Optimization and Application of In Vitro and In Vivo Toxicometabolomics Studies

Dissertation
zur Erlangung des Grades
des Doktors der Naturwissenschaften
der Naturwissenschaftlich-Technischen Fakultät
der Universität des Saarlandes

von

Selina Hemmer

Saarbrücken
2024

Tag des Kolloquiums:	22. April 2024
Prodekan:	Prof. Dr.-Ing. Michael Vielhaber
Berichterstatter:	Prof. Dr. Markus R. Meyer
	Prof. Dr. Alexandra K. Kiemer
Vorsitz:	Prof. Dr. med. Veit Flockerzi
Akad. Mitarbeiter/-in:	PD Dr. Jessica Hoppstädter

Vorwort

Die nachfolgende Arbeit entstand unter der Anleitung von Herrn Univ.-Prof. Dr. Markus R. Meyer in der Abteilung Experimentelle und Klinische Toxikologie der Fachrichtung Experimentelle und Klinische Pharmakologie und Toxikologie der Universität des Saarlandes in Homburg von Oktober 2019 bis Januar 2024.

Die Teilergebnisse der vorliegenden Arbeit wurden in den nachfolgenden Studien bereits veröffentlicht oder zur Veröffentlichung eingereicht. Der eigene Anteil umfasste die Durchführung und Evaluierung der Experimente sowie das Verfassen der Manuskripte für alle fünf Studien.

- Optimization of Extraction and Reconstitution Solvents for the Untargeted Metabolomics Analysis of Human and Rat Urine Samples
  Hemmer S, Manier SK, Wagmann L, Meyer MR
  Zur Veröffentlichung eingereicht bei Journal of Chromatography A, 10/2023
- Comparison of Reversed-phase, Hydrophilic Interaction, and Porous Graphitic Carbon Chromatography Columns for an Untargeted Toxicometabolomics Study in Pooled Human Liver Microsomes, Rat Urine, and Rat Plasma
  Hemmer S, Manier SK, Wagmann L, Meyer MR
  Zur Veröffentlichung eingereicht bei Metabolomics, 10/2023
- Comparison of Three Untargeted Data Processing Workflows for Evaluating LC-HRMS Metabolomics Data
  Hemmer S, Manier SK, Fischmann S, Westphal F, Wagmann L, Meyer MR
  Zur Veröffentlichung angenommen bei Metabolites, 2020
- Altered Metabolic Pathways Elucidated via Untargeted In Vivo Toxicometabolomics in Rat Urine and Plasma Samples Collected After Controlled Application of a Human Equivalent Amphetamine Dose
  Hemmer S, Wagmann L, Meyer MR
  Zur Veröffentlichung angenommen bei Archives of Toxicology, 2021
- In Vitro and In Vivo Toxicometabolomics of the Synthetic Cathinone PCYP Studied by Means of LC-HRMS/MS
  Hemmer S, Wagmann L, Pulver B, Westphal F, Meyer MR
  Zur Veröffentlichung angenommen bei Metabolites, 2022

Danksagung

Ein großes Dankeschön geht an meinen Doktorvater Herrn Univ.-Prof. Dr. Markus R. Meyer, für die herzliche Aufnahme in seinem Arbeitskreis, das entgegengebrachte Vertrauen, die Überlassung dieses interessanten und herausfordernden Dissertationsthemas, die hervorragende Betreuung und die Möglichkeit, selbstständig und wissenschaftlich zu arbeiten und aktiv an nationalen und internationalen Fachkongressen teilzunehmen. Seine offene und freundliche Arbeitsatmosphäre, seine sachliche und konstruktive Kritik, sowie sein Ansporn, über sich selbst hinauszuwachsen, habe ich besonders zu schätzen gelernt.

Frau Univ.-Prof. Dr. Alexandra K. Kiemer danke ich für die Übernahme des Koreferats, sowie Herrn Univ.-Prof. Dr. Dr. h. c. Hans H. Maurer für seine Diskussionsbereitschaft und fachliche Unterstützung während den Seminaren.

Frau Dr. Lea Wagmann und Herrn Dr. Sascha K. Manier danke ich für ihre wissenschaftliche Expertise, die Begleitung und Anleitung der Arbeit und fachliche Diskussionsbereitschaft.

Meinen Kolleginnen und Kollegen möchte ich neben dem wissenschaftlichen Austausch besonders für das angenehme Arbeitsklima und die gute Zusammenarbeit trotz Corona-Pandemie und nahenden Kongressdeadlines danken. Ein besonderer Dank geht an meine Kollegen Dr. Sascha K. Manier, Dr. Tanja M. Gampfer und Juel Maalouli Schaar, für ihre fachliche Unterstützung und Zusammenarbeit, sowie der daraus resultierenden Freundschaft.

Herrn Armin A. Weber danke ich für seine unermüdliche Einsatzbereitschaft, Unterstützung und Geduld bei allen technischen Fragestellungen, auch an Feiertagen und Wochenenden. Frau Gabriele Ulrich danke ich für die gewissenhafte Ausführung der Rattenversuche, sowie der gesamten Besatzung des Routine Labors für die gute Zusammenarbeit.

Meinen Freunden (insbesondere Frederike, Tanja, Juel und Julia) danke ich für die grenzenlose Unterstützung, das stets offenes Ohr, die Möglichkeit Frust abzubauen, das Mitfiebern, Miterleben und Aushalten von Höhen und Tiefen einer Promotion und der Unterstützung in schwierigen Zeiten.

Ein herzliches Dankschön geht an meinen Partner, der mich bereits in vielen Lebenssituationen begleitet hat. Lieber Moritz, danke für deine unendliche Geduld und dein Verständnis, deinen Rückhalt und deine Motivation auch nach Rückschlägen und ganz besonders für deine Liebe.

Die letzten Worte dieser Danksagung gehen an meine Familie: Liebe Mama, Lieber Papa, und Liebe Lea, ohne eure bedingungslose Unterstützung in jeglichen Lebenssituationen wäre all das nicht möglich gewesen. Danke, dass ihr immer an mich geglaubt habt, mir den Rücken freigehalten habt und es mir ermöglicht habt, meinen eigenen Weg zu gehen. Ich liebe euch von ganzem Herzen und bin euch unendlich dankbar für alles!

Homburg, Januar 2024

Selina Hemmer

„**N**othing in life is to be feared, it is only to be understood.”

Marie Curie (1867 -1934)

Zusammenfassung

Im Hinblick auf einen besseren Nachweis neuer Drogenmetabolite und Veränderungen des Stoffwechsels nach dem Konsum von Drogen, wurden verschiedene ungezielte Metabolomik-Techniken untersucht und optimiert. Zunächst wurde eine geeignete Probenaufarbeitung für Urinproben untersucht. Nachfolgend wurde die analytische Methode in Bezug auf die verwendeten Flüssigkeitschromatographie Säulen unter Berücksichtigung verschiedener Matrizes optimiert. Zur Gewinnung verwertbarer Informationen aus Rohdaten und Sicherstellung einer aussagekräftigen biologischen Interpretation, wurden im Anschluss verschiedene Arbeitsabläufe zur Datenprozessierung verglichen. Im letzten Schritt wurden zwei Substanzen aufgrund ihres Missbrauchspotentials mithilfe der ungezielten Toxikometabolomik in vitro und in vivo untersucht.

Die Optimierung der verschiedenen Techniken ergab, dass alle Parameter von der Probenentnahme bis zur biologischen Interpretation an die Fragestellung angepasst und zuvor sorgfältig untersucht werden sollten, da jeder Parameter einen Einfluss auf das Ergebnis der Studie hatte. Die beiden nicht-zielgerichteten Metabolom-Studien ergaben, dass Toxikometabolomik-Studien toxikokinetische Daten und Informationen über die Wirkungsweise von Missbrauchsdrogen liefern können. Toxikometabolomik-Studien ermöglichen es, herkömmliche Screening-Methoden zu umgehen, indem sie sowohl Metabolite als auch endogene Biomarker identifizieren können, die nicht zu erwarten gewesen wären.

Summary

To improve the identification of new drug metabolites and to elucidate changes in the endogenous metabolism after drug consumption, several untargeted metabolomics techniques were investigated and optimized. Initially, a suitable sample preparation for urine samples was investigated. Subsequently, the analytical method was optimized for different matrices with respect to the used liquid chromatography columns. To obtain reliable information from the raw data and to ensure a meaningful biological interpretation, different data processing workflows were compared. Finally, two substances of interest due to their potential for abuse were investigated both in vitro and in vivo using untargeted toxicometabolomics.

The optimization of various techniques demonstrated that parameters from sample collection to biological interpretation should be adapted to the research question and carefully considered beforehand, as each parameter has an influence on the outcome of the study. The two untargeted metabolomics studies indicated that the use of toxicometabolomics studies can provide both toxicokinetic data and information on the mode of action of drugs of abuse. Furthermore, toxicometabolomics studies can circumvent conventional screening methods by identifying both metabolites and endogenous biomarkers that would not have been expected.

Table of Contents

1. General Part

1.1. Metabolomics

1.1.1. Principles of Metabolomics

Metabolomics is an interdisciplinary field that combines analytical chemistry, bioinformatics, statistics, and biochemistry to provide a comprehensive analysis of the metabolome within a biological sample.[1-3] The term 'metabolome' was first introduced by Steven Oliver in the 1990s.[4] It is defined as the sum of low-molecular-weight compounds (< 1,500 Da) that can be detected by mass spectrometry (MS) or nuclear magnetic resonance (NMR) analysis of biofluids or tissues.[1,5] Since the composition of the metabolome is influenced by upstream effects of the genome, transcriptome, and proteome, metabolomics as an emerging field is closer to the phenotype than other 'omics' techniques.[3,6] Unlike the aforementioned, the metabolome is also affected by several other factors such as diet, exercise, drugs, and underlying diseases, as well as chemicals that are derived during sample storage or preparation, amongst others.[1,5,7] Due to its complex composition and high susceptibility to external influences, the metabolome can be categorized into four types: endometabolome, exometabolome, microbial metabolome, and xenometabolome. The endometabolome includes all metabolites produced by any cell type, tissue, or organism, while the exometabolome comprises metabolites that are excreted or consumed by cells. The microbial metabolome refers to metabolites produced by microbiota, and the xenometabolome encompasses metabolites derived from xenobiotics, contaminants, or diet.[5] The metabolome can be analyzed using two primary strategies: untargeted and targeted metabolomics. Targeted approaches are hypothesis-driven and usually requires prior knowledge to detect and quantify specific sets of metabolites.[1,8] In contrast, untargeted approaches are used for hypothesis generation and aim to identify as many metabolites as possible without any previous knowledge to find new biomarkers.[1,8]

1.1.2. Untargeted Metabolomics Workflow

Ideally, an untargeted metabolomics approach offers a complete view of all metabolites present in an organism and enhances comprehension of metabolic response to a biological situation or certain stimulus.[9] This assumes that every metabolite can be measured and that every measurement can be translated into biological information. However, in reality, this assumption

is challenging and requires appropriate experimental design and methodology to overcome.[9] The ability to collect data without prior knowledge is one of the major advantages of untargeted metabolomics, but it is also a key challenge to find the appropriate study design to gain the best biological insights.[1,2,10] Therefore, a well-designed experiment and the choice of appropriate methods for samples and data processing are essential for the success of any metabolomics study.[2,11]

Typically, a workflow for untargeted metabolomics studies can be divided into two major parts: First, the data generation which includes all steps from the biological question to data acquisition and second, the data processing which includes data preprocessing, statistical analysis, metabolite annotation, and biological interpretation (Figure 1). Each of these steps holds individual challenges and influences the outcome of a study.[10]

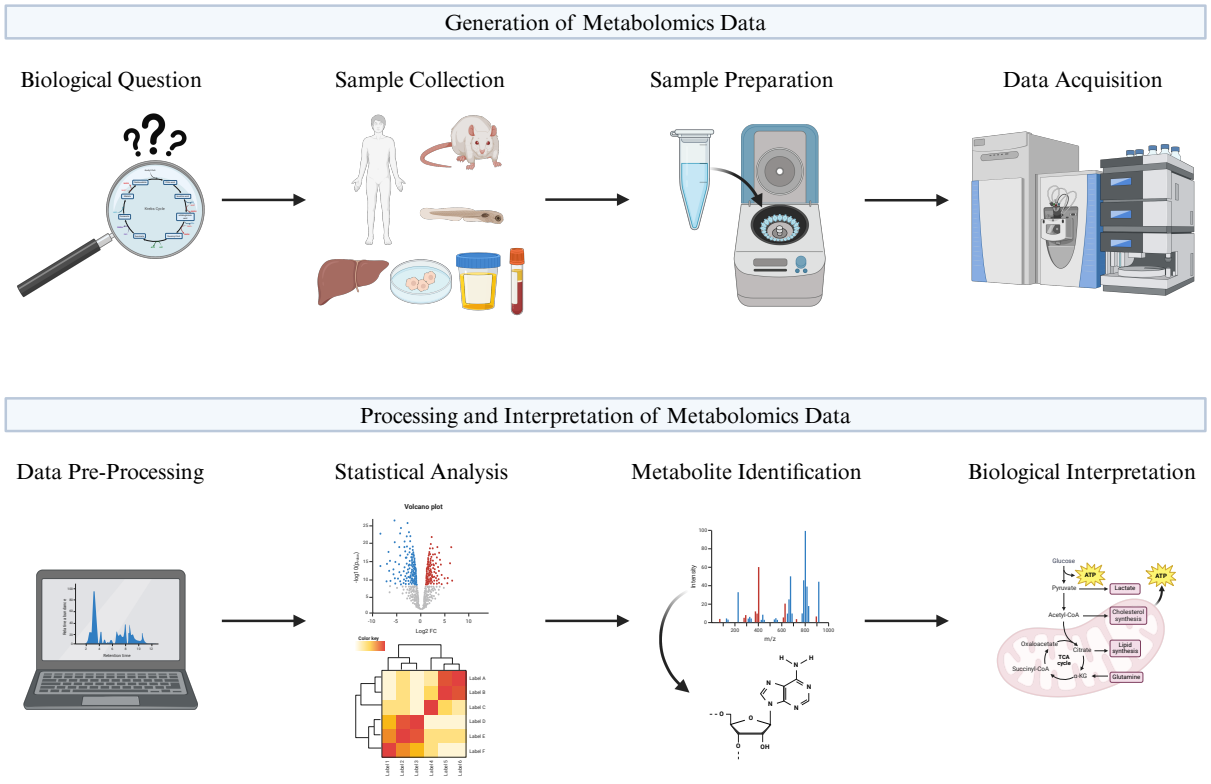

Figure 1. Schematic overview of an untargeted metabolomics workflow. Created with BioRender.com.

The first and most important step is the formulation of the biological question and thus the determination of the experimental design. The definition of the question sets the basis for the study and influences the subsequent steps.[1,5] Once the biological question has been defined, the next step is the sample collection. There is no limitation regarding sample types in metabolomics studies, but both sample type and physicochemical properties of the metabolites predetermine an appropriate sample preparation and also the evaluation and interpretation

varies by biological system.[2] Several studies showed, that preanalytical steps have a significant impact on the outcome of an untargeted study.[12-16] Inadequate sample storage or preparation may lead to a high variability, loss of metabolites, formation of degradation metabolites, or influence with instruments, and therefore must be optimized according to sample type.[5] Since the metabolome is of extremely diverse chemical nature, there is no method for capturing all metabolites.[1] In general, the original biological system must be preserved as far as possible during sample preparation.[2] The next step with considerable variability is the data acquisition. Untargeted metabolomics requires highly analytical instruments for thousands of small molecules with broad chemical diversity and complexity.[3] Most common analytical technologies in untargeted metabolomics are NMR and hyphenated MS.[1,2] While NMR provides no sample alteration, use of small amount of material, identification without reference, and high reproducibility compared with good selectivity, hyphenated MS in contrast exhibits higher sensitivity and a wide dynamic range.[3] These properties make MS coupled to gas chromatography (GC) or liquid chromatography (LC) the most widespread technologies used in untargeted metabolomics.[1,2,17] Chromatographic separation improves the analytical possibilities of MS, as on one hand it reduces ion suppression by separating molecules and thus improves detection. On the other hand, the retention time provides information about the polarity of the molecules.[18,19] Regarding the choice of the chromatographic technique, each comes with advantages and disadvantages. GC-MS is highly reproducible and sensitive, but it is only reliable for measuring small metabolites (< 400 Da) and may not be suitable for measuring unstable molecules that are affected by the heating conditions used for derivatization and chromatography.[1] LC-MS, on the other hand, enables the transfer of charged ions from the liquid phase to the gas phase without derivatization through the use of electrospray ionization or atmospheric pressure ionization interfaces. This offers the possibility of detecting both polar and non-polar metabolites, including lipids, and is therefore, currently the most commonly applied analytical technique in metabolomics.[1,18,20]

The above-mentioned analytical methods, generate huge and high-dimensional amounts of raw data, necessitating powerful software tools to extract valuable information. Data pre-processing includes peak detection, peak alignment, baseline correction, and annotation.[10,21] These steps play a key role to improve signal quality and reduce possible bias. For untargeted data processing a variety of software solutions are available, such as open-source software XCMS[22,23], MetaboAnalyst[24], MZmine[25], or OpenMS[26], and commercial software such as Compound Discoverer, MetaboScape, or MarkerView. Since the underlying algorithms differ, it is very likely, that the outcomes of untargeted studies vary upon the used tools.[27] In order to

compare all the information and to identify compounds and metabolic pathways that are significantly different between investigated groups, a combination of univariate and multivariate analysis are performed. Tools for analyzing include for example *t*-test, analysis of variance (ANOVA), principal component analysis (PCA), or partial least-squares discriminant analysis (PLSDA), among others.[9] While univariate statistic identify specific analytes that altered significantly between cohorts, multivariate statistics distinguish cohorts based on covariances or correlations of the many independent variables.[9,21,28] The main bottleneck in untargeted approaches is translating variables into metabolite identities to draw biological conclusions from untargeted data.[9,10] Metabolite annotation is the crucial link between acquired data and meaningful biological information.[10] The primary challenge for researchers is to objectively investigate the connection between identified metabolites and their biological role.[28,29] In untargeted workflows, the goals are to identify meaningful biomarker(s) and metabolic pathways that forecast or induce a particular phenotype. The former facilitates a fast and immediate implementation. The mechanistic investigation enables a focused exploration of enzyme activity, metabolite transporters, or transcription factors that govern the metabolic process.[21]

However, this approach can prove challenging, as an untargeted approach typically only allows identification of single metabolites within a pathway, making their assignment to definite one often problematic. Therefore, a targeted study is necessary to investigate underlying pathways in order to confirm its impact on the phenotype.[1]

1.2. Drug Abuse

1.2.1. Origin of Drugs of Abuse

The consumption of drugs to modify mental and physical well-being is an ancient practice that can be traced back to the earliest civilizations.[30] In many cultures, their consumption is often related to religious and/or social rituals, but also for medicinal purpose.[31] Throughout the Middle Ages, plants or their components, such as poppy juice or coca leaves were commonly used while the active substances such as morphine or cocaine were first isolated from plants in the 19th century.[32-34] Originally intended for therapeutic effect, morphine was specifically utilized to treat severe pain.[32,33] However, it was discovered that the opiates offered pleasurable effects and thus they were consumed for non-therapeutic purpose. As a result, these substances were quickly adopted as addictive drugs once their medical properties were uncovered.[33] Among other milestones, the isolation of morphine in the 19th century marked the beginning of

the pharmaceutical industry's.[35] After isolation of cocaine from coca leaves in 1855 and first synthesizing of amphetamine in 1887 as a synthetic derivative of the plant alkaloid ephedrine, diacetylmorphine, also known as heroin, was launched on the market by the Bayer company in 1898.[36] Unaware that they had created an even more potent drug, heroin was marketed to reduce the side effects of morphine.[36,37] With the enactment of the German Opium Act in 1929, such classic drugs were available only by prescription and for medical purposes. As part of the modernization of German drug law under the 1961 UN Single Convention, the Opium Act, was replaced in 1971 by the current Narcotics Act (Betäubungsmittelgesetz, BtMG).[38] This increased the search for new drugs of abuse, that were not covered by the law.

The commonly used term drug of abuse (DOA) refers to a psychotropic substance that is illicitly consumed for non-therapeutic or recreational reasons.[39] Classical DOAs include cocaine, heroin, amphetamine, methamphetamine, or methylenedioxymethamphetamine (ecstasy) which have been widely abused for decades and are subject to controlled substance legislation.[36,39,40]

1.2.2. New Psychoactive Substances

Designed to circumvent international drug legislation, new psychoactive substances (NPS) or also known as "legal highs" have spread in the drug market in the last years.[41,42] NPS are an emerging class of compounds, which can chemically be similar to traditional DOAs but also new entities intended to mimic the effects of commonly known illicit substances without being restricted by drug laws.[43,44]

They can be categorized in multiple ways, for example according to their origin – whether plant-based or synthetic, psychotropic effects, or chemical structure.[45] At the end of 2022, the European Monitoring Centre for Drugs and Drug Addiction (EMCDDA) monitored around 930 NPS, 41 of which were first reported in Europe in 2022 of which 24 were synthetic cannabinoids followed by 5 synthetic cathinones.[46]

Both synthetic cannabinoids and synthetic cathinones are excellent examples of the challenges presented by "legal highs". These substances are typically modified chemicals derived from other known DOAs.[47]

As legal alternatives to *Cannabis sativa* L., synthetic cannabinoids have become popular for mimicking the euphoric effects of the main psychotropic constituent, Δ^9-tetrahydrocannabinol (THC).[47-49] This effect is due to the fact that synthetic cannabinoids interact with the human cannabinoid type 1 (CB1) and/or type 2 (CB2) receptors, whereby interactions with CB1 are

primarily responsible for psychoactive effects.[50,51] However, synthetic cannabinoids tend to have higher potency and efficacy at CB receptors than THC, which acts as a partial agonist at both subtypes. This might explain the limited toxicity of cannabis use.[48,49] However, frequent use of synthetic cannabinoids can lead to severe or fatal intoxication, causing side effects such as increased heart rate, high blood pressure, hallucinations, rapid loss of consciousness, seizures, respiratory depression, or coma.[52,53]

Synthetic cathinones commonly sold as "bath salts" are stimulant-like drugs derived from cathinone, the primary psychoactive compound found in *Catha edulis* (Vahl) Forssk. ex Endl..[47] The pharmacological effects of various derivatives rely primarily on the types and positions of the substituents.[47,54,55] Preclinical studies have uncovered two ways in which they interact with monoamine transports. Compounds that either act as monoamine transporter blockers, similar to cocaine, or that act as monoamine transporter substrates, promoting neurotransmitter release, such as amphetamine and 3,4-methylendioxy-*N*-methylamphetamine (MDMA).[56-63] Despite sharing a common phenethylamine core, synthetic cathinones have varying affinity, selectivity, and potency towards monoamine membrane receptors and transporters.[54,62,64] The efficacy, selectivity, and affinity for a particular monoamine system is crucial due to the specific clinical and toxic effects that result from stimulation of different monoamine systems. For instance, the dopaminergic effects manifest in psychostimulant effects and reinforcing properties with a high potential for abuse and addiction, while noradrenergic effects result in sympathomimetic stimulation leading to cardiovascular and psychostimulant effects, and the serotonergic effects induce hyperthermia, seizures, paranoia, and hallucinations.[54,63,65] Since previous studies have demonstrated that synthetic cathinones, which belong to the same chemical family, have diverse pharmacological effects, they are categorized based on their mode of action.[54,59,62,63] Alongside the desirable effects, including increased alertness and attention, euphoria, improved mood and well-being, increased energy or reduced appetite, there are also adverse effects that can occur after acute or chronic intoxication or overdose.[54] These symptoms encompass tachycardia, hyperthermia, restlessness, anxiety, or psychosis, and even multiple organ failure and death.[54,66] Due to the fluctuating presence on the market, the high structural diversity, the associated wide range of clinical manifestations of NPS and the related health and safety hazards, it is challenging for clinical and forensic toxicology to detect ingestion and conduct an appropriate risk assessment.[47,67,68]

1.3. Challenges Related to Drugs of Abuse in Toxicology

Toxicology is defined as the study of potential harmful effects of substances on living organisms and ecosystems. Its goal is to assess the risks of substances to human and animal health while avoiding hazards. Besides the relationship between harmful effects and exposure, it also deals with the mode of action, diagnosis, prevention, and treatment of intoxications.[69,70] Thereby, the processes of toxicokinetic and toxicodynamic play a crucial role. While toxicokinetic deals with the uptake, distribution, biotransformation, and excretion of potentially toxic substances within the body, toxicodynamic examines the interaction of these harmful substances with the target site, resulting in associated biochemical and physiological effects that can lead to adverse effects.[71] During the early stages in drug development process various toxicological tests are utilized to examine the toxicokinetic and toxicodynamic of therapeutic drugs.[67] Typically, these studies are not conducted on DOAs such as NPS prior to their entry into the market, presenting a significant challenge for both clinical and forensic toxicology.[67,72] While forensic toxicology measures drugs in context of death or human performance, clinical toxicology deals with the impact of drugs in both acute poisoning and long-term monitoring/detection of emerging DOAs to confirm intake in case of overdose followed by acute intoxication.[39,68]

On one hand, the structural diversity of NPS leads to an analytical challenge in detecting patient intake and thus a leakage of toxicokinetic information.[68] On the other hand, the lack of information regarding the mode of action of these substances hinders an evaluation of their severity for acute and chronic toxicity. Additionally, the continuously fluctuating number of NPS available in the market complicates regulation and the application of a sufficient risk assessment. Brand et al. described the ongoing evasion of current regulations to promote newly misused drugs as a "cat and mouse game".[73]

However, it is essential to conduct toxicokinetic and toxicodynamic investigations on DOA such as NPS to address those challenges. Due to the lack of preclinical safety data and therefore for ethical reasons, controlled human studies are not possible, so in vitro and in vivo studies are preferred.[67] The emphasis here is mostly on the confirmation of consumption, with a primary focus on the detection of intake. Although stimulants such as synthetic cathinones or piperazines are not extensively metabolized and can also be detected unmetabolized in human urine, most synthetic cannabinoids cannot be detected unmetabolized in urine.[74] Consequently, it is important to continuously adapt existing analytical methods.[75]

1.3.1. Established Toxicology Studies in Clinical and Forensic Toxicology

Due to the rapid emergence of new substances, well established in vitro models such as pooled human liver microsomes (pHLM), pooled human liver S9 fraction, primary human hepatocytes, HepaRG, or HepG2 cells, as well as zebrafish larvae are available to study metabolism of DOAs besides classical in vivo studies.[76-78] Such in vitro models are particularly suitable for elucidating metabolism but also for investigating organ-specific toxicity.[79,80]

Species differences aside, drug excretion patterns are affected by both dose and time, which complicates extrapolation to humans. It's worth noting that excretion patterns are usually dependent on both dose and time, and the substances detected in case of intoxication or overdose may differ from those found after recreational use or during later excretion phases.[67]

For toxicodynamic, there are systematic studies on transporter or receptor interaction profiles in various cell lines, enzyme inhibition screening of selected enzymes, or cytotoxicity tests.[59,62,80-83] However, such in vitro tests do not provide insights into the molecular mechanisms as controlled in vivo tests.

In most of the established toxicokinetic and toxicodynamic methods for NPS, the metabolites are often specifically investigated for the mode of action that can be derived from the general structure and thus targets are specifically searched for. As a result, not only metabolites that would not be expected are missed, but also potential targets remain undiscovered.

1.3.2. Toxicometabolomics

In recent years, toxicometabolomics, a sub-discipline of metabolomics, has become an important tool in toxicology.[3,5,84-88] Compared to other omics techniques, metabolomics is more closely related to the drug response phenotype.[3,7] Therefore, toxicometabolomics observes changes in small molecules that occur in an organism in response to a specific drug-induced stimulus.[84] Given the growing problem of drug abuse worldwide, especially of NPS, the use of metabolomics opens up the possibility of identifying new exogenous and endogenous biomarkers.[84]

Detection of biochemical changes following DOA intake can thus complement conventional approaches by revealing potential biomarkers of organ toxicity, identifying novel metabolites in a time- and dose-dependent manner, and discovering different drug targets, as well as providing insights into metabolic pathways, mechanisms of action, adverse effects, and early toxicity events, even at low doses.[5,89] Therefore, the use of toxicometabolomics of DOAs is of great interest in clinical and forensic toxicology, not only for reliable confirmation of DOA

intake in patients, but also for appropriate risk assessment. Concerning NPS, conventional methods might not be as effective in screening approaches anymore. Thus, in screening methods, detection of drug intake may only be feasible through one or a few distinct metabolites, particularly when the parent compound is not detectable in the samples. However, when numerous structurally related compounds share common primary metabolites, detection of ingestion of a specific illicit drug may require less prominent metabolites.[84] Therefore, in the highly fluctuating market of NPS, metabolomics is an alternative strategy to identify biomarkers, especially with regard to drug biotransformation.

Although metabolomics is an invaluable tool in toxicology, it does have limitations. On the one hand, establishing a direct causal relationship between cause and effect using metabolomics alone can be challenging, since any event can lead to an effect.[87] Additionally, ethical and biological variability concerns often lead to NPS metabolomics studies being performed in vitro or in vivo, which can prove difficult to extrapolate to humans.[85,90]

2. Aims and Scopes

The aims of this study were to evaluate untargeted (toxico-)metabolomics techniques for the identification of drug metabolites and metabolic changes associated with drug consumption, particularly after ingestion of DOAs. Various steps in the untargeted metabolomics workflow should be evaluated, optimized, and applied using both in vitro and in vivo studies. Appropriate sampling strategies, including sample collection and preparation, should be developed. Analytical methods and data preprocessing should be optimized, while statistical analysis should be evaluated to identify significant changes between the investigated groups. Planned studies should finally reveal changes within endogenous and exogenous metabolome after acute exposure to DOAs.

The following steps had to be conducted:

- Development of suitable sample preparation of human and rat urine samples for untargeted liquid chromatography coupled to high resolution mass spectrometry (LC-HRMS) metabolomics

- Optimization of different LC columns using pHLM, rat plasma, and rat urine

- Optimization of different data preprocessing software solutions for evaluation of untargeted metabolomics data

- Investigation of rat metabolome after controlled administration of human equivalent amphetamine dose

- Investigation of in vitro and in vivo metabolic pathways of the synthetic cathinone alpha-pyrrolidinocyclohexanophenone (PCYP) using untargeted toxicometabolomics

3. Results

The results of the studies were published in the following articles:

3.1. Optimization of Extraction and Reconstitution Solvents for the Untargeted Metabolomics Analysis of Human and Rat Urine Samples

This is a pre-copyedited, author-produced version of an article submitted to Journal of Chromatography A (manuscript number: JCA-23-1456).

(Submitted 10/2023, DOI not yet provided)

Author Contributions:
Selina Hemmer conducted and evaluated the experiments as well as composed the manuscript; Sascha K. Manier, Lea Wagmann, and Markus R. Meyer assisted with the design of the experiments, the interpretation of the analytical experiments, and scientific discussions.

Manuscript Click here to view linked References

Optimization of extraction and reconstitution solvents for the untargeted metabolomics analysis of human and rat urine samples

Selina Hemmer, Sascha K. Manier (ORCID: 0000-0002-7126-5263), Lea Wagmann, Markus R. Meyer (ORCID: 0000-0003-4377-6784)

Department of Experimental and Clinical Toxicology, Institute of Experimental and Clinical Pharmacology and Toxicology, Center for Molecular Signaling (PZMS), Saarland University, Homburg, Germany

ABSTRACT

Inadequate sample preparation can result in the loss of important analytes and thus affect the outcome of untargeted metabolomics studies. Different sample preparations may be required for a biological matrix originating from different species. The aim of this study was to optimize the extraction of rat and human urine and the extract reconstitution before untargeted analysis by hydrophilic interaction chromatography or reversed-phase liquid chromatography high-resolution mass spectrometry. The resulting analytical data were evaluated for feature count, feature detectability, and reproducibility of selected compounds. A total of 12 different protein precipitation conditions were tested, combining four different extraction solvents and three different reconstitution solvents. A combination of methanol as extraction and acetonitrile/water (75/25) as reconstitution solvent gave the best results at least in terms of total feature count. In addition, it was found that a higher amount of methanol improved extraction of rat urine among the conditions tested. In comparison, human urine required a lower volume of extraction solvent. Overall, it can be concluded that systematic optimization of both the extraction method and the reconstitution solvent for each analyzed biofluid and analytical setting is encouraged.

Keywords: untargeted metabolomics, human urine, rat urine, extraction methods, reconstitution, sample preparation

1. Introduction

Metabolomics focuses on the analysis of low molecular weight compounds (<1,500 Da) in a biological system [1]. Since these compounds are not only endogenous metabolites but also metabolites from exogenous sources such as drugs, diet, and gut microbiota, a high chemical diversity and complexity is expected. Thus in untargeted metabolomics, it is desirable to use methods that are not biased for or against specific analyte classes but cover a broad range of metabolites [2]. Among others, sample preparation is a critical step with implications for metabolite extraction and their subsequent detection to achieve high quality and comprehensive metabolome coverage [2, 3]. To obtain as many unknown metabolites with various physicochemical properties as possible, the integrity of the samples should be altered as little as possible. Hence, an ideal sample preparation should be non-selective, reproducible, simple, and fast [2, 4]. Due to several advantages such as non-invasive sample collection, large volumes, possibility of repeated sampling, low sample complexity compared to plasma, and reflection of the endogenous as well as exogenous metabolic profile, urine has been established as a key biological matrix in metabolomic studies [5, 6]. Despite these benefits, urine has a wide range of metabolite concentrations and is thus subjected to variable and unpredictable dilution [6]. Due to this fact and the high chemical diversity of metabolites, appropriate sample preparation is required. For urine, recommendations for very simple sample preparations such as filtration, centrifugation, dilution, or combinations thereof can be found in literature, since most analytes are present in sufficiently high concentrations and the protein levels are quite low [1, 4, 7, 8]. However, there are certain classes of compounds such as biogenic amines, lipids, or steroids that are present in lower concentrations and may require additional pre-analytical concentration steps [7]. Furthermore, due to species differences, different sample preparations may be required within the same biological matrix from different origins to cover the respective metabolome.

Therefore, the aim of this study was to systematically test the impact of four different extraction solvents for protein precipitation in combination with three different reconstitution solvents on the analytical data of untargeted liquid chromatography high-resolution mass spectrometry (LC-HRMS) metabolomics analysis of rat and human urine samples. Finally, the most appropriate method for each biofluid was identified.

2. Materials and methods

2.1. Chemicals and reagents

Ammonium formate, ammonium acetate, DL-aspartic acid-d_3 (DL-aspartic acid-2,3,3-d_3), cortisol-d_4 (cortisol-9,11,12,12-d_4), creatinine-d_3, formic acid, D-glucose-d_7 (D-glucose-1,2,3,4,5,6,6-d_7), glycine-^{15}N, palmitic acid-d_{31}, and succinic acid-d_4 were obtained from Merck (Darmstadt, Germany). Acetonitrile, ethanol, and methanol (all LC-MS grade) were from VWR (Darmstadt, Germany). Water was purified with a Millipore filtration unit (18.2 Ω x cm water resistance). L-Tryptophan-d_5 was obtained from Alsachim (Illkirch-Graffenstaden, France). L-Carnitine-d_9, cytosine-d_2, D-fructose-$^{13}C_6$, hypoxanthine-d_4, kynurenic acid-d_5, prostaglandin-E_2-d_9, stearic acid-^{13}C, and thymidine-d_4 were purchased from Cayman Chemical (Ann Arbor, MI, USA). DL-Glutamic acid-d_3 (DL-glutamic-2,4,4-d_3 acid), L-arginine-d_7 (L-arginine-2,3,3,4,4,5,5-d_7), and L-lysine-d_3 (L-lysine-2,6,6-d_3) were obtained from Toronto Research Chemicals (Toronto, Canada).

2.2. Sample collection and preparation

Rat urine (*n* = 5) was used from the control group of a previously published study [9]. Human urine was collected from 10 healthy individuals. Samples were aliquoted and stored at -80°C. Aliquots were thawed at 4°C over night and pooled for each species. Pooled urine was centrifugated at 15,000 x *g* at 4°C for 10 min. For each preparation, 100 µL of supernatants of pooled rat or pooled human urine were transferred into a reaction tube. A total of 12 sample preparations (Table 1) were tested, based on four different extraction solvents. After precipitation, samples were shaken for 2 min at 1,500 rpm, precipitated at -20°C for 30 min, and then centrifuged at 15,000 x *g* and 4°C for 10 min. The supernatant was transferred in new reaction tubes and evaporated to dryness using a vacuum centrifuge at 1,400 rpm and 24 °C. The obtained residues were reconstituted in 50 µL using three different reconstitution solvents (Table 1). Each sample was prepared in quintuplets (*n* = 5). Pooled quality control (QC) samples were prepared by transferring 10 µL of each sample into one MS vial.

Extraction solvents and reconstitution solvents were fortified with a total of 19 different internal standards of various endogenous compound classes (see *Experimental section* in *Supporting information*).

2.3. LC-HRMS/MS apparatus

Analysis was performed according to previous published studies [9, 10]. Details can be found in *Experimental section* of *Supporting information*.

2.4. Data evaluation

Data processing was performed in an R environment [11, 12]. Thermo Fisher Scientific LC-HRMS raw files were converted into mzXML files using ProteoWizard [13]. XCMS parameters were optimized according to Manier et al. [12]. Peak-picking and alignment parameters are summarized in Table S2. Peak picking was performed using XCMS 3 (version 3.20.0) [14] in an R environment and the R package CAMERA [15] was used for annotation of adducts, artifacts, and isotopes. Feature abundances containing the value zero were replaced by the lowest measured abundance as a surrogate limit of detection and the whole dataset was then log 10 transformed. Peak areas were normalized to the different ratios of extraction solvents. To evaluate the number of features that can be detected by the used analysis, total feature count was assessed. Therefore, the number of features which peak area was not declared as not available ("NA") was summed up for each analysis. For the reproducibility, the coefficient of variation (CV) was determined from the peak areas of each sample preparation. In addition to the total feature count, peak areas of spiked internal standards were evaluated to compare each preparation in terms of different compound classes. Statistical evaluation was done using one-way ANOVA as well as Welch's two sample *t*-test for significance comparing total feature count of each group in rat or human urine samples.

R script can be found on GitHub (https://github.com/sehem/urine_preparation.git) and mzXML files are available via Metabolights (study identifier MTBLS8237).

3. Results and discussion

Results after analysis using hydrophilic interaction chromatography (HILIC) and positive and negative electrospray ionization are shown in Figure 1-3. Those of the analysis using reversed-phase chromatography (RP) are shown in Figure S1-3 in *Supporting information*.

The extraction and reconstitution solvents were selected based on their frequency in the literature. Most published extractions were based on methanol (MeOH) and/or

acetonitrile (ACN) in different ratios [8, 16-19]. Since elevated concentrations of water (H_2O) might impair the performance of HILIC, cause instability, or poor solubilization of certain analytes, different ratios for ACN and H_2O were evaluated as reconstitution solvents in addition to the previously described composition of ACN and MeOH [17, 18].

Untargeted metabolomic studies aim to detect as many metabolites as possible to best describe the metabolome. Therefore, the size of the total feature count was used as one main parameter to compare the influence of (pre-)analytical methods. It need to be mentioned that the total feature count was also described as inappropriate parameter for such investigations in general, since it can be widely differ due to artifactual interference and therefore a method that detects the maximum number of features is not always the method that provides the broadest metabolome coverage. Such artifactual interference can be caused by contamination during metabolite extraction, carryover from previous experiments, background noise detected by MS, or misannotation of data during bioinformatic processing, amongst others [20]. Since this study followed a highly standardized procedure and almost the same conditions for each sample, the variability in the total feature count caused by artifactual interference should be rather small compared to the variability caused by different extractions of metabolites.

Regarding the total feature count, each preparation condition was able to provide many features and there was no condition that was the optimal one for all four analytical methods and both species matrices. However, the total feature count mainly depended on the reconstitution solvent. For rat urine (Figure 1A+B and S1A+B), the highest feature count was observed for reconstitution solvent ACN/H_2O (+0.1% formic acid) (75/25) over all four analytical methods. Compared to rat urine, differences were observed for human urine with respect to the used chromatographic method (Figure 1C+D and S1C+D). For HILIC, reconstitution solvent ACN/H_2O (+0.1% formic acid) (25/75) showed the highest effect using positive ionization and for RP, reconstitution solvent ACN/H_2O (+0.1% formic acid) (75/25) using both polarities.

In addition to total feature count, the reproducibility of the features was also evaluated using an accepted CV<20% (Figure 2 and S2). Overall, no clear trend was observed for one single sample preparation for all four analytical methods. Nevertheless, it can be assumed that the reproducibility of rat urine preparation was higher when using a ratio of 1:8 instead of 1:4 urine:MeOH. For human urine preparation, less extraction

solvents were required in general. This is most probably because rat urine contains a higher protein concentration than human urine and therefore requires a larger amount of solvent for protein precipitation [21]. Again, reconstitution solvents exerted a major impact. The highest reproducibility after preparation of rat urine and analyzing using positive ionization mode was for the reconstitution solvent ACN/H_2O (+0.1% formic acid) (25/75) across all extractions, whereas using negative ionization mode no clear trend was observed. The reproducibility of peak areas after preparation of human urine using different reconstitution solvents highly depended on the used analytical method. Since the impact of the feature count and its reproducibility might be discussed, the peak areas of selected internal standards were also investigated in each analysis. For this purpose, various isotope labeled endogenous compounds were spiked into the extraction or reconstitution solvent at physiological concentrations (Table S1) [22]. Results of the mean peak areas of each isotope labeled compound for each preparation of rat and human urine are shown in Figure 3 for HILIC and in Figure S3 for RP as heat maps. Cortisol-d_4, DL-aspartic acid-d_3, glycine-^{15}N, hypoxanthine-d_4, and stearic acid-^{13}C could not be detected at their physiological concentrations in any sample and even not the neat solvents. This may have been due to low concentration and/or poor ionization. Since most analytes in urine can be considered as hydrophilic, most compounds were detected after HILIC (Figure 3). Most hydrophilic labeled compounds eluted within the first 60 sec on RP columns, which may lead to an increased risk of ion suppression. As already described for total feature count, the reconstitution solvents showed a greater impact compared to extraction solvents. For rat urine, reconstitution solvent ACN/H_2O (+0.1% formic acid) (75/25) showed the best results. No fatty acids were detected using a higher amount of water and very hydrophilic labeled compounds showed smaller peak areas after using ACN/MeOH (70/30). With respect to extraction solvent, MeOH resulted in the largest peak areas. In human urine, a similar trend was observed as for rat urine, except for the two analytes cytosine-d_2 and thymidine-d_4. Both analytes were not detected most likely due to matrix effects as the analytes were detected in the respective neat solvents.

Based on all results described above, it can be summarized that reconstitution solvents have a greater impact on compound recovery compared to extraction solvents during sample preparation of urine. Also, the used chromatographic system was important in selection of the extraction or reconstitution solvent. However, the use of multiple extraction and/or reconstitution solvents is expected to be unfeasible in most

circumstances, as it is time-consuming and costly. It therefore appears to be more reasonable to select solvents that fit for each chromatographic system. Nevertheless, this study also showed that it is not recommended to use the same sample preparation for the same matrix of different species in general. Even if rat and human urine differ slightly, it should not be assumed in future that the same preparation will lead to the same results. However, the results of this study are limited to the investigated compounds and matrix. Therefore, described suitable preparations are not universally applicable and this type of study should be done for each workflow to evaluate the most suitable solvents.

4. Conclusion

The study aimed to systematically evaluate the effects of four extraction solvents, three reconstitution solvents in combination with HILIC- or RP-LC, and positive or negative electrospray ionization HRMS on metabolome coverage represented by detectable features/compounds and feature reproducibility in both rat and human urine samples. The metabolome coverage represented by the number of detectable features/compounds and feature reproducibility of rat and human urine was evaluated. Results of this study shows indicated that the feature count and detected compounds were predominantly influenced by the reconstitution solvents used. Extraction solvents were required in higher amounts for rat urine preparation as compared to human urine. Considering the data of this study, it is recommended to use a combination of methanol for extraction and acetonitrile/water (75/25) as the reconstitution solvent. However, for optimal metabolome coverage, it is essential to adapt the preparation under consideration of the investigated biomatrix/species and the chromatographic system used.

Conflict of interest

The authors declare no conflict of interest.

Data availability

The R script can be found on GitHub ((https://github.com/sehem/urine_preparation.git) and the mzXML files used in this study are available via Metabolights (www.ebi.ac.uk/metabolights/MTBLS8237)

Acknowledgements

The authors would like to thank Armin A. Weber, Aline C. Vollmer, Carsten Schröder, Cathy M. Jacobs, Fabian Frankenfeld, Gabriele Ulrich, Juel Maalouli Shaar, Philip Schippers, and Tanja M. Gampfer for their support and/or helpful discussions.

Supplementary materials

Electronic supplementary material associated with this article can be found online.

References

[1] S. Barnes, H.P. Benton, K. Casazza, S.J. Cooper, X. Cui, X. Du, J. Engler, J.H. Kabarowski, S. Li, W. Pathmasiri, J.K. Prasain, M.B. Renfrow, H.K. Tiwari, Training in metabolomics research. I. Designing the experiment, collecting and extracting samples and generating metabolomics data, J. Mass Spectrom. 51(7) (2016) 461-75. https://doi.org/10.1002/jms.3782.

[2] J. Ivanisevic, E.J. Want, From Samples to Insights into Metabolism: Uncovering Biologically Relevant Information in LC-HRMS Metabolomics Data, Metabolites 9(12) (2019). https://doi.org/10.3390/metabo9120308.

[3] Z.G. Gong, J. Hu, X. Wu, Y.J. Xu, The Recent Developments in Sample Preparation for Mass Spectrometry-Based Metabolomics, Crit Rev Anal Chem 47(4) (2017) 325-331. https://doi.org/10.1080/10408347.2017.1289836.

[4] M.M. Khamis, D.J. Adamko, A. El-Aneed, Mass spectrometric based approaches in urine metabolomics and biomarker discovery, Mass Spectrom. Rev. 36(2) (2017) 115-134. https://doi.org/10.1002/mas.21455.

[5] D. Ryan, K. Robards, P.D. Prenzler, M. Kendall, Recent and potential developments in the analysis of urine: a review, Anal. Chim. Acta 684(1-2) (2011) 8-20. https://doi.org/10.1016/j.aca.2010.10.035.

[6] E.J. Want, I.D. Wilson, H. Gika, G. Theodoridis, R.S. Plumb, J. Shockcor, E. Holmes, J.K. Nicholson, Global metabolic profiling procedures for urine using UPLC-MS, Nat. Protoc. 5(6) (2010) 1005-18. https://doi.org/10.1038/nprot.2010.50.

[7] J. Rodriguez-Morato, O.J. Pozo, J. Marcos, Targeting human urinary metabolome by LC-MS/MS: a review, Bioanalysis 10(7) (2018) 489-516. https://doi.org/10.4155/bio-2017-0285.

[8] D. Rojo, C. Barbas, F.J. Ruperez, LC-MS metabolomics of polar compounds, Bioanalysis 4(10) (2012) 1235-43. https://doi.org/10.4155/bio.12.100.

[9] S. Hemmer, L. Wagmann, B. Pulver, F. Westphal, M.R. Meyer, In Vitro and In Vivo Toxicometabolomics of the Synthetic Cathinone PCYP Studied by Means of LC-HRMS/MS, Metabolites 12(12) (2022). https://doi.org/10.3390/metabo12121209.

[10] S.K. Manier, A. Keller, J. Schaper, M.R. Meyer, Untargeted metabolomics by high resolution mass spectrometry coupled to normal and reversed phase liquid chromatography as a tool to study the in vitro biotransformation of new psychoactive substances, Sci. Rep. 9(1) (2019) 2741. https://doi.org/10.1038/s41598-019-39235-w.

[11] S. Hemmer, L. Wagmann, M.R. Meyer, Altered metabolic pathways elucidated via untargeted in vivo toxicometabolomics in rat urine and plasma samples collected after controlled application of a human equivalent amphetamine dose, Arch. Toxicol. 95(10) (2021) 3223-3234. https://doi.org/10.1007/s00204-021-03135-8.

[12] S.K. Manier, A. Keller, M.R. Meyer, Automated optimization of XCMS parameters for improved peak picking of liquid chromatography-mass spectrometry data using the coefficient of variation and parameter sweeping for untargeted metabolomics, Drug Test Anal 11(6) (2019) 752-761. https://doi.org/10.1002/dta.2552.

[13] R. Adusumilli, P. Mallick, Data Conversion with ProteoWizard msConvert, Methods Mol. Biol. 1550 (2017) 339-368. https://doi.org/10.1007/978-1-4939-6747-6_23.

[14] C.A. Smith, E.J. Want, G. O'Maille, R. Abagyan, G. Siuzdak, XCMS: processing mass spectrometry data for metabolite profiling using nonlinear peak alignment, matching, and identification, Anal. Chem. 78(3) (2006) 779-87. https://doi.org/10.1021/ac051437y.

[15] C. Kuhl, R. Tautenhahn, C. Bottcher, T.R. Larson, S. Neumann, CAMERA: an integrated strategy for compound spectra extraction and annotation of liquid chromatography/mass spectrometry data sets, Anal. Chem. 84(1) (2012) 283-9. https://doi.org/10.1021/ac202450g.

[16] J. Chen, W. Wang, S. Lv, P. Yin, X. Zhao, X. Lu, F. Zhang, G. Xu, Metabonomics study of liver cancer based on ultra performance liquid chromatography coupled to mass spectrometry with HILIC and RPLC separations, Anal. Chim. Acta 650(1) (2009) 3-9. https://doi.org/10.1016/j.aca.2009.03.039.
[17] W. Zou, J. She, V.V. Tolstikov, A comprehensive workflow of mass spectrometry-based untargeted metabolomics in cancer metabolic biomarker discovery using human plasma and urine, Metabolites 3(3) (2013) 787-819. https://doi.org/10.3390/metabo3030787.
[18] M.A. Fernández-Peralbo, M.D. Luque de Castro, Preparation of urine samples prior to targeted or untargeted metabolomics mass-spectrometry analysis, TrAC Trends in Analytical Chemistry 41 (2012) 75-85. https://doi.org/https://doi.org/10.1016/j.trac.2012.08.011.
[19] C. Martias, N. Baroukh, S. Mavel, H. Blasco, A. Lefevre, L. Roch, F. Montigny, J. Gatien, L. Schibler, D. Dufour-Rainfray, L. Nadal-Desbarats, P. Emond, Optimization of Sample Preparation for Metabolomics Exploration of Urine, Feces, Blood and Saliva in Humans Using Combined NMR and UHPLC-HRMS Platforms, Molecules 26(14) (2021). https://doi.org/10.3390/molecules26144111.
[20] N.G. Mahieu, X. Huang, Y.J. Chen, G.J. Patti, Credentialing features: a platform to benchmark and optimize untargeted metabolomic methods, Anal. Chem. 86(19) (2014) 9583-9. https://doi.org/10.1021/ac503092d.
[21] H. Idborg, L. Zamani, P.O. Edlund, I. Schuppe-Koistinen, S.P. Jacobsson, Metabolic fingerprinting of rat urine by LC/MS Part 1. Analysis by hydrophilic interaction liquid chromatography-electrospray ionization mass spectrometry, J. Chromatogr. B Analyt. Technol. Biomed. Life Sci. 828(1-2) (2005) 9-13. https://doi.org/10.1016/j.jchromb.2005.07.031.
[22] D.S. Wishart, A. Guo, E. Oler, F. Wang, A. Anjum, H. Peters, R. Dizon, Z. Sayeeda, S. Tian, B.L. Lee, M. Berjanskii, R. Mah, M. Yamamoto, J. Jovel, C. Torres-Calzada, M. Hiebert-Giesbrecht, V.W. Lui, D. Varshavi, D. Varshavi, D. Allen, D. Arndt, N. Khetarpal, A. Sivakumaran, K. Harford, S. Sanford, K. Yee, X. Cao, Z. Budinski, J. Liigand, L. Zhang, J. Zheng, R. Mandal, N. Karu, M. Dambrova, H.B. Schioth, R. Greiner, V. Gautam, HMDB 5.0: the Human Metabolome Database for 2022, Nucleic Acids Res. 50(D1) (2022) D622-D631. https://doi.org/10.1093/nar/gkab1062.

Table 1

Overview of the used sample preparation conditions. Ratio and percent refer to urine or solvent volume. MeOH = methanol, ACN = acetonitrile, and H_2O = purified water.

Preparation	Extraction solvent	Reconstitution solvent
1_1	Urine:MeOH (1:4)	ACN/MeOH (70/30)
1_2	Urine:MeOH (1:4)	ACN/H_2O (+0.1% formic acid) (75/25)
1_3	Urine:MeOH (1:4)	ACN/H_2O (+0.1% formic acid) (25/75)
2_1	Urine:MeOH (1:8)	ACN/MeOH (70/30)
2_2	Urine:MeOH (1:8)	ACN/H_2O (+0.1% formic acid) (75/25)
2_3	Urine:MeOH (1:8)	ACN/H_2O (+0.1% formic acid) (25/75)
3_1	Urine:ACN (1:8)	ACN/MeOH (70/30)
3_2	Urine:ACN (1:8)	ACN/H_2O (+0.1% formic acid) (75/25)
3_3	Urine:ACN (1:8)	ACN/H_2O (+0.1% formic acid) (25/75)
4_1	Urine:ACN:MeOH (2:1:1)	ACN/MeOH (70/30)
4_2	Urine:ACN:MeOH (2:1:1)	ACN/H_2O (+0.1% formic acid) (75/25)
4_3	Urine:ACN:MeOH (2:1:1)	ACN/H_2O (+0.1% formic acid) (25/75)

Legends to the figures

Fig. 1. Results of statistical evaluation using one-way ANOVA and Welch's two sample *t*-test comparing total feature count of each group in rat and human urine samples. Analysis was done using hydrophilic interaction chromatography (HILIC) in positive (pos) and negative (neg) ionization mode. A = rat urine pos, B = rat urine neg, C = human urine pos, D = human urine neg. ns not significant; *$p < 0.05$; **$p < 0.01$; ***$p < 0.001$; ****$p < 0.0001$.

Fig. 2. Histogram of the total feature count extracted for each preparation and their respective reproducibility evaluated by CV (coefficient of variation) in rat urine (A) and human urine (B) using hydrophilic interaction chromatography (HILIC) in positive (pos) and negative (neg) ionization mode. Black or gray filled area indicates the number of features with a CV <20%.

Fig. 3. Heat map of the mean peak areas of internal standards (log 10 transformed) for each preparation in rat urine (A) and human urine (B) using hydrophilic interaction chromatography (HILIC) in positive or negative ionization mode depending on internal standard.

Figure 1

Click here to access/download;Figure;FIgure_1.jpg

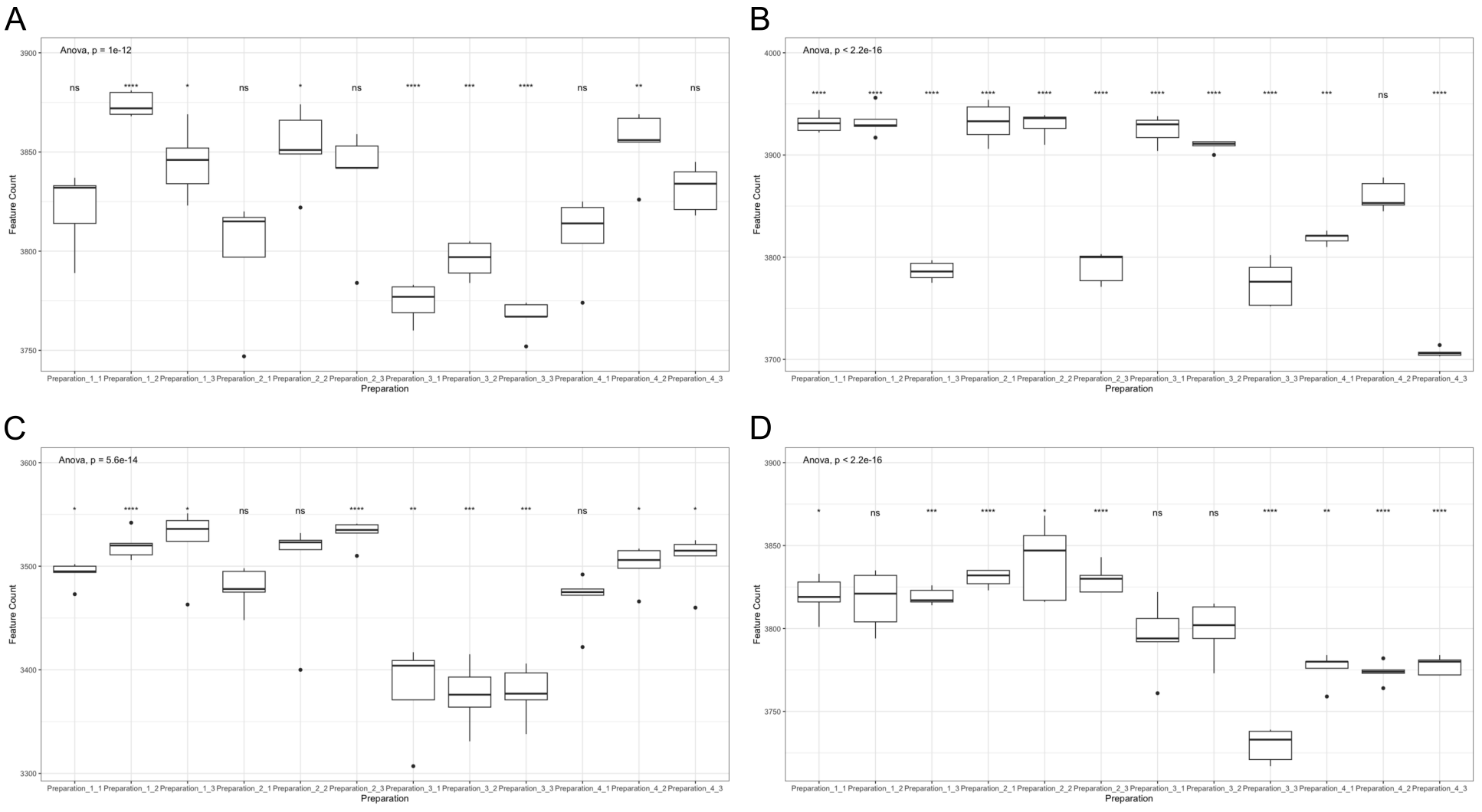

Figure 2

Click here to access/download;Figure;Figure_2.jpg

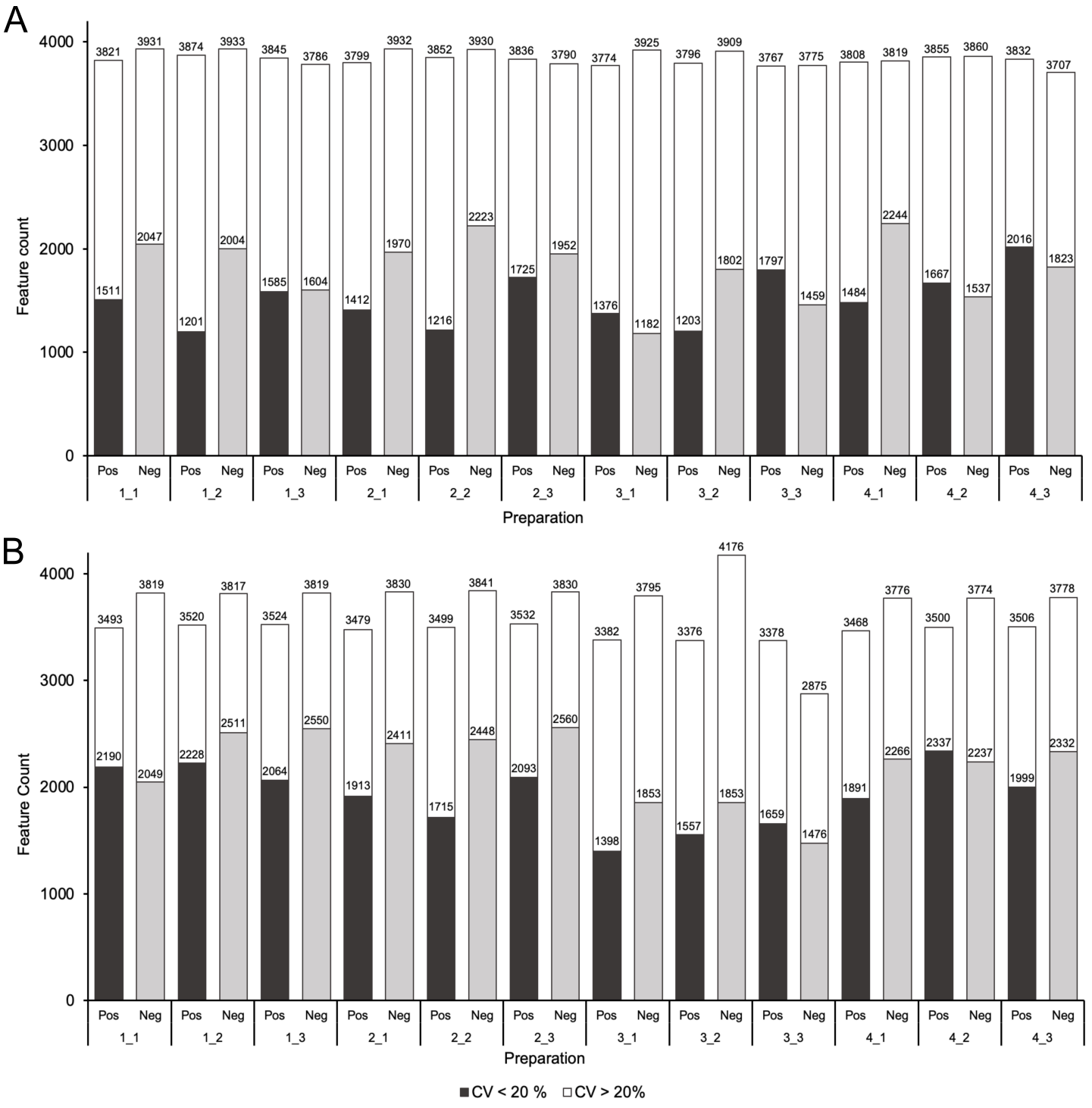

Figure 3

Click here to access/download;Figure;Figure 3.jpg

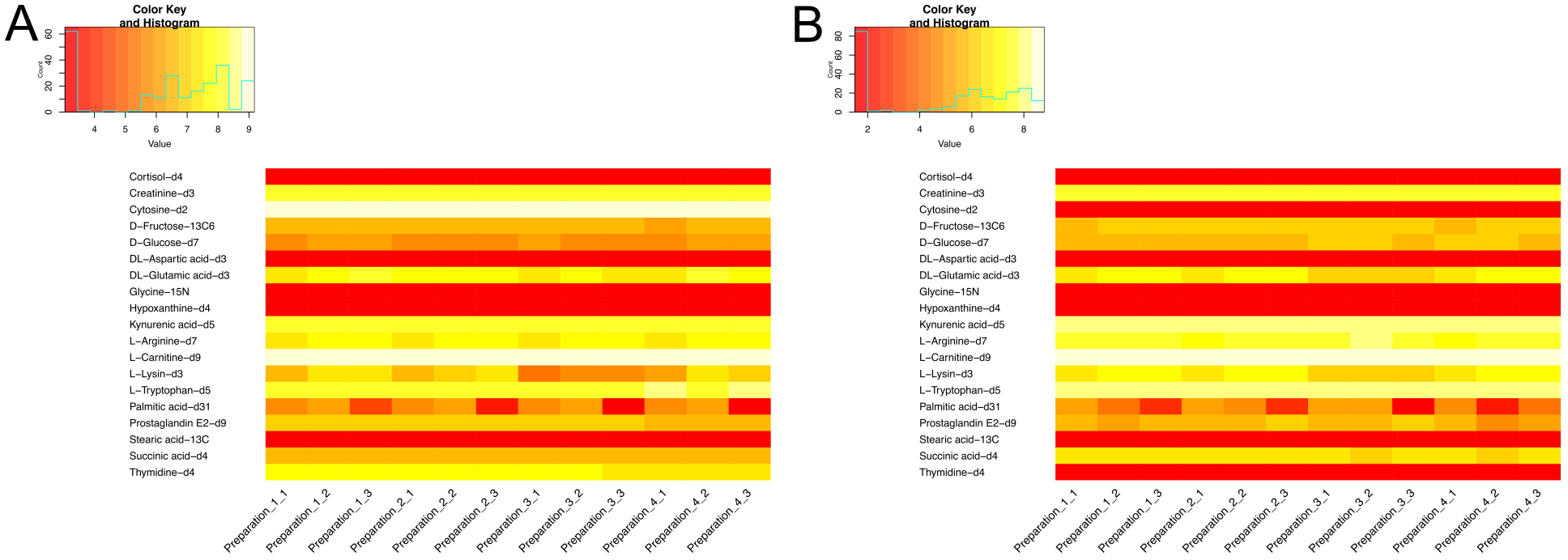

Supporting Information

Optimization of extraction and reconstitution solvents for the untargeted metabolomics analysis of human and rat urine samples

Selina Hemmer, Sascha K. Manier, Lea Wagmann, Markus R. Meyer*

Department of Experimental and Clinical Toxicology, Institute of Experimental and Clinical Pharmacology and Toxicology, Center for Molecular Signaling (PZMS), Saarland University, Homburg, Germany

Corresponding author

*Markus R. Meyer, email: markus.meyer@uks.eu

Experimental section

Preparation of extraction and reconstitution solvents

Each extraction and reconstitution solvent was spiked with a total for 19 different internal standards of various isotope labeled endogenous compounds. Therefore, two different standard solutions representing the analytes' physiological concentrations according to human metabolome database (HMDB) [1] were spiked (Table S1).

Table S1. Overview of the used isotope labeled endogenous compounds, their corresponding urine concentrations from human metabolome database (HMDB) [1], and the finally used concentration in the respective solvents.

Solvent	Compound	Urine concentration according to HMDB, µM/mmol creatinine	Concentration in corresponding solvent, µM/mmol creatinine
Extraction solvent	D-Fructose-$^{13}C_6$	129	26.9
	DL-Glutamic acid-d_3	0.3-218	166.6
	Hypoxanthine-d_4	2.3-25	35.7
	Kynurenic acid-d_5	0.8-4.2	2.6
	L-Carnitine-d_9	0.62-15.2	7.4
	L-Lysin-d_3	1.7-75	6.5
	L-Tryptophan-d_5	2.04-29.4	23.9
	Palmitic acid-d_{31}	2.6-24.3	17.4
	Prostaglandin E_2-d_9	0.000057-0.02	0.3
	Succinic acid-d_4	0.3-33.3	8.2
Reconstitution solvent	Cortisol-d_4	0.012-0.021	0.03
	Creatinine-d_3	500-35000	8.6
	Cytosine-d_2	1.1-10.7	2.2
	D-Glucose-d_7	10.3-111.7	53.5
	DL-Aspartic acid-d_3	0.4-27	7.4
	Glycine-N^{15}	24-600	65.8
	L-Arginine-d_7	0.2-23	5.5
	Stearic acid-^{13}C	0.1-7.7	3.5
	Thymidine-d_4	0.7-11	4.1

LC-HRMS/MS apparatus

Analyses were performed using a Thermo Fisher Scientific (TF, Dreieich, Germany) Dionex UltiMate 3000 RS pump consisting of a degasser, a quaternary pump, and an UltiMate Atosampler, coupled with a TF Q Exactive Plus equipped with a heated electrospray ionization (HESI)-II source [2-4]. Performance of the columns and the mass spectrometer was tested using a test mixture described by Maurer et al. [5]. Gradient reversed-phase (RP) elution was performed on a Waters (Eschborn, Germany) ACQUITY UPLC BEH C_{18} column (100 mm x 2.1 mm, 1.7 µm) and gradient hydrophilic interaction chromatography (HILIC) elution using a Merck (Darmstadt, Germany) SeQuant ZIC HILIC (150 mm x 2.1 mm, 3.0 µm). The mobile phase for the RP chromatography consisted of 10 mM aqueous ammonium acetate containing acetonitrile (1%, *v/v*) and formic acid (0.1%, *v/v*, pH 3, eluent A) and acetonitrile containing formic acid (0.1%, *v/v*, eluent B). The flow rate was set from 0 to 10 min to 500 µL/min and from 10 to 13.5 to 800 µL/min using the following gradient: 0-1 min hold 99% A, 1-10 min to 1% A, 10-11.5 min hold 1% A, and 11.5-13.5 min hold 99% A. The gradient elution for HILIC was performed using aqueous ammonium acetate (200 mM, eluent C) and acetonitrile containing formic acid (0.1%, *v/v*, eluent D). The flow rate was set to 500 µL/min using the following gradient: 0-1 min hold 2% C, 1-5 min to 20% C, 5-8.5 min to 60% C, 8.5-10 min hold 60% C, and 10-12 min hold 2% C. Injection volume was set to 1 µL for all samples. For preparation and cleaning of the injection system, isopropanol:water (90:10, *v/v*) was used. The following settings were used: wash volume, 100 µL; wash speed, 4000 nL/s; loop wash factor, 2. Column temperature for every analysis was set to 40°C, maintained by a Dionex UltiMate 3000 RS analytical column heater. HESI-II source conditions were as follows: ionization mode, positive or negative; sheath gas, 60 AU; auxiliary gas, 10 AU; sweep gas, 3 AU; spray voltage, 3.5 kV in positive and -4.0 kV in negative mode; heater temperature 320°C; ion transfer capillary temperature, 320°C; and S-lens RF level, 50.0. Mass spectrometry for untargeted metabolomics was performed according to a previously optimized workflow [2, 6]. The settings for full scan (FS) data acquisition were as follows: resolution 140,000 at *m/z* 200; microscan, 1; automatic gain control (AGC) target, 5e5; maximum injection time, 200 ms; scan range, *m/z* 50–750; spectrum data type; centroid. All samples were analyzed in randomized order, to avoid potential analyte instability or instrument performance to confound data interpretation. Additionally, one QC injection was performed every ten samples to monitor batch

effects, as described by Wehrens et al. [7]. TF Xcalibur software version 3.0.63 was used for data handling.

Table S2. Overview of the peak picking and alignment parameters used for preprocessing for the respective species. HILIC = hydrophilic interaction chromatography, RP = reversed-phase chromatography, pos = positive, neg = negative, ppm = allowed ppm deviation of mass traces for peak picking, snthresh = signal to noise threshold, mzdiff = minimum difference in m/z for two peaks to be considered as separate, prefilter 1 = minimum of scan points, prefilter 2 = minimum abundance, bw = bandwidth for grouping of peaks across separate chromatograms.

Species	Column	Polarity	Peakwidth, min	Peakwidth, max	ppm	sntresh	mzdiff	Prefilter 1	Prefilter 2	bw
Rat	RP	pos	8.9	19	2.3	55	0.098	5	100	0.4
		neg	8.9	15	2.5	83	0.098	10	100	1.0
	HILIC	pos	8.9	85	2.5	15	0.074	14	100	1.0
		neg	8.9	100	2.5	11	0.1	11	100	1.0
Human	RP	pos	7.8	15	2.5	75	0.034	5	100	1.0
		neg	8.9	15	2.5	50	0.1	6	100	1.0
	HILIC	pos	8.9	31	2.5	19	0.098	9	100	1.0
		neg	8.9	37	2.5	14	0.054	9	100	1.0

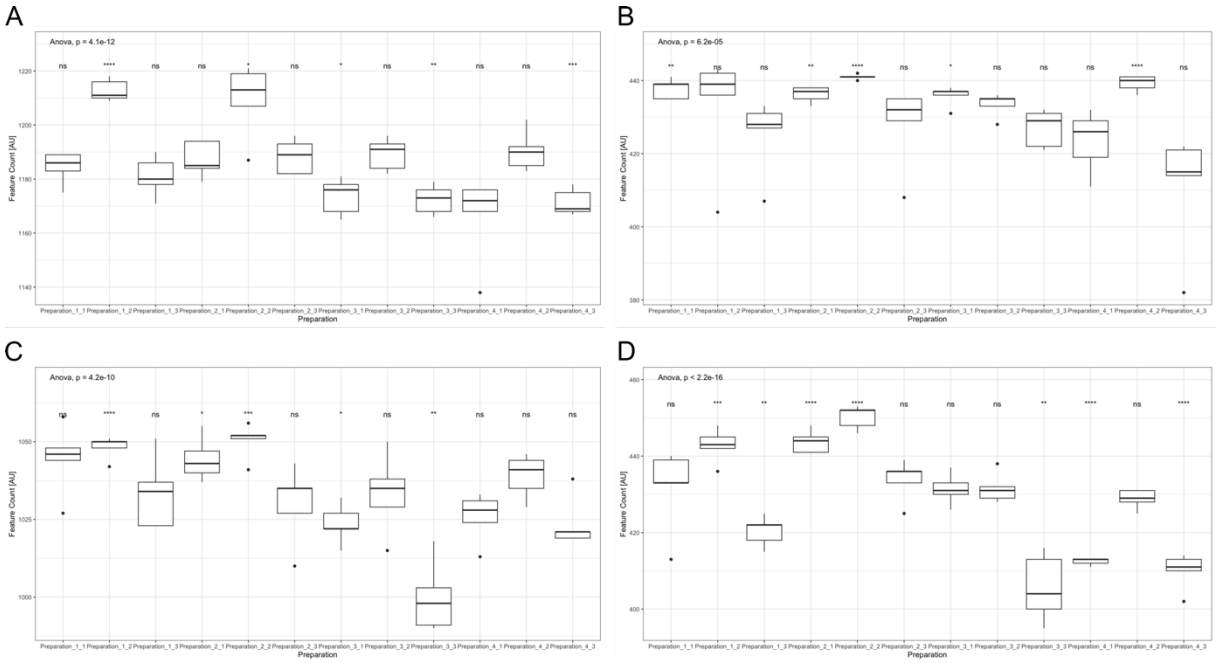

Figure S1. Results of statistical evaluation using one-way ANOVA and Welch's two sample *t*-test comparing total feature count of each group in rat and human urine samples. Analysis was done using reversed-phase (RP) chromatography in positive (pos) and negative (neg) ionization mode. A = rat urine pos, B = rat urine neg, C = human urine pos, D = human urine neg. *ns* not significant; * $p < 0.05$; ** $p < 0.01$; *** $p < 0.001$; **** $p < 0.0001$.

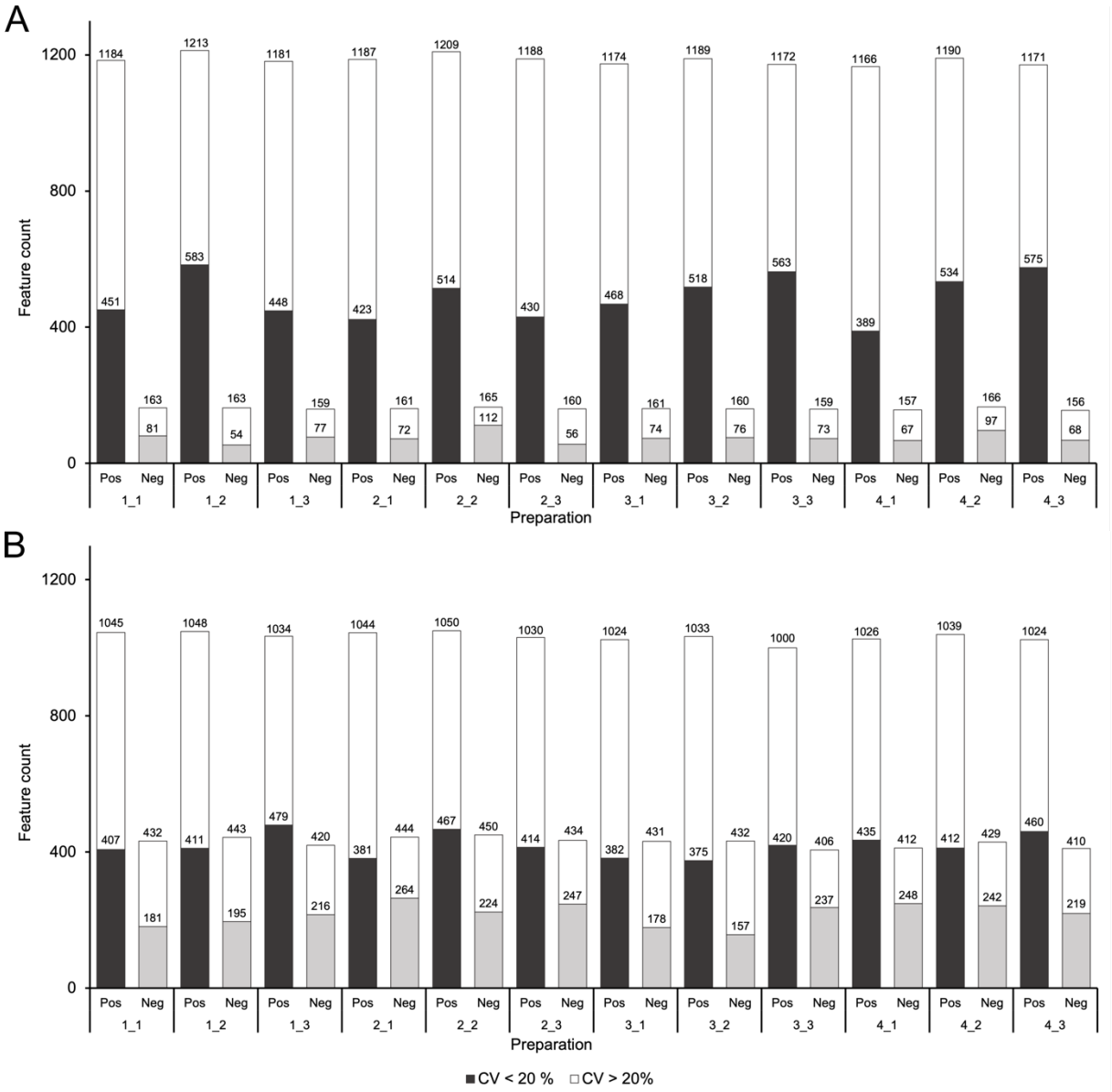

Figure S2. Histogram of the total feature count extracted for each preparation and their respective reproducibility evaluated by CV (coefficient of variation) in rat urine (A) and human urine (B) using reversed-phase (RP) chromatography in positive (pos) and negative (neg) ionization mode. Black or gray filled area indicates the number of features with a CV <20%

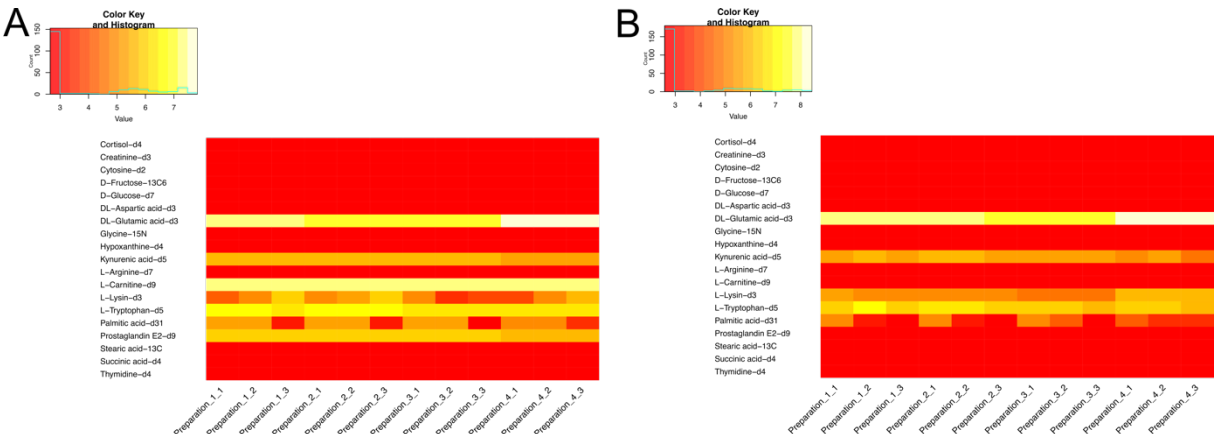

Figure S3. Heat map of the mean peak areas of internal standards (log 10 transformed) for each preparation in rat urine (A) and human urine (B) using reversed-phase (RP) chromatography in positive or negative ionization mode depending on internal standard.

References

[1] D.S. Wishart, A. Guo, E. Oler, F. Wang, A. Anjum, H. Peters, R. Dizon, Z. Sayeeda, S. Tian, B.L. Lee, M. Berjanskii, R. Mah, M. Yamamoto, J. Jovel, C. Torres-Calzada, M. Hiebert-Giesbrecht, V.W. Lui, D. Varshavi, D. Varshavi, D. Allen, D. Arndt, N. Khetarpal, A. Sivakumaran, K. Harford, S. Sanford, K. Yee, X. Cao, Z. Budinski, J. Liigand, L. Zhang, J. Zheng, R. Mandal, N. Karu, M. Dambrova, H.B. Schioth, R. Greiner, V. Gautam, HMDB 5.0: the Human Metabolome Database for 2022, Nucleic Acids Res. 50(D1) (2022) D622-D631. https://doi.org/10.1093/nar/gkab1062.

[2] S.K. Manier, A. Keller, J. Schaper, M.R. Meyer, Untargeted metabolomics by high resolution mass spectrometry coupled to normal and reversed phase liquid chromatography as a tool to study the in vitro biotransformation of new psychoactive substances, Sci. Rep. 9(1) (2019) 2741. https://doi.org/10.1038/s41598-019-39235-w.

[3] S. Hemmer, S.K. Manier, S. Fischmann, F. Westphal, L. Wagmann, M.R. Meyer, Comparison of Three Untargeted Data Processing Workflows for Evaluating LC-HRMS Metabolomics Data, Metabolites 10(9) (2020). https://doi.org/10.3390/metabo10090378.

[4] S. Hemmer, L. Wagmann, M.R. Meyer, Altered metabolic pathways elucidated via untargeted in vivo toxicometabolomics in rat urine and plasma samples collected after controlled application of a human equivalent amphetamine dose, Arch. Toxicol. 95(10) (2021) 3223-3234. https://doi.org/10.1007/s00204-021-03135-8.

[5] H.H. Maurer, M.R. Meyer, A.G. Helfer, A.A. Weber, Maurer/Meyer/Helfer/Weber MMHW LC-HR-MS/MS library of drugs, poisons, and their metabolites, Wiley-VCH, Weinheim, Germany, 2018.

[6] S.K. Manier, A. Keller, M.R. Meyer, Automated optimization of XCMS parameters for improved peak picking of liquid chromatography-mass spectrometry data using the coefficient of variation and parameter sweeping for untargeted metabolomics, Drug Test Anal 11(6) (2019) 752-761. https://doi.org/10.1002/dta.2552.

[7] R. Wehrens, J.A. Hageman, F. van Eeuwijk, R. Kooke, P.J. Flood, E. Wijnker, J.J. Keurentjes, A. Lommen, H.D. van Eekelen, R.D. Hall, R. Mumm, R.C. de Vos, Improved batch correction in untargeted MS-based metabolomics, Metabolomics 12 (2016) 88. https://doi.org/10.1007/s11306-016-1015-8.

3.2. Comparison of Reversed-phase, Hydrophilic Interaction, and Porous Graphitic Carbon Chromatography Columns for an Untargeted Toxicometabolomics Study in Pooled Human Liver Microsomes, Rat Urine, and Rat Plasma

This is a pre-copyedited, author-produced version of an article submitted in the journal Metabolomics (submission ID: 40c91f6e-eb76-469f-b9db-11d2cf901f33).

(Submitted 10/2023, DOI not yet provided)

Author Contributions:

Selina Hemmer conducted and evaluated the experiments as well as composed the manuscript; Sascha K. Manier, Lea Wagmann, and Markus R. Meyer assisted with the design of the experiments, the interpretation of the analytical experiments, and scientific discussions.

Comparison of reversed-phase, hydrophilic interaction, and porous graphitic carbon chromatography columns for an untargeted toxicometabolomics study in pooled human liver microsomes, rat urine, and rat plasma

Selina Hemmer, Sascha K. Manier, Lea Wagmann, Markus R. Meyer*

Department of Experimental and Clinical Toxicology, Institute of Experimental and Clinical Pharmacology and Toxicology, Center for Molecular Signaling (PZMS), Saarland University, Homburg, Germany

Corresponding author

*Markus R. Meyer, email: markus.meyer@uks.eu

ABSTRACT:

Introduction Untargeted metabolomics studies are expected to cover a wide range of compound classes with high chemical diversity and complexity. Thus, optimizing (pre-)analytical parameters such as the analytical liquid chromatography (LC) column is crucial. The selection of the column depends amongst others on the investigated biological matrix, the sample preparation, and the study purpose.

Objectives The current investigation aimed to compare six different analytical columns. First, by comparing the chromatographic resolution of selected compounds. Second, on the outcome of an untargeted toxicometabolomics study using pooled human liver microsomes, rat plasma, and rat urine as matrices.

Methods Separation and analysis was performed using three different reversed-phase (Phenyl-Hexyl, BEH C_{18} and Gold C_{18}), two hydrophilic interaction chromatography (HILIC) (ammonium-sulfonic acid and sulfobetaine), and one porous graphitic carbon (PGC) columns coupled to high-resolution mass spectrometry (HRMS). Their impact was evaluated based on the performance of the columns and the size of feature count, amongst others.

Results All three RP columns showed a similar performance, whereas the PGC column was superior compared to both HILIC columns at least for polar compounds. Comparing the size of feature count across all datasets, most features were detected using the Phenyl-Hexyl or sulfobetaine column.

Conclusion The results underlined that the outcome of this untargeted toxicometabolomic study LC-HRMS metabolomic study was highly influenced by the analytical column, with the Phenyl-Hexyl or sulfobetaine column being the most suitable. However, the column selection may also depend on the investigated compounds as well as on the investigated matrix.

Keywords:

untargeted metabolomics, LC-HRMS, reversed-phase columns, hydrophilic interaction chromatography columns, quality assurance

1. Introduction

Metabolomics studies can in general be divided into untargeted and targeted approaches. Whereas targeted metabolomics aims to detect and quantify specific metabolites of known structures and pathways, untargeted metabolomic studies, as a global approach, aim to detect as many metabolites as possible (Agin *et al.*, 2016; Barnes *et al.*, 2016a). Due to several advantages, liquid chromatography (LC) and mass spectrometry (MS) are meanwhile the major techniques used in metabolomics (Naz *et al.*, 2014; Yao *et al.*, 2019). The impact of LC is mainly influenced by the used stationary phase amongst others (Harrieder *et al.*, 2022; Liu and Locasale, 2017). While normal- or hydrophilic interaction-phase chromatography (HILIC) columns are often used for retention of polar molecules such as amino acids or sugars, reversed-phase (RP) columns are used for non to mid polar molecules such as fatty acids or lipids. Thus, a broad range of compounds can be covered by using both types. However, as several stationary HILIC and RP phases are available, their choice is crucial, which was already discussed extensively elsewhere (Diamantidou *et al.*, 2023; Elmsjo *et al.*, 2018; Si-Hung *et al.*, 2017; Sonnenberg *et al.*, 2019; Wernisch and Pennathur, 2016). Not only the different stationary phases but also the geometry and particle size of columns can affect the outcome of metabolomic studies.

Most of the published studies on analytical column comparison are within the field of targeted metabolomics, investigated metabolite libraries with and without matrix, or developed a scoring approach for the comparison of different column types. To date, there are only a few studies available that did a column comparison within the field of untargeted metabolomics. One main issue in untargeted analysis are the heterogenous physicochemical properties of analytes, which are often even unknown beforehand. Thus, a more universal separation (and detection) system should be used (Harrieder *et al.*, 2022; van de Velde *et al.*, 2020). Multiple chromatographic methods are often used to enable a broad analyte coverage (Barnes *et al.*, 2016a; Harrieder *et al.*, 2022). Additionally, in order to ensure correct interpretation of differences in specific metabolites and for appropriate biological interpretation, a reliable and suitable overall approach is required (Naz *et al.*, 2014).

Therefore, the aim of this study was to compare of six different stationary phases, three reversed-phase, two hydrophilic interaction, and one porous graphitic carbon phase. First, by comparing the chromatographic resolution of selected compounds. Second, their impact the outcome of an untargeted toxicometabolomics study (Hemmer *et al.*,

2022). The (toxico-)metabolome of three different biological matrices should be investigated after exposure to the model compound PCYP. Analytical columns were evaluated based on their performance (chromatographic resolution of analytes) the number and quality of detected features after HRMS analysis. Finally, the study should show, which combination of columns may be suitable for which matrix in future studies.

2. Experimental section

2.1. Sample preparation and analysis of selected compounds

Various mixtures consisting of different compound classes such as amino acids, biogenic amines, carboxylic acids, fatty acids, sugars, and others were analyzed at a concentration level of 50 µg/mL using the six columns Phenyl-Hexyl, Gold C_{18} (Gold), BEH C_{18} (BEH), ammonium-sulfonic acid (Nucleodur), sulfobetaine (ZicHILIC), and porous graphitic carbon particle (PGC) (Table S1). Further information on sample preparation of the neat standard mixtures can be found in the *Supplementary Information*.

2.2. Sample handling of datasets.

Study design, sample collection, sample preparation for pHLM, rat blood plasma, and rat urine were as described by Hemmer et al. (Hemmer *et al.*, 2022). pHLM incubations were performed using a final PCYP concentration of 0 (blank group) or 50 µM (PCYP group) and pHLM. For each group, 5 replicates were prepared. Urine and plasma samples were collected from five control and five rats having PCYP administered. For each matrix and rat, three replicates were prepared and the corresponding 50 µL of them were added together, resulting in 150 µL per rat. Pooled quality control samples (QC group) were prepared for each matrix by transferring 50 µL of each sample into one MS vial. QC samples were used for optimization of peak-picking parameters, evaluating of column performance, and identification of significant features, as described in *Experimental Section* of *Supplementary Information.* QC samples, each sample of control rats and PCYP rats, were aliquoted into six separate MS vials and stored until use at -80 °C. For each run with each column, one of the corresponding vials was retrieved from the freezer and measured. Thus, the same conditions were given for all columns.

2.3. LC-HRMS apparatus

Analyses were performed using a Thermo Fisher Scientific (TF, Dreieich, Germany) Dionex UltiMate 3000 RS pump consisting of a degasser, a quaternary pump, and an UlitMate Autosampler, coupled to a TF Q Exactive Plus equipped with a heated electrospray ionization (HESI)-II source according to previous published studies (Hemmer *et al.*, 2022; Manier *et al.*, 2019a; Manier *et al.*, 2019b). Performance of the columns and the mass spectrometer was tested before each batch using a test mixture described in the *Experimental Section* in the *Supplementary Information*. The used columns and their corresponding flow rates, gradients, and mobile phases are shown in Table 1. More details about LC-HRMS analysis can be found in the *Supplementary Information*.

2.4. Data processing and statistical analysis

Data processing for untargeted metabolomics was performed in a R environment according to previously published workflows (Hemmer *et al.*, 2021; Manier *et al.*, 2019a). Details can be found in the *Supplementary Information*, the R scripts on GitHub (https://github.com/sehem/Columns_Metabolomics) and the mzXML files are available via Metabolights (study identifier MTBLS5082). The total feature count was used to evaluate the number of features detected by each analysis. Therefore, all adducts, artifacts, and isotopes annotated by CAMERA were removed (Kuhl *et al.*, 2012). Subsequently, the QCs of each analysis were considered, since all features present in QCs should also be present in experimental groups. For the reproducibility of the features, the coefficient of variation (CV) was determined from the peak areas of the QCs. Significant changes of features between control and PCYP respectively blank and PCYP group were assumed after Welch's two-sample *t*-test and Bonferroni correction for pHLM (Broadhurst and Kell, 2006), p-value < 0.01 for urine, and p-value < 0.05 for plasma. Principal component analysis (PCA) and hierarchal clustering were used to investigate patterns in the datasets. For pHLM, *t*-distributed stochastic neighborhood embedding (*t*-SNE) (van der Maaten, 2014; van der Maaten and Hinton, 2008) were used in addition to PCA. Names for features were adopted from XCMS using "M" followed by rounded mass and "T" followed by the retention time in seconds. After visual inspection of the extracted ion chromatograms (EIC) of significant features, based on the peak shape quality, the significant features were divided into true and false features (Hemmer *et al.*, 2020).

Table 1. Overview of the used columns and their corresponding flow rates, gradients, and mobile phases.

Column	**Phenyl-Hexyl**	**Gold**	**BEH**	**Nucleodur**	**ZicHILIC**	**PGC**
Chemistry	Phenyl/hexyl	C_{18}	C_{18}	Ammonium-sulfonic acid	Sulfobetaine	Porous graphitic carbon particle
Phase	Spherical, solid core, ultrapure silica	Spherical, fully porous, ultrapure silica	Ethylene bridged hybrid (BEH) particle technology	Fully porous particles	Fully porous particles	
Specification	Thermo Fisher Accucore Phenyl-Hexyl column	Thermo Fisher Hypersil Gold C_{18} column	Waters ACQUITY UPLC BEH C_{18} column	Macherey-Nagel HILIC Nucleodur column	Merck SeQuant ZIC HILIC	Merck PGC Supel™ Carbon LC
Dimensions	100 mm x 2.1 mm, 2.6 µm	100 mm x 2.1 mm, 1.9 µm	100 mm x 2.1 mm, 1.7 µm	125 mm x 3 mm, 3 µm	150 mm x 2.1 mm, 3 µm	150 mm x 2.1 mm, 2.7 µm
Flow rate	500 µL/min (1-10 min); 800 µL/min (10-13.5 min)			500 µL/min		
Gradient	0-1min 99 % A, 1-10 min to 1 % A, 10-11.5 min hold 1 % A, 11.5-13.5 min hold 99 % A			0-1 min 2 % A, 1-5 min to 20 % A, 5-8.5 min to 60 % A, 8.5-10 min hold 60 % A, 10-12 min hold 2 % A		0-1min 99 % A, 1-10 min to 1 % A, 10-11.5 min hold 1 % A, 11.5-13.5 min hold 99 % A
Mobile phase	Eluent A: aqueous ammonium formate (2 mM), acetonitrile (1 %, *v/v*) and formic acid (0.1 %, *v/v*, pH 3) Eluent B: ammonium formate solution (2 mM) in acetonitrile:methanol (1:1, *v/v*), water (1 %, *v/v*), and formic acid (0.1 %, *v/v*)	Eluent A: 10 mM aqueous ammonium acetate containing acetonitrile (1 %, *v/v*) and formic acid (0.1 %, *v/v*, pH 3) Eluent B: acetonitrile containing formic acid (0.1 %, *v/v*)		Eluent A: aqueous ammonium acetate (200 mM) Eluent B: acetonitrile containing formic acid (0.1 %, *v/v*).		Eluent A: water containing difluoroacetic acid (0.1 %, *v/v*) Eluent B: acetonitrile containing difluoroacetic acid (0.1 %, *v/v*).

3. Results and discussion

An overview of the workflow used in this study is given in Figure 1. Since the aim of this study was to evaluate the influence of different analytical LC columns on the resolution of selected endogenous compounds and the results of untargeted metabolomics analyses, only columns were changed and other parameters remained unchanged. However, eluents and gradients had to be adopted and were selected according to the column types and as used in other studies (Hemmer *et al.*, 2022; Manier *et al.*, 2019b; Merck, 2019, 2020; Michely and Maurer, 2018). In addition, the choice of mobile phases was evaluated by the detectability of different compound classes using a system suitability test mixture described in the *Experimental Section* of the *Supplementary Information*. Sample preparations and all other LC-HRMS parameters such as column oven temperature, and MS settings were identical for all columns according to previously published studies (Hemmer *et al.*, 2022; Manier *et al.*, 2019b).

The Phenyl-Hexyl and Nucleodur columns were already used in previous studies and therefore used as reference for RP and HILIC analyses, respectively (Hemmer *et al.*, 2020; Hemmer *et al.*, 2021; Manier *et al.*, 2019b; Manier and Meyer, 2020; Manier *et al.*, 2020a; Manier *et al.*, 2020b). However, since C_{18} columns are the most common RP columns (Harrieder *et al.*, 2022), two differently linked C_{18} stationary phases were chosen over C_4 or C_8 phases. Criscuolo et al. showed that not all C_{18} columns are efficient for lipid separation and not only the chemistry of the stationary phase, but also the different types of particles or their sizes must be considered (Criscuolo *et al.*, 2019). The Gold column, using spherical fully porous particles, was often used for screening and metabolomics methods (Imbert *et al.*, 2021; Liu *et al.*, 2021; Thevenot *et al.*, 2015). The last of the selected RP columns, the BEH, consisted of a C_{18} modification with ethylene bridged hybrid (BEH) particles. It is expected to be a universal column with a wide pH range and was also used in other metabolomics studies previously (Gika *et al.*, 2008; Tobin *et al.*, 2021; Zhao *et al.*, 2018).

Concerning HILIC, different stationary phase chemistries such as aminopropyl silane, alkyl amide, silica, or sulfobetaine groups are available. Amide or amino columns are one of the most frequently used HILIC columns. However, since these columns showed a reduced lifetime at elevated pH values, they were not included in this study (Harrieder *et al.*, 2022). Instead, a sulfobetaine (ZicHILIC) column was selected, since it was often used in other metabolomics studies and showed suitable separation by its

zwitterionic stationary phase (Abdalkader *et al.*, 2021; K Trivedi *et al.*, 2012; Steuer *et al.*, 2020). The in-house HILIC reference column, an ammonium-sulfonic acid (Nucleodur), has also a zwitterionic functional group.

According to the manufacturer, the porous graphitic carbon (PGC) column offers high column efficiency for polar compounds and improved retention of compounds normally only be retained with HILIC (Merck, 2019). PGC is also expected to show high robustness regarding the eluents, pH range, and pressure. Therefore, the PGC column was grouped together with the two HILIC columns but in contrast, PGC should demonstrate elevated stability with respect to pH value and allow retention of polar molecules without HILIC conditions (Bapiro *et al.*, 2016; Hanai, 2003; Knox *et al.*, 2006; Pereira, 2010). The performance of each column was tested before each run using the system suitability test mixture. In addition, the columns were equilibrated before each analysis as described in their care and use instructions.

Besides selected endogenous compounds such as amino acids, fatty acids, and sugars, three different datasets were generated and investigated by analyzing the following matrices. 1) pHLM incubations, a well-characterized in vitro model, which is commonly used in drug metabolism studies, since its ease of use and low variability (Asha and Vidyavathi, 2010; Richter *et al.*, 2017). 2) Rat urine, a matrix to reflect the complexity of an *in vivo* model and which is rich in hydrophilic substances (Khamis *et al.*, 2017; Wagmann *et al.*, 2022). 3) Rat plasma, as a more complex matrix covering a broad spectrum of endogenous compound classes compared to urine.

3.1. Resolution of selected endogenous compounds

Artificial mixtures of 34 compounds from classes such as amino acids, fatty acids, and sugars, were investigated to conclude, which column might be most suitable for which compound class. The individual compounds and analytical results are shown in Table S1. The Phenyl-Hexyl and BEH columns exhibited quite similar behavior in terms of compound retention and retention time. In contrast, analytes eluted later by using the Gold column. With regard to mid- and non-polar substances, both arachidic acid and vitamin D_2 were sufficiently retained using the Gold column in comparison to the Phenyl-Hexyl column. Regarding the HILIC columns, amino acids, carboxylic acids, and sugars could be sufficiently separated using both Nucleodur and ZicHILIC. Compared to the Nucleodur column, more amino acids and the carboxylic acids citrate and succinate were separated using the ZicHILIC column. With respect to biogenic

amines, noradrenalin could not be retained by using any HILIC column. The PGC column was the only one of the six columns capable to retain the amino acid threonine. With respect to mid- and non-polar compounds, the PGC column was able to separate fewer substances than the two HILIC columns.

In summary, separation and retention of polar substances such as amino acids, carboxylic acids, biogenic amines, and sugars, ZicHILIC showed the best performance amongst all six columns, followed by Nucleodur. PGC was only able to separate and retain amino acids used in this study. Concerning the mid- and non-polar compounds, most of them were separated using the Gold column followed by the BEH and Phenyl-Hexyl columns. Compared to the Phenyl-Hexyl column, the used C_{18} columns are more suitable for separation of long-chain fatty acids, since Phenyl-Hexyl columns are mainly designed to retain aromatic hydrocarbons.

3.2. Column performance

The performance of each column in terms of separation and chromatographic sensitivity (signal to noise ratio) was evaluated based on the peak-picking parameters obtained using QC samples (Table S2). Chromatographic peak width is important since narrow chromatographic peaks usually improve chromatographic sensitivity but in turn may reduce detection probability in slow mass analyzers. Broader peak shape usually leads to lower peak height (lower chromatographic sensitivity) and thus lower probability for being e.g., selected for fragmentation in data dependent approaches (Criscuolo *et al.*, 2019). To evaluate the performance of each column, the minimum peak width was used to calculate peak capacity. Peak capacity is defined as the maximum number of peaks that can be chromatographically separated with a unit resolution within a retention time window using gradient elution and is directly proportional to the average peak resolution (Gilar *et al.*, 2004; Wang *et al.*, 2006). For this purpose, Equation 1 was used to obtain the peak capacity *Pc* from the elution time t_g and the average peak width at baseline *W* (Neue, 2005).

$$\boldsymbol{Pc = 1 + \frac{t_g}{W}} \qquad \textbf{(1)}$$

Overall, the highest peak capacity for all three matrices was found after using PGC (Table S2). Compared to the HILIC columns, only slightly differences were observed between the three RP columns.

The sensitivity of a system relates to the detector signal and the ability of peak to be chosen for MS/MS (Criscuolo *et al.*, 2019). For evaluation of the sensitivity of each column, signal-to-noise threshold (snthresh) was used, which is defined as the ratio between the peak height from analytes to the peak height of background noise (Coleman *et al.*, 2001). The highest snthresh ratio overall was shown using Gold and PGC column after analyzing rat urine and plasma (Table S2). For analyzing pHLM, Nucleodur showed the highest snthresh, whereas no differences were observed after using RP columns.

In addition to peak capacity and snthresh, the total ion chromatograms (TIC) were visually evaluated. The TIC is described as the sum of all separated ion currents carried by the ions of different *m/z* contributing to a complete mass spectrum or in a specific *m/z* range of a mass spectrum (Murray *et al.*, 2013). TICs for each column in both ionization modes after analyzing pHLM, rat urine, and rat plasma are shown in Figure S1-6. Both C_{18} columns showed no obvious difference after visual inspection. The peak shapes improved after approximately 200 seconds, which may indicate that the C_{18} columns required an extended equilibration phase compared to the Phenyl-Hexyl column. For the HILIC columns, the Nucleodur and PGC columns showed a similar behavior. Among the HILIC columns, the ZicHILIC showed the visually best TIC.

3.3. Feature count

Features are chromatographic peaks detected by an algorithm and described by their retention time and their *m/z* (Mahieu *et al.*, 2014). The size of the detected feature count is crucial for a sufficient description of e.g., the metabolome. Therefore, it can be assumed that the more features were detected after peak picking, the better the metabolome of the biosample was analytically described. However, it should be considered that the size of feature count can be influenced by non-matrix dependent parameters such as artifactual interference. These are peaks that originated from contaminants, chemical noise, and bioinformatic noise. In contrast, biologically derived features originated from metabolites of the analyzed biological sample. Therefore, a method that detects the maximum number of features is not always the method that provides the greatest metabolome coverage (Mahieu *et al.*, 2014). In this study, the aim was to identify columns, that provide a sufficient metabolic coverage in term of number of feature count. In addition, the reproducibility of the features was also assessed by CV<10%, to exclude possible artifactual interference. Figure 2 shows the

feature count detected after peak picking (without isotopes and adducts detected by CAMERA) and their respective reproducibility evaluated by CV after analyzing all three matrices by using the six analytical columns and MS positive and negative ionization mode.

The feature count differed widely amongst the columns. The Phenyl-Hexyl and ZicHILIC columns allowed detection of most features across all three datasets. The urine metabolome, currently described by about 3,100 metabolites (Bouatra *et al.*, 2013) seemed to be best covered after analysis using the BEH (1,960 features) and ZicHILIC columns (2,092 features) in positive mode. In contrast, the plasma metabolome was best described by the Phenyl-Hexyl and ZicHILIC columns. Since there are no data available on the number of metabolites in the plasma metabolome, the serum metabolome database was used as reference, which contains 4,651 small molecule metabolites (Psychogios *et al.*, 2011). In comparison to the two other HILIC columns, significantly fewer features were detected in urine and plasma samples using the PGC. Reasons for this might be an inappropriate sample preparation, especially regarding the reconstitution solvent, or other LC parameters that were not further optimized in this study. Same patterns were observed for the reproducibility evaluated by CV <10%. Again, both columns Phenyl-Hexyl and ZicHILIC show the highest number of reproducible features over all three matrices.

However, it should be considered that not all detected features are required to be of biological origin (Mahieu *et al.*, 2014). Since the same samples of a dataset were always used for all six columns in this study, the number of artifactual features in the different analytical methods should be as low as possible and comparable. Contaminations originating from the samples themselves or from the sample processing can be excluded for the most part. However, differences in contamination may have occurred, for example due to the different eluents or stationary phases in the individual methods.

3.4. Univariate and multivariate statistic

Univariate statistics aimed to identify those features that were significantly altered between control and experimental groups (Barnes *et al.*, 2016b). They were done using Welch's two-sample *t*-test. An overview of all detected significant features can be found in Table S3 (sheet 1-3) in the *Supplementary Information*. No significant features were found after analyzing pHLM using MS in negative ionization mode

independent from the used column. In addition, no significant features were found after analyzing rat urine by PGC and MS in negative mode as well as after analyzing rat plasma by the Gold column and MS in negative mode as well as PGC and MS in positive and negative mode.

Nevertheless, the columns were also evaluated according to the peak shape quality of the significant features. Since the EIC of some significant features turned out to be false features, they were divided into true and false features based on the peak shape quality of their EIC according to the criteria used by Hemmer et al. (Hemmer *et al.*, 2020). Therefore, the ratio of false vs true features was calculated (Table S4). Over all three datasets, the Phenyl-Hexyl column and the ZicHILIC showed the lowest ratio followed by Gold and Nucleodur columns.

Besides univariate statistics, the different columns were also evaluated regarding the results of multivariate statistics to identify the largest changing features and specific signatures in the data. Since multivariate statistics can only be performed if there were at least two significant features, no data were available for datasets containing no or only one significant feature. In this study, PCA and hierarchical clustering were used to discover differences between the columns. The figures for the different datasets can be found in the *Supporting Information* (Figure S7-20). It was shown that groups blank vs PCYP and control vs PCYP, were distinct from each other independent from the used column and investigated matrix. Since the results of the variance of the first principal component indicated that the pHLM datasets were highly linear (Figure S7-8), the patterns in pHLM dataset were evaluated using *t*-SNE (van der Maaten and Hinton, 2008). Results of the *t*-SNEs (Figure S13-14) showed similar cluster patterns for all columns. Regarding hierarchical clustering, there was in general a high distance between samples from blank or control group to those from PCYP and QC group (Figure S15-20), again independent from the used columns and investigated matrix. Therefore, it can be assumed that with respect to the multivariate statistics, there should be no significant influence of the used column on its outcome. After separation using PGC, no significant features were found in the plasma data, and thus, no multivariate statistics were performed. One explanation for this might be the different compositions of plasma and urine. While lipids and similar compounds predominate in plasma, more polar substances are present in urine (Bouatra *et al.*, 2013; Psychogios *et al.*, 2011). The PGC column should be much better suited for polar substances, such as those found in urine.

3.5. Summary of column comparison

Table 2 provides a brief summary of the results described above for each column. With respect to the different matrices, the Phenyl-Hexyl column was well suited for all three matrices, concerning both the overall number of features and the reproducibility of them. In addition, the Phenyl-Hexyl column exhibits a low false feature rate compared to C_{18} columns. Compared to the Phenyl-Hexyl column, the two C_{18} columns performed similarly. BEH showed significantly more features in urine compared to both other columns.

Regarding the different matrices, the ZicHILIC column showed the best performance for analysis of urine and pHLM represented by e.g., the lowest false feature rate. Compared to the other two HILIC columns, the lowest number of features were detected after PGC separation. One explanation for this might be, that more analytical parameters need to be optimized for this column, such as eluents, gradient, column oven temperature, amongst others. However, this was not the aim of the study, thus optimizations are still needed for this column. Another explanation might be the composition of the metabolites in the different matrices. Compared to plasma, urine contains more polar compounds, which can be better separated by PGC (Bouatra *et al.*, 2013; Psychogios *et al.*, 2011). Nevertheless, PGC showed better peak capacity and snthresh than the HILIC columns. In terms of compound classes, the PGC column performed well for separation of amino acids. The ZicHILIC and Nucleodur column were equally suitable for the separation of polar substances such as amino acids or sugars.

In summary, even though the chemistry of the stationary phase remains the same, there are significant differences between the investigated columns. Results of this study revealed that the LC columns should be adapted to both the matrix and metabolites being investigated.

3.6. Limitations of the study

The present study provides only a small insight into how different analytical columns can affect the outcome of an untargeted metabolomics study. The study also used only a limited selection from a huge pool of columns and the dimensions of the different columns were not identical. It is known that the column geometry and the particle size can play a crucial role (Criscuolo *et al.*, 2019).

As preliminary experiments had shown that not every eluent was suitable for all columns, eluents could not be kept consistent and had to be slightly adopted. Since the study was primarily based on an untargeted approach, selected endogenous compounds were still used to detect any differences between the columns with respect to different compound classes. Nevertheless, it seems to be necessary to adapt the analytical method to the research question. Does the researcher want to detect as many metabolites as possible or does is the focus on certain compound classes? Does the researcher want to keep the analytical setup the same for all investigated matrices or does the researcher chose the more time-consuming and cost-intensive way and evaluate a suitable analytical method for each matrix?

4. Conclusion

Using LC-(MS), the choice of analytical columns plays a crucial role since the metabolome includes many compound classes with high chemical diversity and complexity. Thus, the influence of different reversed-phase, HILIC, and PGC columns was investigated on the outcome of an untargeted metabolomic study using three different matrices. Evaluation criteria included e.g., peak capacity, size of feature count, and results of multivariate statistics.

The study showed that a combination of BEH and ZicHILIC might be a suitable choice for analysis of urine samples and a combination of Phenyl-Hexyl and ZicHILIC might be suitable for analysis of plasma samples. Over all three datasets, the best results were obtained by using a combination of Phenyl-Hexyl and ZicHILIC. However, concerning the use of Phenyl-Hexyl column for reversed-phase, it should be considered that mainly non-polar metabolites with aromatic hydrocarbon structure can be retained, and that e.g., fatty acids may not retain. Considering the results of this study, it can be concluded that if researchers want to achieve the best possible results, they should test and adapt the analytical method for each matrix and set of investigated substances.

REFERENCES

Abdalkader, R., Chaleckis, R., Meister, I., Zhang, P., Wheelock, C.E. and Kamei, K.I. (2021) Untargeted LC-MS Metabolomics for the Analysis of Micro-scaled Extracellular Metabolites from Hepatocytes. *Anal Sci* **37,** 1049-1052.

Agin, A., Heintz, D., Ruhland, E., Chao de la Barca, J.M., Zumsteg, J., Moal, V., Gauchez, A.S. and Namer, I.J. (2016) Metabolomics – an overview. From basic principles to potential biomarkers (part 1). *Médecine Nucléaire* **40,** 4-10.

Asha, S. and Vidyavathi, M. (2010) Role of human liver microsomes in in vitro metabolism of drugs-a review. *Appl Biochem Biotechnol* **160,** 1699-722.

Bapiro, T.E., Richards, F.M. and Jodrell, D.I. (2016) Understanding the Complexity of Porous Graphitic Carbon (PGC) Chromatography: Modulation of Mobile-Stationary Phase Interactions Overcomes Loss of Retention and Reduces Variability. *Anal Chem* **88,** 6190-4.

Barnes, S., Benton, H.P., Casazza, K., Cooper, S.J., Cui, X., Du, X., Engler, J., Kabarowski, J.H., Li, S., Pathmasiri, W., Prasain, J.K., Renfrow, M.B. and Tiwari, H.K. (2016a) Training in metabolomics research. I. Designing the experiment, collecting and extracting samples and generating metabolomics data. *J Mass Spectrom* **51,** 461-75.

Barnes, S., Benton, H.P., Casazza, K., Cooper, S.J., Cui, X., Du, X., Engler, J., Kabarowski, J.H., Li, S., Pathmasiri, W., Prasain, J.K., Renfrow, M.B. and Tiwari, H.K. (2016b) Training in metabolomics research. II. Processing and statistical analysis of metabolomics data, metabolite identification, pathway analysis, applications of metabolomics and its future. *J Mass Spectrom* **51,** 535-548.

Bouatra, S., Aziat, F., Mandal, R., Guo, A.C., Wilson, M.R., Knox, C., Bjorndahl, T.C., Krishnamurthy, R., Saleem, F., Liu, P., Dame, Z.T., Poelzer, J., Huynh, J., Yallou, F.S., Psychogios, N., Dong, E., Bogumil, R., Roehring, C. and Wishart, D.S. (2013) The human urine metabolome. *PLoS One* **8,** e73076.

Broadhurst, D.I. and Kell, D.B. (2006) Statistical strategies for avoiding false discoveries in metabolomics and related experiments. *Metabolomics* **2,** 171-196.

Coleman, J., Wrzosek, T., Roman, R., Peterson, J. and McAllister, P. (2001) Setting system suitability criteria for detectability in high-performance liquid chromatography methods using signal-to-noise ratio statistical tolerance intervals. *J Chromatogr A* **917,** 23-7.

Criscuolo, A., Zeller, M., Cook, K., Angelidou, G. and Fedorova, M. (2019) Rational selection of reverse phase columns for high throughput LC-MS lipidomics. *Chem Phys Lipids* **221,** 120-127.

Diamantidou, D., Sampsonidis, I., Liapikos, T., Gika, H. and Theodoridis, G. (2023) Liquid chromatography-mass spectrometry metabolite library for metabolomics: Evaluating column suitability using a scoring approach. *J Chromatogr A* **1690,** 463779.

Elmsjo, A., Haglof, J., Engskog, M.K.R., Erngren, I., Nestor, M., Arvidsson, T. and Pettersson, C. (2018) Method selectivity evaluation using the co-feature ratio in LC/MS metabolomics: Comparison of HILIC stationary phase performance for the analysis of plasma, urine and cell extracts. *J Chromatogr A* **1568,** 49-56.

Gika, H.G., Theodoridis, G.A. and Wilson, I.D. (2008) Hydrophilic interaction and reversed-phase ultra-performance liquid chromatography TOF-MS for metabonomic analysis of Zucker rat urine. *J Sep Sci* **31,** 1598-608.

Gilar, M., Daly, A.E., Kele, M., Neue, U.D. and Gebler, J.C. (2004) Implications of column peak capacity on the separation of complex peptide mixtures in single- and two-dimensional high-performance liquid chromatography. *J Chromatogr A* **1061,** 183-92.

Hanai, T. (2003) Separation of polar compounds using carbon columns. *J Chromatogr A* **989,** 183-96.

Harrieder, E.M., Kretschmer, F., Bocker, S. and Witting, M. (2022) Current state-of-the-art of separation methods used in LC-MS based metabolomics and lipidomics. *J Chromatogr B Analyt Technol Biomed Life Sci* **1188,** 123069.

Hemmer, S., Manier, S.K., Fischmann, S., Westphal, F., Wagmann, L. and Meyer, M.R. (2020) Comparison of Three Untargeted Data Processing Workflows for Evaluating LC-HRMS Metabolomics Data. *Metabolites* **10**.

Hemmer, S., Wagmann, L. and Meyer, M.R. (2021) Altered metabolic pathways elucidated via untargeted in vivo toxicometabolomics in rat urine and plasma samples collected after controlled application of a human equivalent amphetamine dose. *Arch Toxicol* **95,** 3223-3234.

Hemmer, S., Wagmann, L., Pulver, B., Westphal, F. and Meyer, M.R. (2022) In Vitro and In Vivo Toxicometabolomics of the Synthetic Cathinone PCYP Studied by Means of LC-HRMS/MS. *Metabolites* **12**.

Imbert, A., Rompais, M., Selloum, M., Castelli, F., Mouton-Barbosa, E., Brandolini-Bunlon, M., Chu-Van, E., Joly, C., Hirschler, A., Roger, P., Burger, T., Leblanc, S., Sorg, T., Ouzia, S., Vandenbrouck, Y., Medigue, C., Junot, C., Ferro, M., Pujos-Guillot, E., de Peredo, A.G., Fenaille, F., Carapito, C., Herault, Y. and Thevenot, E.A. (2021) ProMetIS, deep phenotyping of mouse models by combined proteomics and metabolomics analysis. *Sci Data* **8,** 311.

K Trivedi, D., Jones, H., Shah, A. and K Iles, R. (2012) Development of Zwitterionic Hydrophilic Liquid Chromatography (ZIC®HILIC-MS) Metabolomics Method for Shotgun Analysis of Human Urine. *Journal of Chromatography & Separation Techniques* **03,** 144.

Khamis, M.M., Adamko, D.J. and El-Aneed, A. (2017) Mass spectrometric based approaches in urine metabolomics and biomarker discovery. *Mass Spectrom Rev* **36,** 115-134.

Knox, J.H., Unger, K.K. and Mueller, H. (2006) Prospects for Carbon as Packing Material in High-Performance Liquid Chromatography. *Journal of Liquid Chromatography* **6,** 1-36.

Kuhl, C., Tautenhahn, R., Bottcher, C., Larson, T.R. and Neumann, S. (2012) CAMERA: an integrated strategy for compound spectra extraction and annotation of liquid chromatography/mass spectrometry data sets. *Anal Chem* **84,** 283-9.

Liu, H., Zhu, J., Li, Q., Wang, D., Wan, K., Yuan, Z., Zhang, J., Zou, L., He, X. and Miao, J. (2021) Untargeted metabolomic analysis of urine samples for diagnosis of inherited metabolic disorders. *Funct Integr Genomics* **21,** 645-653.

Liu, X. and Locasale, J.W. (2017) Metabolomics: A Primer. *Trends Biochem Sci* **42,** 274-284.

Mahieu, N.G., Huang, X., Chen, Y.J. and Patti, G.J. (2014) Credentialing features: a platform to benchmark and optimize untargeted metabolomic methods. *Anal Chem* **86,** 9583-9.

Manier, S.K., Keller, A. and Meyer, M.R. (2019a) Automated optimization of XCMS parameters for improved peak picking of liquid chromatography-mass spectrometry data using the coefficient of variation and parameter sweeping for untargeted metabolomics. *Drug Test Anal* **11,** 752-761.

Manier, S.K., Keller, A., Schaper, J. and Meyer, M.R. (2019b) Untargeted metabolomics by high resolution mass spectrometry coupled to normal and reversed phase liquid chromatography as a tool to study the in vitro biotransformation of new psychoactive substances. *Sci Rep* **9,** 2741.

Manier, S.K. and Meyer, M.R. (2020) Impact of the used solvent on the reconstitution efficiency of evaporated biosamples for untargeted metabolomics studies. *Metabolomics* **16,** 34.

Manier, S.K., Schwermer, F., Wagmann, L., Eckstein, N. and Meyer, M.R. (2020a) Liquid Chromatography-High-Resolution Mass Spectrometry-Based In Vitro Toxicometabolomics of the Synthetic Cathinones 4-MPD and 4-MEAP in Pooled Human Liver Microsomes. *Metabolites* **11**.

Manier, S.K., Wagmann, L., Flockerzi, V. and Meyer, M.R. (2020b) Toxicometabolomics of the new psychoactive substances alpha-PBP and alpha-PEP studied in HepaRG cell incubates by means of untargeted metabolomics revealed unexpected amino acid adducts. *Arch Toxicol* **94,** 2047-2059.

Merck (2019) Care & Use Guide for 2.7 µm SupelTM Carbon LC Column.

Merck (2020) Application Note: LC-MS/MS Analysis of 20 Underivatized Amino Acids on Supel Carbon LC column.

Michely, J.A. and Maurer, H.H. (2018) A multi-analyte approach to help in assessing the severity of acute poisonings - Development and validation of a fast LC-MS/MS quantification approach for 45 drugs and their relevant metabolites with one-point calibration. *Drug Test Anal* **10,** 164-176.

Murray, K.K., Boyd, R.K., Eberlin, M.N., Langley, G.J., Li, L. and Naito, Y. (2013) Definitions of terms relating to mass spectrometry (IUPAC Recommendations 2013). *Pure and Applied Chemistry* **85,** 1515-1609.

Naz, S., Vallejo, M., Garcia, A. and Barbas, C. (2014) Method validation strategies involved in non-targeted metabolomics. *J Chromatogr A* **1353,** 99-105.

Neue, U.D. (2005) Theory of peak capacity in gradient elution. *J Chromatogr A* **1079,** 153-61.

Pereira, L. (2010) Porous Graphitic Carbon as a Stationary Phase in HPLC: Theory and Applications. *Journal of Liquid Chromatography & Related Technologies* **31,** 1687-1731.

Psychogios, N., Hau, D.D., Peng, J., Guo, A.C., Mandal, R., Bouatra, S., Sinelnikov, I., Krishnamurthy, R., Eisner, R., Gautam, B., Young, N., Xia, J., Knox, C., Dong, E., Huang, P., Hollander, Z., Pedersen, T.L., Smith, S.R., Bamforth, F., Greiner, R., McManus, B., Newman, J.W., Goodfriend, T. and Wishart, D.S. (2011) The human serum metabolome. *PLoS One* **6,** e16957.

Richter, L.H.J., Flockerzi, V., Maurer, H.H. and Meyer, M.R. (2017) Pooled human liver preparations, HepaRG, or HepG2 cell lines for metabolism studies of new psychoactive substances? A study using MDMA, MDBD, butylone, MDPPP, MDPV, MDPB, 5-MAPB, and 5-API as examples. *J Pharm Biomed Anal* **143,** 32-42.

Si-Hung, L., Causon, T.J. and Hann, S. (2017) Comparison of fully wettable RPLC stationary phases for LC-MS-based cellular metabolomics. *Electrophoresis* **38,** 2287-2295.

Sonnenberg, R.A., Naz, S., Cougnaud, L. and Vuckovic, D. (2019) Comparison of underivatized silica and zwitterionic sulfobetaine hydrophilic interaction liquid chromatography stationary phases for global metabolomics of human plasma. *J Chromatogr A* **1608,** 460419.

Steuer, A.E., Kaelin, D., Boxler, M.I., Eisenbeiss, L., Holze, F., Vizeli, P., Czerwinska, J., Dargan, P.I., Abbate, V., Liechti, M.E. and Kraemer, T. (2020) Comparative Untargeted Metabolomics Analysis of the Psychostimulants 3,4-Methylenedioxy-Methamphetamine (MDMA), Amphetamine, and the Novel Psychoactive Substance Mephedrone after Controlled Drug Administration to Humans. *Metabolites* **10**.

Thevenot, E.A., Roux, A., Xu, Y., Ezan, E. and Junot, C. (2015) Analysis of the Human Adult Urinary Metabolome Variations with Age, Body Mass Index, and Gender by Implementing a Comprehensive Workflow for Univariate and OPLS Statistical Analyses. *J Proteome Res* **14,** 3322-35.

Tobin, N.H., Murphy, A., Li, F., Brummel, S.S., Taha, T.E., Saidi, F., Owor, M., Violari, A., Moodley, D., Chi, B., Goodman, K.D., Koos, B. and Aldrovandi, G.M. (2021) Comparison of dried blood spot and plasma sampling for untargeted metabolomics. *Metabolomics* **17,** 62.

van de Velde, B., Guillarme, D. and Kohler, I. (2020) Supercritical fluid chromatography - Mass spectrometry in metabolomics: Past, present, and future perspectives. *J Chromatogr B Analyt Technol Biomed Life Sci* **1161,** 122444.

van der Maaten, L. (2014) Accelerating t-SNE using Tree-Based Algorithms. *Journal of Machine Learning Research* **15,** 3221-3245.

van der Maaten, L. and Hinton, G. (2008) Visualizing Data using t-SNE. *Journal of Machine Learning Research* **9,** 2579-2605.

Wagmann, L., Jacobs, C.M. and Meyer, M.R. (2022) New Psychoactive Substances: Which Biological Matrix is the Best for Clinical Toxicology Screening? *Ther Drug Monit*.

Wang, X., Stoll, D.R., Schellinger, A.P. and Carr, P.W. (2006) Peak capacity optimization of peptide separations in reversed-phase gradient elution chromatography: fixed column format. *Anal Chem* **78,** 3406-16.

Wernisch, S. and Pennathur, S. (2016) Evaluation of coverage, retention patterns, and selectivity of seven liquid chromatographic methods for metabolomics. *Anal Bioanal Chem* **408,** 6079-91.

Yao, L., Sheflin, A.M., Broeckling, C.D. and Prenni, J.E. (2019) Data Processing for GC-MS- and LC-MS-Based Untargeted Metabolomics. *Methods Mol Biol* **1978,** 287-299.

Zhao, H., Liu, Y., Li, Z., Song, Y., Cai, X., Liu, Y., Zhang, T., Yang, L., Li, L., Gao, S., Li, Y. and Yu, C. (2018) Identification of essential hypertension biomarkers in human urine by non-targeted metabolomics based on UPLC-Q-TOF/MS. *Clin Chim Acta* **486,** 192-198.

Acknowledgements

The authors would like to thank Armin A. Weber, Aline C. Vollmer, Carsten Schröder, Cathy M. Jacobs, Fabian Frankenfeld, Gabriele Ulrich, Juel Maalouli Shaar, Matthias J. Richter, Philip Schippers, and Tanja M. Gampfer for their support and/or helpful discussions.

Funding

This research received no external funding.

Author contributions

S.H., S.K.M., L.W., and M.R.M. designed the experiments; S.H. performed the experiments; S.H. analyzed the data; S.H., S.K.M., L.W., and M.R.M. interpreted the data; S.H. wrote the first draft of the manuscript; S.H. prepared the figures; S.H., S.K.M., L.W., and M.R.M. reviewed the manuscript. All authors have read and agreed to the published version of the manuscript.

Corresponding author

Correspondence to Markus R. Meyer.

Ethics declarations

Conflict of interest

The authors declare no conflict of interest.

Ethical approval

The animal study protocol was approved by the Ethcis Committee of Landesamt für Verbraucherschutz, Saarbrücken, Germany (protocol code 33/2019)

Additional information

Data availability

The R script can be found on GitHub (https://github.com/sehem/Columns_Metabolomics) and the mzXML files used in this study are available via Metabolights (www.ebi.ac.uk/metabolights/MTBLS5082).

Supplementary information

Below is the link to the electronic supplementary material.

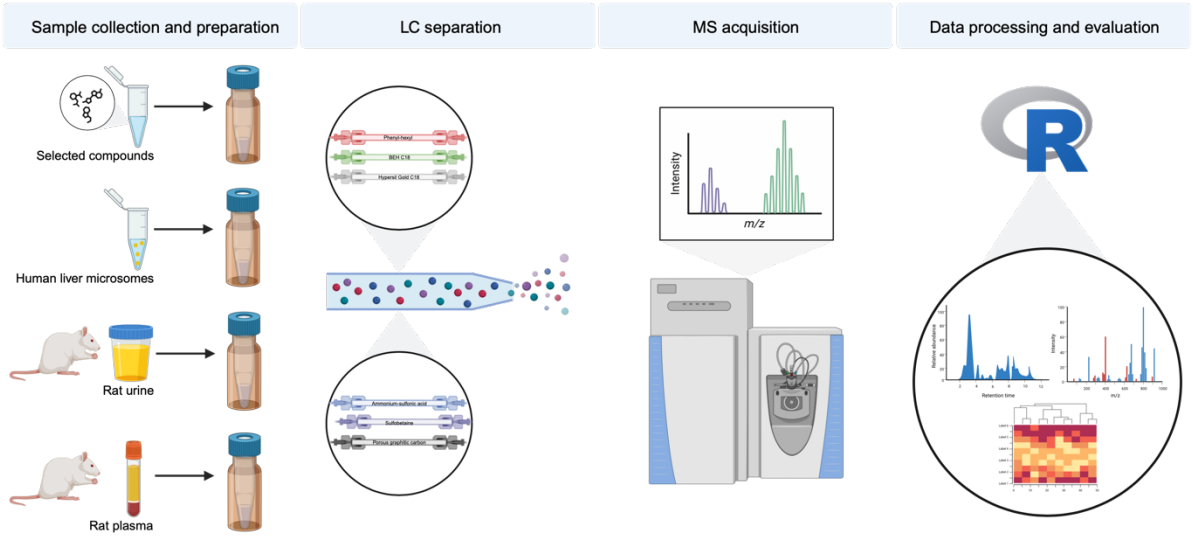

Figure 1. Overview of the analytical workflow used in this study. Sample types were prepared with different preparation methods; samples were then separated on different reversed-phase and hydrophilic interaction-phase columns; mass spectrometry acquisition was performed in positive and negative ionization mode; data processing and evaluation was done using an in-house R script based on XCMS; columns were compared in terms of their different outcomes. (Created with BioRender.com)

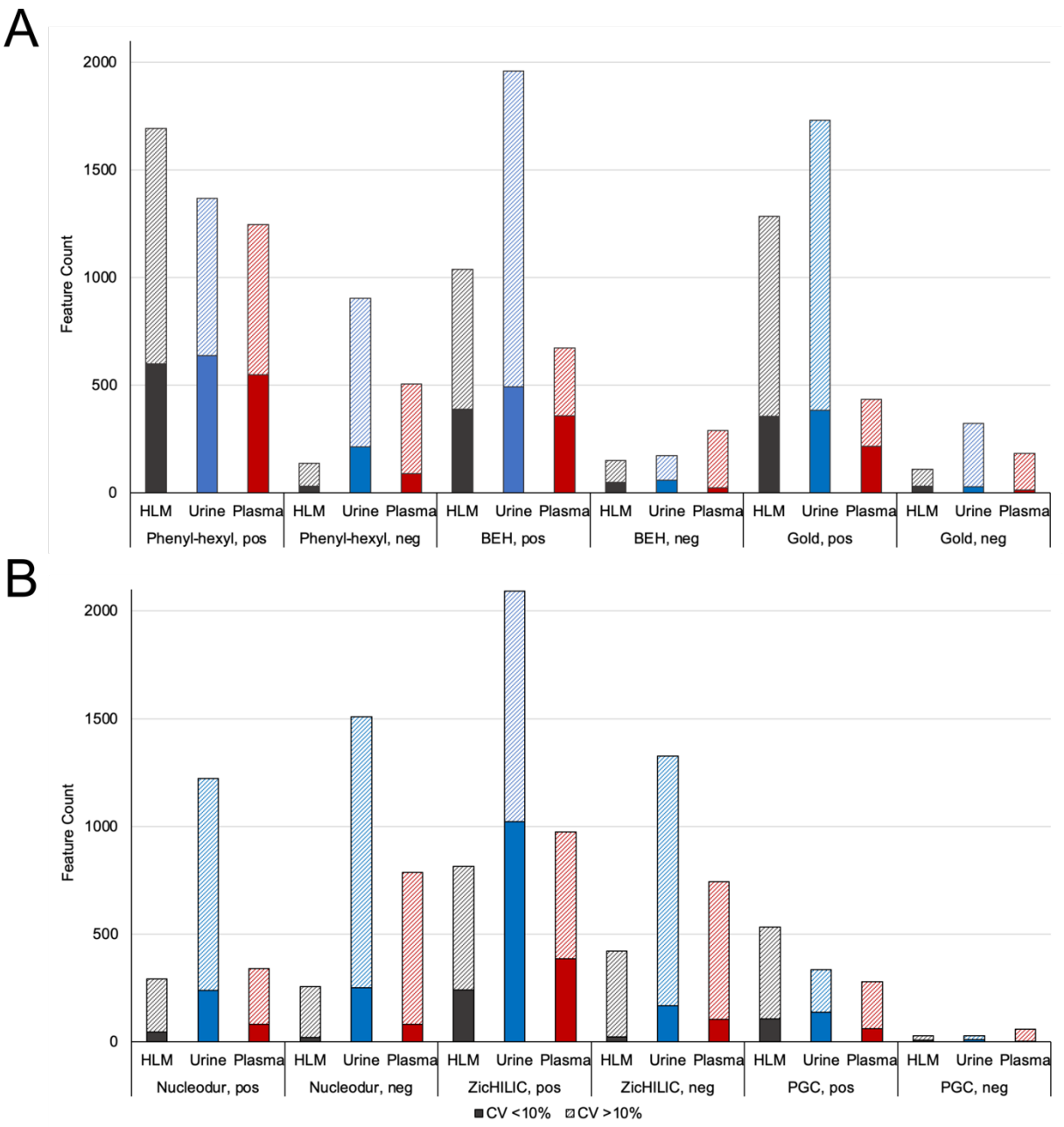

Figure 2. Bar chart showing feature count detected after peak picking and their respective reproducibility evaluated by CV (coefficient of variation) in pooled human liver microsomes (HLM), rat urine, and rat plasma using different reversed-phase (A) and HILIC (B) columns. pos = positive, neg = negative, BEH = BEH C_{18}, Gold = Hypersil Gold C_{18}, Nucleodur = ammonium-sulfonic acid, ZicHILIC = sulfobetaine, PGC = porous graphitic carbon.

Table 2. Summary of study factors and the respective results from this study. Each column is compared within their chromatographic technique. BEH = BEH C_{18}, Gold = Hypersil Gold C_{18}, Nucleodur = ammonium-sulfonic acid, ZicHILIC = sulfobetaine, PGC = porous graphitic carbon, AA = amino acids, CA = carboxylic acids, BA = biogenic amines, FA = Fatty acids, H = pooled human liver microsome, U = rat urine, P = rat plasma.

Parameter	**Reversed-phase columns**			**Hydrophilic interaction columns**		
	Phenyl-Hexyl	**BEH**	**Gold**	**Nucleodur**	**ZicHILIC**	**PGC**
High chromatographic resolution	Short FA, Steroids	Long FA	FA, steroids	AA, BA, sugars	AA, BA, CA, sugars	AA
Column performance (peak width, peak capacity, snthresh)	High	Low	High	Low	Low	High
Feature count	High	Low	Low	Low	High	Low
Reproducibility feature count	High	Low	Low	Low	High	Low
False feature rate	Low	High	Low	High	Low	Low
Recommended matrix	H, U, P	H, U	H, U	P	H, U, P	H

Metabolomics

Supplementary Information

Comparison of reversed-phase, hydrophilic interaction, and porous graphitic carbon chromatography columns for an untargeted toxicometabolomics study in pooled human liver microsomes, rat urine, and rat plasma

Selina Hemmer, Sascha K. Manier, Lea Wagmann, Markus R. Meyer*

Department of Experimental and Clinical Toxicology, Institute of Experimental and Clinical Pharmacology and Toxicology, Center for Molecular Signaling (PZMS), Saarland University, Homburg, Germany

Corresponding author

*Markus R. Meyer, email: markus.meyer@uks.eu

Contents

List of tables and figures

1. Experimental section

1.1. Material and chemicals

PCYP hydrochloride was provided by the State Bureau of Criminal Investigation Schleswig-Holstein (EU project ADEBAR plus, Kiel, Germany) for research purposes. The chemical purity of >93% and identity of the compound were verified by MS and nuclear magnetic resonance analysis.

25-HO Cholesterol, adenosine 5' diphosphate, ammonium formate, ammonium acetate, arachidic acid, ascorbate, carnosine, chloroform, cholesteryl oleate, citrate, cortisone, creatinine, creatinine-d_3, D-fructose, D-glucose, D-glucose-d_7, D-ribose, dipotassium phosphate, dopamine, formic acid, glutamine, glutaminic acid, guanosine 5' triphosphate, histamine, inosine, isocitrate dehydrogenase, isocitrate, kynurenine, lauric acid, lysin, magnesium chloride, maltose, NAD, noradrenalin, palmitic acid-d_{31}, pregnenolone, proline, retinol, riboflavin, serotonin, spermidine, succinate, superoxide dismutase, threonine, tripotassium phosphate, tryptophane, and vitamine D2 were obtained from Merck (Darmstadt, Germany). Acetonitrile, ethanol, methanol (all LC-MS grade), and NADP-Na_2 were from VWR (Darmstadt, Germany). L-Tryptophan-d_5 was obtained from Alsachim (Illkirch-Graffenstaden, France). 1-Palmitoyl-d_9-2-palmitoyl-*sn*-glycero-3-PC and prostaglandin-E3-d_9 were from Cayman Chemical (Michigan, USA). Difluoroacetic acid (DFA) was obtained from Acros organics (Geel, Belgium). Water was purified with a Millipore filtration unit (18.2 Ω x cm water resistance). pHLM (20 mg microsomal protein x mL^{-1}, 360 pmol total CYP/mg, 26 donors) were obtained from Corning (Amsterdam, The Netherlands). After delivery, pHLM were thawed at 37 °C, aliquoted, snap-frozen in liquid nitrogen, and stored at -80 °C until use.

1.2. Sample preparation and analysis of selected compounds

Various mixtures consisting of different compound classes such as amino acids, biogenic amines, carboxylic acids, fatty acids, sugars, and others were analyzed at a concentration level of 50 µg/mL using the six columns (Table S1). Amino acids, carboxylic acids, biogenic amines, polyamines, nucleotides, coenzymes, and vitamins were dissolved in a water/methanol (95:5, *v/v*) mixture, sugars in Millipore water, and fatty acids, lipids, steroids, and hormones in chloroform/methanol (1:1, *v/v*) mixture.

1.3. Performance test of each column using a system suitability test mixture

The performance of each column was tested before each measurement. For this purpose, a test mixture was used, which contained the following analytes: Glucose-d_7 (10 mg/L), creatinine-d_3 (1 mg/L), tryptophane-d_5 (10 mg/L), cortisol (10 mg/L), pregnenolone (10 mg/L), prostaglandin-E3-d_9 (10 mg/L), 1-palmitoyl-d_9-2-palmitoyl-*sn*-glycero-3-PC (10 mg/L), and palmitic acid-d_{31} (20 mg/L). The analytes were spiked in methanol for the phenyl-hexyl column. For the Hypersil Gold C_{18} (Gold), BEH C_{18} (BEH), ammonium-sulfonic acid (Nucleodur), and sulfobetaine (ZicHILIC) columns, analytes were spiked in acetonitrile, and for porous graphitic carbon (PGC) column analytes were spiked in water containing DFA (0.1 %, *v/v*).

1.4. Additional information about the LC-HRMS apparatus

For preparation and cleaning of the injection system, isopropanol:water (90:10, *v/v*) was used. The following settings were used: wash volume, 100 µL; wash speed, 4000 nL/s; loop wash factor, 2. Column temperature for every analysis was set to 40 °C, maintained by a Dionex UltiMate 3000 RS analytical column heater. Injection volume was set to 1 µL for all samples, except for samples of the compound classes. HESI-II source conditions were as follow: ionization mode, positive or negative; sheath gas, 60 AU; auxiliary gas, 10 AU; sweep gas, 3 AU; spray voltage, 3.5 kV in positive and -4.0 kV in negative mode; heater temperature 320 °C; ion transfer capillary temperature, 320 °C; and S-lens RF level, 50.0. Mass spectrometry for untargeted metabolomics was performed according to a previously optimized workflow (Manier *et al.*, 2019a; Manier *et al.*, 2019b). The settings for full scan (FS) data acquisition were as follows: resolution 140,000 at *m/z* 200; microscan, 1; automatic gain control (AGC) target, 5e5; maximum injection time, 200 ms; scan range, *m/z* 50–750; spectrum data type; centroid. All study samples were analyzed in randomized order, to avoid potential analyte instability or instrument performance to confound data interpretation. Additionally, one QC injection was performed every five samples to monitor batch effects, as described by Wehrens et al. (Wehrens *et al.*, 2016). Significant features were subsequently identified using parallel reaction monitoring (PRM). Settings for PRM data acquisition were as follow: resolution, 35,000 at *m/z* 200; microscans, 1; AGC target, 5e5; maximum injection time, 200 ms; isolation window, *m/z* 1.0; collisions energy (CE), 10, 20, 35, or 40 eV; spectrum data type, centroid. The inclusion list contained the monoisotopic masses of all significant features, and a time window of

their retention time ± 60 s. The injection volume for the different mixture of compound classes was set to 2 µL and MS was carried out in full scan mode with subsequent data-dependent acquisition of MS^2 ($ddMS^2$) in positive and negative ionization mode. Following FS settings were used: resolution 35,000 at *m/z* 200; microscan, 1; AGC target, 5e4; maximum injection time, 120 ms; scan range, *m/z* 50–750. For $ddMS^2$ mode the following settings were used: resolution 17,500 at *m/z* 200; microscan, 1; AGC target, 5e4; maximum injection time, 250 ms; scan range, *m/z* 50–750; isolation window, *m/z* 1.0; high collision dissociation cell with stepped normalized collision energy (NCE), 17.5, 35, and 52.5 eV; exclude isotopes, on; dynamic exclusion, 5 s; spectrum data type, profile. TF Xcalibur software version 3.0.63 was used for data handling.

1.5. Data processing and statistical analysis

Thermo Fisher LC-HRMS/MS RAW files were converted into mzXML files using ProteoWizard (Adusumilli and Mallick, 2017). XCMS parameters were optimized using a previously developed strategy as mentioned by Manier et al. (Manier *et al.*, 2019a). Peak picking and alignment parameters are summarized in Table S2. Peak picking was performed using XCMS in an R environment (Smith *et al.*, 2006; Team) and the R package CAMERA (Kuhl *et al.*, 2012) was used for the annotation of adducts, artifacts, and isotopes. Feature abundance with a value zero were replaced by the lowest measured abundance as a surrogate limit of detection and the whole dataset was then log 10 transformed (Wehrens *et al.*, 2016). Normalization was performed for urine samples using the area of endogenous creatinine from those samples analyzed using HILIC column and positive ionization mode. For plasma samples, normalization was performed using the area of L-tryptophane-d_5.

1.6. Identification of significant features

Significant features were identified by recording MS/MS spectra using the PRM method mentioned above. After conversion to mzXML format using ProteoWizard (Adusumilli and Mallick, 2017), spectra were imported to NIST MS Search version 2.3 Library and the settings for library, and MS/MS search were used according to published procedures (Hemmer *et al.*, 2020; Hemmer *et al.*, 2021; Hemmer *et al.*, 2022; Manier *et al.*, 2020). Metabolites of the synthetic cathinone PCYP were

tentatively identified by interpreting their spectra in comparison to that of the parent compound. Identified features were classified on the different levels of identification according to the Metabolomics Standards Initiative (MSI) (Sumner *et al.*, 2007).

Table S1. Overview of the detected compound classes using different reversed-phase and hydrophilic interaction chromatography columns sorted by compound class. Retention times of the compounds detected utilizing the respective columns are given in seconds (s). BEH = BEH C_{18}, Gold = Hypersil Gold C_{18}, Nucleodur = ammonium-sulfonic acid, ZicHILIC = sulfobetaine, PGC = porous graphitic carbon. Hyphen (-) means that neither a peak nor a MS^2 were detected for this compound using the corresponding column.

Compound class	Compound	RT reversed-phase, s			RT HILIC, sec		
		Phenyl-hexyl	BEH	Gold	Nucleodur	ZicHILIC	PGC
Amino acid	Creatinine	26	29	59	356	293	191
Amino acid	Glutamine	26	27	57	511	466	73
Amino acid	Glutaminic acid	26	27	57	533	488	81
Amino acid	Histidine	23	27	55	552	484	103
Amino acid	Kynurenine	88	127	188	446	364	296
Amino acid	Lysin	23	27	55	550	518	47
Amino acid	Proline	28	29	59	490	436	61
Amino acid	Threonine	-	-	-	-	-	53
Amino acid	Tryptophane	149	172	217	452	380	344
Biogenic amine	Carnosine	24	28	52	550	506	190
Biogenic amine	Dopamine	38	57	95	443	400	239
Biogenic amine	Histamine	22	28	50	500	440	89
Biogenic amine	Noradrenalin	26	32	59	-	-	-
Biogenic amine	Serotonin	71	126	179	434	381	-
Biogenic amine	Spermidine	22	37	50	620	649	-
Carboxylic acid	Citrate	35	33	76	538	503	-
Carboxylic acid	Succinate	52	61	109	-	456	-
Coenzyme	NAD	32	52	80	-	-	-
Fatty acid	Arachidic acid	-	697	674	82	44	-
Fatty acid	Lauric acid	421	-	-	-	-	-
Lipide	Cholesteryl oleate	-	-	-	-	-	-
Nucleotide	Adenosine 5' Diphosphate	-	-	-	-	-	-
Nucleotide	Guanosine 5' Triphosphate	-	-	-	-	-	-
Nucleotide	Inosine	61	98	151	367	329	349

Steroid	25-HO Cholesterol	-	-	-	-	-	-
Steroid	Cortisone	331	310	323	92	52	-
Steroid	Vitamin D2	-	-	699	-	-	-
Sugar	D-Fructose	-	-	-	490	707	-
Sugar	D-Glucose	25	28	43	481	445	-
Sugar	D-Ribose	26	29	44	503	296	-
Sugar	Maltose	26	29	41	257	463	
Vitamin	Ascorbate	-	-	-	536	713	-
Vitamin	Riboflavin	211	214	245	329	263	-
Vitamin	Retinol	-	-	-	-	-	-

Table S2. Overview of peak picking and alignment parameters used for preprocessing and calculation of peak capacity for different columns and respective matrices. BEH = BEH C_{18}, Gold = Hypersil Gold C_{18}, Nucleodur = ammonium-sulfonic acid, ZicHILIC = sulfobetaine, PGC = porous graphitic carbon, pos = positive, neg = negative, ppm = allowed ppm deviation of mass traces for peak picking, snthresh = signal-to-noise threshold, mzdiff = minimum difference in *m/z* for two peaks to be considered as separate, prefilter 1 = minimum of scan points, prefilter 2 = minimum abundance, bw = bandwidth for grouping of peaks across separate chromatograms.

Column	Matrix	Polarity	Peak width, s	Peak width, max	ppm	sntresh	mzdiff	Prefilter 1	Prefilter 2	bw	Peak capacity
Phenyl-hexyl	pHLM	pos	8.9	100	1.8	10	0.018	7	100	5	92
		neg	8.9	15	1.7	27	0.094	5	100	1	92
	Urine	pos	8.9	19	1	12	0.012	7	100	2.5	92
		neg	7.8	15	2.5	18	-0.098	6	100	4.5	105
	Plasma	pos	8.9	33	1.3	12	0.1	7	100	1	92
		neg	6.8	100	1.8	16	0.01	5	100	1	102
BEH	pHLM	pos	8.9	12	1.6	13	0.016	5	100	1.5	92
		neg	8.9	33	1.4	15	0.1	7	100	1	92
	Urine	pos	7.8	21	2.4	12	-0.098	6	100	1	105
		neg	8.9	10	1.4	22	0.002	8	100	1.5	92
	Plasma	pos	9.9	12	1.5	14	0.096	6	100	0.2	83
		neg	8.9	93	2.5	13	-0.002	5	100	0.3	92
Gold	pHLM	pos	8.9	15	2.5	12	0.1	6	100	2	92
		neg	8.9	15	1.2	30	-0.002	7	100	1	92
	Urine	pos	8.9	17	2.5	12	0.004	5	100	1	92
		neg	7.8	100	1.4	23	-0.1	1	2100	0.8	105
	Plasma	pos	8.9	15	2.5	54	0.1	6	100	0.2	92
		neg	7.8	100	2.5	45	0.1	5	100	1	105

Table S2. Continued.

Column	Matrix	Polarity	Peak width, s	Peak width, max	ppm	sntresh	mzdiff	Prefilter 1	Prefilter 2	bw	Peak capacity
Nucleodur	pHLM	pos	9.9	100	2.5	42	0.1	5	100	1.5	74
		neg	7.8	15	2.1	56	0.1	7	8000	1	93
	Urine	pos	9	20	2.5	14	0.0059	7	100	1.5	81
		neg	8.9	37	2.5	18	0.038	7	100	1	82
	Plasma	pos	7.8	91	1.1	13	0.014	1	100	1	93
		neg	8.9	33	2.5	11	0.014	1	100	0.9	82
ZicHILIC	pHLM	pos	7.8	29	1.6	17	0.006	6	100	0.5	93
		neg	7.8	17	2.5	51	0.01	6	1300	1	93
	Urine	pos	8.9	21	1.9	16	0.02	8	100	1.5	82
		neg	8.9	35	1.3	15	0.022	8	100	1.5	82
	Plasma	pos	8.9	46	1.4	6	0.034	6	100	0.2	82
		neg	8.9	25	2.5	15	0.034	6	100	0.9	82
PGC	pHLM	pos	7.8	15	1.2	12	0.002	6	100	1	105
		neg	8.9	15	1.4	25	0.1	16	100	0.5	92
	Urine	pos	9	15	1.5	30	0.024	5	100	1	91
		neg	7.9	12	1.8	14	0.002	36	100	0.5	104
	Plasma	pos	8.9	12	1.2	42	0.066	6	100	0.9	92
		neg	5.8	44	2	4	0.1	54	100	1	141

Table S3. Overview of the significant features using different columns in the corresponding matrices, namely pooled human liver microsome (pHLM) incubation (sheet 1), rat urine (sheet 2), and rat plasma (sheet 3) in which the features showed significant changes between PCYP and blank or control group. Features are sorted according to *m/z* values, followed by the polarity, the retention time (RT) for the corresponding column in seconds (s), identity, and the identification level according to MSI. BEH = BEH C_{18}, Gold = Hypersil Gold C_{18}, Nucleodur = ammonium-sulfonic acid, ZicHILIC = sulfobetaine, PGC = porous graphitic carbon. Hyphen (-) means that the feature was not significant using the corresponding column.

Table S4. Overview of the calculated ratio of false vs true significant features for different columns and the respective matrices. Pos = positive, neg = negative, BEH = BEH C_{18}, Gold = Hypersil Gold C_{18}, Nucleodur = ammonium-sulfonic acid, ZicHILIC = sulfobetaine, PGC = porous graphitic carbon

	Phenyl-hexyl pos	Phenyl-hexyl neg	BEH pos	BEH neg	Gold pos	Gold neg
pHLM	0 %	-	4 %	-	0 %	-
Urine	10 %	59 %	53 %	0 %	55 %	57 %
Plasma	13 %	100 %	50 %	0 %	0 %	-
	Nucleodur pos	Nucleodur neg	ZicHILIC pos	ZicHILIC neg	PGC pos	PGC neg
pHLM	0 %	50 %	8 %	-	0 %	-
Urine	25 %	55 %	29 %	35 %	0 %	-
Plasma	15 %	63 %	17 %	40 %	-	-

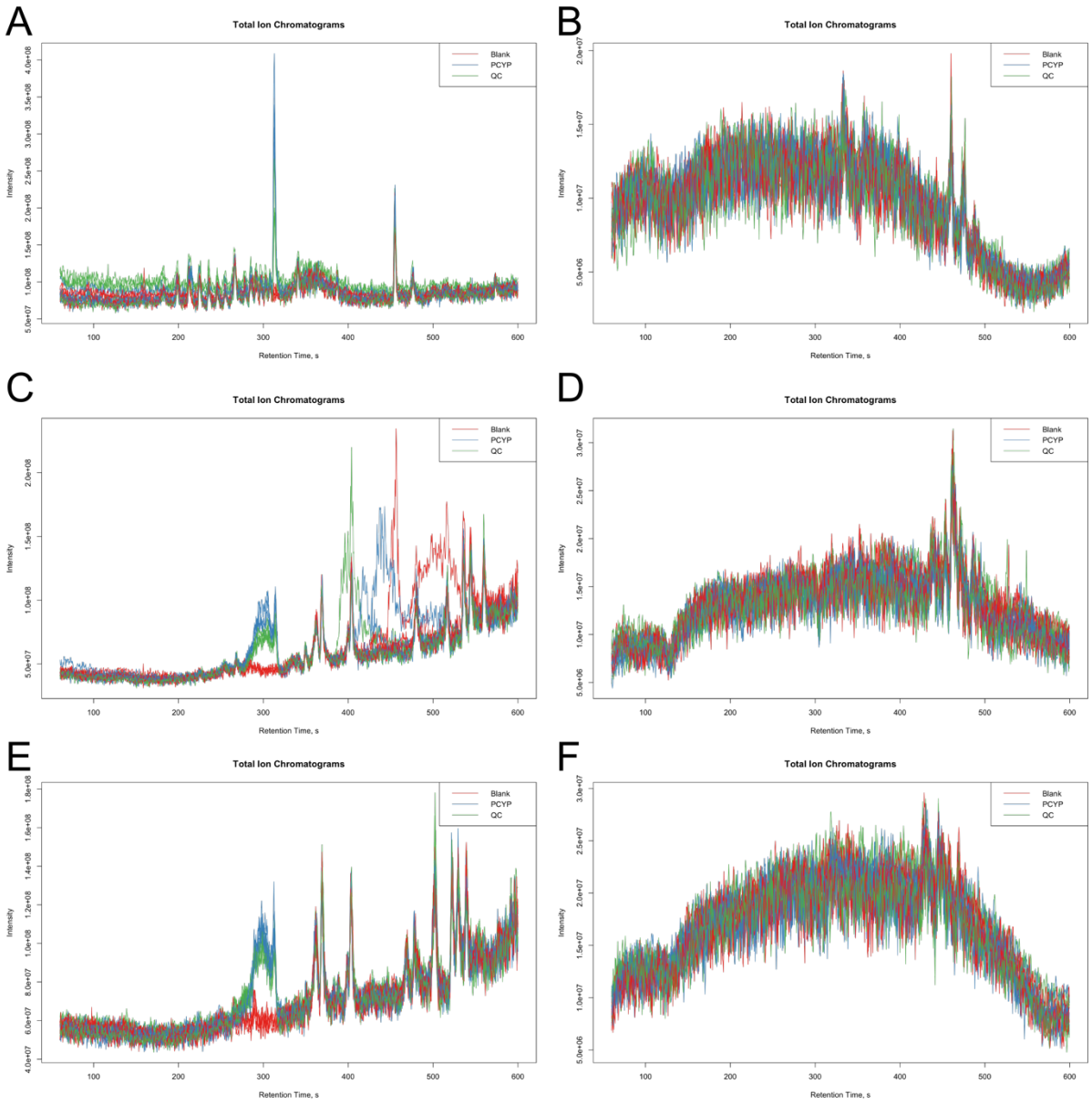

Figure S1. Total ion chromatograms (TIC) of reversed-phase chromatography in pooled human liver microsomes (pHLM) in positive (pos) and negative (neg) ionization mode. A = Phenyl-hexyl pos, B = Phenyl-hexyl neg, C = BEH pos, D = BEH neg, E = Gold pos, and F = Gold neg.

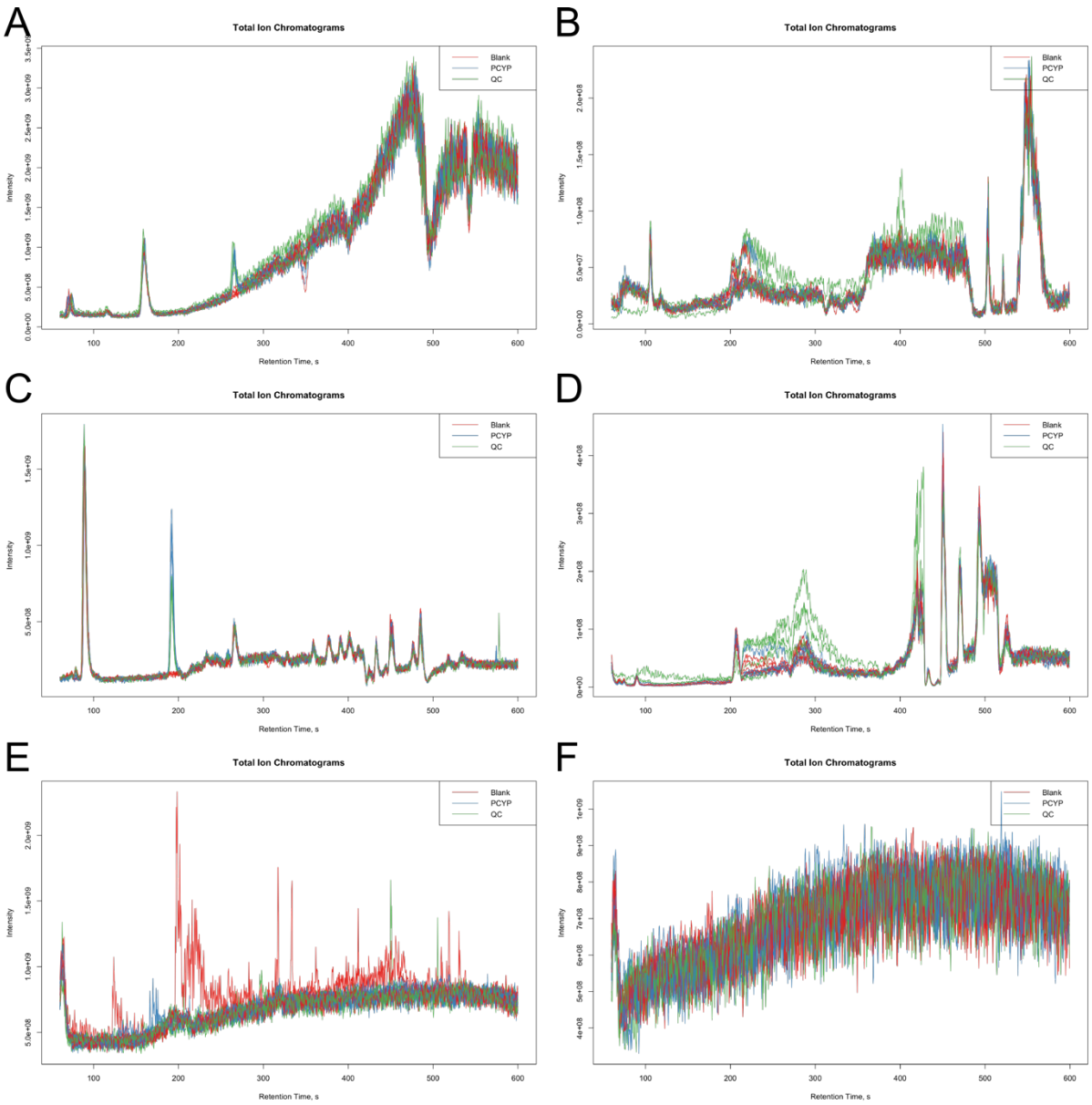

Figure S2. Total ion chromatograms (TIC) of hydrophilic interaction chromatography in pooled human liver microsomes (pHLM) in positive (pos) and negative (neg) ionization mode. A = Nucleodur pos, B = Nucleodur neg, C = ZicHILIC pos, D = ZicHILIC neg, E = PGC pos, and F = PGC neg

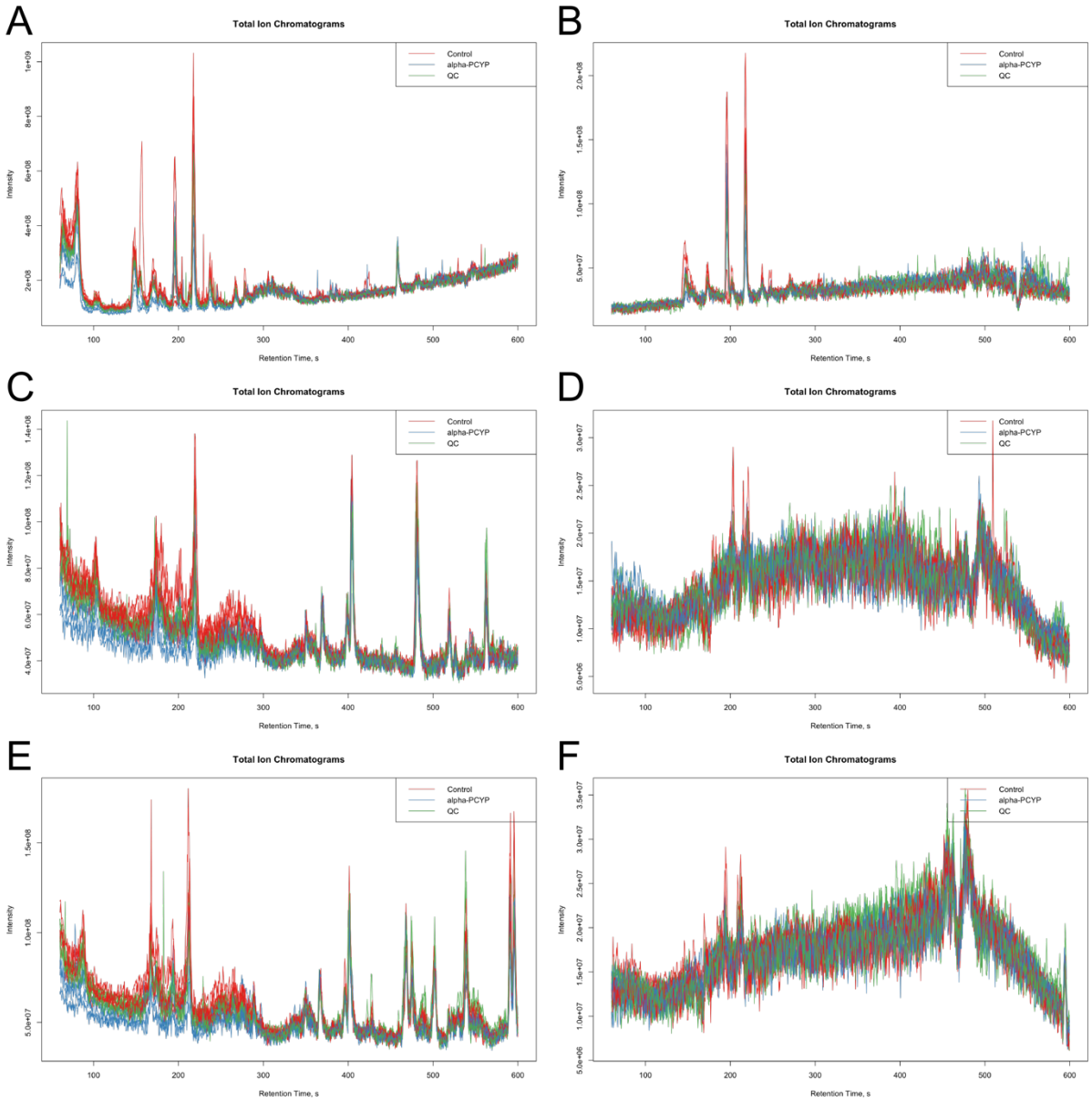

Figure S3. Total ion chromatograms (TIC) of reversed-phase chromatography in rat urine in positive (pos) and negative (neg) ionization mode. A = Phenyl-hexyl pos, B = Phenyl-hexyl neg, C = BEH pos, D = BEH neg, E = Gold pos, and F = Gold neg

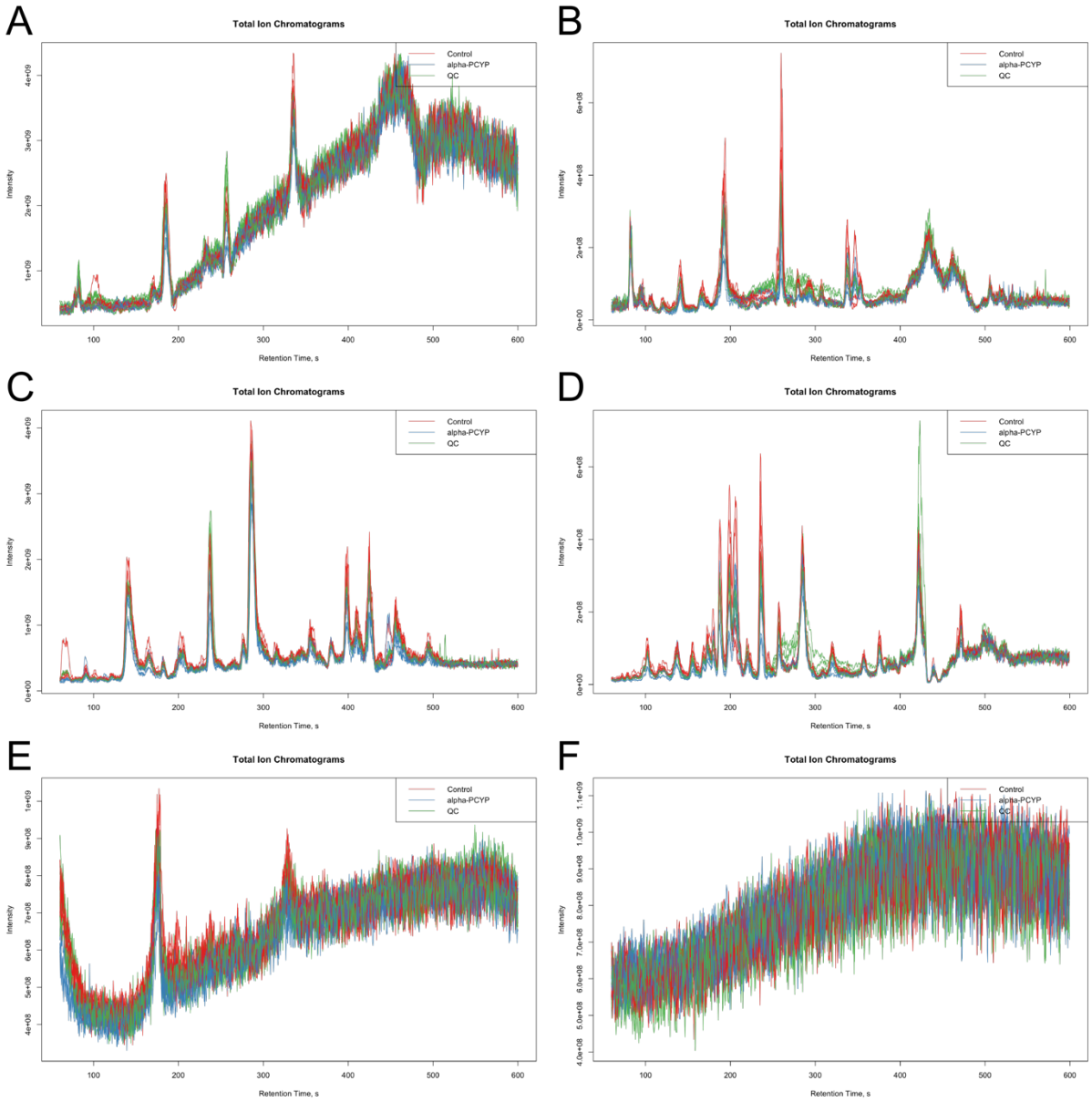

Figure S4. Total ion chromatograms (TIC) of hydrophilic interaction chromatography in rat urine in positive (pos) and negative (neg) ionization mode. A = Nucleodur pos, B = Nucleodur, C = ZicHILIC pos, D = ZicHILIC neg, E = PGC pos, and F = PGC neg.

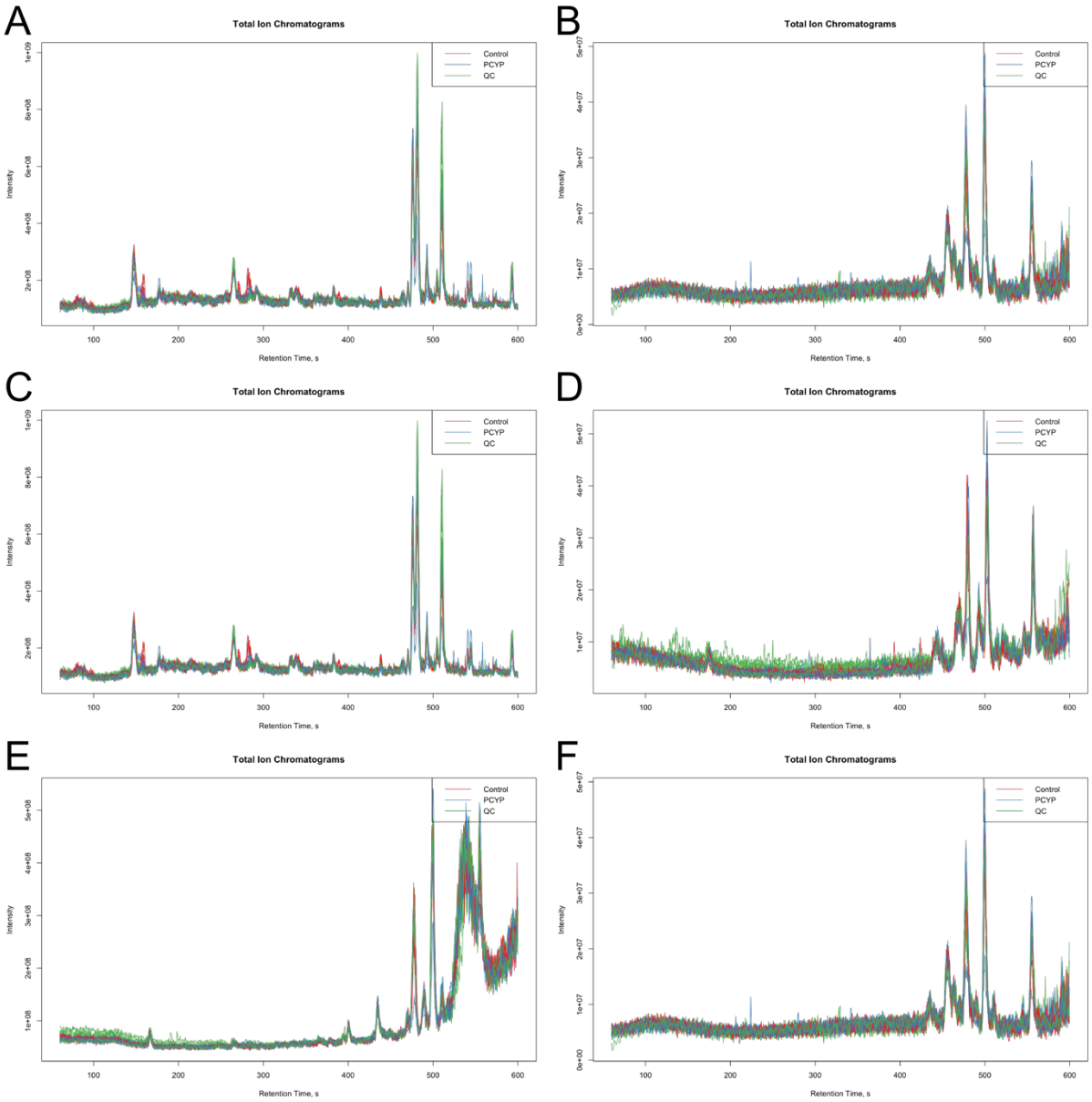

Figure S5. Total ion chromatograms (TIC) of the reversed-phase chromatography in rat plasma in positive (pos) and negative (neg) ionization mode. A = Phenyl-hexyl pos, B = Phenyl-hexyl neg, C = BEH pos, D = BEH neg, E = Gold pos, and F = Gold neg.

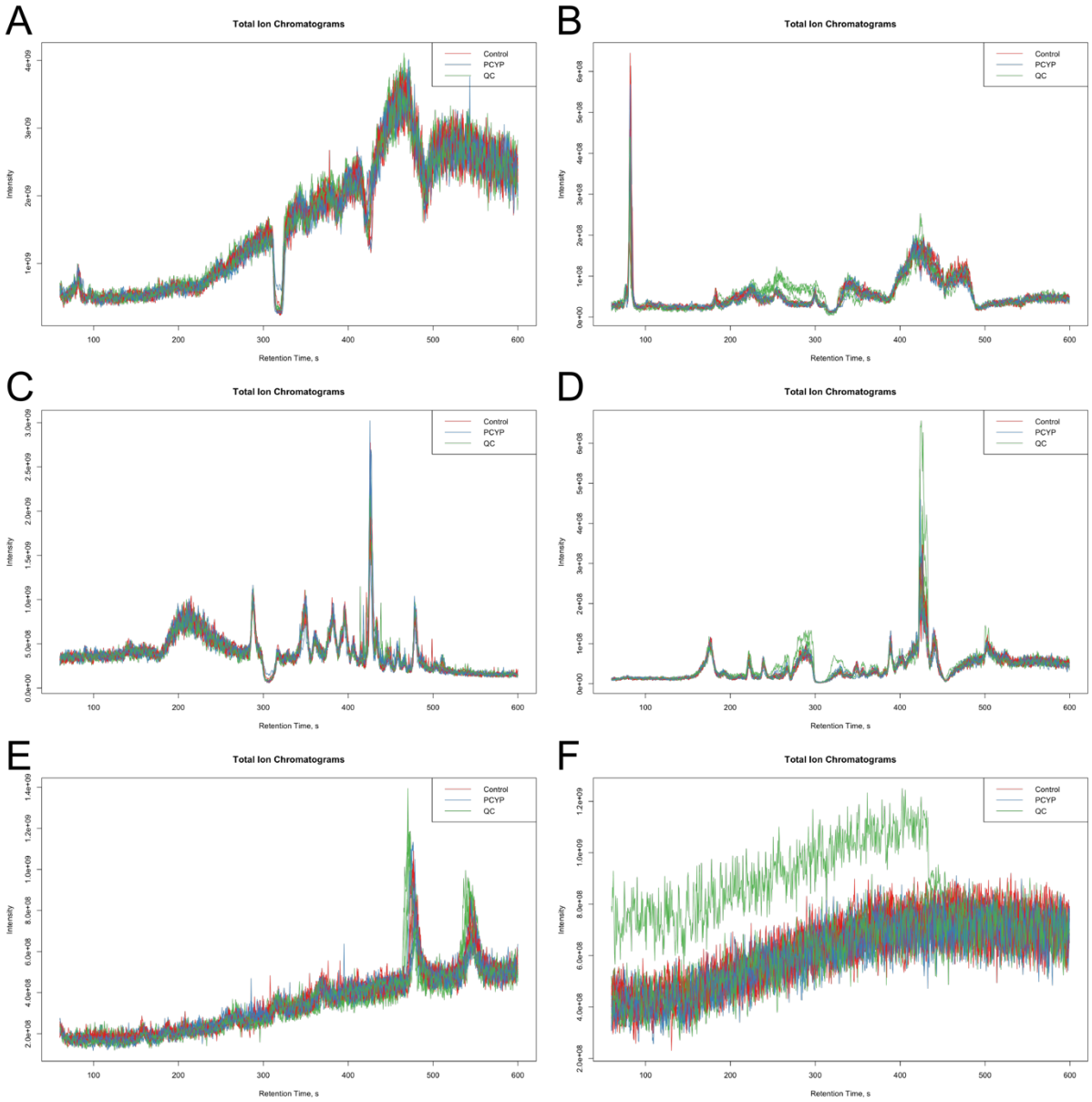

Figure S6. Total ion chromatograms (TIC) of hydrophilic interaction chromatography in rat plasma in positive (pos) and negative (neg) ionization mode. A = Nucleodur pos, B = Nucleodur neg, C = ZicHILIC pos, D = ZicHILIC neg, E = PGC pos, and F = PGC neg.

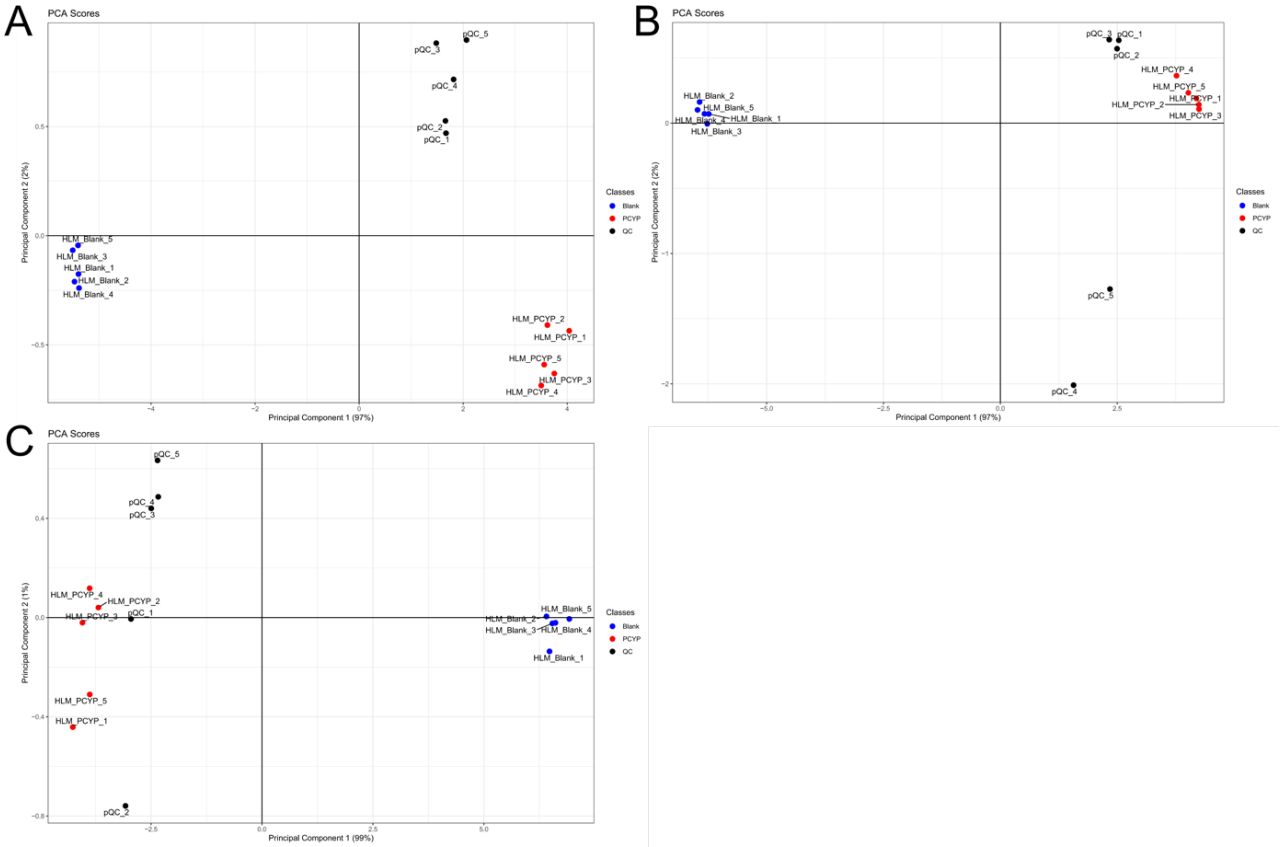

Figure S7. Scores of principal component analysis of pooled human liver microsome samples after analysis using reversed-phase chromatography in positive ionization mode. A = Phenyl-hexyl, B = BEH, and C = Gold.

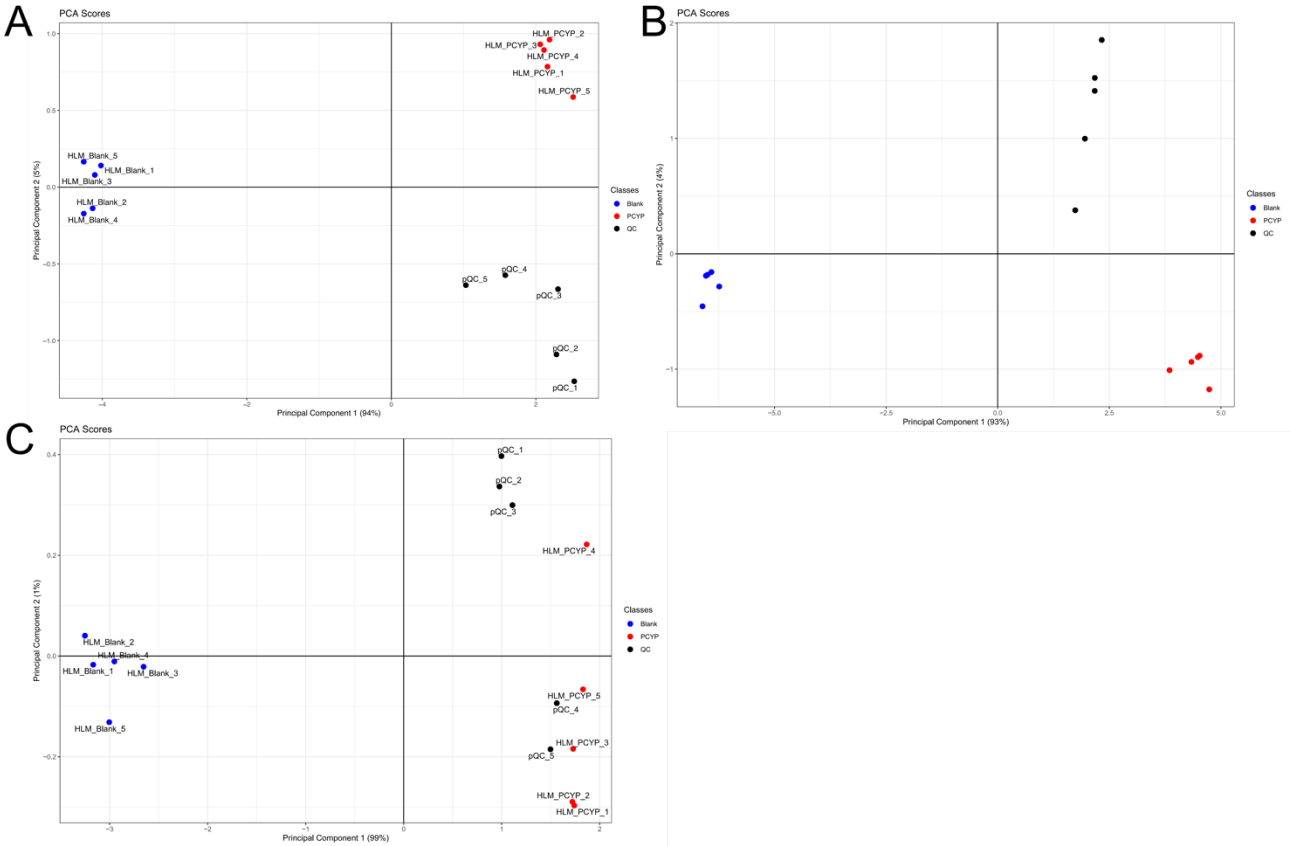

Figure S8. Scores of principal component analysis of pooled human liver microsome samples after analysis using hydrophilic interaction chromatography in positive ionization mode. A = Nucleodur, B = ZicHILIC, and C = PGC.

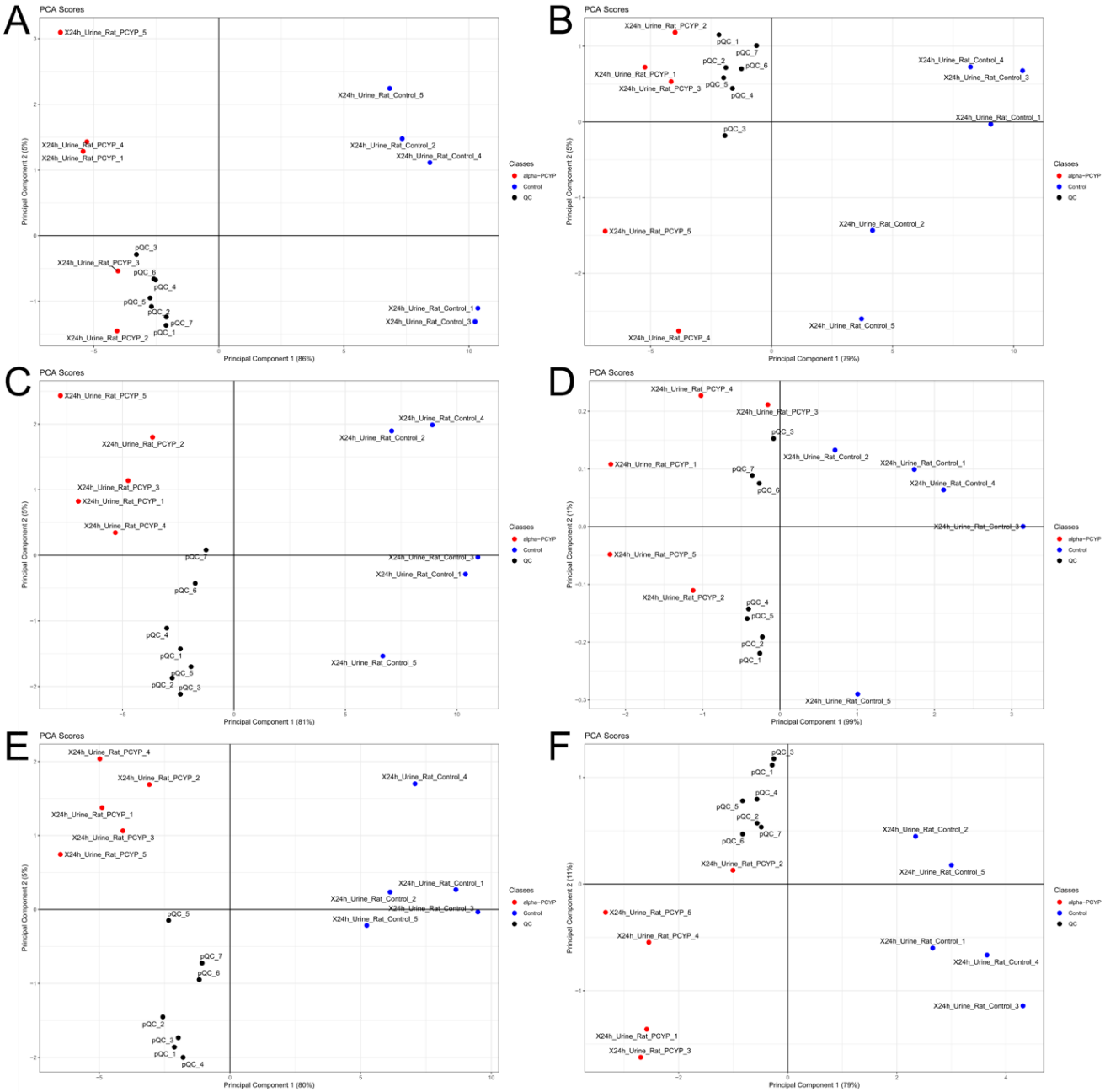

Figure S9. Scores of principal component analysis of rat urine samples after analysis using reversed-phase chromatography in positive (pos) and negative (neg) ionization mode. A = Phenyl-hexyl pos, B = Phenyl-hexyl neg, C = BEH pos, D = BEH neg, D = Gold pos, and F = Gold neg.

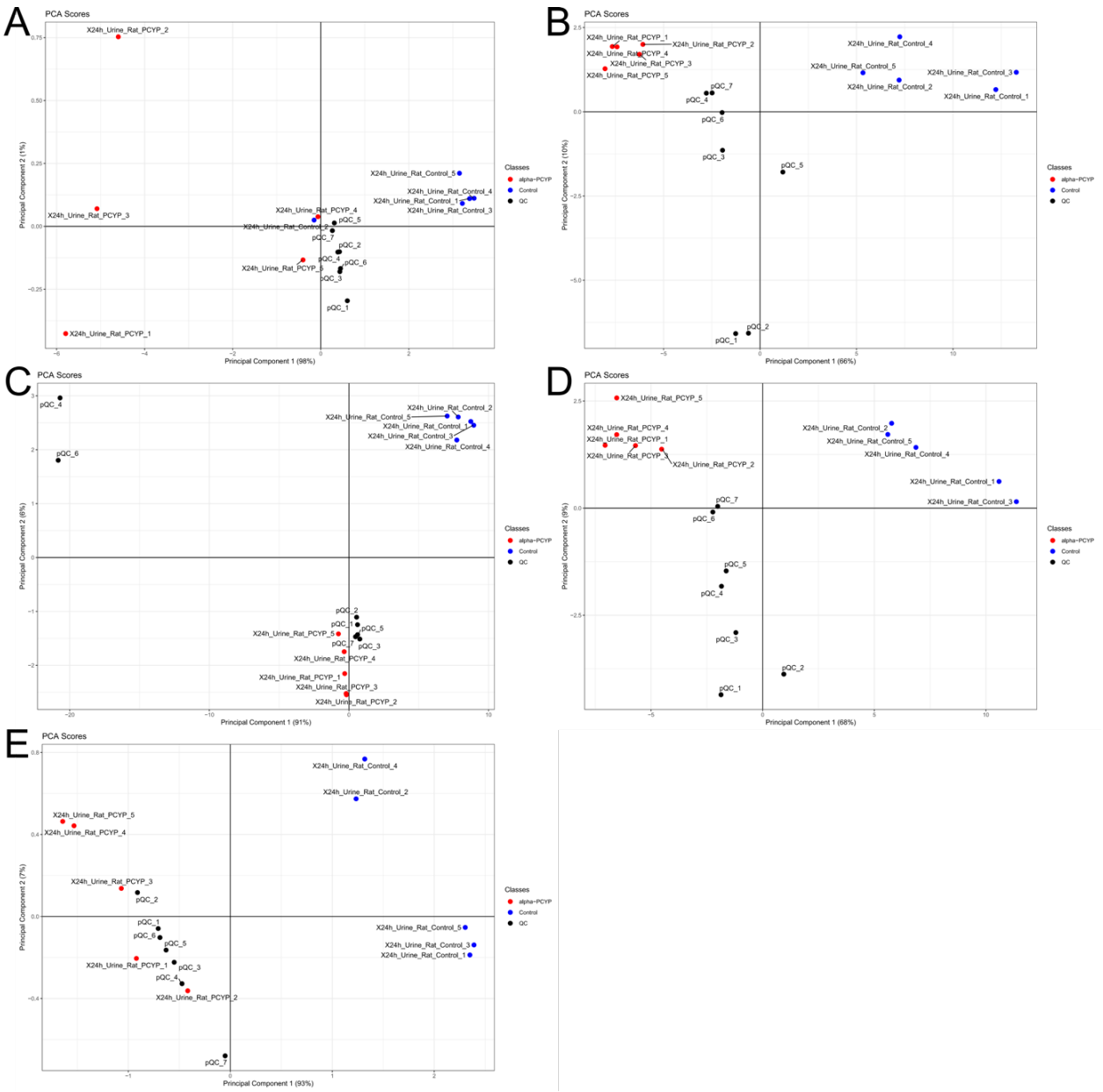

Figure S10. Scores of principal component analysis of rat urine samples after analysis using hydrophilic interaction chromatography in positive (pos) and negative (neg) ionization mode. A = Nucleodur pos, B = Nucleodur neg, C = ZicHILIC pos, D = ZicHILIC neg, and E = PGC pos.

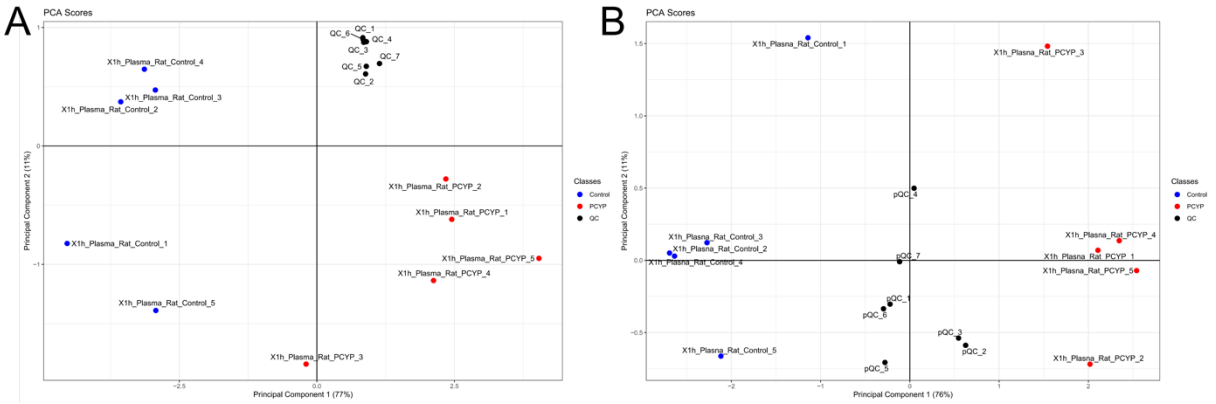

Figure S11. Scores of principal component analysis of rat plasma samples after analysis using reversed-phase chromatography in positive ionization mode. A = Phenyl-hexyl and B = BEH.

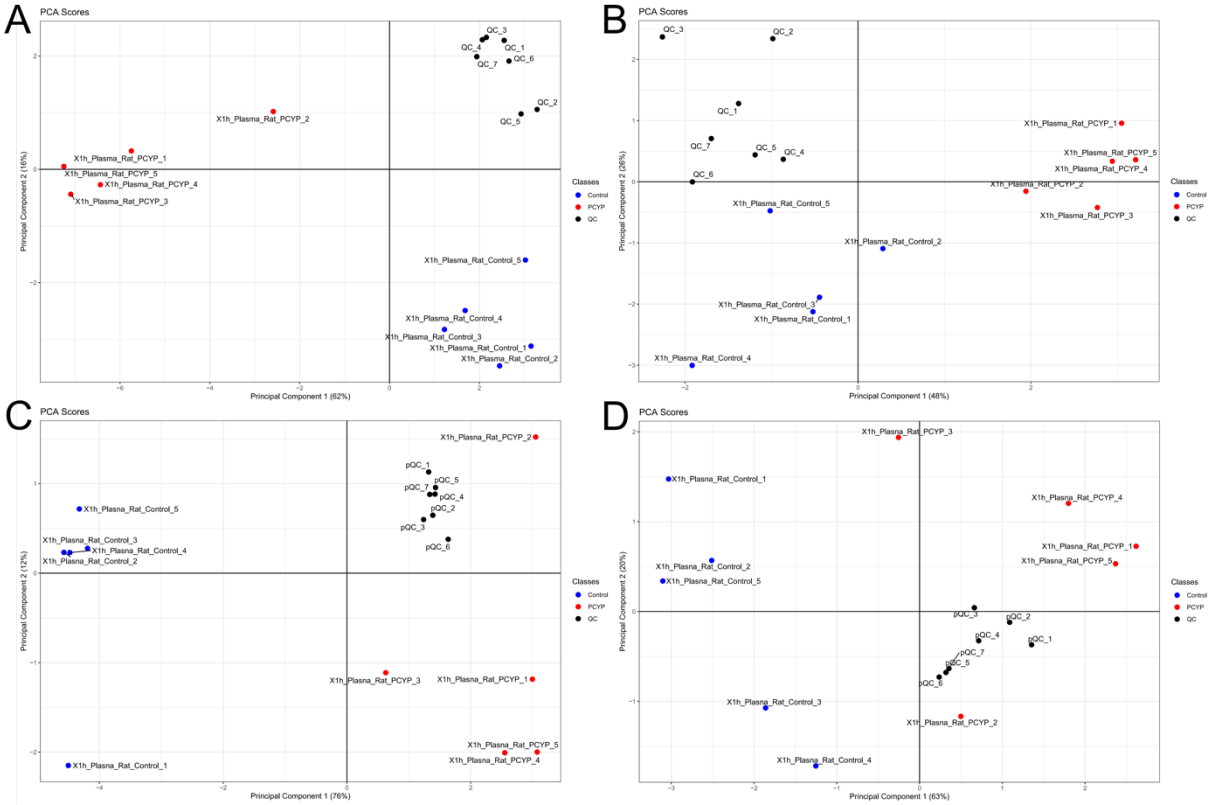

Figure S12. Scores of principal component analysis of rat plasma samples after analysis using hydrophilic interaction chromatography in positive (pos) and negative (neg) ionization mode. A = Nucleodur pos, B = Nucleodur neg, C = ZicHILIC pos, and D = ZicHILIC neg.

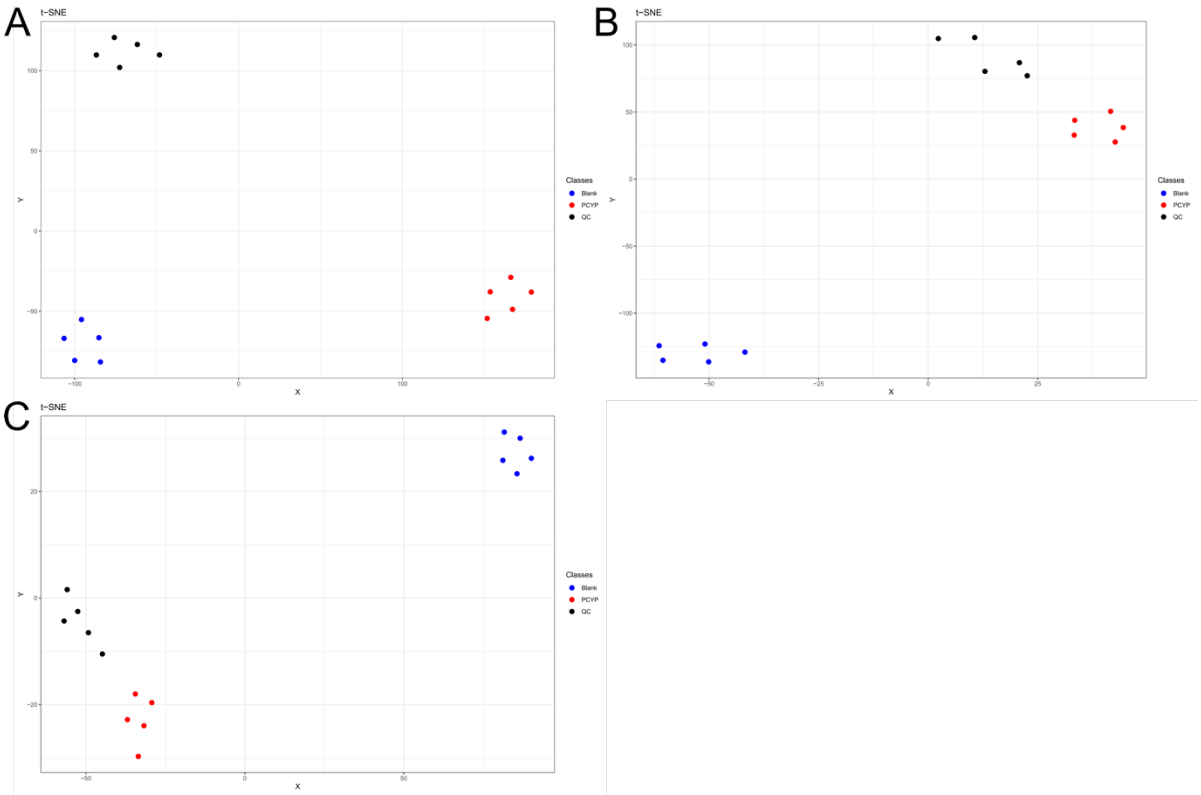

Figure S13. Results of *t*-distributed stochastic neighborhood embedding (*t*-SNE) of pooled human liver microsome samples after analysis using reversed-phase chromatography in positive ionization mode. A = Phenyl-hexyl, B = BEH, and C = Gold.

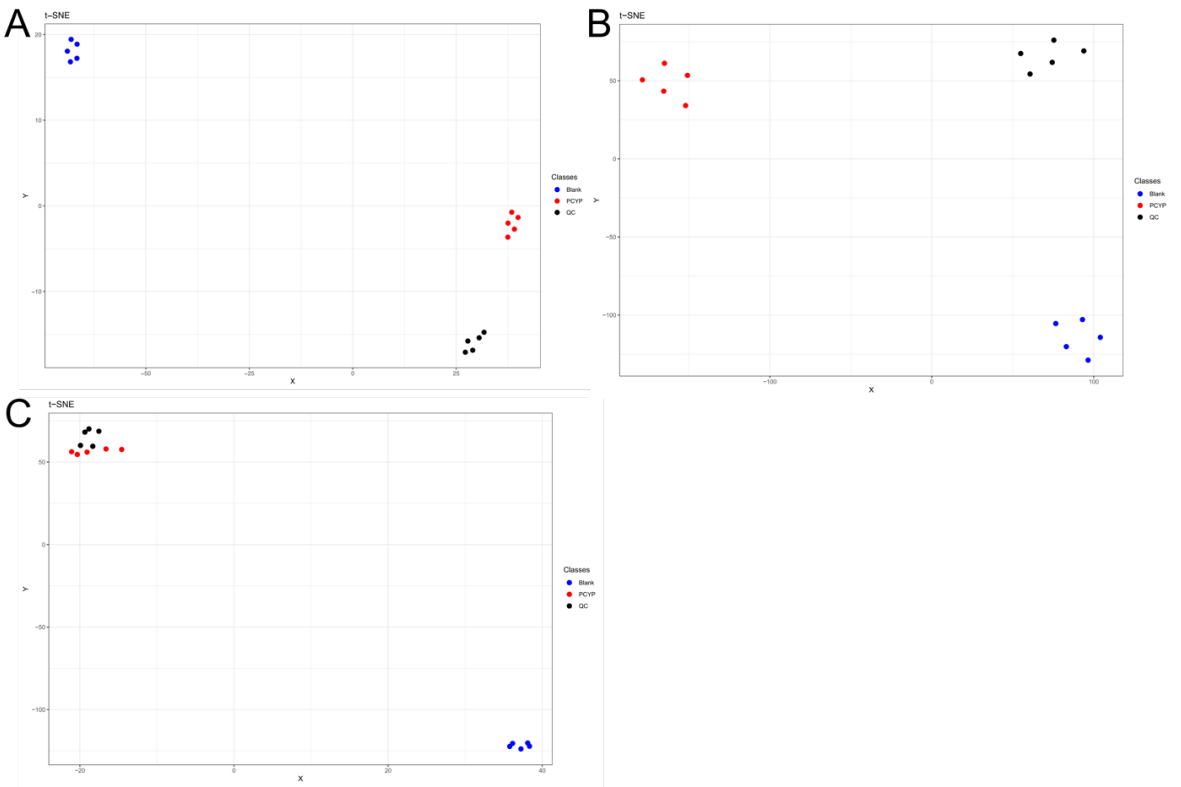

Figure S14. Results of *t*-distributed stochastic neighborhood embedding (*t*-SNE) of pooled human liver microsome samples after analysis using hydrophilic interaction chromatography in positive ionization mode. A = Nucleodur, B = ZicHILIC, and C = PGC.

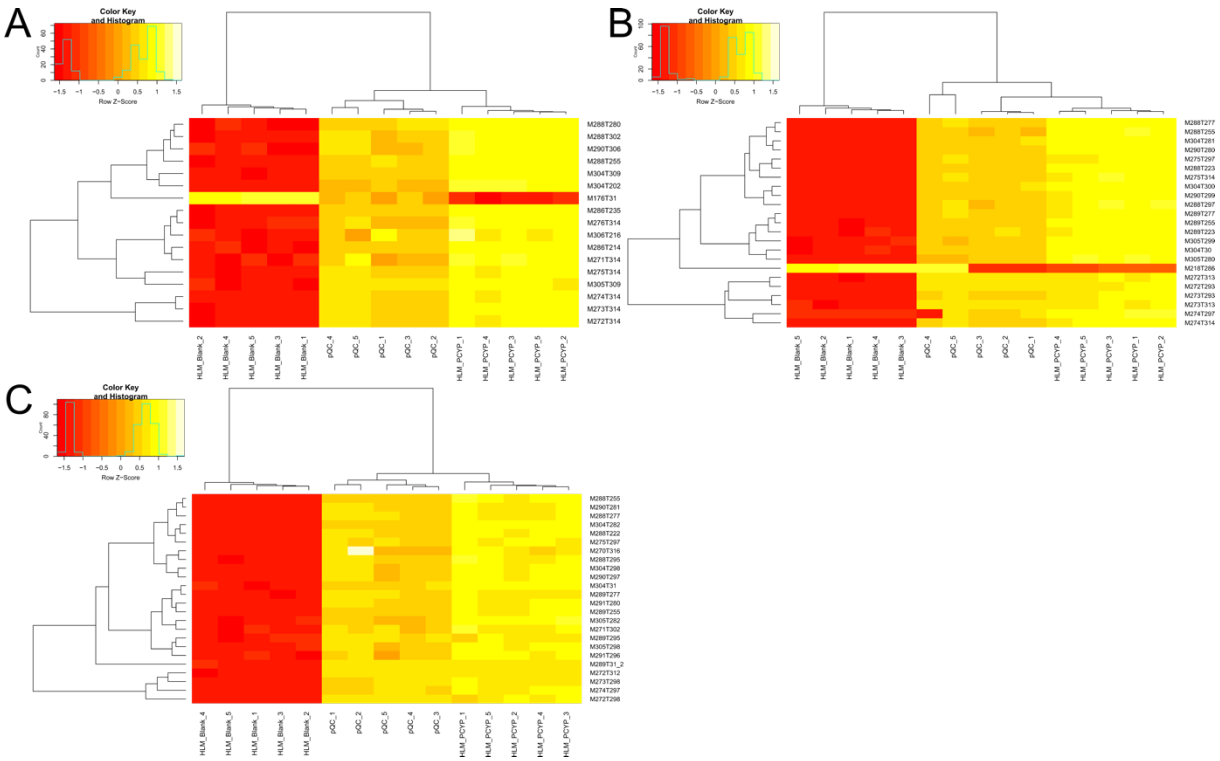

Figure S15. Results of heat map of hierarchical clustering of pooled human liver microsome samples after analysis using reversed-phase chromatography in positive ionization mode. A = Phenyl-hexyl, B = BEH, and C = Gold.

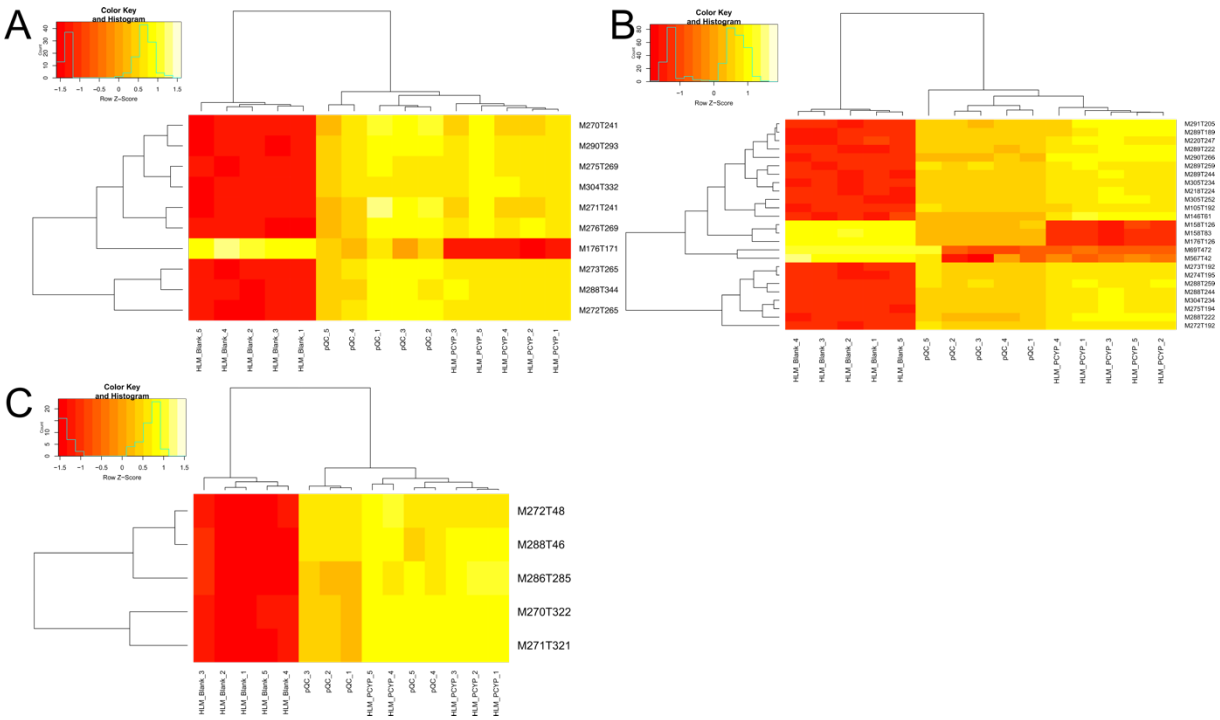

Figure S16. Results of heat map of hierarchical clustering of pooled human liver microsome samples after analysis using hydrophilic interaction chromatography in positive ionization mode. A = Nucleodur, B = ZicHILIC, and C = PGC.

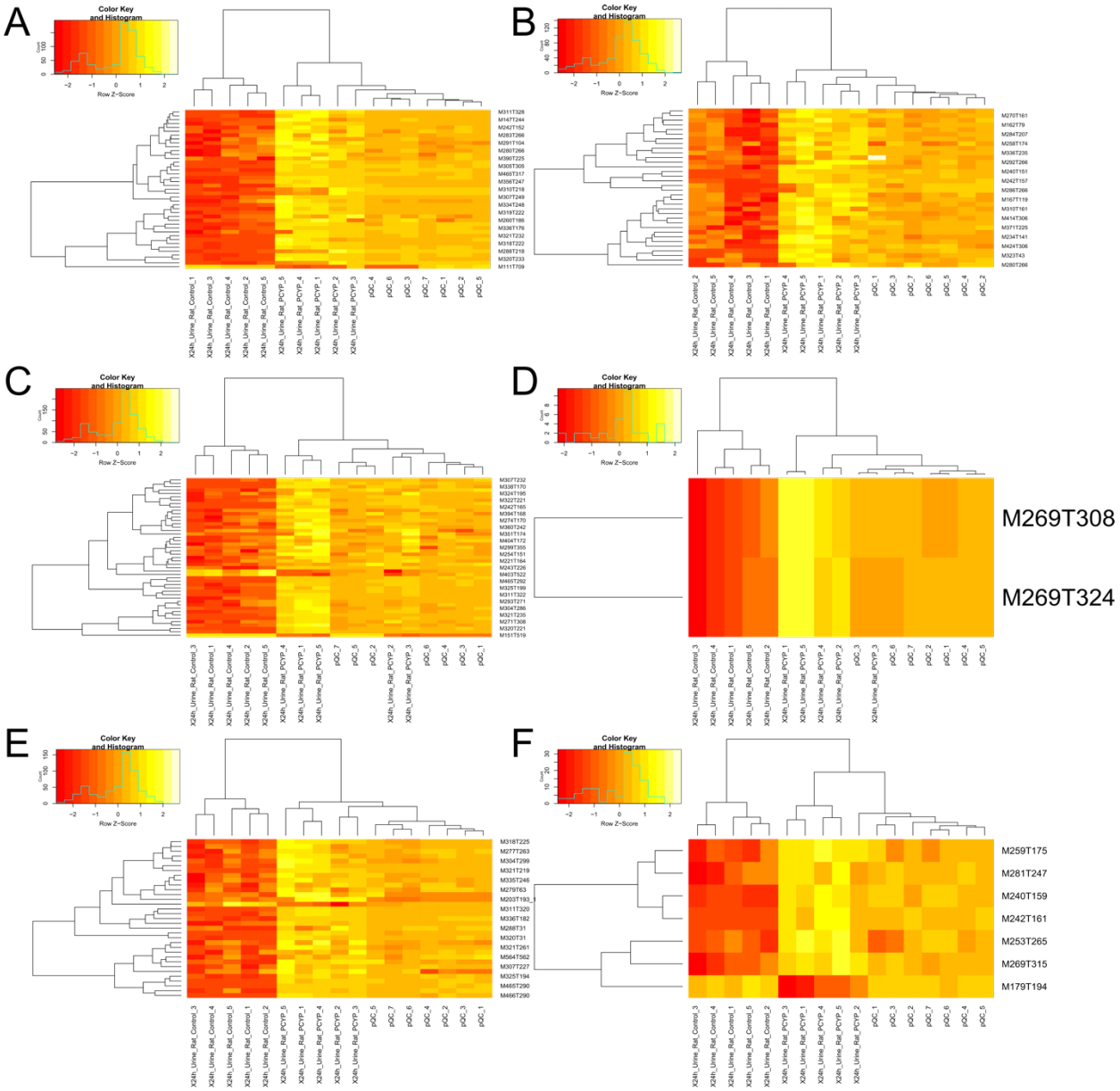

Figure S17. Results of heat map of hierarchical clustering of rat urine samples after analysis using reversed-phase chromatography in positive (pos) and negative (neg) ionization mode. A = Phenyl-hexyl pos, B = Phenyl-hexyl neg, C = BEH pos, D = BEH neg, D = Gold pos, and F = Gold neg.

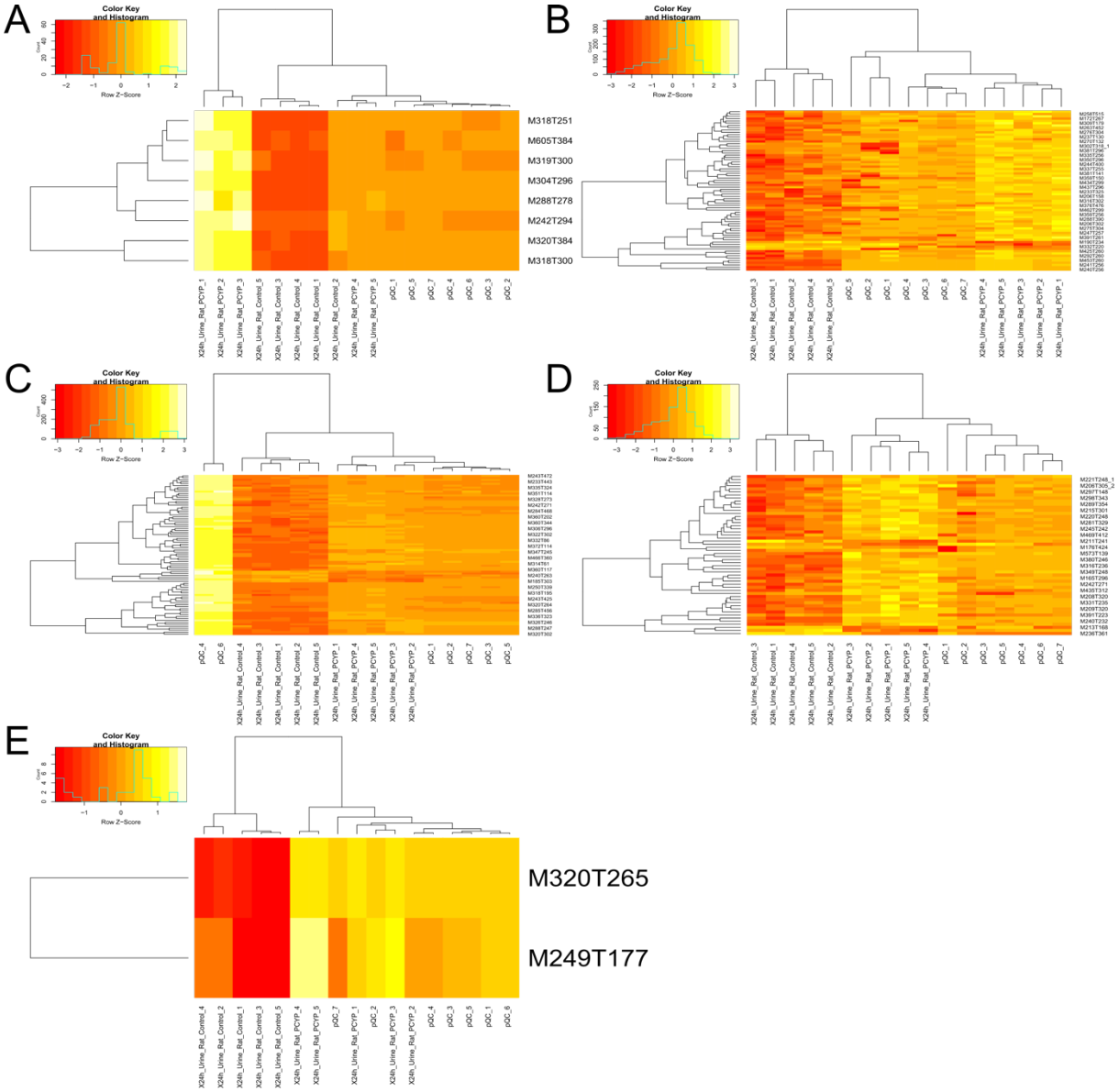

Figure S18. Results of heat map of hierarchical clustering of rat urine samples after analysis using hydrophilic interaction chromatography in positive (pos) and negative (neg) ionization mode. A = Nucleodur pos, B = Nucleodur neg, C = ZicHILIC pos, D = ZicHILIC neg, and E = PGC pos.

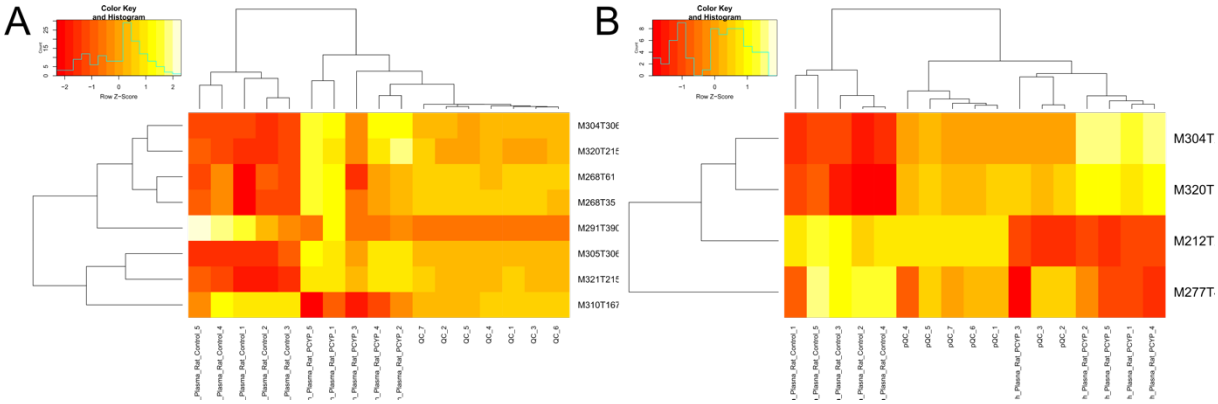

Figure S19. Results of heat map of hierarchical clustering of rat plasma samples after analysis using reversed-phase chromatography in positive ionization mode. A = Phenyl-hexyl and B = BEH.

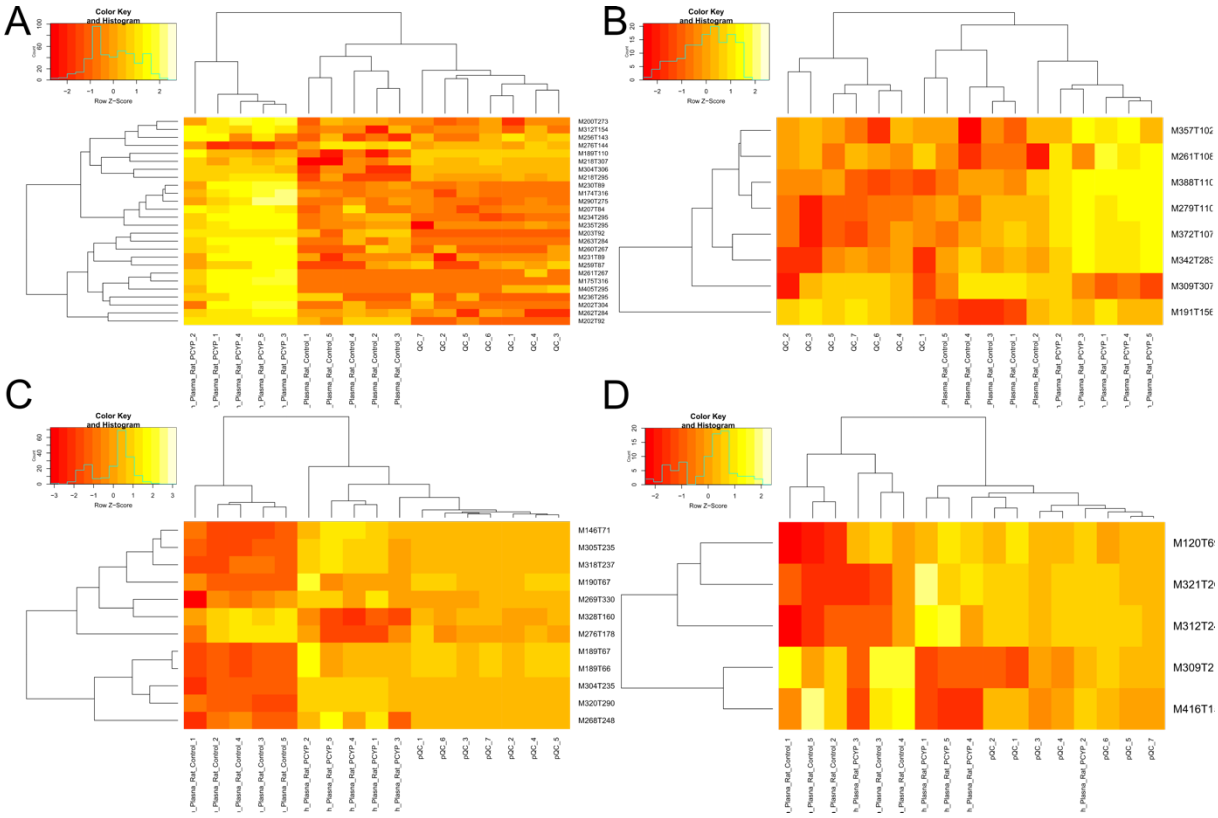

Figure S20. Results of heat map of hierarchical clustering of rat plasma samples after analysis using hydrophilic interaction chromatography in positive and negative ionization mode. A = Nucleodur pos, B = Nucleodur neg, C = ZicHILIC pos, and D = ZicHILIC neg.

References

Adusumilli, R. and Mallick, P. (2017) Data Conversion with ProteoWizard msConvert. *Methods Mol Biol* **1550,** 339-368.

Hemmer, S., Manier, S.K., Fischmann, S., Westphal, F., Wagmann, L. and Meyer, M.R. (2020) Comparison of Three Untargeted Data Processing Workflows for Evaluating LC-HRMS Metabolomics Data. *Metabolites* **10**.

Hemmer, S., Wagmann, L. and Meyer, M.R. (2021) Altered metabolic pathways elucidated via untargeted in vivo toxicometabolomics in rat urine and plasma samples collected after controlled application of a human equivalent amphetamine dose. *Arch Toxicol* **95,** 3223-3234.

Hemmer, S., Wagmann, L., Pulver, B., Westphal, F. and Meyer, M.R. (2022) In Vitro and In Vivo Toxicometabolomics of the Synthetic Cathinone PCYP Studied by Means of LC-HRMS/MS. *Metabolites* **12**.

Kuhl, C., Tautenhahn, R., Bottcher, C., Larson, T.R. and Neumann, S. (2012) CAMERA: an integrated strategy for compound spectra extraction and annotation of liquid chromatography/mass spectrometry data sets. *Anal Chem* **84,** 283-9.

Manier, S.K., Keller, A. and Meyer, M.R. (2019a) Automated optimization of XCMS parameters for improved peak picking of liquid chromatography-mass spectrometry data using the coefficient of variation and parameter sweeping for untargeted metabolomics. *Drug Test Anal* **11,** 752-761.

Manier, S.K., Keller, A., Schaper, J. and Meyer, M.R. (2019b) Untargeted metabolomics by high resolution mass spectrometry coupled to normal and reversed phase liquid chromatography as a tool to study the in vitro biotransformation of new psychoactive substances. *Sci Rep* **9,** 2741.

Manier, S.K., Wagmann, L., Flockerzi, V. and Meyer, M.R. (2020) Toxicometabolomics of the new psychoactive substances alpha-PBP and alpha-PEP studied in HepaRG cell incubates by means of untargeted metabolomics revealed unexpected amino acid adducts. *Arch Toxicol* **94,** 2047-2059.

Smith, C.A., Want, E.J., O'Maille, G., Abagyan, R. and Siuzdak, G. (2006) XCMS: processing mass spectrometry data for metabolite profiling using nonlinear peak alignment, matching, and identification. *Anal Chem* **78,** 779-87.

Sumner, L.W., Amberg, A., Barrett, D., Beale, M.H., Beger, R., Daykin, C.A., Fan, T.W., Fiehn, O., Goodacre, R., Griffin, J.L., Hankemeier, T., Hardy, N., Harnly, J., Higashi, R., Kopka, J., Lane, A.N., Lindon, J.C., Marriott, P., Nicholls, A.W., Reily, M.D., Thaden, J.J. and Viant, M.R. (2007) Proposed minimum reporting standards for chemical analysis Chemical Analysis Working Group (CAWG) Metabolomics Standards Initiative (MSI). *Metabolomics* **3,** 211-221.

Team, R.C. R: A Language and Environment for Statistical Computing, R Foundation for Statistical Computing.

Wehrens, R., Hageman, J.A., van Eeuwijk, F., Kooke, R., Flood, P.J., Wijnker, E., Keurentjes, J.J., Lommen, A., van Eekelen, H.D., Hall, R.D., Mumm, R. and de Vos, R.C. (2016) Improved batch correction in untargeted MS-based metabolomics. *Metabolomics* **12,** 88.

Significant features in pHL (sheet 1)

m/z	Polarity	Reversed-phase chromatography RT, sec			Hiydrophilic interaction chromatography RT, sec			Identity	Identification level according to MS
		Phenyl-hexyl	BEH	Gold	Nucleodur	ZicHILIC	PGC		
105.0331	Positive	-	-	-	-	192	-	PCYP artifact	3
146.0812	Positive	-	-	-	-	61	-	Unknown	4
158.0812	Positive	-	-	-	-	83, 126	-	Unknown	4
176.0918	Positive	31	-	-	171	126	-	Unknown	4
218.1539	Positive	-	286	-	-	224	-	PCYP-M (*N*-dealkyl-) (M5)	3
220.1696	Positive	-	-	-	-	247	-	Unknown	4
270.1851	Positive	-	-	316	241	-	322	PCYP-M (dehydro-) (M4)	3
271.1884	Positive	314	-	302	241	-	321	PCYP-M (dehydro-) isotope	3
272.2008	Positive	314	293, 313	298, 312	265	192	48	PCYP	1
273.2041	Positive	314	293, 313	298,	265	192	-	PCYP isotope	3
274.2164	Positive	314	297, 314	297	-	195	-	PCYP isotope	3
275.2197	Positive	314	297, 314	297	269	194	-	PCYP isotope	3
276.223	Positive	314	-	-	269	-	-	PCYP isotope	3
286.1801	Positive	214, 235	-	-	-	-	285	PCYP-M (oxo-) (M9)	3
286.181	Negative	-	-	-	308	-	-	Unknown	4
288.1957	Positive	280, 302, 255	223, 255, 277, 297	222, 255, 277, 295	344	222, 259, 24	46	PCYP-M (hydroxy-) (M1, M2, M3)	3
289.199	Positive	-	255, 277, 223	31, 255, 277,295	-	1[illegible], 222, 259, 24	-	PCYP-M (hydroxy-) isotope	3
290.2113	Positive	306	299, 280	297, 281	293	266	-	PCYP-M (ring opened hydroxy) (M12)	3
291.2146	Positive	-	-	280, 296	-	20[illegible]	-	PCYP-M (ring opened hydroxy)) isotope	3
304.1907	Positive	202, 309	30, 281, 300	31, 282, 298	332	[illegible]84	-	PCYP-M (dihydroxy) (M6, M14)	3
305.1939	Positive	309	280, 299	282, 298	-	234, 252	-	PCYP-M (dihydroxy) isotope	3
305.6789	Negative	-	-	-	27[illegible]	-	-	Unknown	4
306.2063	Positive	216	-	-	-	-	-	PCYP-M (ring opened dihydroxy) (M13)	3
566.5508	Positive	-	-	-	-	42	-	Unknown	4

Table S5

Significant features in rat plas (sheet 2)

m/z	Polarity	Reversed-phase chromatography RT, sec			Hydrophilic interaction chromatography RT, sec			Identity	Identification level according to MSI
		Phenyl-hexyl	BEH	Gold	Nucleodur	ZicHILIC	PGC		
146.0602	Positive	244	-	-	-	70	-	Unknown	4
147.0635	Positive	244	-	-	-	-	-	Unknown	4
148.0965	Positive	-	-	-	-	456	-	Unknown	4
162.0551	Positive	-	-	-	-	230	-	Quinoline-2,4-diol	2 (NIST msms)
163.0584	Positive	-	-	-	-	230	-	Quinoline-2,4-diol isotope	2 (NIST msms)
179.0536	Negative	-	-	194	-	-	-	Unknown	4
185.0437	Positive	-	-	-	-	303	-	Kynurenic acid	2 (massbank)
186.0470	Positive	-	-	-	-	303	-	Kynurenic acid isotope	2 (massbank)
189.0582	Positive	156	-	-	-	67	322	Unknown	4
190.0503	Negative	-	-	-	-	176	-	Unknown	4
190.0614	Positive	-	-	-	-	67	-	Unknown	4
208.1183	Negative	-	-	-	-	398	-	Unknown	4
208.4951	Negative	-	-	-	-	320	-	Unknown	4
208.9913	Negative	-	-	-	-	320	-	Unknown	4
211.0401	Positive	156	-	-	-	-	48	Unknown	4
215.0013	Negative	-	-	-	-	301	-	Unknown	4
219.9996	Negative	-	-	-	-	248	-	Unknown	4
220.9920	Negative	-	-	-	-	248	-	Unknown	4
221.0448	Negative	226	-	-	-	-	-	Unknown	4
221.1215	Positive	-	164	-	-	-	-	Unknown	4
239.9966	Negative	203, 151	-	-	256	232, 271	-	Unknown	4
240.0539	Positive	-	-	-	-	263	-	Unknown	4
240.9999	Negative	-	-	-	256, 294		-	Unknown	4
242.0118	Positive	152	165	159	294	271	-	Unknown	4
242.0122	Negative	-	-	-	260	245	-	Unknown	4
242.0123	Negative	157	-	-	-	-	-	Unknown	4
242.1000	Positive	-	164	-	-	-	-	Unknown	4
243.0155	Negative	-	-	-	260	-	-	Unknown	4
243.0977	Positive	-	-	-	-	472	-	Unknown	4
243.1817	Positive	-	-	-	-	425	-	Unknown	4
245.0924	Negative	-	-	-	-	242	-	Unknown	4
247.9776	Negative	238	-	-	-	-	-	Unknown	4
250.1439	Positive	-	-	-	-	[illegible]	-	PCYP artifact	3
253.0500	Negative	-		265	-	-	-	Daidzein	2 (massbank)
254.1613	Positive	-	151	-	-	-	-	Unknown	4
255.0653	Positive	-	-	-	-	22[illegible]	-	Daidzein	2 (massbank)
255.0743	Positive	-	94	-	-	-	-	Unknown	4
260.0588	Positive	186	-	-	-	-	-	Unknown	4
269.0449	Negative	-	308, 324	315	-	-	-	Genistein	2 (massbank)
270.0483	Negative	336	-	-	-	-	-	Unknown	4
271.0390	Negative	-	-	-	-	226	-	Unknown	4
271.0819	Negative	-	-	-	-	107	-	Unknown	4
271.1884	Positive	-	308	300	-*	-	-	PCYP-M (dehydro-) isotope	3
276.1920	Positive	-	153	-	-	-	-	Unknown	4
281.1136	Negative	266	-	-	-	329	-	Unknown	4
283.1290	Positive	266	-	-	-	-	-	Unknown	4
283.9306	Negative	207, 238	-	-	-	-	-	Unknown	4
284.1242	Positive	-	-	-	-	468	-	Unknown	4
285.2286	Positive	-	-	-	-	456	-	Unknown	4
285.8645	Negative	266	-	-	-	-	-	Unknown	4
286.0793	Positive	-	-	289	-	455	-	Unknown	4
287.1139	Positive	208	214	210	-	-	-	Unknown	4
288.0901	Positive	218	-	-	278	247	-	Unknown	4
288.1957	Positive	-	-	-	-	222	-	PCYP-M (HO-) (M3)	3
289.0324	Negative	-	-	-	-	354	-	Unknown	4
290.9998	Negative	-	-	-	-	246	-	Unknown	4
293.0212	Positive	-	271	-	-	-	-	Unknown	4
297.0973	Negative	-	-	-	-	148	-	Unknown	4
299.0916	Positive	-	355	-	-	-	-	Unknown	4
299.8808	Negative	122	-	-	-	-	-	Unknown	4
302.1422	Positive	-	-	-	-	68	-	Unknown	4
302.2108	Positive	-	-	-	-	366	-	Unknown	4
303.1704	Positive	-	-	-	-	271	-	Unknown	4
303.2109	Positive	-	-	-	-	366	-	Unknown isotope	4
304.0070	Negative	-	-	-	-	320	-	Unknown	4
304.1910	Positive	305	286, 301	284, 299	296	232	-	PCYP-M (di HO-) (M6)	3
305.1942	Positive	305	-	-	-	-	-	PCYP-M (di HO-) isotope	3
306.1701	Positive	204	-	-	-	296	-	PCYP-M (HO + pyrrolidin cleavage with oxidation to COOH) (M16)	3

Table S3

307.0578	Positive	312	-	-	-	-	-	Unknown	4
307.0749	Positive	249	232	227	-	-	-	Unknown	4
309.0067	Negative	-	-	-	-	247	-	Unknown	4
310.0720	Positive	218	-	-	-	247	-	Unknown	4
311.2119	Positive	320	328, 335	322	-	218	-	Unknown	4
312.2151	Positive	-	-	-	-	218	-	Unknown isotope	4
316.1546	Negative	-	-	-	-	236	-	Unknown	4
317.0329	Negative	-	-	-	-	241	-	Unknown	4
318.1702	Positive	222	228, 31	225, 32	251, 300	195, 233, 318	-	PCYP-M (di HO-, oxo) (M10)	3
319.1266	Positive	245	-	-	-	-	-	Unknown	4
319.1734	Positive	222	-	-	300	233, 318	-	PCYP-M (di HO-, oxo) isotope	3
320.1859	Positive	214, 232	221, 30	219, 31	384	264, 302	-	PCYP-M (tri HO-) (M15)	3
321.1892	Positive	214, 232	221, 235	219, 261	-	302	-	PCYP-M (tri HO-) isotope	3
322.2015	Positive	193	204	201	-	-	-	Unknown	4
323.2048	Positive	192	-	-	-	296	-	Unknown isotope	4
324.9200	Negative	-	-	-	-	234	-	Unknown	4
325.0855	Positive	206	199	194	-	305	-	Unknown	4
326.0460	Positive	-	-	-	-	246	-	Unknown	4
327.1079	Negative	-	-	-	-	176	-	Unknown	4
327.2069	Positive	243	-	-	-	273	-	Unknown	4
331.0851	Negative	-	-	-	-	235	-	Unknown	4
332.1491	Positive	-	-	-	-	86	-	Unknown	4
334.0101	Negative	-	-	-	-	226	-	Unknown	4
334.1108	Positive	-	-	-	-	69	-	Unknown	4
334.1651	Positive	188, 248	-	-	-	115, 324	-	PCYP-M (tri HO-, oxo) (M11)	3
335.0223	Positive	-	252	246	-	324	-	PCYP-M (tri HO-, oxo) isotope	3
335.9012	Negative	235	-	-	-	-	-	Unknown	4
336.1807	Positive	176, 197	186, 202	182	-	323, 341	-	PCYP-M (tetra HO-) (M8)	3
337.0379	Negative	-	-	-	255	-	-	Unknown	4
337.1807	Positive	176	-	-	-	323, 341	-	PCYP-M (tetra HO-) isotope	3
338.0414	Negative	-	-	-	-	241	-	Unknown	4
341.1861	Positive	210	-	-	-	375	-	Unknown	4
343.2019	Positive	-	-	-	-	321	-	Unknown	4
343.8885	Negative	182	-	-	-	-	-	Unknown	4
346.1433	Positive	-	-	-	-	245	-	Unknown	4
347.1466	Positive	-	-	-	-	245	-	Unknown	4
347.2541	Positive	-	-	-	-	74	-	Unknown	4
349.0703	Negative	-	-	-	-	248	-	Unknown	4
351.0858	Positive	-	174	-	-	176	-	Unknown	4
352.0487	Positive	-	-	-	-	225	-	Unknown	4
352.0569	Negative	-	-	-	214	-	-	Unknown	4
353.0329	Negative	-	-	-	-	245	-	Unknown	4
356.1471	Positive	247	-	226	-	-	-	Unknown	4
360.1920	Positive	-	242	-	-	202, 344	-	Unknown	4
361.1952	Positive	-	-	-	-	344	-	Unknown isotope	4
365.2357	Negative	-	-	-	-	146	-	Unknown	4
367.0484	Negative	-	-	-	-	240	-	Unknown	4
371.1338	Negative	225	-	-	-	-	-	Unknown	4
372.1212	Positive	-	-	-	-	114	-	Unknown	4
376.1426	Positive	271	-	-	-	-	-	Unknown	4
377.0690	Negative	-	-	-	200	-	-	Unknown	4
380.0548	Negative	-	-	-	-	246	-	Unknown	4
390.1762	Positive	225	214	-	-	-	-	Unknown	4
391.0682	Negative	-	-	-	-	223	-	Unknown	4
393.2862	Positive	-	411	-	-	-	-	Unknown	4
402.2102	Positive	-	522	-	-	-	-	Unknown	4
402.2103	Positive	-	-	510	-	-	-	Unknown	4
403.2134	Positive	-	522	-	-	-	-	Unknown isotope	4
404.2060	Positive	-	172	167	-	-	-	Unknown	4
410.1293	Negative	-	-	-	294	-	-	Unknown	4
426.1333	Positive	-	-	-	-	247	-	Unknown	4
453.0057	Negative	-	-	-	260	-	-	Unknown	4
462.0523	Negative	-	-	-	-	320	-	Unknown	4
464.2285	Positive	-	219	216	-	393	-	PCYP-M (HO-glucuronide) (M18)	3
465.2155	Positive	317	292	290	-	360	-	Unknown	4
466.2189	Positive	-	292	290	-	360	-	Unknown isotope	4
563.2661	Positive	-	594	-	-	-	-	Unknown	4
564.2695	Positive	-	594	562	-	-	-	Unknown isotope	4
573.3299	Negative	-	-	-	-	139	-	Unknown	4
605.2931	Positive	-	-	-	384	-	-	Unknown	4
573.3299	Negative	-	-	-	-	139	-	Unknown	4

Table S3

Significant features in rat plas (sheet 3)

m/z	Polarity	Reversed-phase chromatography RT, sec			Hydrophilic interaction chromatography RT, sec			Identity	Identification level according to MSI
		Phenyl-hexyl	BEH	Gold	Nucleodur	ZicHILIC	PGC		
146.0599	Positive	-	-	-	-	71	-	Quinolin-2-ol	2 (NIST msms)
172.9909	Negative	-	-	-	-	-		Unknown	4
174.1852	Positive	-	-	-	316	-	-	Unknown	4
175.1885	Positive	-	-	-	316	-	-	Unknown Isotop	4
189.0579	Positive	-	-	-	110	66	-	3-Methyladipic acid	2 (NIST msms)
189.0579	Positive	-	-	-	-	67	-	Unknown	4
190.0613	Positive	-	-	-	-	67	-	Unknown	4
200.2372	Positive	-	-	-	273	-	-	Unknown	4
202.1801	Positive	-	-	-	90	-	-	Unknown	4
202.2164	Positive	-	-	-	304	-	322	Unknown	4
203.1835	Positive	-	-	-	92	-	48	Unknown Isotop	4
207.1589	Positive	-	-	-	84	-	-	Triethylene glycol monobutyl ether	2 (NIST msms)
212.1182	Positive	-	-	238	-	-	-	1,3-Diphenylguanidine	2 (massbank)
218.2114	Positive	-	-	-	295	-	-	Unknown	4
218.2114	Positive	-	-	-	307	-	-	Unknown	4
230.2113	Positive	-	-	-	89		-	Unknown	4
231.2147	Positive	-	-	-	89		-	Unknown Isotop	4
234.2063	Positive	-	-	-	295	-	-	Unknown	4
235.2096	Positive	-	-	-	295		-	Unknown Isotop	4
236.2128	Positive	-	-	-	295	-	-	Unknown Isotop	4
256.1906	Positive	-	-	-	143	-	-	Pentaethylen glycol	2 (NIST msms)
259.2461	Positive	-	-	-	87	-	-	Unknown	4
262.2375	Positive	-	-	-	284	-	-	Unknown	4
263.2409	Positive	-	-	-	284	-	-	Unknown Isotop	4
268.1038	Positive	35,61	-	-	-	248		Adenosin	2 (NIST msms)
269.0878	Positive	-	-	-	-	330		Unknown	4
276.2685	Positive	-	-	-	144	178		Unknown	4
290.2687	Positive	-	-	-	275			Unknown	4
291.2721	Positive	390	-	-	-	-		Unknown	4
304.1904	Positive	306	-	282	306	235		PCYP-M (di HO-) (M6)	3
305.1939	Positive	306	-	-	-	235		PCYP-M (di HO-) isotope	3
309.1010	Negative	-	-	-	307	215		Unknown	4
310.1493	Positive	167	-	-	-	-		Unknown	4
312.0945	Negative	-	-	-	-	248		Unknown	4
312.2015	Positive	-	-	-	154			Unknown	4
318.1699	Positive	-	-	-	-	237		PCYP-M (di HO-, oxo) (M7)	3
320.1856	Positive	215	32	32	-	290		PCYP-M (tri HO-) (M10)	3
321.0432	Negative	-	-	-	-	206		Unknown	4
321.1886	Positive	215	-	-	-	-		PCYP-M (tri HO-) isotope	3
328.3845	Positive	-	-	-	-	160		Unknown	4
357.1747	Negative	-	-	-	102	-		Unknown	4
372.1660	Negative	-	-	-	107	-		Unknown	4
388.1610	Negative	-	-	-	110	-		Unknown	4
405.2949	Positive	-	-	-	295	-		Unknown	4
416.3740	Negative	-	-	-	-	159		Unknown	4
562.5880	Negative	24	24	-	-	-		Unknown	4

Table S3

3.3. Comparison of Three Untargeted Data Processing Workflows for Evaluating LC-HRMS Metabolomics Data

(DOI: 10.3390/metabo10090378)[91]

(DOI: 10.3390/metabo10110432)[92]

Author Contributions:

Selina Hemmer conducted and evaluated the experiments as well as composed the manuscript; Sascha K. Manier developed the used code for R and assisted scientific discussions; Svenja Fischmann and Folker Westphal provided the investigated new psychoactive substance; Lea Wagmann and Markus R. Meyer assisted with the design of the experiments, the interpretation of the analytical experiments, and scientific discussions.

metabolites

MDPI

Article

Comparison of Three Untargeted Data Processing Workflows for Evaluating LC-HRMS Metabolomics Data

Selina Hemmer [1], Sascha K. Manier [1], Svenja Fischmann [2], Folker Westphal [2], Lea Wagmann [1] and Markus R. Meyer [1,*]

[1] Department of Experimental and Clinical Toxicology, Institute of Experimental and Clinical Pharmacology and Toxicology, Center for Molecular Signaling (PZMS), Saarland University, 66421 Homburg, Germany; selina.hemmer@uks.eu (S.H.); sascha.manier@uks.eu (S.K.M.); lea.wagmann@uks.eu (L.W.)

[2] State Bureau of Criminal Investigation Schleswig-Holstein, 24116 Kiel, Germany; Svenja.Dr.Fischmann@polizei.landsh.de (S.F.); Folker.Dr.Westphal@polizei.landsh.de (F.W.)

* Correspondence: markus.meyer@uks.eu

Received: 21 August 2020; Accepted: 21 September 2020; Published: 21 September 2020

Abstract: The evaluation of liquid chromatography high-resolution mass spectrometry (LC-HRMS) raw data is a crucial step in untargeted metabolomics studies to minimize false positive findings. A variety of commercial or open source software solutions are available for such data processing. This study aims to compare three different data processing workflows (Compound Discoverer 3.1, XCMS Online combined with MetaboAnalyst 4.0, and a manually programmed tool using R) to investigate LC-HRMS data of an untargeted metabolomics study. Simple but highly standardized datasets for evaluation were prepared by incubating pHLM (pooled human liver microsomes) with the synthetic cannabinoid A-CHMINACA. LC-HRMS analysis was performed using normal- and reversed-phase chromatography followed by full scan MS in positive and negative mode. MS/MS spectra of significant features were subsequently recorded in a separate run. The outcome of each workflow was evaluated by its number of significant features, peak shape quality, and the results of the multivariate statistics. Compound Discoverer as an all-in-one solution is characterized by its ease of use and seems, therefore, suitable for simple and small metabolomic studies. The two open source solutions allowed extensive customization but particularly, in the case of R, made advanced programming skills necessary. Nevertheless, both provided high flexibility and may be suitable for more complex studies and questions.

Keywords: untargeted metabolomics; LC-HRMS; data processing; feature detection; A-CHMINACA

1. Introduction

Metabolomics is defined as the analysis of the whole metabolome of a biological system and therefore, aims to detect as many metabolites as possible in a biological sample [1,2]. However, the metabolic profile is not limited to endogenous metabolites but also metabolites of exogenous sources like drugs, diet, and gut microbiota may be added in. Furthermore, metabolomic studies can be divided into two major strategies, untargeted and targeted approaches. Targeted metabolomics usually aims to detect and quantify specific metabolites of known structures. The untargeted or global approach usually aims to identify as many metabolites as possible without having any previous knowledge about them [1,3].

Due to its high selectivity and sensitivity, liquid chromatography coupled to high-resolution mass spectrometry (LC-HRMS) is currently the most commonly applied analytical technique in metabolomics [4–6]. To correctly interpret differences in specific metabolites and to gain a proper

biological interpretation, a reliable and suitable entire approach is necessary [4,5]. The part of data processing includes a series of steps such as peak detection, peak alignment, baseline correction, and annotation [7–9]. Data processing of LC-HRMS raw data is a key step in untargeted metabolomic studies, which establishes a sound basis to accurately identify significant changes. It involves reducing the complexity of raw data by extracting features, and usually transforming them in order to subsequently perform adequate statistical tests [9,10].

A variety of software solutions are available for untargeted data processing, such as the open source software XCMS, MZmine, OpenMS [11], MetAlign, MetaboAnalyst [12] and the commercial software MarkerView, Compound Discoverer (CD), MetaboScape etc. In the case of open source software, modules are often based on the programming language R [7].

Since the underlying algorithms differ, it is very likely that the outcome of a metabolomic study might vary upon the tools used. Li et al. compared the performance of five software solutions (MS-Dial, MZmine, XCMS, MarkerView, and CD) on a benchmark dataset from standard mixtures. All five software solutions revealed similar performance in detecting true features. Nevertheless, to select true discriminating markers, they recommended the combination of MZmine 2 and XCMS [13]. Fernández-Ochoa et al. determined that Agilent Profinder showed good quality of the graphs and was characterized by its ease of use, whereas the R pipeline seemed to be better suited for studies with a large number of samples [7].

Since further studies are missing and the selection of an appropriate tool is essential for the quality and outcome of the statistical evaluation, the present study aimed to compare three different data processing workflows to investigate LC-HRMS data of an untargeted metabolomics study, namely the commercially available software CD 3.1, the open source online tool XCMS Online in combination with MetaboAnalyst 4.0 (XCMS/MetaboAnalyst), and a manually programmed tool using the language R based on different R packages [14]. XCMS, MetaboAnalyst, and the R script were chosen as they were identified as suitable and were successfully used in previous studies [15–17]. Simple but highly standardized datasets for evaluation should be used by incubating pooled human liver microsomes (pHLM) with the synthetic cannabinoid A-CHMINACA (1(-cyclohexylmethyl)-*N*-tricyclo[3.3.1.1^{3,7}]dec-1-yl-1H-indazole-3-carboxamide). The outcome of each workflow should be evaluated by its number of significant features, the quality of the peaks, and the results of multivariate statistics. Additionally, the metabolite profile of A-CHMINACA in pHLM should be elucidated.

2. Results and Discussion

2.1. Study Design

Due to the ease of use and low variability of individual pHLM incubations and the fact that it is a very well characterized in vitro model for drug metabolism studies, incubations of pHLM with the synthetic cannabinoid A-CHMINACA were prepared to generate simple datasets [18]. The incubation mixtures were then analyzed using LC-HRMS/MS and finally, three different software tools for untargeted data processing were applied to identify significant features. Software evaluation in this study included the commercial software CD 3.1, which was developed for the used type of MS instrument; open source software workflows including a combination of XCMS Online and MetaboAnalyst 4.0; and a manually programmed tool using R. While XCMS-based software tools might be one of the best solutions for LC-HRMS/MS untargeted metabolomics, XCMS was used as a preprocessing tool in the case of the two open source workflows [15,19–22]. After data processing, significant features were identified and the metabolic fate of A-CHMINACA in pHLM was elucidated. The three untargeted data processing workflows were extensively evaluated with regards to their number of significant features, the peak quality of the significant feature, their false positive rate, and the results of the multivariate statistics.

2.2. Untargeted Metabolomics

2.2.1. Parameter Optimization for the Three Different Workflows of Untargeted Metabolomics

In untargeted data processing, the optimization of various parameters is important to allow for the detection of chromatographic peaks, construct extracted ion chromatograms (EICs), annotate features, and for chromatogram alignment [19]. Since the two open source software tools XCMS/MetaboAnalyst and R are not already optimized, peak picking and alignment parameters were optimized using a previously optimized workflow [15]. The optimized XCMS parameters are summarized in Table S1. Using the R workflow, all eight parameters could be transferred in exactly the same way. For XCMS Online, prefilter 1 was limited up to 10. If this parameter was greater than 10, 10 was used for XCMS Online. Additionally, the parameter bandwidth could only be specified in positive integer numbers in XCMS Online, so if this parameter was less than 1, 1 was used. Since the commercial software CD was developed specifically in combination with the used MS instrument type, an already existing workflow for untargeted metabolomics, namely "Untargeted Metabolomics with statistics detect unknowns with ID using Online Database and mzLogic", was chosen without changing any parameters.

2.2.2. Comparison of Significant Features of the Three Different Workflows

Univariate statistics was done using one-way analysis of variance (ANOVA) for all three workflows (Figure S1). False positive results were prevented using Bonferroni correction as a multiple testing correction technique [23]. Since the settings of XCMS Online did not allow a change from the Kruskal–Wallis test to ANOVA in multi-group comparisons for no evident reason, XCMS Online was only used for peak picking and alignment. The resulting table was then reduced to the peak areas and retention times between 1 and 10 min. The entire statistical evaluation was performed using MetaboAnalyst 4.0. Visual inspection of the plotted ANOVA results (Figure S1) of the two open source workflows revealed that they were similar to each other concerning significant features and their corresponding *p*-values. In contrast to this, differential analysis over all three groups was not possible using CD, because the software does not allow one to do a statistical evaluation of more than two groups. Thus, statistical evaluation using a Welch *t*-test in combination with the corresponding fold change had to be performed for blank vs. low, blank vs. high, and low vs. high. A feature was considered significant if it was significant between one of the two groups. In terms of number of significant features, 15 significant features were obtained for CD, 32 for the XCMS/MetaboAnalyst solution, and 28 for R using normal phase chromatography and positive ionization mode. In the case of using a reversed phase chromatography and positive ionization mode, 5 significant features were received for CD, 13 for XCMS/MetaboAnalyst, and 11 for R. None of the analyses indicated significant features using negative ionization mode. The Venn diagram in Figure 1A shows the composition of all significant features obtained after using the three data processing workflows and the two analytical columns. In total, 11 of the significant features were detected after using each of the three workflows, 31 significant features were determined after using both open source workflows, and 17 after using CD. While the manually programmed R tool used the R package CAMERA to identify isotopes and adducts in the dataset, CD annotated neither isotopes nor adducts. In CD, isotopes and adducts were merely labeled in the spectrum of the related compound, but not listed in the compound list and therefore, not annotated as significant features. Taking this into account, the number of significant features identified by the two open source workflows that are neither isotopes nor adducts could be reduced to 9 (Figure 1B).

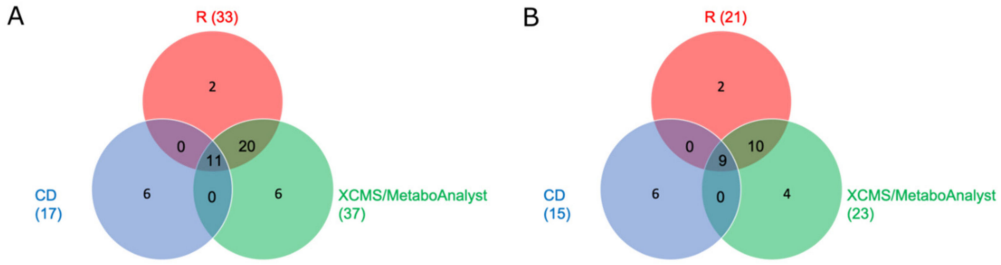

Figure 1. Comparison of the significant features of the three data processing workflows R (red), XCMS Online combined with MetaboAnalyst (green), and Compound Discoverer (CD, blue) displayed as Venn Diagram; (**A** = with isotopes and adducts; **B** = without isotopes and adducts).

In addition to the number of significant features, the three workflows were also evaluated according to the peak shape quality of these features. Since the extracted ion chromatogram (EIC) of some detected significant features appeared to be false positive hits, the significant features were divided into true and false features based on the peak shape quality of their EIC. Therefore, peak quality was divided into two main categories. The first category included non-existent group differences, which means that in the EIC of the respective significant features, there was no clear separation of peak intensity between the four groups Blank, Low, High, and QC. The second category included the non-correct peak integration, which means that in the EIC, the integrated peak could not be separated from the baseline. By comparing the quality of the peaks based on the two categories mentioned above, the overall true features for the three different workflows were 17 for CD, 28 for XCMS Online/MetaboAnalyst, and 24 for R. The significant features detected by CD were all identified as true features, which can be explained by the fact that this workflow does not show isotopes or adducts as significant features. Furthermore, in comparison to the two open source workflows, CD used a fold change of 1 in addition to the *p*-value in order to filter the features in one of the group comparisons. The true features are listed in Tables 1 and 2.

Table 1. Overview of significant features of A-CHMINACA after untargeted analysis using reversed-phase chromatography in positive mode of all three workflows.

Feature	Measured Mass, *m/z*	Retention Time, s	Found with	Identity
M296T431	296.1768	431	XM, CD	**A-CHMINACA-M (*N*-dealkyl-)**
M424T443	424.2610	443	R, XM	**A-CHMINACA-M (di-HO-)**
M408T474	408.2661	474	R, XM, CD	**A-CHMINACA-M (HO-)**
M409T474	409.2693	474	R, XM	A-CHMINACA-M (HO-) ^{13}C isotope
M430T474	430.2481	474	R, XM	A-CHMINACA-M (HO-) adduct $[M + Na]^+$
M392T547	392.2710	547	R, XM, CD	A-CHMINACA
M393T547	393.2743	547	R, XM	A-CHMINACA ^{13}C isotope
M394T547	394.2775	547	R, XM	A-CHMINACA $^{13}C_2$ isotope
M414T547	414.2530	547	R, XM, CD	A-CHMINACA adduct $[M + Na]^+$
M415T547	415.2562	547	R, XM	A-CHMINACA adduct $[M + Na]^+$ ^{13}C isotope
M430T547	430.2270	547	R, XM, CD	A-CHMINACA adduct $[M + K]^+$
M437T547	437.3290	547	R, XM	A-CHMINACA adduct
M438T547	438.3320	547	XM	A-CHMINACA adduct ^{13}C isotope

Features are ordered by retention time and *m/z*. Isotopes were annotated by the R package CAMERA and not further identified. Metabolites are indicated by bold font. XM = XCMS Online/MetaboAnalyst, CD = Compound Discoverer.

Table 2. Overview of significant features of A-CHMINACA after untargeted analysis using a normal phase (HILIC) column in positive mode of all three workflows.

Feature	Measured Mass, *m/z*	Retention Time, s	Found with	Identity
M355T70	355.2392	70	R, XM	Unknown
M430T71	430.2270	71	XM	A-CHMINACA adduct $[M + K]^+$
M392T72	392.2710	72	R, XM, CD	A-CHMINACA
M393T72	393.2743	72	R, XM	A-CHMINACA ^{13}C isotope
M394T72	394.2775	72	R, XM	A-CHMINACA $^{13}C_2$ isotope
M395T72	395.2809	72	R, XM	A-CHMINACA $^{13}C_3$ isotope
M356T74	356.1802	74	XM	Unknown
M135T76	135.1174	76	CD	A-CHMINACA artifact (adamantyl-ring)
M408T83	408.2661	83	R, XM, CD	**A-CHMINACA-M (HO-)**
M409T83	409.2693	83	R, XM	A-CHMINACA-M (HO-) ^{13}C isotope
M296T86	296.1768	86	R, XM, CD	**A-CHMINACA-M (*N*-dealkyl-)**
M297T86	297.1800	86	XM	A-CHMINACA-M (*N*-dealkyl-) ^{13}C isotope
M408T88	408.2661	88	CD	**A-CHIMINACA-M (HO-)**
M422T92	422.2453	92	R, XM	**A-CHIMINACA-M (HO, Oxo)**
M424T93	424.2610	93	CD	**A-CHMINACA-M (di-HO-)**
M424T96	424.2610	96	R, XM, CD	**A-CHMINACA-M (di-HO-)**
M425T96	425.2644	96	R, XM	A-CHMINACA-M (di-HO-) ^{13}C isotope
M274T113	274.1559	113	R, XM	**A-CHMINACA-M (HO-) (*N*-dealkyl-)**
M312T115	312.1715	115	R, XM, CD	**A-CHMINACA-M (HO-) (*N*-dealkyl-)**
M146T116	146.0819	116	CD	A-CHMINACA artifact (indazole-core)
M440T117	440.2561	117	CD	**A-CHMINACA-M (tri-HO-)**
M440T122	440.2565	122	CD	**A-CHMINACA-M (tri-HO-)**
M176T135	176.0924	135	R, XM, CD	Unknown
M158T135	158.0818	135	R, XM, CD	$[M + H - H_2O]$+175.086
M188T170	188.1288	170	R, XM, CD	Unknown
M158T174	158.0818	174	R, XM	$[M + H - H_2O]$+175.086
M176T174	176.0924	174	R, XM, CD	Unknown
M341T219	341.2447	219	R, XM	Unknown
M313T253	313.2649	253	R, XM	Unknown
M248T270	248.2382	270	XM	Unknown

Features are ordered by retention time and *m/z*. Isotopes were annotated by the R package CAMERA and not further identified. Metabolites are indicated by bold font. XM = XCMS Online/MetaboAnalyst, CD = Compound Discoverer.

2.2.3. Comparison of Multivariate Statistics of the Three Different Software Workflows

In addition to univariate statistics, datasets are usually also analyzed using multivariate methods to identify the largest changing features and specific signatures in the data [2]. In this study, principal component analysis (PCA) and hierarchical clustering were used to evaluate differences between the three workflows.

PCA, as a non-supervised method, does not use any group information to find the principal component. It is a data reduction technique, which enables high dimensional datasets to be reduced to a few major principal components (PC) [24]. The scores of these components, which are the weighted sum of the contribution of each metabolite to a principal component, are plotted. It can be seen that each incubation group is distinct from another one. In addition to the score plot, the loading plot provides information on which metabolites are contributing the most to the separations between groups [24]. The results of the scores of PCA of all three workflows are shown in Figure 2. The corresponding scree plots are shown in Figure S2. Regarding the variance of the first principal component (PC1), differences between the three workflows became visible. While PC1 accounts for 97% of variance in R, it dropped to 60.6% in CD when using a PhenylHexyl column in positive ionization mode. One explanation for this difference could be the different peak picking parameters. While the two open source workflows are highly adaptable methods regarding the optimization of parameters, CD is a black box with limited possibilities for optimization. Another explanation for the different PC1 could be that R and CD revealed a different amount of significant features. In contrast to the two open source workflows, CD did not detect any isotopes or adducts of the parent compound and its metabolites as significant features. This led to a low amount of compounds in relation to other substances within the incubation mixture and therefore, the variability between the group Blank and the groups Low and High are much higher. Figure S3 shows an example of the scores of PCA of the

two open source workflows without isotopes and adducts using a PhenylHexyl column and ESI in positive ionization mode.

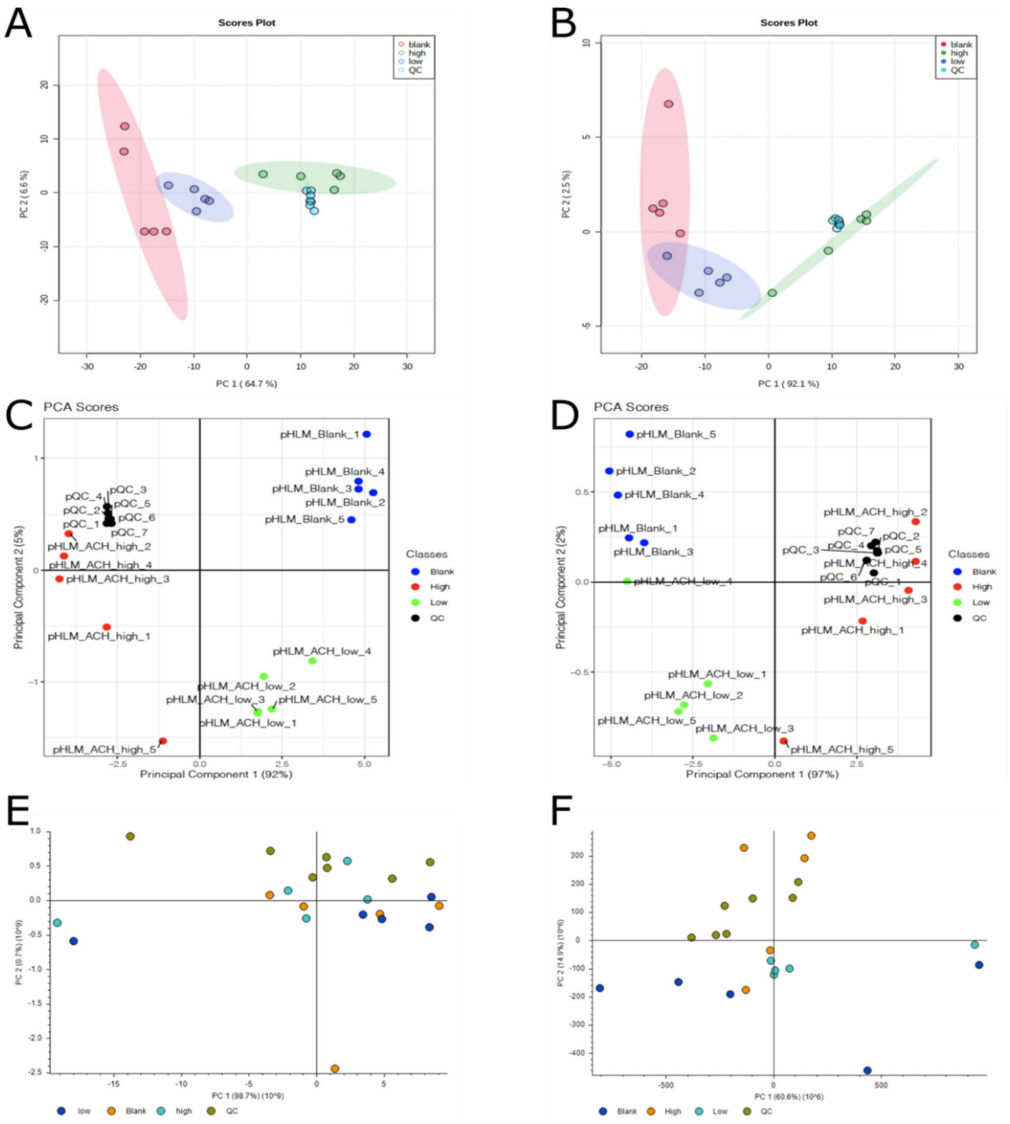

Figure 2. Scores of principal component analysis. (**A** = XCMS Online/MetaboAnalyst, HILIC column, positive mode; **B** = XCMS Online/MetaboAnalyst, PhenylHexyl column, positive mode; **C** = R, HILIC column, positive mode; **D** = R, PhenylHexyl column, positive mode; **E** = Compound Discoverer, HILIC column, positive mode; **F** = Compound Discoverer, PhenylHexyl column, positive mode).

Another technique for statistical data analysis, which was used to assess the difference of the three workflows, was hierarchical clustering. Hierarchal cluster analysis refers to a specific family of distance-based procedures for cluster analysis. Clusters consist of objects that are less distant from each other than objects in other clusters. In untargeted metabolomic studies, heat maps of hierarchical clustering can be used to discover clustering patterns in the datasets. Figure 3 shows the resulting heatmaps for all three workflows. Except for the heatmap of CD when using a PhenylHexyl column, all other heatmaps showed a clear discrimination between samples from the group Blank and groups Low and High. Blank samples appear very close or within the cluster of samples from group Low. This could be explained by the concentration of the parent compound that was very low in group Low and therefore, this concentration could not sufficiently form as many metabolites as in group High. QC samples belonged to the cluster of samples from group High. Since pooled sample QC consisted

of a mixture of every incubation sample, it contained the parent compound and its metabolites in a concentration of the samples from group High and Low. As shown in Figure 3F, only two samples of group High showed a clear discrimination between the other samples. The most likely explanation could be the low number of significant features. In comparison to the two open source workflows, CD detected only five significant features including the parent compound and four metabolites of A-CHMINACA, which showed their highest intensity in sample group High.

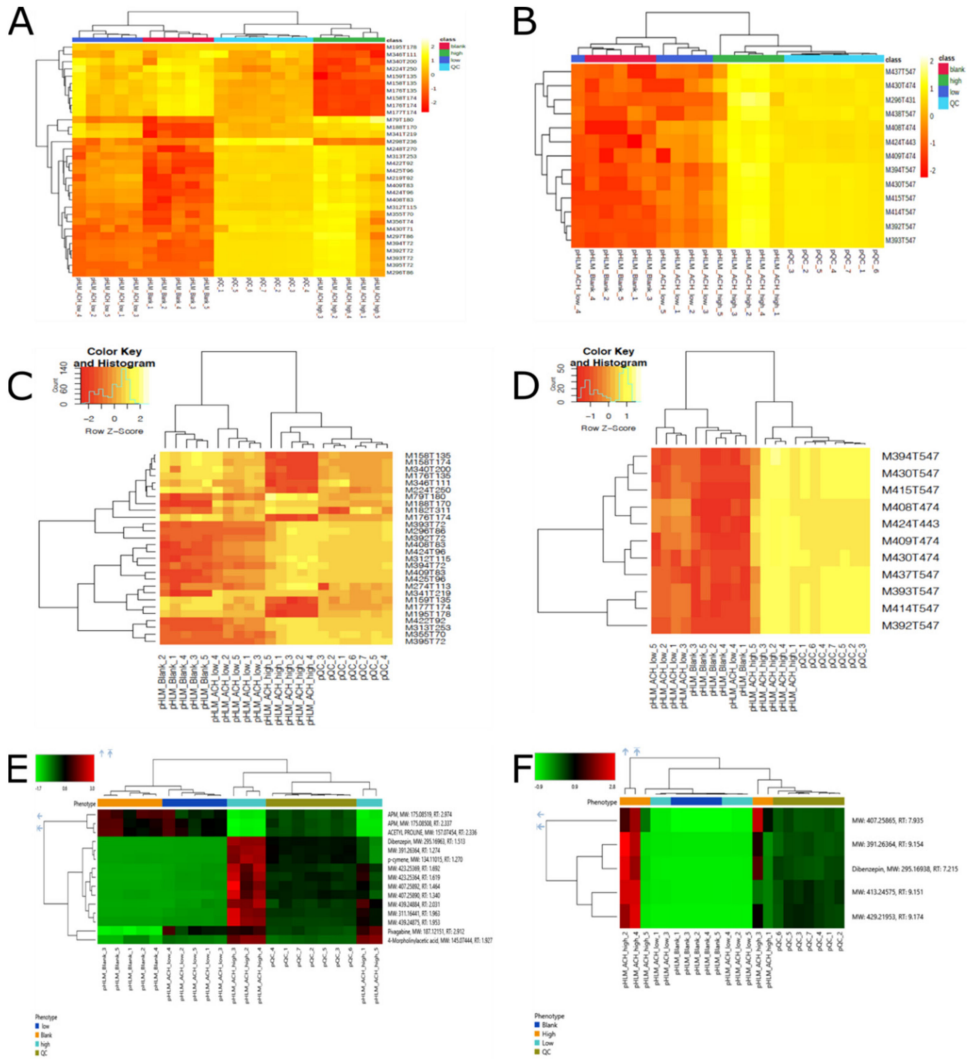

Figure 3. Heat map of hierarchical clustering. (**A** = XCMS Online/MetaboAnalyst, HILIC column, positive mode; **B** = XCMS Online/MetaboAnalyst, PhenylHexyl column, positive mode; **C** = R, HILIC column, positive mode; **D** = R, PhenylHexyl column, positive mode; **E** = Compound Discoverer, HILIC column, positive mode; **F** = Compound Discoverer, PhenylHexyl column, positive mode).

2.3. Targeted Metabolomics

2.3.1. Identification of Significant Features

The results of the identification of significant features are summarized in Tables 1 and 2. Annotated isotopes by CAMERA were not further analyzed. All other features were analyzed using the parallel reaction monitoring (PRM) method described below and the mass spectra are shown in Figure S4. Proposed structural formulas of the metabolites were deducted by comparing their spectra with those of the parent compound or reference spectra using the METLIN and Human Metabolome Database (HMBD) [25,26]. According to the Metabolomics Standards Initiative, this approach referred

to category two, which means a putatively annotated compound [25]. It applies to all of the identified compounds except for 10 significant features, which are yet unknown and therefore, belongs to category four. Concerning the incubations using A-CHMINACA, significant features consisted of eight isotopes, two artifacts, nine metabolites, and four adducts.

2.3.2. Metabolism of A-CHMINACA in pHLM

From here onwards, only exact masses will be used for characterization of the parent compound and its respective metabolites. The proposed phase I metabolic pathways of A-CHMINACA in pHLM are summarized in Figure 4. After incubation with pHLM, nine metabolites were found in total. The main metabolic reaction was the hydroxylation of the adamantyl-ring, which has already been described for other synthetic cannabinoids containing such structure [27,28]. Protonated ions for hydroxylation were observed with *m*/*z* 408.2661 ($C_{25}H_{34}N_3O_2$), *m*/*z* 424.2610 ($C_{25}H_{34}N_3O_3$), and *m*/*z* 440.2565 ($C_{25}H_{34}N_3O_4$) corresponding to mono-, di-, and trihydroxylated derivates, respectively. Monohydroxylation of the adamantyl-ring concerning M408T83 (PH: M408T474) was identified by the occurrence of the highly abundant fragment ion with *m*/*z* 151.1117 ($C_{10}H_{15}O$) (Figure S4). Additionally, the occurrence of the fragment ion with *m*/*z* 133.1012 ($C_{10}H_{13}$), which resulted from water loss on the adamantyl-ring, supported this theory. M424T96 revealed an unmodified indazole-3-carbaldehyde moiety by the occurrence of the fragment ion with *m*/*z* 241.1335 ($C_{15}H_{17}N_2O$), suggesting that this molecule was hydroxylated twice at the adamantyl-ring. The fragment ion with *m*/*z* 167.1067 ($C_{10}H_{15}O_2$) also strongly indicated that both hydroxylations occurred at the adamantyl-ring. Since M440T117 and M440T122 had the same MS2 spectra, both gave rise to a fragment ion with *m*/*z* 422.2438 ($C_{25}H_{32}N_3O_3$) indicating the loss of water from the species with *m*/*z* 440.2544 ($C_{25}H_{34}N_3O_4$). The observed fragment ion with *m*/*z* 167.1067 ($C_{10}H_{15}O_2$) corresponded to the dihydroxylation at the adamantyl-ring. The loss of water at the adamantyl-ring resulted in a fragment ion with *m*/*z* 149.0961 ($C_{10}H_{13}O$). Whereas the monohydroxylation and dihydroxylation could be found significant by all three workflows, trihydroxylation was only found by CD. In comparison to M424T96 (PH: M424T434), the feature M424T93 gave rise to a fragment ion with *m*/*z* 151.1117 ($C_{10}H_{15}O$), indicating that hydroxylation occurred once at the adamantyl-ring. Hydroxylation and oxidation at the adamantyl-ring of M422T92 were identified by the occurrence of fragmentation with *m*/*z* 165.0910 ($C_{10}H_{13}O_2$), while the fragment ion with *m*/*z* 404.2332 ($C_{25}H_{30}N_3O_2$) resulted from water loss on the adamantyl-ring. Features M296T86 (PH: M296T431), M274T113, and M312T115 were formed after *N*-dealkylation of the indazole-3-carbaldeyde moiety, which was also described by Erratico et al. [29] in the in vitro metabolism of AB-CHMINACA. Using the current incubation conditions, no phase II metabolites were expected to be formed and were thus, not detected.

2.4. Comparison of the Three Software Workflows

Based on the usage of the three software workflows during this study and the results in the previous sections, an overview of the pros and cons concerning important criteria is given in Table 3.

In comparison to the two open source workflows, the commercial software CD is characterized by its ease of use as a user-friendly black box. Thermo Fisher LC-HRMS/MS RAW files can be uploaded directly, and the desired workflow can be selected. The first results are available after a few mouse clicks. For statistical evaluation, only p-value and fold change have to be specified. Limitations for this kind of workflow are given by the preprocessing parameters, the normalization techniques, and the statistical analysis. Looking at the results in this study, this commercial software showed a low false positive rate for significant features, but neither isotopes nor adducts were detected that usually help in identifying significant features. Since CD is limited to its statistical test of Welch's t-test, it does not allow one to do statistical evaluation of more than two groups and therefore, it is not a suitable workflow for complex datasets. The open source combination of XCMS Online and MetaboAnalyst 4.0 allowed for more intervention in the processing steps than CD. In XCMS Online, almost all parameters could be taken over with a few exceptions and MetaboAnalyst allowed a wide range of statistical tests. The report

of MetaboAnalyst allowed an interpretation of the results. Both online tools were also based on the programming language R, but in contrast to the manually programmed R tool, less programming skills were required. The disadvantage is that due to the limited statistical test equipment of XCMS Online, a combination of these two online platforms was necessary. When comparing the results of the two open source workflows, both showed an almost identical false positive rate. The difference between the two workflows can only be seen in the user handling and the minimal difference in the number of significant features. The latter can be attributed to the not quite perfectly adjusted peak picking parameters using XCMS Online.

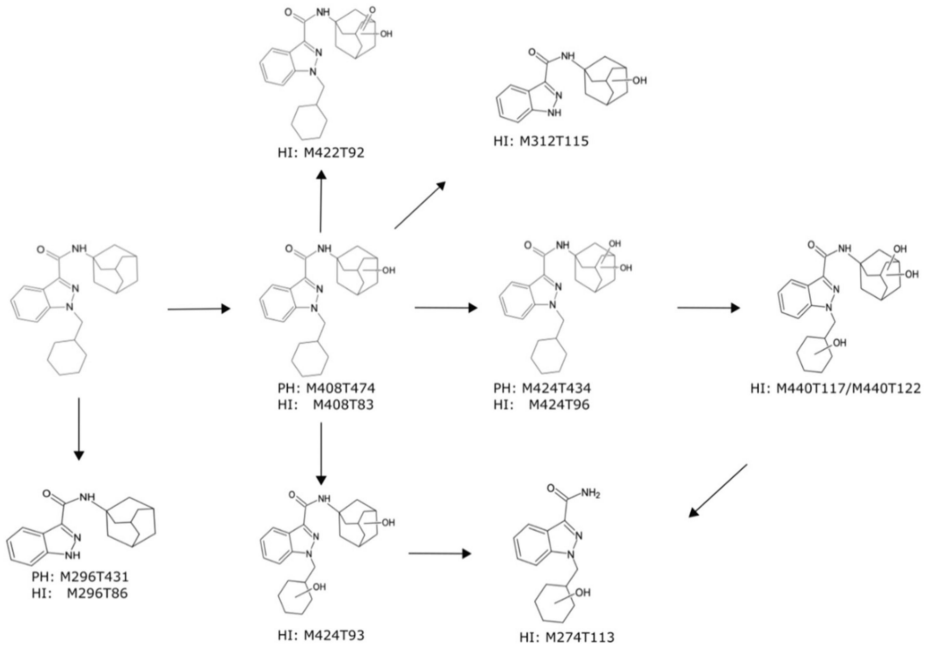

Figure 4. Metabolic pathways of A-CHMINACA in incubations with pooled human liver microsomes. Undefined hydroxylation position is indicated by unspecific bonds. Metabolites are annotated with their feature identity from untargeted metabolomics analysis. PH = PhenylHexyl column, HI = HILIC column.

Table 3. Overview of important criteria by which the three workflows can be classified.

Criteria	Compound Discoverer	XCMS Online/ MetaboAnalyst 4.0	Manually Programmed R Tool
Open source	-	+	+
Low false-positive rate	+	-	+
Flexibility	-	-/+	+
Complex datasets	-	+	+
Using raw data	+	-	-
Required prior knowledge	-	-	+
Annotation of isotopes and adducts	-	+	+

Evaluation criteria: + = available/good; - = not available/bad.

In the case of complex datasets, the manually programmed R tool should be the best option. Due to its high number of packages, functions, and methods, it offers a great adaptability also with regard to statistical analysis. However, this open source workflow requires advanced programming skills.

Regarding the results, the most relevant difference between the two open source workflows and the commercial software might be the optimization of the peak picking parameters. In contrast to the two open source workflows, the vendor-based software CD was used without changing any parameter (used as a black box as intended by the manufacturer). On the other hand, the two XCMS-based

workflows are neutral for a broad range of data and therefore, they need parameter optimization because they are not usable under standard settings [15,19–21].

In summary, all three workflows have found the most important metabolites, but (toxico-)metabolomics includes not only exogenous metabolites but also endogenous ones. However, it must also be said that the investigated set was rather simple and less complex. Due to the minimal fluctuations, it was not necessary to normalize the dataset, for example, using an internal standard. This might be necessary when analyzing plasma or urine samples. The choice of the appropriate method should therefore depend on the complexity of the dataset and on previous knowledge. Complex datasets in this context mean that there are more than two groups in one study and that due to the complexity of the matrix, normalization to an endogenous biomarker is necessary. Previous knowledge basically means that the user has previously programmed with R or other programming languages. The manually programmed R tool required far more programming skills than the open source combination of XCMS Online and MetaboAnalyst 4.0. The commercial software CD on the other hand required almost no prior knowledge of metabolomics data processing.

3. Materials and Methods

3.1. Chemicals and Reagents

A-CHMINACA was provided by the EU project ADEBAR/State Bureau of Criminal Investigation Schleswig-Holstein (Kiel, Germany) for research purpose. The chemical purity and identity of the compound were verified by MS and nuclear magnetic resonance analysis. Ammonium formate, ammonium acetate, formic acid, isocitrate dehydrogenase, isocitrate, dipotassium phosphate, tripotassium phosphate, magnesium chloride, and superoxide dismutase were obtained from Sigma (Taufkirchen, Germany). Acetonitrile (LC-MS grade), methanol (LC-MS grade), and NADP-Na_2 were from VWR (Darmstadt, Germany). pHLM (20 mg microsomal protein mL^{-1}) was obtained from Corning (Amsterdam, The Netherlands). After delivery, pHLM were thawed at 37 °C, aliquoted, snap-frozen in liquid nitrogen, and stored at −80 °C until use.

3.2. pHLM Incubation

According to published procedures [16,30,31], incubations using pHLM were prepared as follows. A-CHMINACA was freshly dissolved in methanol and subsequently diluted with 100 mM phosphate buffer to obtain the required concentrations. Incubations were performed at 37 °C using final A-CHMINACA concentrations of 0 (Blank group), 5 (Low group), or 50 µM (High group) and 1 mg protein mL^{-1} pHLM. Final incubation mixtures also contained 90 mM phosphate buffer, 5 mM isocitrate, 5 mM Mg^{2+}, 1.2 mM $NADP^+$, 200 U mL^{-1} superoxide dismutase, and 0.5 U mL^{-1} isocitrate dehydrogenase. The final incubation volume was 50 µL. The reaction was stopped after 60 min by adding 50 µL of ice-cold acetonitrile and then, centrifugated for 2 min at 18,407× *g*. Every group consisted of five replicates. Pooled quality samples (QC group) were prepared by transferring 10 µL of each incubation into one MS vial. These were also used for optimization of the peak picking parameters, batch correction, and identification of significant features, as described below. An aliquot of 70 µL of the remaining supernatant was transferred into separate MS vials and used for metabolomics analysis, as described below.

3.3. LC-HRMS/MS Apparatus

In accordance with Manier et al. [16], analyses were performed by using a Thermo Fisher Scientific (TF, Dreieich, Germany) Dionex UltiMate 3000 RS pump consisting of a degasser, a quaternary pump, and an UltiMate Autosampler, coupled to a TF Q-Exactive Plus system including a heated electrospray ionization (HESI)-II source. Prior to every experiment, the performance of the columns and mass spectrometer was tested using a test mixture as described by Maurer et al. [32,33]. Gradient normal phase elution was performed on a Macherey-Nagel (Düren, Germany) HILIC Nucleodur column (125 mm × 3 mm, 3 µm) and

reversed phase elution using a TF Accucore PhenylHexyl column (100 mm × 2.1 mm, 2.6 µm). The mobile phase and gradient for the PhenylHexyl column consisted of 2 mM aqueous ammonium formate containing acetonitrile (1%, *v*/*v*) and formic acid (0.1%, *v*/*v*, pH 3, eluent A), as well as 2 mM ammonium formate solution with acetonitrile:methanol (1:1, *v*/*v*) containing water (1%, *v*/*v*) and formic acid (0.1%, *v*/*v*, eluent B). The flow rate was set from 1–10 min to 500 µL min^{-1} and from 10–13.5 min to 800 µL min^{-1} using the following gradient: 0–1.0 min hold 99% A, 1–10 min to 1% A, 10–11.5 min hold 1% A, 11.5–13.5 min hold 99% A. The gradient elution for normal phase chromatography was performed using aqueous ammonium acetate (200 mM, eluent C) and acetonitrile containing formic acid (0.1%, *v*/*v*, eluent D). The flow rate was set to 500 µL × min^{-1} using the following gradient: 0–1 min hold 2% C, 1–5 min to 20% C, 5–8.5 min to 60% C, 8.5–10 min hold 60% C, 10–12 min hold 2% C. For preparation and cleaning of the injection system, isopropanol:water (90:10, *v*/*v*) was used. Due to the lipophilic properties of A-CHMINACA, eluent D was used for the flushing of both columns. The following settings were used: wash volume, 100 µL; wash speed, 4000 nL s^{-1}; loop wash factor, 2. Column temperature for every analysis was set to 40 °C, maintained by a Dionex UltiMate 3000 RS analytical column heater. Injection volume was set to 1 µL. HESI-II source conditions were as follows: ionization mode, positive or negative; sheath gas, 60 AU; auxiliary gas, 10 AU; sweep gas, 3 AU; spray voltage, 3.5 kV in positive and −4.0 kV in negative mode; heater temperature, 320 °C; ion transfer capillary temperature, 320 °C; and S-lens RF level, 50.0. Mass spectrometry for untargeted metabolomics was performed according to a previously optimized workflow [15,16]. The settings for full scan (FS) data acquisition were as follows: resolution, 140,000 fwhm; microscan, 1; automatic gain control (AGC) target, 5×10^5; maximum injection time, 200 ms; scan range, *m*/*z* 50–750; spectrum data type; centroid. Significant features were subsequently identified using PRM. Settings for PRM data acquisition were as follows: resolution, 70,000 fwhm; microscans, 1; AGC target, 5×10^5; maximum injection time, 200 ms; isolation window, 0.4 *m*/*z*; collisions energy (CE), 10, 20, 30, or 40 eV; spectrum data type, centroid. The inclusion list contained the monoisotopic masses of all significant features and a time window of their retention time ±60 s. TF Xcalibur software version 3.0.63 was used for data handling. Due to the carry-over effect of A-CHMINACA, the analysis was performed using the following sequence order: five injections of eluent D samples at the beginning of the sequence for apparatus equilibration, followed by five injections of pooled QC samples, five blank groups, five low groups, and five high groups. Additionally, one QC injection was performed every five samples to monitor batch effects, as described by Wehrens et al. [34].

3.4. Dataset Processing with Different Software

For the two open source software workflows, Proteo Wizard was used to convert Thermo Fisher LC-HRMS/MS RAW files into mzXML files [35]. Optimization of the XCMS parameters was done by using a comprehensive parameter sweeping approach [15]. Table S1 summarizes the peak picking and alignment parameters used for the two open source workflows.

In the case of using R, peak picking was performed using XCMS in an R environment [14,36] and the R package CAMERA [37] was used for the annotation of isotopes, adducts, and artifacts. The dataset was filtered keeping merely those features with a p-value using Bonferroni correction [23]. Feature abundances with a value of zero were replaced by the lowest measured abundance as a surrogate limit of detection and the whole dataset was subsequently log10 transformed [34]. Batch correction was performed for those features that were detected in every QC sample. Corresponding feature abundances were corrected using a linear model to extrapolate abundance drift between QC samples [34]. Principal component analysis (PCA) and hierarchical clustering were used to investigate patterns in the dataset. Names for the features were adopted from XCMS using "M" followed by rounded mass and "T" followed by the retention time in seconds. The R script and the mzXML files can be found at https://github.com/sehem/HLM_Metabolomics.git.

For the combination of XCMS Online and MetaboAnalyst 4.0, first, XCMS Online was used for peak picking and alignment using the optimized parameters listed in Table S1. The resulted table of XCMS Online was then processed by removing all features under a retention time of 1 min and above 10 min and all columns were removed except the peak areas of each feature in each sample. The modified

table was then uploaded to MetaboAnalyst 4.0 for statistical analysis. For normalization of the dataset, the following settings were used: sample normalization, none; data scaling, none; and data transformation, log transformation. Subsequently, one-way ANOVA was selected using Bonferroni correction for *p*-value. To investigate patterns in the dataset, PCA and hierarchical clustering using heat maps and dendrograms were selected. For hierarchical clustering, distance measures using Euclidean distances and clustering algorithms using complete were chosen.

In the case of CD, Thermo Fisher LC-HRMS/MS RAW files were uploaded and definitions of study factors in the form of categorical factors were entered. Subsequently, the ratios blank/low, blank/high, and low/high were defined. Afterwards, a predefined untargeted workflow named "Untargeted Metabolomics with statistics detect unknowns with ID using Online Database and mzLogic" was used. This workflow included findings and identified the differences between samples, performed retention time alignment, identified compounds using mzCloud, ChemSpider, and calculated differential analysis such as ANOVA, determined *p*-values, and fold changes. Bonferroni correction for *p*-value and fold-change of 1 were used for ANOVA.

3.5. Identification of Significant Features

Identification of significant features was done by recording MS/MS spectra using the PRM method mentioned above. Spectra were imported to NIST MSSEARCH version 2.3, after conversion to mzXML format using ProteoWizard [35]. According to Manier et al. [17], a library search for identification was conducted using the following settings: spectrum search type, identity (MS/MS); precursor ion *m*/*z*, in spectrum; spectrum search options, none; presearch, off; other options, none. MS/MS search was conducted using the following settings: precursor tolerance, ±5 ppm; product ion tolerance, ±10 ppm; ignoring peaks around precursor, ±*m*/*z* 1. The search was conducted by using the following libraries: NIST 14 (nist_msms and nist_msms2 sublibraries) and Wiley METLIN Mass Spectral Database. Metabolites of the investigated synthetic cannabinoid A-CHMINACA were tentatively identified by interpreting their spectra in comparison to that of the parent compound.

4. Conclusions

In this study, a dataset of pHLM incubations of the synthetic cannabinoid A-CHMINACA was used to evaluate data processing of three different software workflows under their respective optimal parameter settings. The commercial software CD is a vendor-based software, which was specifically developed for the type of MS instrument used in this study. The two open source workflows, XCMS Online/MetaboAnalyst and R, both use the "gold standard" XCMS for peak picking and alignment for untargeted metabolomics data evaluation after LC-HRMS/MS analysis.

While the two open source workflows were highly adaptable methods regarding the optimization of parameters, CD is a user-friendly black box with limited possibilities for optimization. Additionally, the metabolic profile of A-CHMINACA in pHLM was determined to compare the three software solutions. The main metabolic reactions were the hydroxylation of the adamantyl-ring and *N*-dealkylation of the indazole-3-carbaldeyde moiety.

In relation to the results of this study, CD as an all-in-one solution is characterized by its ease of use and therefore, seems suitable for simple and small metabolomic studies, as the dataset used in this study. However, it is not possible to use the right statistical test, since the dataset exists of three groups. Taking this into account, the statistical results of the used dataset can be better represented with the two open source workflows. Both open source workflows allowed extensive customization but particularly in the case of R, advanced programming skills are required, while XCMS Online/MetaboAnalyst is an almost entirely point-and-click experience. Nevertheless, both provided high flexibility and may be suitable for more complex studies and questions. The metabolic fate of A-CHMINACA in pHLM was identified best by the two open source workflows.

Supplementary Materials: The supplementary materials are available online at http://www.mdpi.com/2218-1989/10/9/378/s1.

Author Contributions: S.H., S.K.M., L.W. and M.R.M. designed the experiments; S.H. performed the experiments; S.H., S.K.M., and M.R.M. analyzed and interpreted the data. S.F. and F.W. provided the reference standard of A-CHMINACA. S.H. and M.R.M. wrote and edited the manuscript; S.H. prepared the figures; S.H., S.K.M., L.W., S.F., F.W. and M.R.M. reviewed the manuscript. All authors have read and agreed to the published version of the manuscript.

Funding: This research received no external funding.

Acknowledgments: The authors would like to thank the EU funded project ADEBAR (IZ25-5793-2016-27) for the supply of the chemical standard, as well as Cathy M. Jacobs, Tanja M. Gampfer, Thomas P. Bambauer, Matthias J. Richter, Carsten Schröder, Gabriele Ulrich, and Armin A. Weber for their support.

Conflicts of Interest: The authors declare no conflict of interest.

References

1. Barnes, S.; Benton, H.P.; Casazza, K.; Cooper, S.J.; Cui, X.; Du, X.; Engler, J.; Kabarowski, J.H.; Li, S.; Pathmasiri, W.; et al. Training in metabolomics research. I. Designing the experiment, collecting and extracting samples and generating metabolomics data. *J. Mass Spectrom.* **2016**, *51*, 461–475. [CrossRef] [PubMed]
2. Liu, X.; Locasale, J.W. Metabolomics: A Primer. *Trends Biochem. Sci.* **2017**, *42*, 274–284. [CrossRef] [PubMed]
3. Agin, A.; Heintz, D.; Ruhland, E.; Chao de la Barca, J.M.; Zumsteg, J.; Moal, V.; Gauchez, A.S.; Namer, I.J. Metabolomics—An overview. From basic principles to potential biomarkers (part 1). *Méd. Nucl.* **2016**, *40*, 4–10. [CrossRef]
4. Naz, S.; Vallejo, M.; Garcia, A.; Barbas, C. Method validation strategies involved in non-targeted metabolomics. *J. Chromatogr. A* **2014**, *1353*, 99–105. [CrossRef] [PubMed]
5. Yao, L.; Sheflin, A.M.; Broeckling, C.D.; Prenni, J.E. Data Processing for GC-MS- and LC-MS-Based Untargeted Metabolomics. *Methods Mol. Biol.* **2019**, *1978*, 287–299. [CrossRef] [PubMed]
6. Rurik, M.; Alka, O.; Aicheler, F.; Kohlbacher, O. Metabolomics Data Processing Using OpenMS. *Methods Mol. Biol.* **2020**, *2104*, 49–60. [CrossRef] [PubMed]
7. Fernandez-Ochoa, A.; Quirantes-Pine, R.; Borras-Linares, I.; Cadiz-Gurrea, M.L.; Precisesads Clinical, C.; Alarcon Riquelme, M.E.; Brunius, C.; Segura-Carretero, A. A Case Report of Switching from Specific Vendor-Based to R-Based Pipelines for Untargeted LC-MS Metabolomics. *Metabolites* **2020**, *10*. [CrossRef]
8. Sugimoto, M.; Kawakami, M.; Robert, M.; Soga, T.; Tomita, M. Bioinformatics Tools for Mass Spectroscopy-Based Metabolomic Data Processing and Analysis. *Curr. Bioinform.* **2012**, *7*, 96–108. [CrossRef]
9. Katajamaa, M.; Oresic, M. Data processing for mass spectrometry-based metabolomics. *J. Chromatogr. A* **2007**, *1158*, 318–328. [CrossRef] [PubMed]
10. Castillo, S.; Gopalacharyulu, P.; Yetukuri, L.; Orešič, M. Algorithms and tools for the preprocessing of LC–MS metabolomics data. *Chemom. Intell. Lab. Syst.* **2011**, *108*, 23–32. [CrossRef]
11. Spicer, R.; Salek, R.M.; Moreno, P.; Canueto, D.; Steinbeck, C. Navigating freely-available software tools for metabolomics analysis. *Metabolomics* **2017**, *13*, 106. [CrossRef] [PubMed]
12. Cambiaghi, A.; Ferrario, M.; Masseroli, M. Analysis of metabolomic data: Tools, current strategies and future challenges for omics data integration. *Brief. Bioinform.* **2017**, *18*, 498–510. [CrossRef] [PubMed]
13. Li, Z.; Lu, Y.; Guo, Y.; Cao, H.; Wang, Q.; Shui, W. Comprehensive evaluation of untargeted metabolomics data processing software in feature detection, quantification and discriminating marker selection. *Anal. Chim. Acta* **2018**, *1029*, 50–57. [CrossRef]
14. Smith, C.A.; Want, E.J.; O'Maille, G.; Abagyan, R.; Siuzdak, G. XCMS: Processing mass spectrometry data for metabolite profiling using nonlinear peak alignment, matching, and identification. *Anal. Chem.* **2006**, *78*, 779–787. [CrossRef] [PubMed]
15. Manier, S.K.; Keller, A.; Meyer, M.R. Automated optimization of XCMS parameters for improved peak picking of liquid chromatography-mass spectrometry data using the coefficient of variation and parameter sweeping for untargeted metabolomics. *Drug Test Anal* **2019**, *11*, 752–761. [CrossRef]
16. Manier, S.K.; Keller, A.; Schaper, J.; Meyer, M.R. Untargeted metabolomics by high resolution mass spectrometry coupled to normal and reversed phase liquid chromatography as a tool to study the in vitro biotransformation of new psychoactive substances. *Sci. Rep.* **2019**, *9*, 2741. [CrossRef]

17. Manier, S.K.; Wagmann, L.; Flockerzi, V.; Meyer, M.R. Toxicometabolomics of the new psychoactive substances alpha-PBP and alpha-PEP studied in HepaRG cell incubates by means of untargeted metabolomics revealed unexpected amino acid adducts. *Arch. Toxicol.* **2020**, *94*, 2047–2059. [CrossRef]
18. Asha, S.; Vidyavathi, M. Role of human liver microsomes in in vitro metabolism of drugs-a review. *Appl. Biochem. Biotechnol.* **2010**, *160*, 1699–1722. [CrossRef]
19. Myers, O.D.; Sumner, S.J.; Li, S.; Barnes, S.; Du, X. Detailed Investigation and Comparison of the XCMS and MZmine 2 Chromatogram Construction and Chromatographic Peak Detection Methods for Preprocessing Mass Spectrometry Metabolomics Data. *Anal. Chem.* **2017**, *89*, 8689–8695. [CrossRef]
20. Lange, E.; Tautenhahn, R.; Neumann, S.; Gropl, C. Critical assessment of alignment procedures for LC-MS proteomics and metabolomics measurements. *BMC Bioinform.* **2008**, *9*, 375. [CrossRef]
21. Garcia, C.J.; Yang, X.; Huang, D.; Tomas-Barberan, F.A. Can we trust biomarkers identified using different non-targeted metabolomics platforms? Multi-platform, inter-laboratory comparative metabolomics profiling of lettuce cultivars via UPLC-QTOF-MS. *Metabolomics* **2020**, *16*, 85. [CrossRef]
22. Coble, J.B.; Fraga, C.G. Comparative evaluation of preprocessing freeware on chromatography/mass spectrometry data for signature discovery. *J. Chromatogr. A* **2014**, *1358*, 155–164. [CrossRef] [PubMed]
23. Broadhurst, D.I.; Kell, D.B. Statistical strategies for avoiding false discoveries in metabolomics and related experiments. *Metabolomics* **2006**, *2*, 171–196. [CrossRef]
24. Barnes, S.; Benton, H.P.; Casazza, K.; Cooper, S.J.; Cui, X.; Du, X.; Engler, J.; Kabarowski, J.H.; Li, S.; Pathmasiri, W.; et al. Training in metabolomics research. II. Processing and statistical analysis of metabolomics data, metabolite identification, pathway analysis, applications of metabolomics and its future. *J. Mass Spectrom.* **2016**, *51*, 535–548. [CrossRef] [PubMed]
25. Sumner, L.W.; Amberg, A.; Barrett, D.; Beale, M.H.; Beger, R.; Daykin, C.A.; Fan, T.W.; Fiehn, O.; Goodacre, R.; Griffin, J.L.; et al. Proposed minimum reporting standards for chemical analysis Chemical Analysis Working Group (CAWG) Metabolomics Standards Initiative (MSI). *Metabolomics* **2007**, *3*, 211–221. [CrossRef] [PubMed]
26. Wishart, D.S.; Tzur, D.; Knox, C.; Eisner, R.; Guo, A.C.; Young, N.; Cheng, D.; Jewell, K.; Arndt, D.; Sawhney, S.; et al. HMDB: The Human Metabolome Database. *Nucleic Acids Res.* **2007**, *35*, D521–D526. [CrossRef]
27. Gandhi, A.S.; Zhu, M.; Pang, S.; Wohlfarth, A.; Scheidweiler, K.B.; Liu, H.F.; Huestis, M.A. First characterization of AKB-48 metabolism, a novel synthetic cannabinoid, using human hepatocytes and high-resolution mass spectrometry. *AAPS J.* **2013**, *15*, 1091–1098. [CrossRef] [PubMed]
28. Kadomura, N.; Ito, T.; Kawashima, H.; Matsuhisa, T.; Kinoshita, T.; Soda, M.; Kohyama, E.; Iwaki, T.; Nagai, H.; Kitaichi, K. In vitro metabolic profiles of adamantyl positional isomers of synthetic cannabinoids. *Forensic Toxicology* **2020**. [CrossRef]
29. Erratico, C.; Negreira, N.; Norouzizadeh, H.; Covaci, A.; Neels, H.; Maudens, K.; van Nuijs, A.L. In vitro and in vivo human metabolism of the synthetic cannabinoid AB-CHMINACA. *Drug Test Anal.* **2015**, *7*, 866–876. [CrossRef] [PubMed]
30. Welter, J.; Meyer, M.R.; Wolf, E.U.; Weinmann, W.; Kavanagh, P.; Maurer, H.H. 2-methiopropamine, a thiophene analogue of methamphetamine: Studies on its metabolism and detectability in the rat and human using GC-MS and LC-(HR)-MS techniques. *Anal. Bioanal. Chem.* **2013**, *405*, 3125–3135. [CrossRef] [PubMed]
31. Richter, L.H.; Kaminski, Y.R.; Noor, F.; Meyer, M.R.; Maurer, H.H. Metabolic fate of desomorphine elucidated using rat urine, pooled human liver preparations, and human hepatocyte cultures as well as its detectability using standard urine screening approaches. *Anal. Bioanal. Chem.* **2016**, *408*, 6283–6294. [CrossRef] [PubMed]
32. Maurer, H.H.; Pfleger, K.; Weber, A.A. *Mass Spectral Data of Drugs, Poisons, Pesticides, Pollutants and Their Metabolites*; Wiley-VCH: Weinheim, Germany, 2016.
33. Maurer, H.H.; Meyer, M.R.; Helfer, A.G.; Weber, A.A. *Maurer/Meyer/Helfer/Weber MMHW LC-HR-MS/MS Library of Drugs, Poisons, and Their Metabolites*; Wiley-VCH: Weinheim, Germany, 2018.
34. Wehrens, R.; Hageman, J.A.; van Eeuwijk, F.; Kooke, R.; Flood, P.J.; Wijnker, E.; Keurentjes, J.J.; Lommen, A.; van Eekelen, H.D.; Hall, R.D.; et al. Improved batch correction in untargeted MS-based metabolomics. *Metabolomics* **2016**, *12*, 88. [CrossRef] [PubMed]
35. Adusumilli, R.; Mallick, P. Data Conversion with ProteoWizard msConvert. *Methods Mol. Biol.* **2017**, *1550*, 339–368. [CrossRef] [PubMed]

36. R Core Team. *R: A Language and Environment for Statistical Computing*; R Foundation for Statistical Computing: Vienna, Austria, 2020.
37. Kuhl, C.; Tautenhahn, R.; Bottcher, C.; Larson, T.R.; Neumann, S. CAMERA: An integrated strategy for compound spectra extraction and annotation of liquid chromatography/mass spectrometry data sets. *Anal. Chem.* **2012**, *84*, 283–289. [CrossRef] [PubMed]

© 2020 by the authors. Licensee MDPI, Basel, Switzerland. This article is an open access article distributed under the terms and conditions of the Creative Commons Attribution (CC BY) license (http://creativecommons.org/licenses/by/4.0/).

Supplementary materials

Comparison of Three Untargeted Data Processing Workflows for Evaluating LC-HRMS Metabolomics Data

Selina Hemmer [1], Sascha K. Manier [1], Svenja Fischmann [2], Folker Westphal [2], Lea Wagmann [1]and Markus R. Meyer [1,*]

[1] Department of Experimental and Clinical Toxicology, Institute of Experimental and Clinical Pharmacology and Toxicology, Center for Molecular Signaling (PZMS), Saarland University, 66421 Homburg, Germany; selina.hemmer@uks.eu (S.H.); sascha.manier@uks.eu (S.K.M.); lea.wagmann@uks.eu (L.W.)

[2] State Bureau of Criminal Investigation Schleswig-Holstein, 24116 Kiel, Germany; Svenja.Dr.Fischmann@polizei.landsh.de (S.F.); Folker.Dr.Westphal@polizei.landsh.de (F.W.)

* Correspondence: markus.meyer@uks.eu

Table S1. Peak picking and alignment parameters used for preprocessing using R and XCMS Online.

Column	Polarity	Peakwidth, min	Peakwidth, max	ppm	Snthresh	Mzdiff	Prefilter 1	Prefilter 2	bw
HI	pos	10	22	1.0	39	0.07	7	900	0.1 (1*)
HI	neg	10	12	1.9	69	0.016	5	6100	0.1 (1*)
PH	pos	9.3	12	1.2	83	0.02	10	5400	0.1 (1*)
PH	neg	9.3	12	1.0	96	0.068	6	8200	0.5 (1*)

HI = HILIC, PH = PhenylHexyl, pos = positive, neg = negative, ppm = allowed ppm deviation of mass traces for peak picking, snthresh = signal to noise threshold, mzdiff = minimum difference in m/z for two peaks to be considered as separate, prefilter 1 = minimum of scan points, prefilter 2 = minimum abundance, bw = bandwidth for grouping of peaks across separate chromatograms, * value used for XCMS Online.

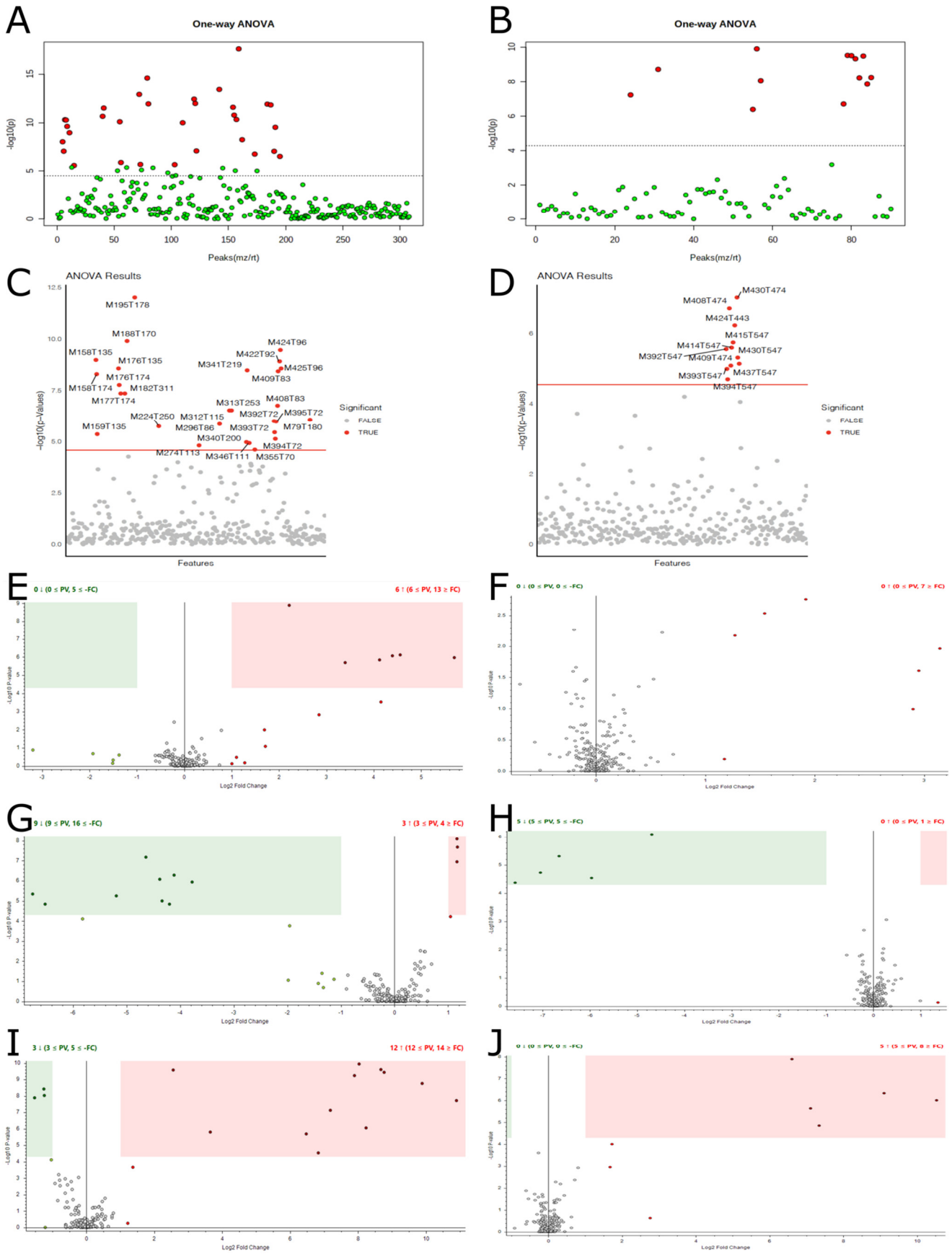

Figure S1. Results of one-way ANOVA for A-CHMINACA incubations analyzed in positive ionization mode. **A** = XCMS Online/MetaboAnalyst, HILIC column; **B** = XCMS Online/MetaboAnalyst, PhenylHexyl column; **C** = R, HILIC column; **D** = R, PhenylHexyl column; **E** = Compound Discoverer, Low and Blank, HILIC column; **F** = Compound Discoverer, Low and Blank,

PhenylHexyl column; **G** = Compound Discoverer, Low and High, HILIC column; **H** = Compound Discoverer, Low and High, PhenylHexyl column; **I** = Compound Discoverer, High and Blank, HILIC column; **J** = Compound Discoverer, High and Blank, PhenylHexyl column.

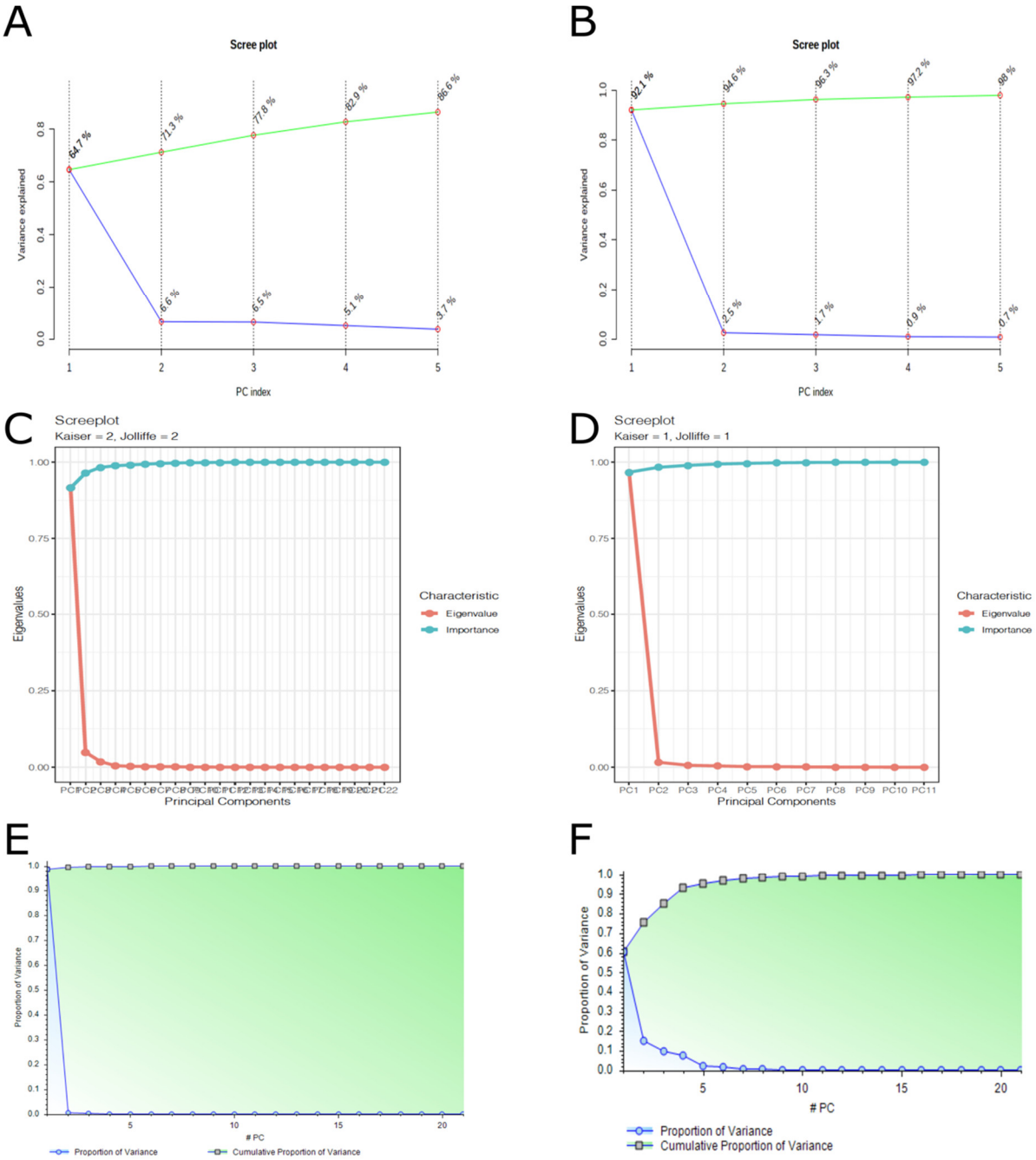

Figure S2. Results of scree plots for A-CHMINACA incubations analyzed in positive ionization mode. **A** = XCMS Online/MetaboAnalyst, HILIC column; **B** = XCMS Online/MetaboAnalyst, PhenylHexyl column; **C** = R, HILIC column; **D** = R, PhenylHexyl column; **E** = Compound Discoverer, HILIC column; **F** = Compound Discoverer, PhenylHexyl column.

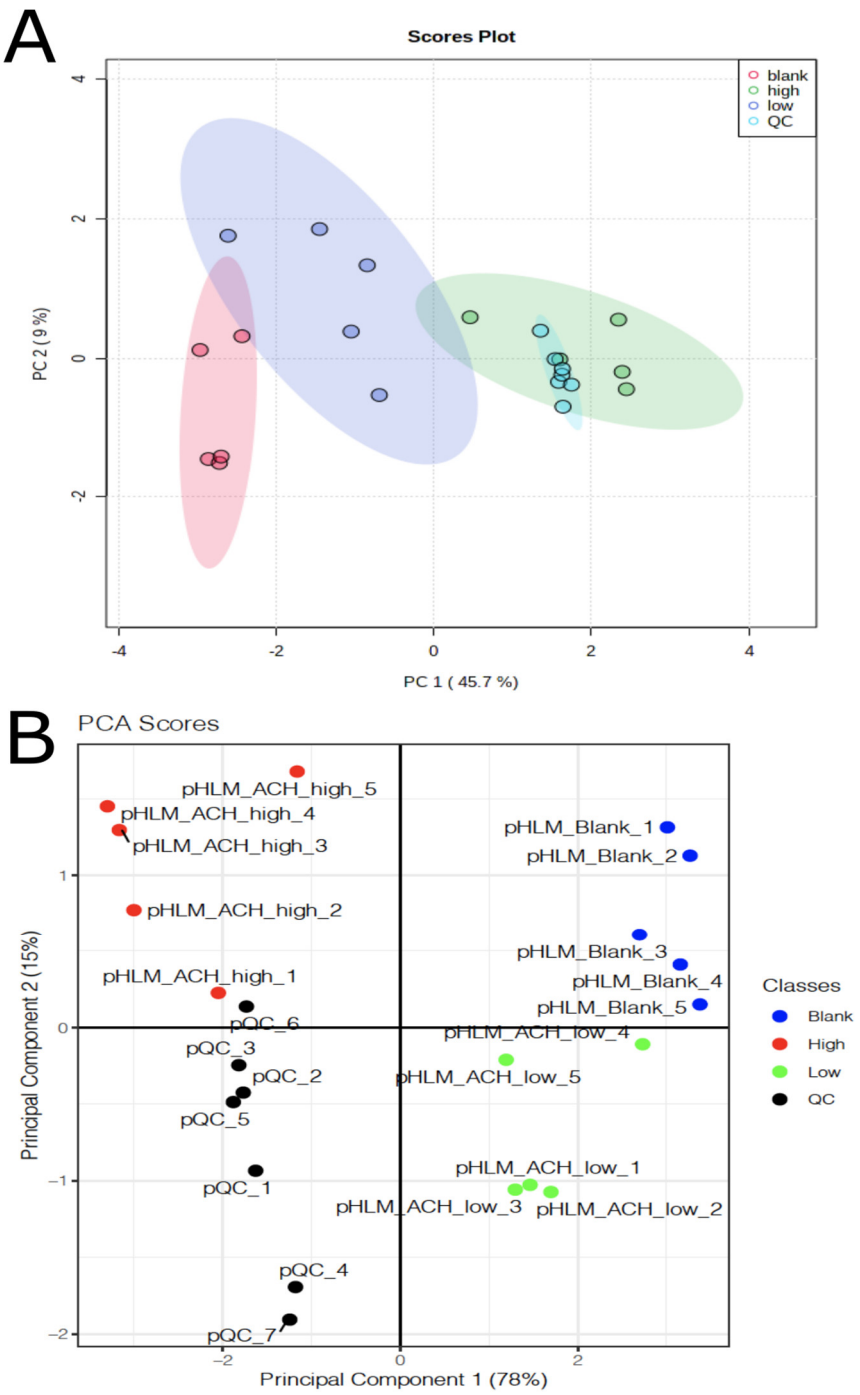

Figure S3. Results of scores of principal component analysis for A-CHMINACA incubations analyzed in positive ionization mode without isotopes and adducts. **A** = XCMS Online/MetaboAnalyst, PhenylHexyl column; **B** = R, PhenylHexyl column.

M392T72, A-CHMINACA

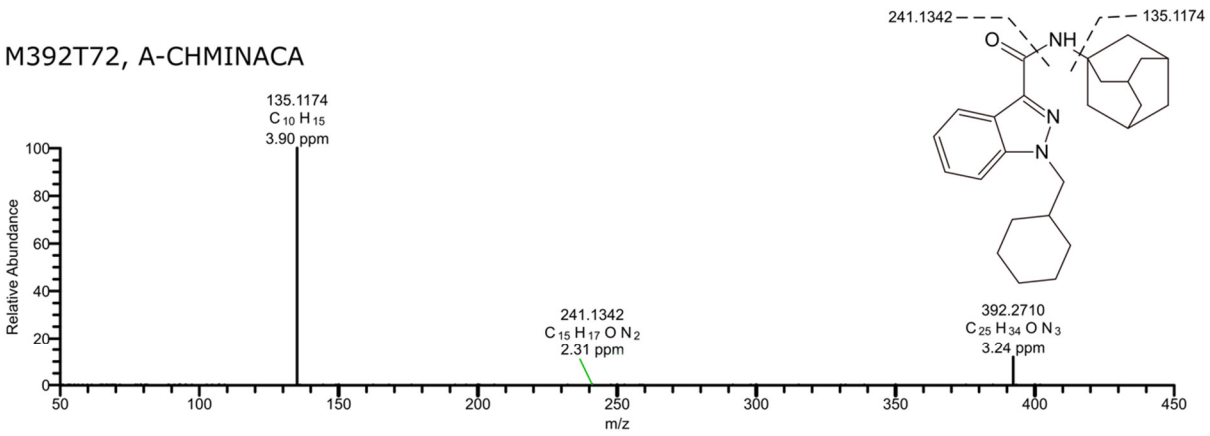

M296T86, A-CHMINACA (*N*-dealkyl-)

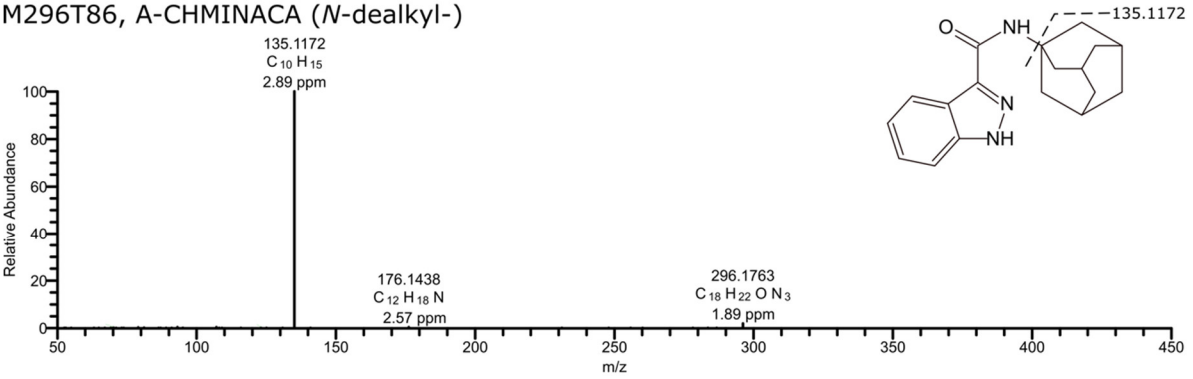

M408T83, A-CHMINACA-M (HO-)

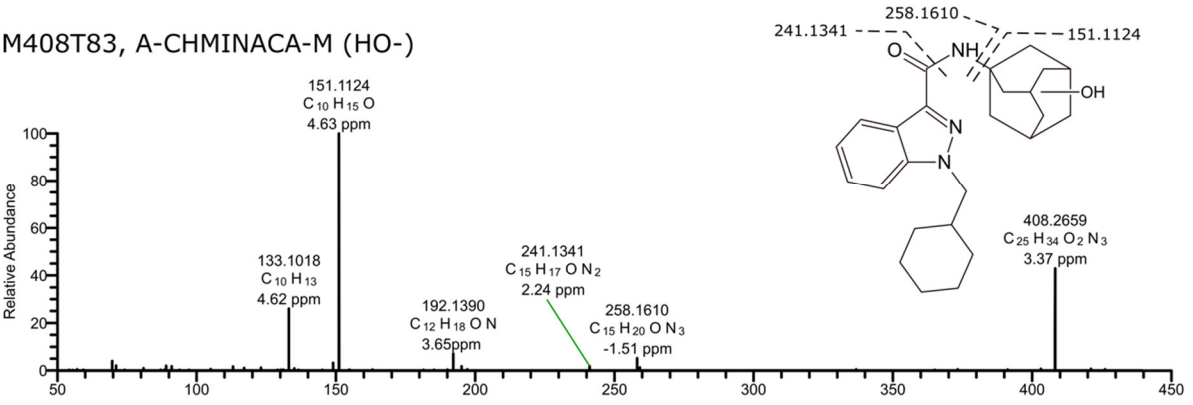

M422T92, A-CHMINACA-M (HO, Oxo)

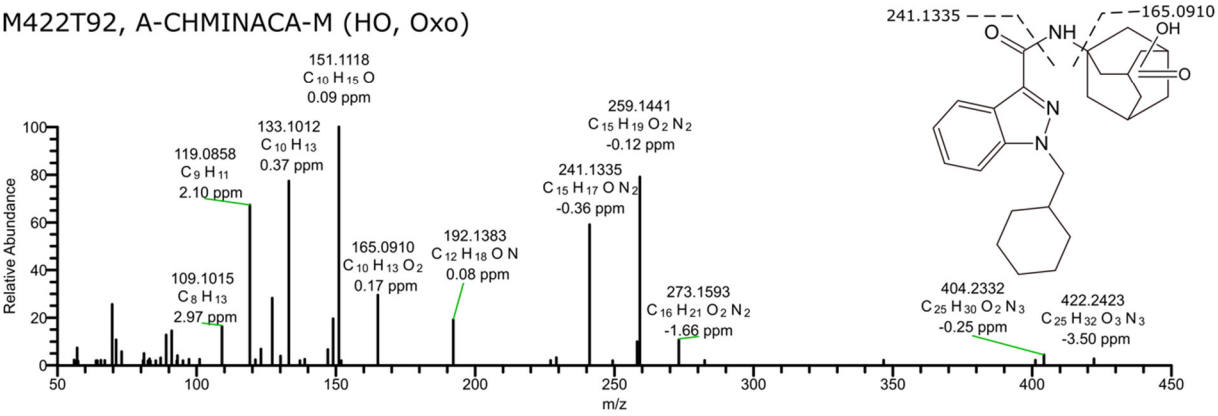

M424T96, A-CHMINACA-M (di-HO-)

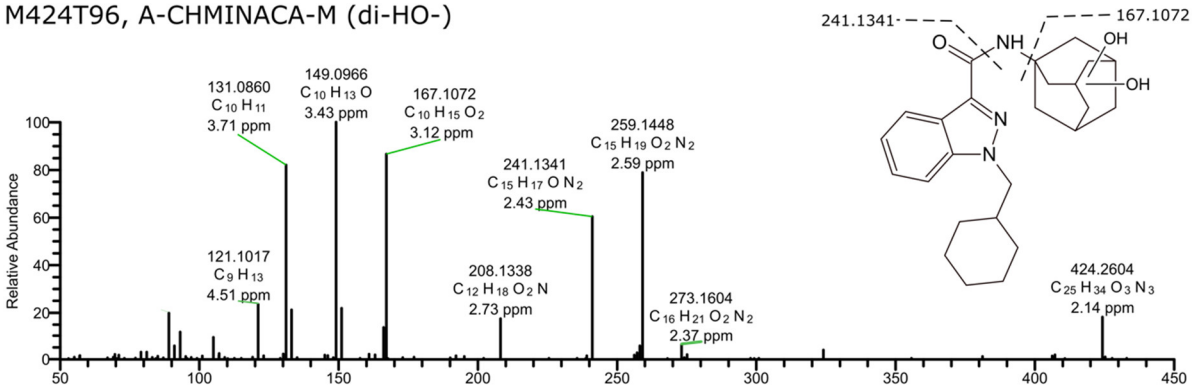

M424T93, A-CHMINACA-M (di-HO-)

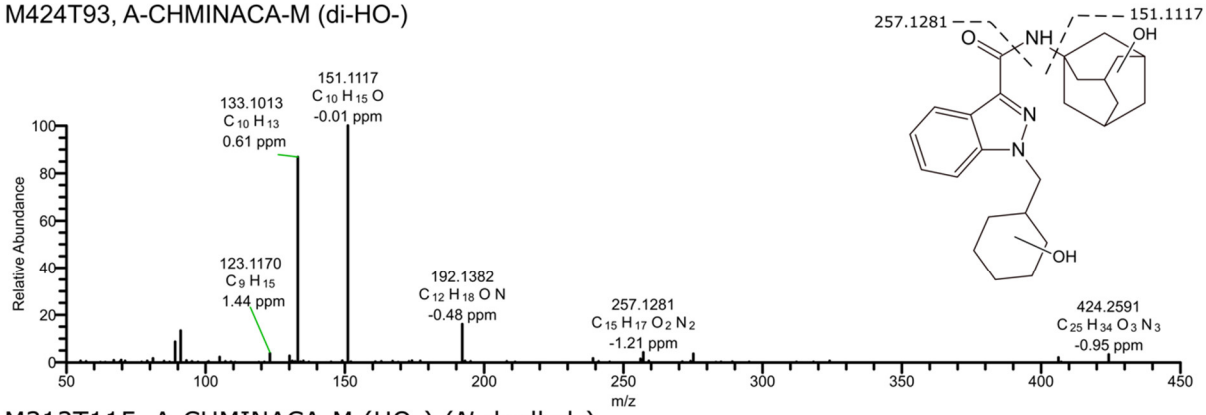

M312T115, A-CHMINACA-M (HO-) (*N*-dealkyl-)

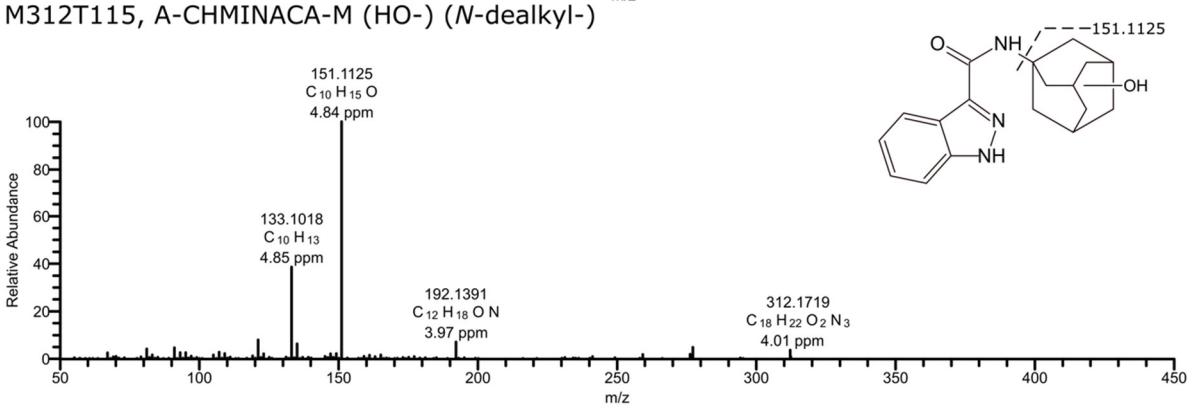

M274T113, A-CHMINACA-M (HO-) (*N*-dealkyl-)

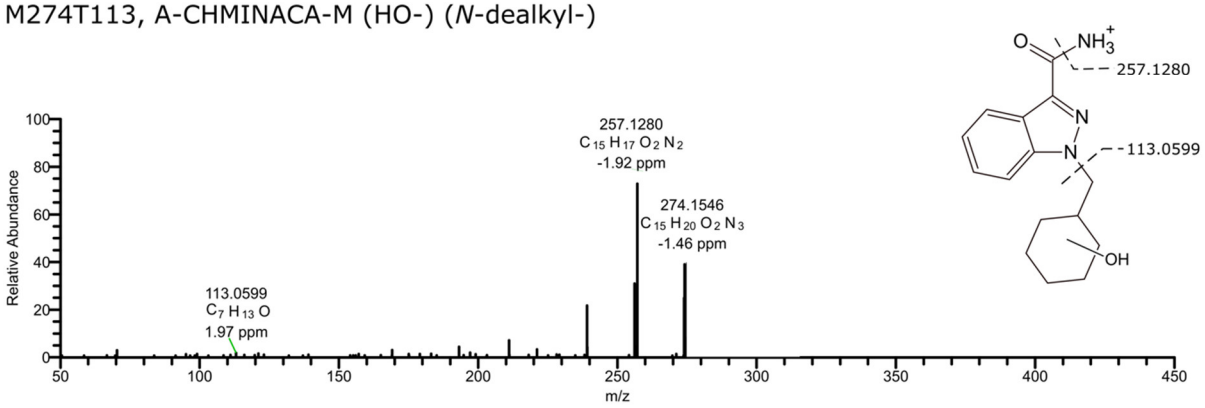

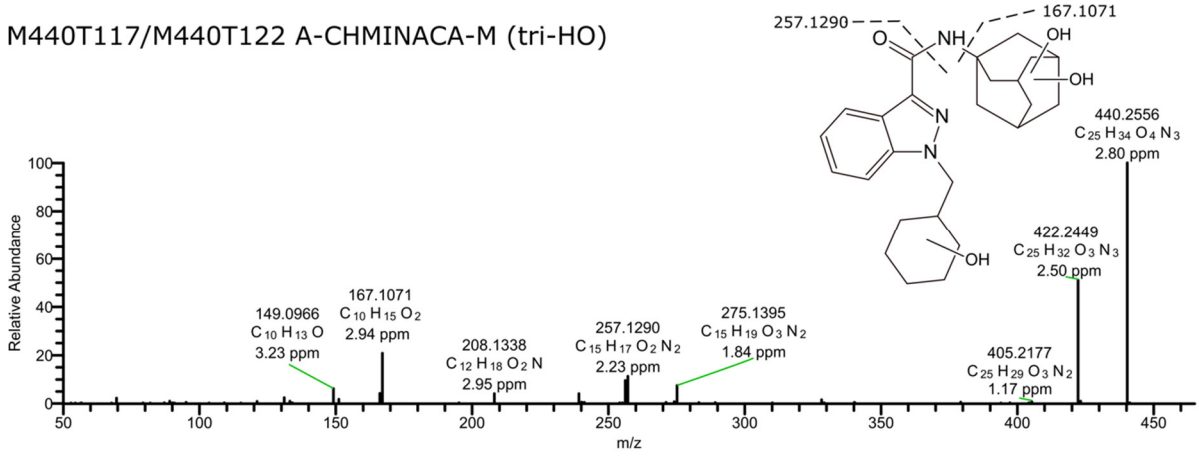

Figure S4. LC-HRMS/MS spectra of significant features in A-CHMINACA incubations analyzed with a HILIC column in positive ionization mode. Fragments with accurate mass, calculated elemental formula, and mass error value in parts per million (ppm).

metabolites

MDPI

Addendum

Addendum: Hemmer, S., et al. Comparison of Three Untargeted Data Processing Workflows for Evaluating LC-HRMS Metabolomics Data. *Metabolites* 2020, *10*, 378

Selina Hemmer [1], Sascha K. Manier [1], Svenja Fischmann [2], Folker Westphal [2], Lea Wagmann [1] and Markus R. Meyer [1,*]

[1] Department of Experimental and Clinical Toxicology, Institute of Experimental and Clinical Pharmacology and Toxicology, Center for Molecular Signaling (PZMS), Saarland University, 66421 Homburg, Germany; selina.hemmer@uks.eu (S.H.); Sascha.manier@uks.eu (S.K.M.); lea.wagmann@uks.eu (L.W.)

[2] State Bureau of Criminal Investigation Schleswig-Holstein, 24116 Kiel, Germany; Svenja.Dr.Fischmann@polizei.landsh.de (S.F.); Folker.Dr.Westphal@polizei.landsh.de (F.W.)

* Correspondence: markus.meyer@uks.eu

Received: 21 October 2020; Accepted: 22 October 2020; Published: 27 October 2020

The authors wish to make the following comment to this paper [1].

To avoid any misunderstandings and misleading interpretations regarding the general possibilities of Compound Discoverer (CD) when reading the paper, we would like to add the following comment. We used Compound Discoverer (CD) with an already existing workflow for untargeted metabolomics namely "Untargeted Metabolomics with statistics detect unknowns with ID using Online Database and mzLogic" without changing any parameters ("out-of-the-box"). Therefore, some features of CD were not used, such as direct evaluation of isotopes and adducts, Scripting node for normalization, and comparing three groups visually after ANOVA, as it was carried out for the other two workflows.

Readers should be aware that CD is nevertheless able to determine isotopic patterns and elemental composition, integrate Scripting node that can then be used to integrate R or Python scripts, and is capable of comparing multiple groups, performing ANOVA with Tukey as a post-hoc test, and nested designs.

The authors would like to apologize for any misunderstandings appearing from the original manuscript. These comments do not affect the scientific results.

Author Contributions: S.H., S.K.M., L.W. and M.R.M. designed the experiments; S.H. performed the experiments; S.H., S.K.M., and M.R.M. analyzed and interpreted the data. S.F. and F.W. provided the reference standard of A-CHMINACA. S.H. and M.R.M. wrote and edited the manuscript; S.H. prepared the figures; S.H., S.K.M., L.W., S.F., F.W. and M.R.M. reviewed the manuscript. All authors have read and agreed to the published version of the manuscript.

Funding: This research received no external funding.

Conflicts of Interest: The authors declare no conflict of interest.

Reference

1. Hemmer, S.; Manier, S.K.; Fischmann, S.; Westphal, F.; Wagmann, L.; Meyer, M.R. Comparison of Three Untargeted Data Processing Workflows for Evaluating LC-HRMS Metabolomics Data. *Metabolites* **2020**, *10*, 378. [CrossRef] [PubMed]

Publisher's Note: MDPI stays neutral with regard to jurisdictional claims in published maps and institutional affiliations.

© 2020 by the authors. Licensee MDPI, Basel, Switzerland. This article is an open access article distributed under the terms and conditions of the Creative Commons Attribution (CC BY) license (http://creativecommons.org/licenses/by/4.0/).

3.4. Altered Metabolic Pathways Elucidated via Untargeted In Vivo Toxicometabolomics in Rat Urine and Plasma Samples Collected After Controlled Application of a Human Equivalent Amphetamine Dose

(DOI: 10.1007/s00204-021-03135-8)[93]

Author Contributions:

Selina Hemmer conducted and evaluated the experiments as well as composed the manuscript; Lea Wagmann and Markus R. Meyer assisted with the design of the experiments, the interpretation of the analytical experiments, and scientific discussions.

Archives of Toxicology (2021) 95:3223–3234
https://doi.org/10.1007/s00204-021-03135-8

TOXICOKINETICS AND METABOLISM

Altered metabolic pathways elucidated via untargeted in vivo toxicometabolomics in rat urine and plasma samples collected after controlled application of a human equivalent amphetamine dose

Selina Hemmer[1] · Lea Wagmann[1] · Markus R. Meyer[1]

Received: 2 June 2021 / Accepted: 11 August 2021 / Published online: 19 August 2021
© The Author(s) 2021

Abstract
Amphetamine is widely consumed as drug of abuse due to its stimulating and cognitive enhancing effects. Since amphetamine has been on the market for quite a long time and it is one of the most commonly used stimulants worldwide, to date there is still limited information on its effects on the metabolome. In recent years, untargeted toxicometabolomics have been increasingly used to study toxicity-related pathways of such drugs of abuse to find and identify important endogenous and exogenous biomarkers. In this study, the acute effects of amphetamine intake on plasma and urinary metabolome in rats were investigated. For this purpose, samples of male Wistar rats after a single dose of amphetamine (5 mg/kg) were compared to a control group using an untargeted metabolomics approach. Analysis was performed using normal and reversed phase liquid chromatography coupled to high-resolution mass spectrometry using positive and negative ionization mode. Statistical evaluation was performed using Welch's two-sample *t* test, hierarchical clustering, as well as principal component analysis. The results of this study demonstrate a downregulation of amino acids in plasma samples after amphetamine exposure. Furthermore, four new potential biomarkers *N*-acetylamphetamine, *N*-acetyl-4-hydroxyamphetamine, *N*-acetyl-4-hydroxyamphetamine glucuronide, and amphetamine succinate were identified in urine. The present study complements previous data and shows that several studies are necessary to elucidate altered metabolic pathways associated with acute amphetamine exposure.

Keywords Untargeted metabolomics · Toxicometabolomics · Amphetamine · LC-HRMS/MS

Introduction

Once introduced as a treatment against narcolepsy, mild depression, post-encephalitic parkinsonism, and several other disorders (Heal et al. 2013), amphetamine nowadays has a limited therapeutic use but is widely consumed as a drug of abuse (DOA) due to its stimulating properties (Carvalho et al. 2012). In 2018, amphetamine was one of the world's most commonly used stimulants, along with cocaine and methamphetamine (UNODC 2020). In addition to the desired effects such as feelings of energy, sociability, and confidence, many adverse effects including hypertension, tachycardia, anxiety, paranoia or auditory and visual hallucinations are associated with its use (Bonisch and Bruss 2006; Steinkellner et al. 2011). These effects are based on its pharmacological ability to act as an indirect sympathomimetic and to increase the release of different neurotransmitters such as noradrenaline and dopamine and/or inhibit their respective reuptake transporter in the presynaptic membrane (Carvalho et al. 2012; de la Torre et al. 2004). Although amphetamine is consumed since decades, there is still little knowledge available regarding its effects on the metabolic state of the organism (Steuer et al. 2020). Conventional in vitro toxicological studies, e.g., using human dopaminergic differentiated SH-SY5Y cells revealed a neurotoxic effect, which caused mitochondrial dysfunction at a concentration of 3.5 mM (Carvalho et al. 2012; Feio-Azevedo et al. 2017).

✉ Markus R. Meyer
markus.meyer@uks.eu

[1] Department of Experimental and Clinical Toxicology, Center for Molecular Signaling (PZMS), Institute of Experimental and Clinical Pharmacology and Toxicology, Saarland University, 66421 Homburg, Germany

Metabolomics in general is used for discovery of novel biomarkers, investigation of physiologic status, or identification of perturbed biochemical pathways (Nicholson and Lindon 2008) and can provide a snapshot analysis of the whole metabolome in a biological system (Liu and Locasale 2017). Toxicometabolomics, a sub-discipline of metabolomics, is dedicated to elucidate the pattern of small molecules (usually below 1500 Da) within an in vitro or in vivo system related to a certain stimulus such as DOA intake. Under highly controlled study conditions, changes of the metabolome can be observed that may indicate or be the result of a certain drug intake (Wang et al. 2016). Toxicometabolomics can, therefore, be used to study toxicity-related pathways such as the mode of action of xenobiotics or in screening of drug induced cellular or organ toxicity, or to discover new biomarkers (Bouhifd et al. 2013; Ramirez et al. 2013). In recent years, toxicometabolomics have been increasingly used in the field of DOA (Araujo et al. 2021; Manier et al. 2020a, b; Steuer et al. 2020; Zaitsu et al. 2016). Its application may allow to find exogenous biomarkers, which could be new drug metabolites, and on the other hand to identify endogenous biomarkers, which could not only be indications of acute drug ingestion or sample manipulation but also provide information in the mechanism of drug action, consumption behavior, or can be used to assess the severity of intoxications (Steuer et al. 2019; Wang et al. 2016). Steuer et al. (2020) investigated changes of the plasma metabolome after amphetamine intake in a controlled human study of 13 participants and identified an increased energy and steroid metabolism. However, since there is no method that can reveal the complete metabolome and since the plasma metabolome is highly dynamic and influenced by various factors, further studies are needed. In vivo studies in laboratory animals are suitable for this purpose. Under well-standardized and comparable conditions such as controlled diet, sleep cycles and little genetic variability, it is possible to better delineate the metabolome changes caused by amphetamine use. Furthermore, to the best of our knowledge, there are no studies on the urinary metabolome after amphetamine exposure available.

This study should provide the metabolic profiling of rat plasma and urine in response to acute amphetamine exposure, provide additional metabolites/biomarker in urine for detection of amphetamine intake and should complement previous studies. Data should allow to observe changes in the metabolome caused by amphetamine and allow to identify biological pathways affected by its intake, which are necessary to further understand its acute and chronic effects and support further targeted analysis. The analysis should be done by liquid chromatography coupled to high-resolution tandem mass spectrometry (LC–HRMS/MS).

Materials and methods

Chemicals and reagents

Racemic D-/L-amphetamine sulfate was purchased from Lipomed (Weil am Rhein, Germany). Acetonitrile, ethanol, and methanol (all LC–MS grade) were obtained from VWR (Darmstadt, Germany), ammonium formate, ammonium acetate, and formic acid, amino acids standards solution, D-Glucose-1,2,3,4,5,6,6-d_7, palmitic acid-d_{31}, and creatinine-d_3 from Merck (Darmstadt, Germany). L-Tryptophan-d_5 was obtained from Alsachim (Illkirch-Graffenstaden, France). Water was purified with a Millipore filtration unit (18.2 Ω × cm water resistance).

Study design

Ten adolescent male Wistar rats (Charles River, Sulzfeld, Germany) were housed in a controlled environment (temperature 22 °C, humidity 57 ± 2%, and 12 h light/dark cycles). Studies have been approved by an ethics committee (33/2019—Landesamt für Verbraucherschutz, Saarbrücken, Germany). A single dose of 5 mg/kg body weight (BW) racemic D-/L-amphetamine was administered as aqueous suspension by gastric intubation to five rats. Five control rats were administrated only with water. During the study, rats were housed in metabolism cages for 24 h, having water ad libitum. Animal general health aspects were assessed at the time points 30 min, 60 min, 120 min, 360 min, and 24 h after amphetamine intake. The animals were then monitored including only some general aspects such as body weight, clean orifices, clear eyes, and sleep behavior. Detailed changes expected after intake of stimulants such as heart rate, radial maze for cognitive function or plus maze to determine activity and anxiety behavior were not and could not be monitored as this was not the focus of the current study.

The selected dose of 5 mg/kg BW D-/L-amphetamine is equivalent to 50 mg in a 60 kg human according to the allometric scaling principles of Nair and Jacob (2016). This would correspond to a human D-amphetamine dose of 25 mg, which is in line with the work by Dolder et al. (2017) and 50 mg of a racemic mixture, which is used as recreational drug (http://psychoaktivesubstanzen.de/amphetamin. Accessed 26-May-2020, 9:30).

Sample collection

Urine was collected separately from the feces over a period of eight or 24 h after administration, aliquoted, and frozen at − 80 °C until use. Blood samples were collected 1, 2, and

8 h after administration. For blood sampling, animals were anesthetized with diethyl ether and blood was withdrawn from the *Vena caudalis mediana* using a heparin-coated syringe. Blood samples were centrifuged (1503 rcf, 5 min, 24 °C), and plasma was removed and immediately stored at − 80 °C until analysis.

Sample preparation

According to Manier and Meyer (2020), plasma samples were prepared as follow. A volume of 50 µL plasma was transferred into a reaction tube and precipitated using 200 µL of a mixture of methanol and ethanol (1:1, v/v). The mixture contained 48 µM L-tryptophan-d_5, 8.6 µM creatinine-d_3, 34.8 µM palmitic acid-d_{31}, and 53.4 µM D-glucose-d_7 as internal standards. Samples were shaken for 2 min at 2000 rpm and subsequently centrifuged for 30 min at 21,130 rcf and 2 °C. 150 µL of the supernatant was transferred into a new reaction tube and evaporated to dryness using a vacuum centrifuge at 1400 rpm and 24 °C for 20 min. The obtained residues were reconstituted in 50 µL of a mixture of acetonitrile and methanol (70:30, v/v).

In accordance with Barnes et al. (2016), urine samples were centrifugated at 13,523 rcf at 4 °C for 10 min to remove any precipitates. 50 µL of urine were transferred in a reaction tube and 200 µL methanol including 48 µM L-tryptophan-d_5, 8.6 µM creatinine-d_3, 34.8 µM palmitic acid-d_{31}, and 53.4 µM D-glucose-d_7 as internal standards were added. Samples were cooled to − 20 °C for 20 min and then centrifugated for 10 min at 13,523 rcf and 4 °C. 150 µL of the supernatant were transferred into a new reaction tube and evaporated to dryness using a vacuum centrifuge at 1400 rpm and 24 °C. The obtained residues were reconstituted in 50 µL of a mixture of acetonitrile and methanol (70:30, v/v).

For each matrix and the corresponding timepoint, one pooled quality control (QC) sample was prepared by transferring 10 µL of each sample into one MS vial. These QC samples were also used for optimization of the peak picking parameters and identification of significant features, as described below (QC group).

LC-HRMS/MS apparatus

According to Manier et al. (2019b), analyses were performed using a Thermo Fisher Scientific (TF, Dreieich, Germany) Dionex UltiMate 3000 RS pump consisting of a degasser, a quaternary pump, and an UltiMate Autosampler, coupled to a TF Q-Exactive Plus system including a heated electrospray ionization (HESI)-II source. Performance of the columns and the mass spectrometer was tested using a test mixture as described by Maurer et al. (Maurer et al. 2018, 2016). Gradient reversed phase (RP) elution was performed on a TF Accucore Phenyl-Hexyl column (100 mm × 2.1 mm, 2.6 µm) and normal phase (NP) elution using a Macherey–Nagel (Düren, Germany) HILIC Nucleodur column (125 mm × 3 mm, 3 µm). The mobile phase and gradient for the Phenyl-Hexyl column consisted of 2 mM aqueous ammonium formate containing acetonitrile (1%, v/v) and formic acid (0.1%, v/v, pH 3, eluent A), as well as 2 mM ammonium formate solution with acetonitrile:methanol (1:1, v/v) containing water (1%, v/v) and formic acid (0.1%, v/v, eluent B). The flow rate was set from 1 to 10 min to 500 µL/min and from 10 to 13.5 min to 800 µL/min using the following gradient: 0–1 min hold 99% A, 1–10 min to 1% A, 10–11.5 min hold 1% A, 11.5–13.5 min hold 99% A. The gradient elution for normal phase chromatography was performed using aqueous ammonium acetate (200 mM, eluent C) and acetonitrile containing formic acid (0.1%, v/v, eluent D). The flow rate was set to 500 µL/min using the following gradient: 0–1 min hold 2% C, 1–5 min to 20% C, 5–8.5 min to 60% C, 8.5–10 min hold 60% C, 10–12 min hold 2% C. For preparation and cleaning of the injection system, isopropanol:water (90:10, v/v) was used. The following settings were used: wash volume, 100 µL; wash speed, 4000 nL/s; loop wash factor, 2. Column temperature for every analysis was set to 40 °C, maintained by a Dionex UltiMate 3000 RS analytical column heater. Injection volume was set to 1 µL. HESI-II source conditions were as follows: ionization mode, positive or negative; sheath gas, 60 AU; auxiliary gas, 10 AU; sweep gas, 3 AU; spray voltage, 3.5 kV in positive and − 4.0 kV in negative mode; heater temperature, 320 °C; ion transfer capillary temperature, 320 °C; and S-lens RF level, 50.0. Mass spectrometry for untargeted metabolomics was performed according to a previously optimized workflow (Manier et al. 2019a, b). The settings for full scan (FS) data acquisition were as follows: resolution, 140,000 fwhm; microscan, 1; automatic gain control (AGC) target, 5×10^5; maximum injection time, 200 ms; scan range, *m/z* 50–750; spectrum data type; centroid. All study samples were analyzed in randomized order, to avoid potential analyte instability or instrument performance to confound data interpretation. Additionally, one QC injection was performed every five samples to monitor batch effects, as described by Wehrens et al. (Wehrens et al. 2016).

Significant features were subsequently identified using PRM. Settings for PRM data acquisition were as follow: resolution, 35,000 fwhm; microscans, 1; AGC target, 5×10^5; maximum injection time, 200 ms; isolation window, 1.0 m/z; collisions energy (CE), 10, 20, 35, or 40 eV; spectrum data type, centroid. The inclusion list contained the monoisotopic masses of all significant features and a time window of their retention time ± 60 s. TF Xcalibur software version 3.0.63 was used for data handling.

Data processing and statistical analysis

Thermo Fisher LC-HRMS/MS RAW files were converted into mzXML files using ProteoWizard (Adusumilli and Mallick 2017). Optimization of XCMS parameter was done on a previously optimized strategy as mentioned by Manier et al. (2019a). Peak picking and alignment parameters are summarized in Table S1 in the supplementary data. Peak picking was performed using XCMS in an R environment (Smith et al. 2006; Team) and the R package CAMERA (Kuhl et al. 2012) was used for the annotation of adducts, artifacts, and isotopes. Feature abundance with a value of zero were replaced by the lowest measured abundance as a surrogate limit of detection and the whole dataset was subsequently log10 transformed (Wehrens et al. 2016). Normalization was performed for urine samples using the area of endogenous creatinine from those samples analyzed using normal phase column and positive ionization mode and for plasma samples using the internal standard L-tryptophan-d_5. Significant changes of features between control and amphetamine group were assumed after evaluating their fold change using a threshold of 1.5, as well as after Welch's two-sample *t* test and a p value < 0.025. Principal component analysis (PCA) and hierarchical clustering were used to investigate patterns in the datasets. Names for the features were adopted from XCMS using "M" followed by rounded mass and "T" followed by the retention time in seconds. After visual inspection of the extracted ion chromatograms (EIC) of significant features, the significant features were divided into true and false features based on the peak shape quality of their EIC (Hemmer et al. 2020). The R scripts and the mzXML files can be found at https://github.com/sehem/Amphetamine_Metabolomics.git.

Identification of significant features

Significant features were identified by recording MS/MS spectra using the PRM method mentioned above. After conversion to mzXML format using ProteoWizard (Adusumilli and Mallick 2017), spectra were imported to NIST MSSEARCH version 2.3. Library search for identification was performed using the following settings: spectrum search type, identity (MS/MS); precursor ion *m/z*, in spectrum; spectrum search options, none; presearch, off; other options, none. MS/MS search was conducted using the following settings: precursor tolerance, ± 5 ppm; product ion tolerance, ± 10 ppm; ignoring peaks around precursor, ± *m/z* 1 (Manier et al. 2020b). Following libraries were used: NIST 2014 (nist_msms and nist_msms2 sublibrary) (Linstrom and Mallard 2001), Wiley METLIN Mass Spectral Database (Guijas et al. 2018), LipidBlast (Kind et al. 2013), MMHW (Maurer et al. 2018), the Human Metabolome Database (Wishart et al. 2007) (HMDB, V4.0). Metabolites of amphetamine were tentatively identified by interpreting their spectra in comparison to that of the parent compound. The in-silico fragmentation tool MetFrag (https://msbi.ipb-halle.de/MetFrag/) was applied to MS/MS data to identify potential substructures. Identified features were classified on the different levels of identification according to the Metabolomics Standards Initiative (MSI) (Sumner et al. 2007): affirmation using MS/MS information and co-elution with authentic standards (level 1), affirmation without chemical reference standards, based on comparison of experimental MS/MS spectra with public/commercial spectral libraries (level 2), annotation of putatively characterized compound classes based on characteristic physicochemical properties of a chemical class of compounds, or by spectral similarity to known compounds of a chemical class (level 3), and unidentified or unclassified metabolites (level 4).

Metabolic pathway analysis

To identify the endogenous metabolic pathways affected by amphetamine intake, all compounds identified with level 1 were imported to MetaboAnalyst 5.0 (http://www.metaboanalyst.ca) and searched against *Rattus norvegicus* metabolite database, for each matrix and time points. Scatter plot was selected as visualization method and the hypergeometric test with the relative-betweenness centrality algorithm was used. For further biological interpretation biochemical pathways with a significant level of $p < 0.05$ was used.

Results

Data files in mzXML format and the corresponding R files can be found at https://github.com/sehem/Amphetamine_Metabolomics.git. Results of univariate and multivariate statistic as well as the MS^2 spectra of amphetamine metabolites are available as supplementary data.

Animal general health aspects

Amphetamine exposed animals in this study showed no effect on their stereotyped behavior or exploratory activity after administration. Furthermore, no significant body weight loss could be observed in comparison to the control group.

Untargeted metabolomics: univariate and multivariate statistics

Volcano plots of detected features are shown in Fig. S1–4. An overview of the total number of significant features and their percentage of adducts/artifacts, isotopes, and false-positive results are shown in Table S2. In addition, datasets

were analyzed using multivariate methods in form of PCA and hierarchical clustering, to identify the largest changing features and specific signatures. Results of the hierarchical clustering which are displayed in heatmaps are shown in Fig. S5–8. Results of the scores of PCA of all matrices and time points are shown in Fig. S9–12.

Plasma

Using the four different analytical methods (RP positive, RP negative, NP positive, NP negative), 41 features were found in total to be significant at all three plasma time points after amphetamine administration. Plasma samples which were taken 1 h after administration, revealed 14 significant features after using RP and NP and positive ionization mode, which contained one isotope and two adducts according to CAMERA. However, one of these significant features was manually marked as false-positive, due to its EIC showing a poor peak shape quality. Analyses using RP and NP and negative ionization mode did not reveal any significant changes at that time point. Considering the heat maps, a clear separation between the control group and the amphetamine group is shown by NP (Fig. S5a). The dataset of the plasma samples which were taken 2 h after administration, revealed 13 significant features. These features included nine false-positive features, as well as two isotopes. Again, using RP and negative ionization did not reveal any significant features. Looking at the PCA, the two groups amphetamine and control measured in positive ionization mode separated well (Fig. S9b and S11b). In plasma samples received 8 h after administration, 18 significant features were observed only in positive ionization mode. These features included five false-positive hits and two isotopes. Both heatmaps showed a clear separation of the amphetamine and control group (Fig. S5c and S7c).

Urine

In urine samples, 88 significant features were found in total using the above mentioned four different analytical methods in the samples collected after 8 and 24 h. Sixty-four significant features were found in the 8-h urine samples. These features included 18 false-positive hits, as well as five isotopes and seven artifacts according to CAMERA. Heatmaps showed a good clustering of all groups (Fig. S5d, S6b, S7d, and S8a). Furthermore, in comparison to plasma, amphetamine samples are clustered very closely together in the PCA scores, whereas the control group appears more distributed (Fig. S9d, S10b, S11d, and S12a). Urine samples which were collected 24 h after administration revealed 32 significant features. These features included two false-positive hits, two isotopes, and three artifacts. The four heatmaps displayed a good clustering of the groups (Fig. S5e, S6c, S7e, and S8b). In comparison to the PCA scores after 8 h, the amphetamine group appears more distributed after 24 h.

Identification of significant features

The results of the identification of significant features are summarized in Tables 1 and 2. The given level of identification was in accordance with the MSI (Sumner et al. 2007). Isotopes that were putatively identified by CAMERA were not further identified. No MS^2 spectra could be recorded for several features due to their low abundance.

Plasma

In total, 14 compounds could be identified with a level of 1 or 2 (Table 1). 1 h after administration, most identified compounds were amino acids, which could all be identified with level 1 according to MSI. Additionally, the sesquiterpenoid tocopheronic acid was identified. In comparison to the control group all compounds were downregulated. Amphetamine and its metabolite *N*-acetylamphetamine were identified in samples drawn 2 h after administration. Furthermore, erucamide, an unsaturated fatty amide was upregulated compared to the control group. In plasma samples obtained after the 8 h, the identified compounds were again amino acids and *N*-acylsphingosines such as L-methionine and ceramide. While amounts of most amino acids were decreased compared to control group, all other compounds had increased.

Urine

Table 2 summarizes the 21 compounds which were identified in urine samples. Compared to urine collected after8 h, only amphetamine and its metabolites could be identified in the 24-h urine samples, except for *N*-acetylhistamine. Most of the identified compounds in 8-h urine samples were either amino acids or amphetamine metabolites. All identified compounds had increased in comparison to the control group except for L-tryptophan and spermidine.

Metabolic pathway analysis

since no substances with a level of 1 were identified in plasma samples 2 h after amphetamine administration, only the scatter plots of 1- and 8-h plasma samples are shown in Fig. 1a, b. The identified metabolic pathway in plasma samples 1 h after administration with $p < 0.05$ were aminoacyl-tRNA biosynthesis, phenylalanine, tyrosine, and tryptophan biosynthesis, valine, leucine, and isoleucine biosynthesis, and ubiquinone and other terpenoid-quinone biosynthesis. For the 8-h plasma samples, glycine, serine, and threonine metabolism, aminoacyl-tRNA biosynthesis, and valine, leucine, and isoleucine biosynthesis were found as significantly

Table 1 Identified compounds in plasma samples that showed significant changes between amphetamine (A) and control (C) group, sorted according to compound classes, *m/z* values are given for the highest prevalent ion species

Compound name	Identification level	Compound class	*m/z*	Chromatography	Adducts	Change	*p* (1 h, A vs. C)	*p* (2 h, A vs. C)	*p* (8 h, A vs. C)
Creatine	1	Amino acid	131.0695	RP	M + H	↑	n.s	n.s	*
L-Tryptophan	1	Amino acid	204.0899	RP	M + H, M + H-NH3, M + K*HCOOH, M + 1	↓	**	n.s	n.s
L-Citrulline	1	Amino acid	175.0957	NP	M + H	↓	*	n.s	n.s
L-Histidine	1	Amino acid	155.0695	RP	M + H	↓	**	n.s	n.s
L-Methionine	1	Amino acid	149.0510	RP, NP	M + H	↓	**	n.s	**
L-Proline	1	Amino acid	115.0633	RP, NP	M + H	↓	*	n.s	n.s
L-Threonine	1	Amino acid	119.0582	RP, NP	M + H	↓	**	n.s	*
L-Tyrosine	1	Amino acid	181.0739	RP, NP	M + H	↓	*	n.s	n.s
Amphetamine	1	Amphetamine	135.1048	RP	M + H	↑	n.s	*	n.s
Amphetamine-M (*N*-acetyl)	2 (NIST msms)	Amphetamine	177.1154	RP	M + H	↑	n.s	**	n.s
Ceramide (d18:1/23:0)	2 (Lipidmaps)	*N*-acylsphingosine	635.6216	NP	M + H, M + 1	↑	n.s	n.s	**
Nicotinamide	2 (NIST ms/ms)	Pyridine carboxylic acids	122.0480	NP	M + H	↓	n.s	n.s	*
Tocopheronic acid	3 (hmdb)	Sesquiterpenoids	294.1467	NP	M + H-H2O	↓	**	n.s	n.s
Erucamide	2 (NIST msms)	Unsaturated fatty amide	337.3345	NP	M + H, M + 1	↑	n.s	*	n.s

Identification levels for each metabolite are given according to MSI (Sumner et al. 2007). The corresponding chromatography method is given for normal phase (NP) and for reversed phase (RP) chromatography. Statistical was performed by Welch *t* test ($p < 0.025$): not significant (n.s.) > 0.025

*0.01–0.025

**0.001–0.01

*** < 0.001

changed metabolic pathways. In the 8-h urine samples, only two endogenous metabolites were identified by level 1, therefore, the scatter plot shows only one significant hit for arginine biosynthesis (Fig. 1c). No endogenous metabolites could be identified with level 1 according to MSI in urine 24 h after administration and, therefore, no metabolic pathway analysis was possible.

Discussion

The metabolome is considered as all compounds with molecular weights less than 1500 Da, which could be detected in, e.g., biofluids or tissues (Barnes et al. 2016). These molecules are not necessarily originating from the biological sample but also from, e.g., tubing vials and reagents. Samples such as plasma or urine are particularly complex since the metabolome is affected additionally by, e.g., food, microbiome, and drugs used to anesthetize experimental animals (Barnes et al. 2016). Since there are many parameters, which can influence the human metabolome, animal models are well suited to study changes in the metabolome, as they are less complex than human studies and can be performed under standardized and comparable conditions. Animals are subject to a uniform sleep–wake rhythm, kept under the same conditions, receive the same food and water, and they have the advantage that their genetic variability is very low. Furthermore, a metabolomic study requires significantly fewer animals than would be needed in a human clinical study to obtain reliable results. They are also beneficial compared to in vitro studies, which often represent only certain cells or organs and thus only a part of an entire organism. Thus, ten male adolescents Wistar rats were used in this study. Certain metabolites are released or excreted into blood and urine due to a certain stimulus such as drug of abuse intake. There they can be identified and serve as potential biomarkers (Wang et al. 2016). While plasma is primarily of interest in terms of changes in endogenous metabolites

Table 2 Identified compounds in urine samples that showed significant changes between amphetamine (A) and control (C) group, sorted according to compound classes, *m/z* values are given for the highest prevalent ion species

Compound name	Identification level	Compound class	*m/z*	Chromatography	Adducts	Change	p (8 h, A vs. C)	p (24 h, A vs. C)
4-Hydroxy-6-methyl-2-pyron	2 (NIST msms)		126.0317	NP	M + H	↑	*	n.s
Imidazole lactate	2 (NIST msms)		156.0535	NP	M + H	↑	*	n.s
Histamine	2 (NIST msms)	Amines	111.0796	NP	M + H	↑	**	n.s
L-Pentahomomethionine	2 (METLIN)	Amino acids	219.1293	NP	M + H	↑	*	n.s
L-Tryptophan	1	Amino acids	204.0899	RP	M + H	↓	*	n.s
N-acetyl-L-arginine	2 (NIST msms)	Amino acids	216.1222	NP	M + H	↑	**	n.s
N-acetylhistamine	2 (NIST msms)	Amino acids	153.0902	RP	M + H	↑	n.s	*
N^2, N^5-diacetylornithine	2 (NIST msms)	Amino acids	216.1110	RP	M + H	↑	*	n.s
Spermidine	2 (NIST msms)	Amino acids	145.1579	RP	M + H	↓	*	n.s
γ-Glutamyl-γ-aminobutyraldehyde	2 (NIST msms)	Amino acids	216.1110	NP	M-H	↑	**	n.s
Amphetamine	1	Amphetamine	135.1048	RP, NP	M + H-NH3, M + D-NH3, M + H, M + H, M + D, M + 1, M + 2, M + H-107	↑	**	***
Amphetamine-M (3-OH sulfate)	2 (MMHW)	Amphetamine	231.0565	RP, NP	M + H	↑	**	**
Amphetamine-M (4-hydroxy glucuronide)	3	Amphetamine	327.1318	RP	M + H	↑	**	n.s
Amphetamine-M (4-hydroxy-)	3	Amphetamine	151.0997	RP, NP	M + H, M + H-(107), M + D	↑	***	**
Amphetamine-M (6-oxohexanoic acid-)	3	Amphetamine	263.1521	NP	M + H	↑	***	n.s
Amphetamine-M (*N*-acetyl-4-hydroxy glucuronide)	3	Amphetamine	369.1424	RP, NP	M + H, H–H	↑	**	**
Amphetamine-M (*N*-acetyl-)	3	Amphetamine	177.1154	NP	M + H	↑	n.s	*
Amphetamine-M (*N*-acetyl-4-hydroxy-)	3	Amphetamine	193.1103	NP	M + H	↑	*	n.s
Amphetamine succinate	3	Amphetamine	235.1208	NP	M + H, M + D	↑	***	**
5-Acetylamino-6-amino-3-methyluracil	2 (MetFrag)	*N*-arylamides	198.0753	NP	M + H, M + D	↑	*	n.s
1,3-Dimethyluracil	2 (MetFrag)	Pyrimidines	140.0586	NP	M + H, M + D	↑	*	n.s
Urea	1	Ureas	60.0324	RP	M + Na	↑	*	n.s

Identification levels for each metabolite are given according to MSI (Sumner et al. 2007). The corresponding chromatography method is given for normal phase (NP) and for reversed phase (RP) chromatography. Statistical was performed by Welch *t* test ($p < 0.025$): not significant (n.s.) > 0.025

*0.01–0.025

**0.001–0.01

*** < 0.001

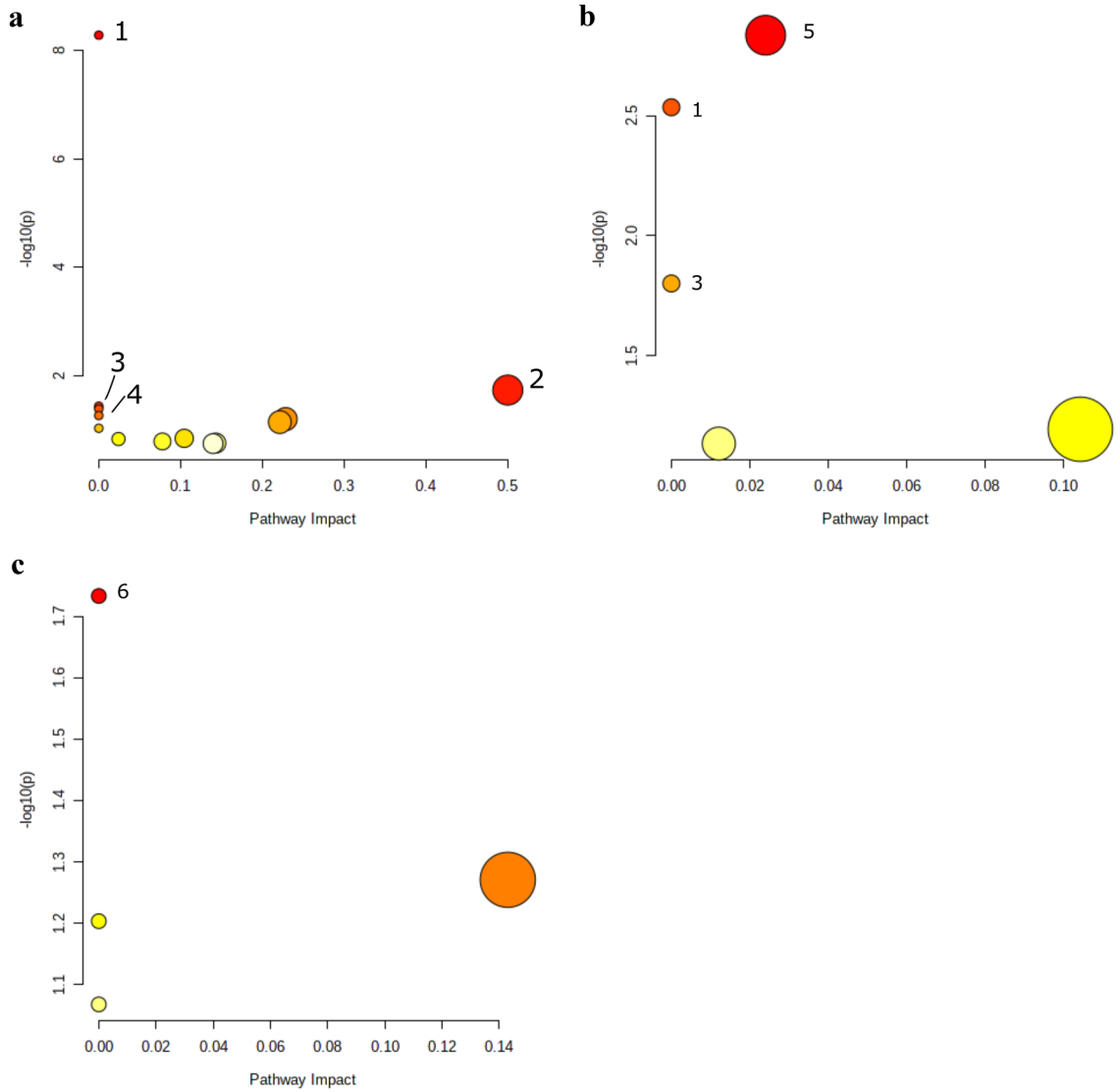

Fig. 1 Overview of the scatter plots of the metabolic pathways changed by a single dose of amphetamine (5 mg/kg) in **a** plasma 1 h, **b** plasma 8 h, and **c** urine 8 h after administration. The color of the dots is based on the negative decadic logarithm of the *p* value. Dark color indicates a more significant pathway. The dots radius complies with the pathway impact value. Statistically significant pathways ($p < 0.05$) are numbered from 1 to 6. 1 = aminoacyl-tRNA-biosynthesis; 2 = phenylalanine, tyrosine and tryptophan biosynthesis; 3 = valine, leucine, and isoleucine biosynthesis; 4 = ubiquinone and other terpenoid-quinone biosynthesis; 5 = glycine, serine and threonine metabolism; 6 = arginine biosynthesis

that may be affected by amphetamine abuse, urine is of interest for detecting metabolites (intake biomarker). The application of untargeted metabolomics to urine may allow the detection of metabolites that may be overseen by conventional pathway analysis methods because they might not be expected. Therefore, both plasma and urine were analyzed in this study to complement and confirm previous studies of the plasma metabolome after amphetamine intake and to detect additional metabolites/biomarker in urine that allow detection of amphetamine abuse. Blood draw time points of 1, 2, and 8 h were chosen to examine both direct and delayed effects of amphetamines on the plasma metabolome. Blood at time point = 0 min was not sampled to avoid additional stress to the animals prior to substance application, which could have influenced the study outcome. Furthermore, individual differences in the animals could be ruled out via the study design as changes in the metabolome between the control and amphetamine group were only assumed to be statistically significant in case they occurred in the complete group. Since the maximum plasma concentration is reached

after 15 min, the first two withdrawal time points were 1 and 2 h (Slezak et al. 2018). 8 h after amphetamine administration, amphetamine or metabolites of them could no longer be detected in plasma. However, effects could possibly still be detected but also some changes may also occur at a later time point and thus be undetectable (Gertsman and Barshop 2018). The two urine collection time points were chosen to be able to detect both direct and delayed effects.

It was not possible to find potential reasons for all identified altered metabolites in this study. Conclusions on a pathway can only be drawn if the pathway could be clearly identified by more than one metabolite. Metabolites that occurred as a single phenomenon of a possible pathway must, therefore, first be considered individually in their function. To be able to make specific statements about the influence of the metabolites in association with amphetamine consumption, a targeted study can be considered in which a specific analysis can be made for metabolites that occur in the proposed metabolic pathways.

Plasma samples collected after controlled amphetamine administration

The complexity of the plasma metabolome was visible comparing the PCA of the plasma datasets to the urine datasets (Fig. S9–12). Urine samples are well clustered in contrast to plasma samples regarding the multivariate statistics. This can be explained by the fact, that in contrast to plasma, most of the identified features in urine belong to amphetamine and its metabolites.

While Steuer et al. (2020) identified in human various metabolites derived from energy metabolism in general, such as acyl carnitines, fatty acids, bile acids, the current study found amino acids to be significantly changed in rat plasma. It needs to be mentioned, that the species may not be directly comparable. The difference in the results between Steuer et al. (2020) and the present study shows that comprehensive studies and different analytical strategies are necessary to study changes within the metabolome. The pathway analysis of time points 1 and 8 h after administration are shown in Fig. 1a and b. Except for creatine, all amino acids were downregulated in the amphetamine-treated rats compared to the control group. The pathway, which was indicated for both time points was the aminoacetyl-tRNA biosynthesis, which is an essential process in protein synthesis (Rubio Gomez and Ibba 2020). While tryptophan, histidine, methionine, threonine, and tyrosine are essential amino acids, proline and tryptophan are functional amino acids, which are important regulators of key metabolic pathways. Such pathways are necessary for maintenance growth, reproduction, and immunity in organism (Wu 2009). In addition to the amino acids, further features were identified, but these belong to MSI level 2 and were, therefore, not included in the pathway analysis. The *N*-acylsphingosine ceramide (d18:1/23:0) was increased in 8-h plasma samples of amphetamine-treated rats. Ceramides are biologically used as membrane stabilizer, energy source and storage, and in inflammatory processes. The observation of amphetamine being able to increase energy metabolism also correlates with other studies conducted both in humans and in rats (Dickson 1998; Tserng and Griffin 2004). Again, species may not be comparable. Another endogenous metabolite, which is associated with the energy metabolism is tocopheronic acid (Fahy et al. 2005; Watson 2006). It is also part of the lipid metabolism and transport and was significantly decreased in comparison to the control group after 1 h of drug administration. Furthermore, nicotinamide was downregulated in amphetamine-treated rats. It is involved in the nicotinamide adenine dinucleotide (NAD^+) signaling pathway. NAD is synthesized from both nicotinamide and degradation products of the amino acid tryptophan (Canto and Auwerx 2011). It has an important role as a cofactor in numerous metabolic processes such as glycolysis, citric acid cycle of cellular respiration, or other cellular functions (Belenky et al. 2007; Ying 2006). In plasma collected after 2 h, only three features were identified. Two of them were identified as amphetamine and its metabolite *N*-acetylamphetamine. The third feature identified was erucamide, which is an endogenous metabolite that causes reduced mobility and slightly decreased awareness in rats (Cravatt et al. 1995; McKinney and Cravatt 2005). Such oleamides could also be originating from disposable laboratory plasticware. To test whether this metabolite was a contaminant from laboratory plasticware or whether it was endogenous in origin, a study was performed according to McDonald et al. (2008) by replacing plasma with methanol. The result showed that erucamide was also found in methanol samples, but compared to plasma, the intensity and peak area was much lower. Additionally, the EIC showed a higher signal in amphetamine-treated plasma than in the control group. Therefore, it might be possible that erucamide was mainly derived from an endogenous source. All identified features except of amphetamine and its metabolite *N*-acetylamphetamine were of endogenous origin and may help to understand acute and long-term effects of amphetamine abuse and are an important complement to already published results.

Urine samples collected after controlled amphetamine administration

Compared to other biofluids such as plasma, urine is characterized by being easy to collect, rich in metabolites, and able to reflect imbalances in all biochemical pathways within an organism (Khamis et al. 2017). It is, amongst others, also well suited for identifying novel exogenous drug metabolites or endogenous biomarkers indicative for drug ingestion so

far, they are not exclusively excreted into feces. This is of particular interest for compounds, which show relatively small detection windows such as amphetamine (Carvalho et al. 2012; Kraemer and Maurer 2002; Musshoff 2000). Therefore, an untargeted metabolomics approach was used in the present study to detect endogenous and (new) exogenous metabolites in rat urine. According to previous studies in mammals (Caldwell 1976; Cho and Wright 1978; Musshoff 2000), expected amphetamine metabolites were formed mainly through (1) hydroxylation in position 4 of the aromatic ring, followed by conjugation of the phenol group with sulfate or glucuronic acid and (2) *N*-deamination and oxidation into corresponding benzoic acid derivatives which were further conjugated with glycine and excreted as hippuric acids (Kraemer and Maurer 2002). However, there might be species differences to be considered. In the present study, seven amphetamine metabolites were found amongst them 4-hydroxyamphetamine and its sulfate and glucuronic acid conjugates. Features, which belong to the *N*-deamination and oxidation pathway were not indicated as statistically significant. However, six metabolites/adducts could be identified (MS^2 spectra shown in Fig. S13). In detail, the *N*-acetylation, which was also found in plasma samples, the *N*-acetylation together with the hydroxylation of the aromatic ring, the glucuronic acid conjugate of *N*-acetyl-4-hydroxyamphetamine, and the conjugate with acid succinic acid. The 6-oxohexanoic acid adduct cannot be explained from a biological point of view. It is possible that this adduct originated exogenously. However, to our knowledge this is the first report of amphetamine bound to succinic acid in rat. In addition to the amphetamine metabolites mentioned above, endogenous metabolites were also detected in urine. These included metabolites, which belong to the histamine metabolism such as *N*-acetylhistamine and histamine itself. Histamine is a powerful vasodilator, stimulant of gastric secretion, and also a centrally acting neurotransmitter. Furthermore, histamine has a considerable impact on mitigating stress-induced adverse effects in rats (Chen et al. 2020). This observation suggests that amphetamine induces additional stress to rats compared to the control group. Spermidine was decreased in amphetamine-treated rats. Polyamines such as spermidine and spermine play important roles in mammalian cells in protein and nucleic acid synthesis, protection from oxidative damage, activity of ion channels, and cell proliferation, differentiation and apoptosis (Pegg 2016). The pathway which was indicated for urine collected 8 h after administration was the arginine biosynthesis (Fig. 1c). Arginine, a semi-essential amino acid, is synthesized from citrulline, which has also been detected in plasma and is metabolized either to ornithine and urea or to citrulline and nitric oxide (NO). The arginine derivatives *N*-acetyl-L-arginine and urea, and N_2, N_5-diacetylornithine, a derivate of ornithine, were also detected in urine (Cynober et al. 1995; Sasso et al. 2014). In rats, arginine acts as a key signal for the activation of ureagenesis during high-protein feeding. Additionally, arginine plays an important role in cell division, ammonia-removing from body, immune function, and hormones release. As a precursor of NO, the smallest signaling molecule in mammalian cells, arginine is thus indirectly involved in the regulation of blood pressure (Cynober et al. 1995). γ-Glutamyl-γ-aminobutyraldehyde, imidazole lactate, 5-acetylamino-6-amino-3-methyluracil, and 1,3-dimethyluracil fluctuated significantly in urine. However, the biological significance of these metabolites is currently unclear.

Limitations of the study

The present study provides only a snapshot of the metabolome in rats and a direct transfer to humans is not possible. Furthermore, individual altered features in this study could only be partly explained in terms of their general function in mammals, but not how they relate to amphetamine abuse. This is due to the fact that it is not possible to draw reliable conclusions about a specific pathway based on a single feature and thus explain processes in the organism. Thus, further studies are needed to draw reliable conclusions. However, the findings of this study may help to first understand the impact of amphetamine on the metabolome of mammals but—and this is much more of relevance—to allow a targeted design of future human studies that need then fewer subjects. Furthermore, the newly detected metabolites in rats may potentially not be formed (at least to this extent) in humans.

Conclusion

Due to the complexity of the metabolome in plasma and urine with its multitude of different metabolites, it is not possible to establish an untargeted metabolomics approach that allows a holistic view on the metabolome. For this reason, the present study is a further piece in the puzzle to elucidate, which metabolic changes occur in an organism after amphetamine intake. In this study, the major endogenous metabolites that were significantly altered belong to the compound class of amino acids. Furthermore, new amphetamine metabolites *N*-acetylamphetamine, *N*-acetyl-4-hydroxyamphetamine, *N*-acethyl-4-hydroxy-glucuronic amphetamine, and an amphetamine succinic acid conjugate were identified, which may be used for detection of amphetamine intake. The example of the succinate metabolite shows that untargeted metabolomics allows to identify metabolites that would otherwise not have been expected or would not have been searched for in a targeted approach.

Supplementary Information The online version contains supplementary material available at https://doi.org/10.1007/s00204-021-03135-8.

Acknowledgements The authors would like to thank Sascha K. Manier, Carsten Schröder, Gabriele Ulrich, and Armin A. Weber for their support and/or helpful discussion.

Funding Open Access funding enabled and organized by Projekt DEAL. This research received no external funding.

Availability of data and material The R scripts and the mzXML files can be found at https://github.com/sehem/Amphetamine_Metabolomics.git.

Declarations

Conflict of interest The authors declare no conflict of interest.

Open Access This article is licensed under a Creative Commons Attribution 4.0 International License, which permits use, sharing, adaptation, distribution and reproduction in any medium or format, as long as you give appropriate credit to the original author(s) and the source, provide a link to the Creative Commons licence, and indicate if changes were made. The images or other third party material in this article are included in the article's Creative Commons licence, unless indicated otherwise in a credit line to the material. If material is not included in the article's Creative Commons licence and your intended use is not permitted by statutory regulation or exceeds the permitted use, you will need to obtain permission directly from the copyright holder. To view a copy of this licence, visit http://creativecommons.org/licenses/by/4.0/.

References

Adusumilli R, Mallick P (2017) Data conversion with proteowizard msconvert. Methods Mol Biol 1550:339–368. https://doi.org/10.1007/978-1-4939-6747-6_23

Araujo AM, Carvalho M, Costa VM et al (2021) In vivo toxicometabolomics reveals multi-organ and urine metabolic changes in mice upon acute exposure to human-relevant doses of 3,4-methylenedioxypyrovalerone (MDPV). Arch Toxicol 95(2):509–527. https://doi.org/10.1007/s00204-020-02949-2

Barnes S, Benton HP, Casazza K et al (2016) Training in metabolomics research. I. Designing the experiment, collecting and extracting samples and generating metabolomics data. J Mass Spectrom 51(7):461–475. https://doi.org/10.1002/jms.3782

Belenky P, Bogan KL, Brenner C (2007) NAD+ metabolism in health and disease. Trends Biochem Sci 32(1):12–19. https://doi.org/10.1016/j.tibs.2006.11.006

Bonisch H, Bruss M (2006) The norepinephrine transporter in physiology and disease. Handb Exp Pharmacol 485(175):485–524. https://doi.org/10.1007/3-540-29784-7_20

Bouhifd M, Hartung T, Hogberg HT, Kleensang A, Zhao L (2013) Review: toxicometabolomics. J Appl Toxicol 33(12):1365–1383. https://doi.org/10.1002/jat.2874

Caldwell J (1976) The metabolism of amphetamines in mammals. Drug Metab Rev 5(2):219–280. https://doi.org/10.3109/03602537609029979

Canto C, Auwerx J (2011) NAD+ as a signaling molecule modulating metabolism. Cold Spring Harb Symp Quant Biol 76:291–298. https://doi.org/10.1101/sqb.2012.76.010439

Carvalho M, Carmo H, Costa VM et al (2012) Toxicity of amphetamines: an update. Arch Toxicol 86(8):1167–1231. https://doi.org/10.1007/s00204-012-0815-5

Chen S, Lu D, Wang W, Chen W, Zhang S, Wei S (2020) Plasma metabolomic profiling of repeated restraint stress in rats. J Chromatogr B Analyt Technol Biomed Life Sci 1160:122294. https://doi.org/10.1016/j.jchromb.2020.122294

Cho AK, Wright J (1978) Pathways of metabolism of amphetamine and related compounds. Life Sci 22(5):363–372. https://doi.org/10.1016/0024-3205(78)90282-5

Cravatt BF, Prospero-Garcia O, Siuzdak G et al (1995) Chemical characterization of a family of brain lipids that induce sleep. Science 268(5216):1506–1509. https://doi.org/10.1126/science.7770779

Cynober L, Boucher JL, Vasson M-P (1995) Arginine metabolism in mammals. J Nutr Biochem 6(8):402–413. https://doi.org/10.1016/0955-2863(95)00066-9

de la Torre R, Farre M, Navarro M, Pacifici R, Zuccaro P, Pichini S (2004) Clinical pharmacokinetics of amfetamine and related substances: monitoring in conventional and non-conventional matrices. Clin Pharmacokinet 43(3):157–185. https://doi.org/10.2165/00003088-200443030-00002

Dickson RC (1998) Sphingolipid functions in saccharomyces cerevisiae: comparison to mammals. Annu Rev Biochem 67:27–48. https://doi.org/10.1146/annurev.biochem.67.1.27

Dolder PC, Strajhar P, Vizeli P, Hammann F, Odermatt A, Liechti ME (2017) Pharmacokinetics and pharmacodynamics of lisdexamfetamine compared with D-amphetamine in healthy subjects. Front Pharmacol 8:617. https://doi.org/10.3389/fphar.2017.00617

Fahy E, Subramaniam S, Brown HA et al (2005) A comprehensive classification system for lipids. J Lipid Res 46(5):839–861. https://doi.org/10.1194/jlr.E400004-JLR200

Feio-Azevedo R, Costa VM, Ferreira LM et al (2017) Toxicity of the amphetamine metabolites 4-hydroxyamphetamine and 4-hydroxynorephedrine in human dopaminergic differentiated SH-SY5Y cells. Toxicol Lett 269:65–76. https://doi.org/10.1016/j.toxlet.2017.01.012

Gertsman I, Barshop BA (2018) Promises and pitfalls of untargeted metabolomics. J Inherit Metab Dis 41(3):355–366. https://doi.org/10.1007/s10545-017-0130-7

Guijas C, Montenegro-Burke JR, Domingo-Almenara X et al (2018) METLIN: a technology platform for identifying knowns and unknowns. Anal Chem 90(5):3156–3164. https://doi.org/10.1021/acs.analchem.7b04424

Heal DJ, Smith SL, Gosden J, Nutt DJ (2013) Amphetamine, past and present–a pharmacological and clinical perspective. J Psychopharmacol 27(6):479–496. https://doi.org/10.1177/0269881113482532

Hemmer S, Manier SK, Fischmann S, Westphal F, Wagmann L, Meyer MR (2020) Comparison of three untargeted data processing workflows for evaluating LC-HRMS metabolomics data. Metabolites. https://doi.org/10.3390/metabo10090378

Khamis MM, Adamko DJ, El-Aneed A (2017) Mass spectrometric based approaches in urine metabolomics and biomarker discovery. Mass Spectrom Rev 36(2):115–134. https://doi.org/10.1002/mas.21455

Kind T, Liu KH, Lee DY, DeFelice B, Meissen JK, Fiehn O (2013) LipidBlast in silico tandem mass spectrometry database for lipid identification. Nat Methods 10(8):755–758. https://doi.org/10.1038/nmeth.2551

Kraemer T, Maurer H (2002) Toxicokinetics of amphetamines: metabolism and toxicokinetic data of designer drugs, amphetamine, methamphetamine, and their N-alkyl derivatives. Ther Drug Monit 24(2):277–289

Kuhl C, Tautenhahn R, Bottcher C, Larson TR, Neumann S (2012) CAMERA: an integrated strategy for compound spectra extraction and annotation of liquid chromatography/mass spectrometry

data sets. Anal Chem 84(1):283–289. https://doi.org/10.1021/ac202450g
Linstrom PJ, Mallard WG (2001) The NIST chemistry webbook: a chemical data resource on the internet†. J Chem Eng Data 46(5):1059–1063. https://doi.org/10.1021/je000236i
Liu X, Locasale JW (2017) Metabolomics: a primer. Trends Biochem Sci 42(4):274–284. https://doi.org/10.1016/j.tibs.2017.01.004
Manier SK, Meyer MR (2020) Impact of the used solvent on the reconstitution efficiency of evaporated biosamples for untargeted metabolomics studies. Metabolomics 16(3):34. https://doi.org/10.1007/s11306-019-1631-1
Manier SK, Keller A, Meyer MR (2019a) Automated optimization of XCMS parameters for improved peak picking of liquid chromatography-mass spectrometry data using the coefficient of variation and parameter sweeping for untargeted metabolomics. Drug Test Anal 11(6):752–761. https://doi.org/10.1002/dta.2552
Manier SK, Keller A, Schaper J, Meyer MR (2019b) Untargeted metabolomics by high resolution mass spectrometry coupled to normal and reversed phase liquid chromatography as a tool to study the in vitro biotransformation of new psychoactive substances. Sci Rep 9(1):2741. https://doi.org/10.1038/s41598-019-39235-w
Manier SK, Schwermer F, Wagmann L, Eckstein N, Meyer MR (2020a) Liquid chromatography-high-resolution mass spectrometry-based in vitro toxicometabolomics of the synthetic cathinones 4-MPD and 4-MEAP in pooled human liver microsomes. Metabolites. https://doi.org/10.3390/metabo11010003
Manier SK, Wagmann L, Flockerzi V, Meyer MR (2020b) Toxicometabolomics of the new psychoactive substances alpha-PBP and alpha-PEP studied in HepaRG cell incubates by means of untargeted metabolomics revealed unexpected amino acid adducts. Arch Toxicol 94(6):2047–2059. https://doi.org/10.1007/s00204-020-02742-1
Maurer HH, Pfleger K, Weber AA (2016) Mass spectral data of drugs, poisons, pesticides, pollutants and their metabolites. Wiley-VCH, Weinheim
Maurer HH, Meyer MR, Helfer AG, Weber AA (2018) Maurer/Meyer/Helfer/Weber MMHW LC-HR-MS/MS library of drugs, poisons, and their metabolites. Wiley-VCH, Weinheim
McDonald GR, Hudson AL, Dunn SM et al (2008) Bioactive contaminants leach from disposable laboratory plasticware. Science 322(5903):917. https://doi.org/10.1126/science.1162395
McKinney MK, Cravatt BF (2005) Structure and function of fatty acid amide hydrolase. Annu Rev Biochem 74:411–432. https://doi.org/10.1146/annurev.biochem.74.082803.133450
Musshoff F (2000) Illegal or legitimate use? Precursor compounds to amphetamine and methamphetamine. Drug Metab Rev 32(1):15–44. https://doi.org/10.1081/dmr-100100562
Nair AB, Jacob S (2016) A simple practice guide for dose conversion between animals and human. J Basic Clin Pharm 7(2):27–31. https://doi.org/10.4103/0976-0105.177703
Nicholson JK, Lindon JC (2008) Systems biology: metabonomics. Nature 455(7216):1054–1056. https://doi.org/10.1038/4551054a
Pegg AE (2016) Functions of polyamines in mammals. J Biol Chem 291(29):14904–14912. https://doi.org/10.1074/jbc.R116.731661
Psychoaktivesubstanzen.de/amphetamin/Amphetamin/Speed/Amphe—Bekannter, verbotener Upper (Substanzinfo). In. http://psychoaktivesubstanzen.de/amphetamin/. Accessed 26 May 2020, 9:30
Ramirez T, Daneshian M, Kamp H et al (2013) Metabolomics in toxicology and preclinical research. Altex 30(2):209–225. https://doi.org/10.14573/altex.2013.2.209
Rubio Gomez MA, Ibba M (2020) Aminoacyl-tRNA synthetases. RNA 26(8):910–936. https://doi.org/10.1261/rna.071720.119
Sasso S, Dalmedico L, Delwing-Dal Magro D, Wyse AT, Delwing-de Lima D (2014) Effect of N-acetylarginine, a metabolite accumulated in hyperargininemia, on parameters of oxidative stress in rats: protective role of vitamins and L-NAME. Cell Biochem Funct 32(6):511–519. https://doi.org/10.1002/cbf.3045
Slezak JM, Mueller M, Ricaurte GA, Katz JL (2018) Pharmacokinetic and pharmacodynamic analysis of d-amphetamine in an attention task in rodents. Behav Pharmacol 29(6):551–556. https://doi.org/10.1097/FBP.0000000000000409
Smith CA, Want EJ, O'Maille G, Abagyan R, Siuzdak G (2006) XCMS: processing mass spectrometry data for metabolite profiling using nonlinear peak alignment, matching, and identification. Anal Chem 78(3):779–787. https://doi.org/10.1021/ac051437y
Steinkellner T, Freissmuth M, Sitte HH, Montgomery T (2011) The ugly side of amphetamines: short- and long-term toxicity of 3,4-methylenedioxymethamphetamine (MDMA, 'Ecstasy'), methamphetamine and D-amphetamine. Biol Chem 392(1–2):103–115. https://doi.org/10.1515/BC.2011.016
Steuer AE, Brockbals L, Kraemer T (2019) Metabolomic strategies in biomarker research-new approach for indirect identification of drug consumption and sample manipulation in clinical and forensic toxicology? Front Chem 7:319. https://doi.org/10.3389/fchem.2019.00319
Steuer AE, Kaelin D, Boxler MI et al (2020) Comparative untargeted metabolomics analysis of the psychostimulants 3,4-methylenedioxy-methamphetamine (MDMA), amphetamine, and the novel psychoactive substance mephedrone after controlled drug administration to humans. Metabolites. https://doi.org/10.3390/metabo10080306
Sumner LW, Amberg A, Barrett D et al (2007) Proposed minimum reporting standards for chemical analysis chemical analysis working group (CAWG) metabolomics standards initiative (MSI). Metabolomics 3(3):211–221. https://doi.org/10.1007/s11306-007-0082-2
Team RC R: A language and environment for statistical computing. 3.4.1 edn. R Foundation for Statistical Computing
Tserng KY, Griffin RL (2004) Ceramide metabolite, not intact ceramide molecule, may be responsible for cellular toxicity. Biochem J 380(Pt 3):715–722. https://doi.org/10.1042/BJ20031733
UNODC (2020) World drug report 2020—booklet 1. United Nations Publication, New York
Wang L, Wu N, Zhao TY, Li J (2016) The potential biomarkers of drug addiction: proteomic and metabolomics challenges. Biomarkers 21(8):678–685. https://doi.org/10.1080/1354750X.2016.1201530
Watson AD (2006) Thematic review series: systems biology approaches to metabolic and cardiovascular disorders. Lipidomics: a global approach to lipid analysis in biological systems. J Lipid Res 47(10):2101–2111. https://doi.org/10.1194/jlr.R600022-JLR200
Wehrens R, Hageman JA, van Eeuwijk F et al (2016) Improved batch correction in untargeted MS-based metabolomics. Metabolomics 12:88. https://doi.org/10.1007/s11306-016-1015-8
Wishart DS, Tzur D, Knox C et al (2007) HMDB: the human metabolome database. Nucleic Acids Res 35:D521–D526. https://doi.org/10.1093/nar/gkl923
Wu G (2009) Amino acids: metabolism, functions, and nutrition. Amino Acids 37(1):1–17. https://doi.org/10.1007/s00726-009-0269-0
Ying W (2006) NAD+ and NADH in cellular functions and cell death. Front Biosci 11:3129–3148. https://doi.org/10.2741/2038
Zaitsu K, Hayashi Y, Kusano M, Tsuchihashi H, Ishii A (2016) Application of metabolomics to toxicology of drugs of abuse: a mini review of metabolomics approach to acute and chronic toxicity studies. Drug Metab Pharmacokinet 31(1):21–26. https://doi.org/10.1016/j.dmpk.2015.10.002

Publisher's Note Springer Nature remains neutral with regard to jurisdictional claims in published maps and institutional affiliations.

Altered metabolic pathways elucidated via untargeted in vivo toxicometabolomics in rat urine and plasma samples collected after controlled application of a human equivalent amphetamine dose

Selina Hemmer[1], Lea Wagmann[1], Markus R. Meyer[1]

[1]Department of Experimental and Clinical Toxicology, Institute of Experimental and Clinical Pharmacology and Toxicology, Center for Molecular Signaling (PZMS), Saarland University, 66421 Homburg, Germany

Electronic Supplementary Material

Table S1. Overview of the peak picking and alignment parameters used for preprocessing for the respective matrices. NP = normal phase chromatography, RP = reversed phase chromatography, pos = positive, neg = negative, ppm = allowed ppm deviation of mass traces for peak picking, snthresh = signal to noise threshold, mzdiff = minimum difference in *m/z* for two peaks to be considered as separate, prefilter 1 = minimum of scan points, prefilter 2 = minimum abundance, bw = bandwidth for grouping of peaks across separate chromatograms.

Matrix, time point	Column	Polarity	Peakwidth, min	Peakwidth, max	ppm	sntresh	mzdiff	Prefilter 1	Prefilter 2	bw
Plasma, 1h	NP	pos	9.9	40	1.0	47	0.038	10	9100	0.5
		neg	7.8	12	1.2	14	0.048	6	3800	0.5
	RP	pos	10.0	10	1.5	100	0.048	15	10000	1.0
		neg	8.9	96	1.0	80	0.002	6	8800	0.5
Plasma, 2h	NP	pos	9.9	22	1.0	26	0.038	9	700	0.5
		neg	9.9	12	1.2	23	0.002	6	6600	0.5
	RP	pos	9.9	11	1.6	96	0.054	16	10000	3.5
		neg	10.0	62	1.0	83	-0.096	1	9000	0.5
Plasma, 8h	NP	pos	10.0	24	1.0	23	0.018	10	9600	0.5
		neg	8.9	10	1.0	74	0.042	8	1900	0.5
	RP	pos	8.9	10	1.6	98	0.010	15	9700	2.1
		neg	9.2	10	1.0	77	0.016	8	9800	0.5
Urine, 8h	NP	pos	9.9	22	1.1	36	0.062	15	300	0.5
		neg	8.9	10	1.2	97	0.038	11	8200	0.5
	RP	pos	10.0	11	1.8	97	0.016	18	500	2.0
		neg	10.0	76	1.2	34	0.044	6	5600	0.5
Urine, 24h	NP	pos	9.9	12	1.0	90	0.090	17	1600	0.5
		neg	8.9	16	1.5	65	0.062	9	7000	0.5
	RP	pos	9.8	12	1.3	61	0.030	19	900	1.5
		neg	9.9	59	1.0	42	0.010	8	300	0.5

Table S2. Overview of the total number of significant features found with all 4 different analytical methods (reversed phase chromatography positive/negative and normal phase chromatography positive/negative) and their percentage of adducts/artifacts, isotopes and false-positive results in the respective matrices. Features found with more than one analytical method count only once.

Matrix	Time point	Number significant features	Adducts/Artifacts	Isotopes	False-positive
Plasma	1h	14	2	1	1
	2h	13	0	2	9
	8h	18	0	2	5
Urine	8h	64	7	5	18
	24h	32	3	2	2

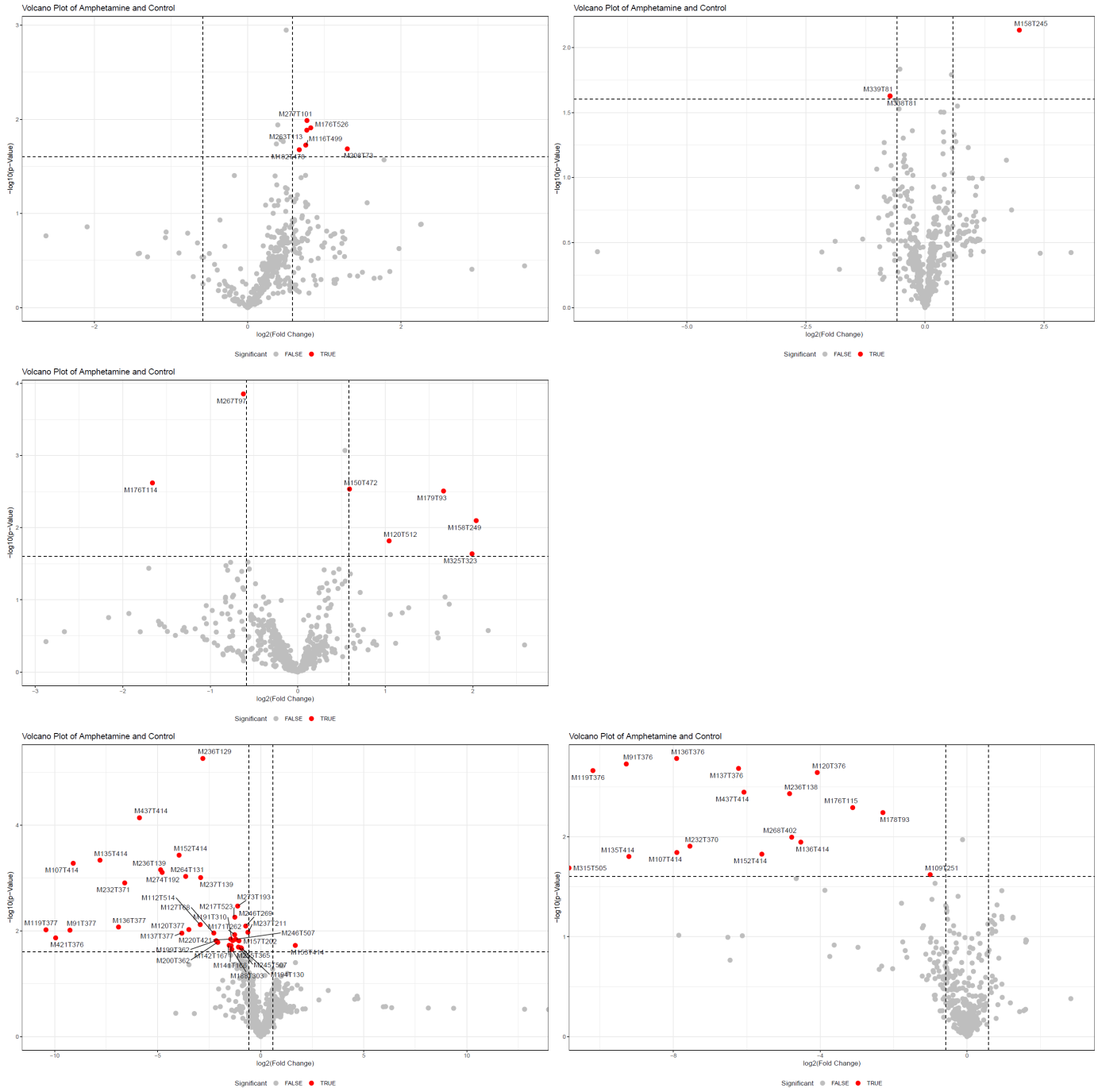

Fig. S1. Results of volcano plot for plasma and urine samples after analysis using normal phase chromatography and positive ionization mode. **a** = plasma 1 h; **b** = plasma 2 h; **c** = plasma 8 h; **d** = urine 8 h; **e** = urine 24 h.

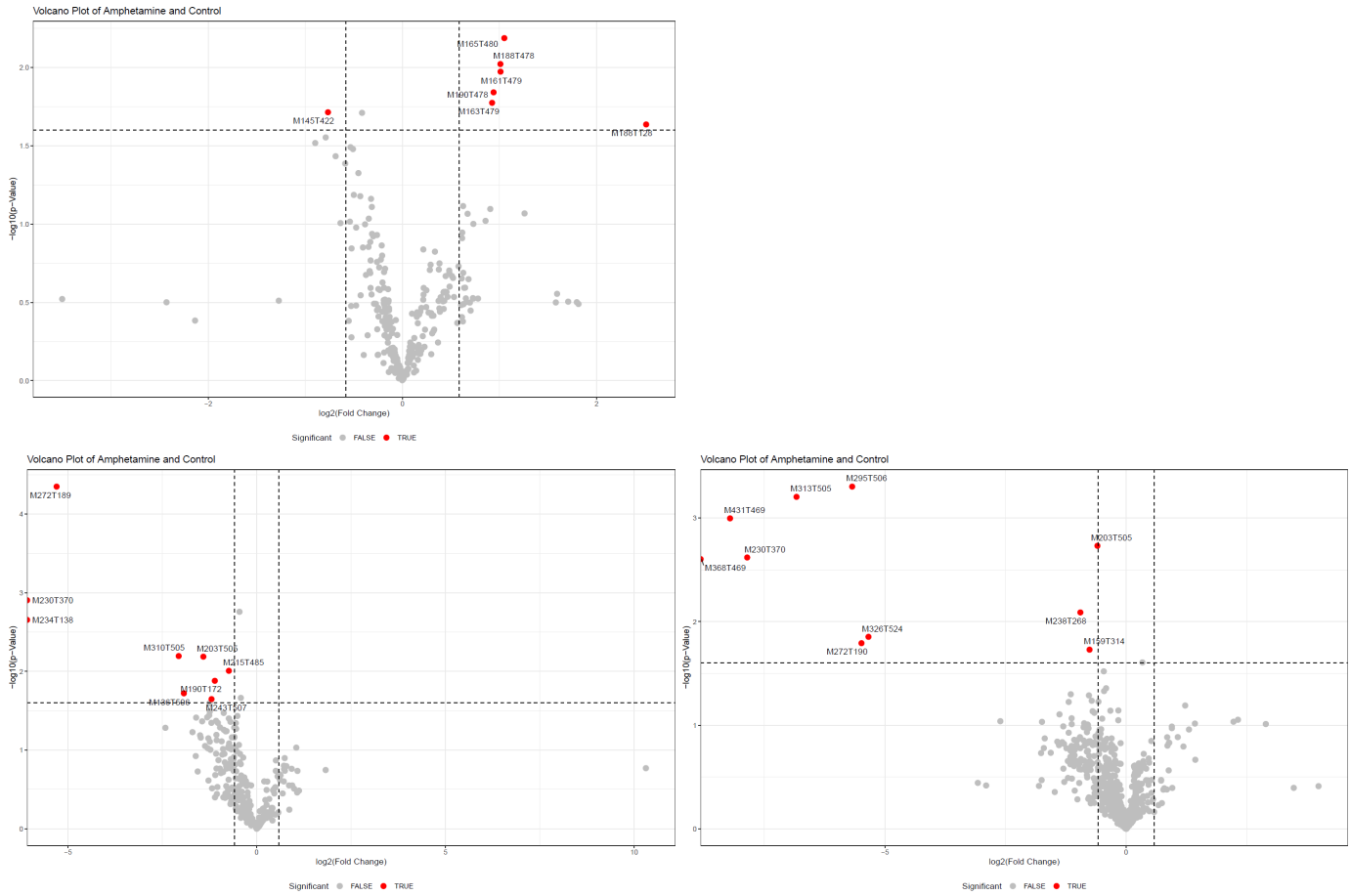

Fig. S2. Results of volcano plot for plasma and urine samples after analysis using normal phase chromatography and negative ionization mode. **a** = plasma 2 h; **b** = urine 8 h; **c** = urine 24 h.

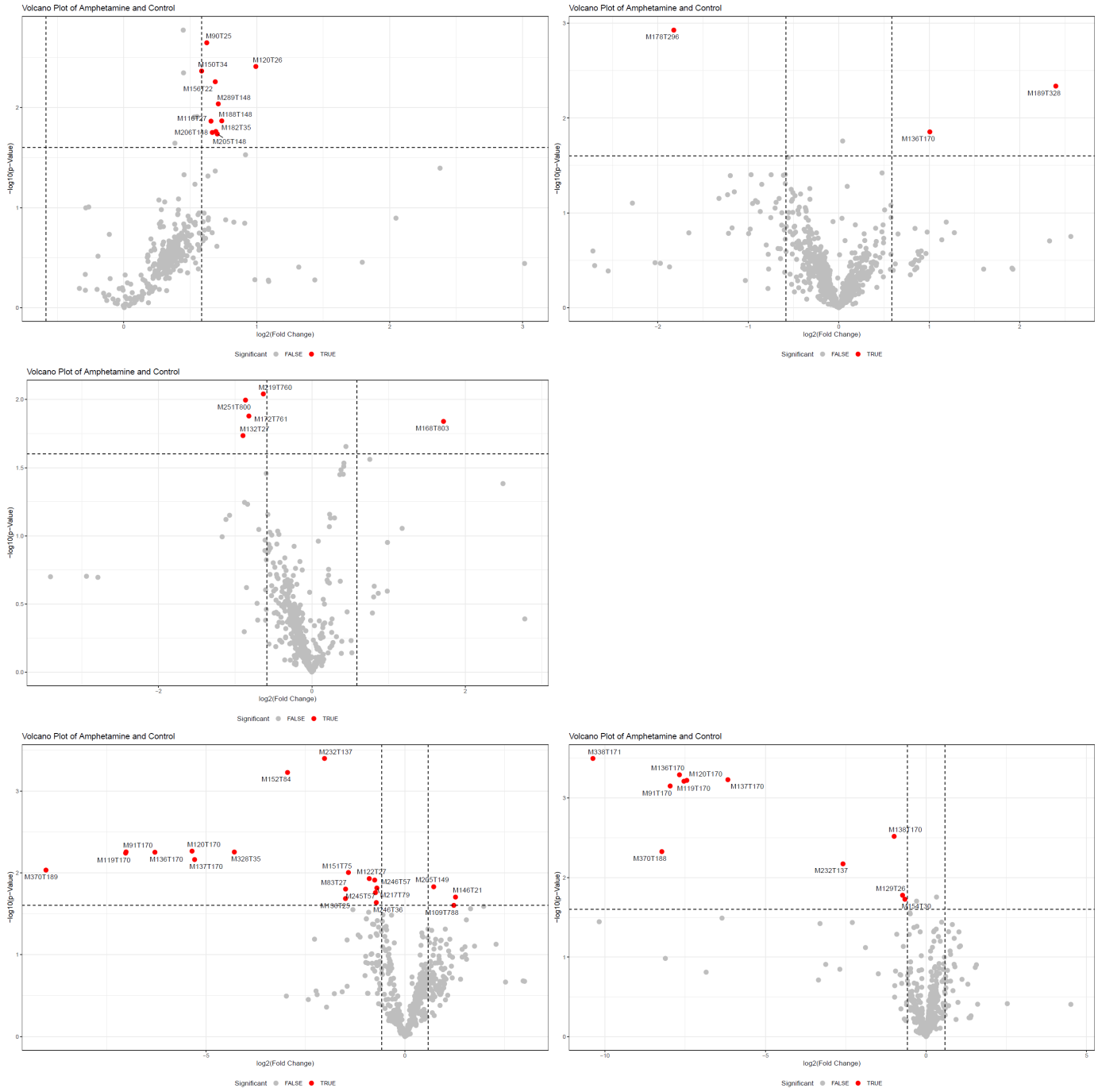

Fig. S3. Results of volcano plot for plasma and urine samples after analysis using reversed phase chromatography and positive ionization mode. **a** = plasma 1 h; **b** = plasma 2 h; **c** = plasma 8 h; **d** = urine 8 h; **e** = urine 24 h.

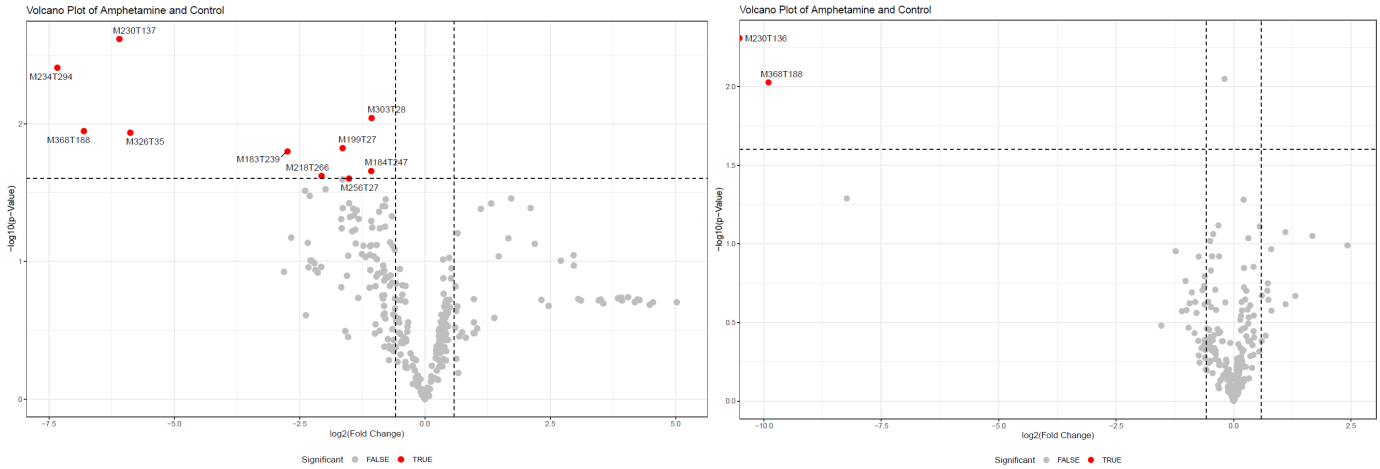

Fig. S4. Results of volcano plot for urine samples after analysis using reversed phase chromatography and negative ionization mode. **a** = urine 8 h; **b** = urine 24 h.

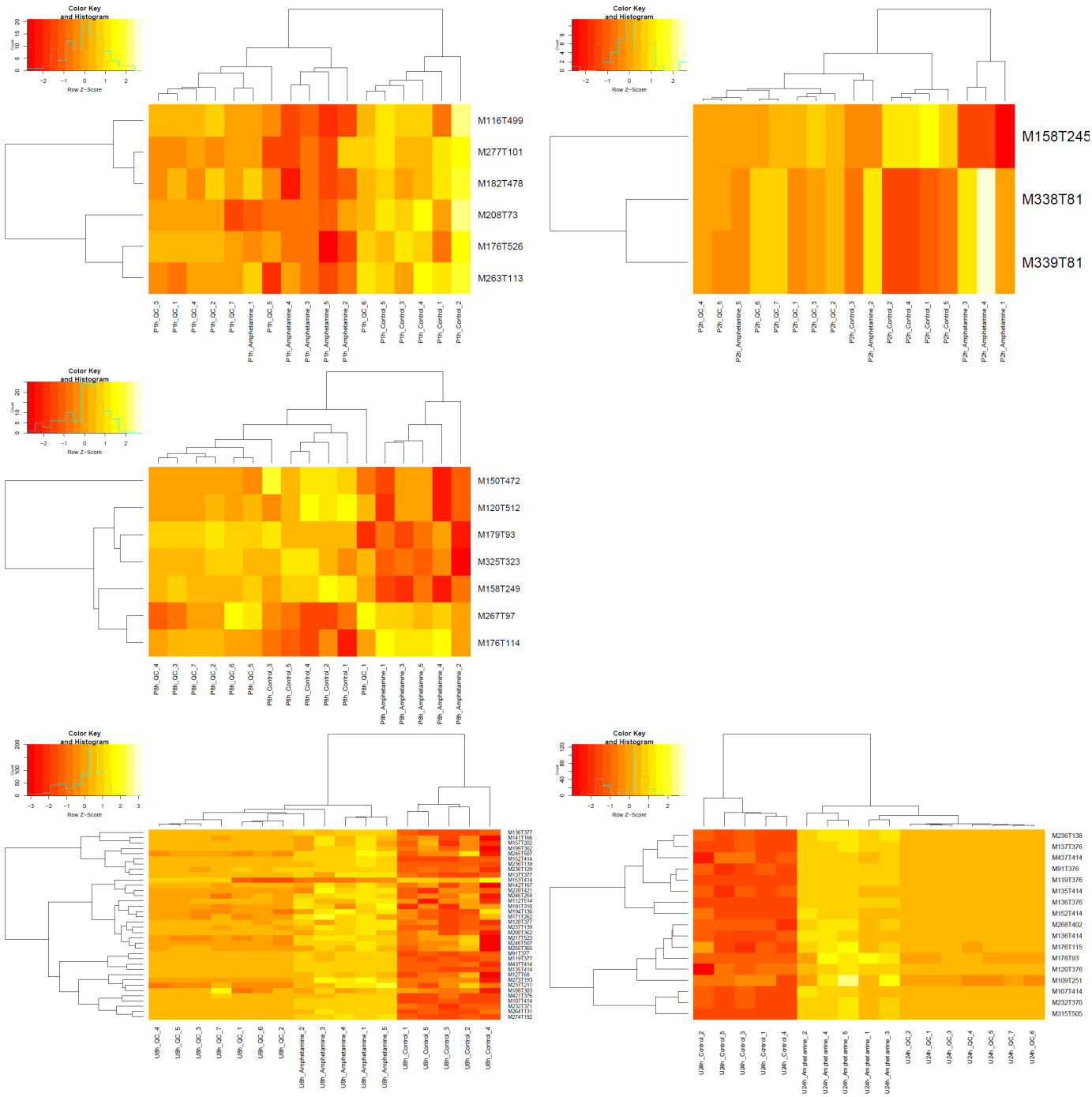

Fig. S5. Results of heat map of hierarchical clustering for plasma and urine samples after analysis using normal phase chromatography and positive ionization mode. **a** = plasma 1 h; **b** = plasma 2 h; **c** = plasma 8 h; **d** = urine 8 h; **e** = urine 24 h.

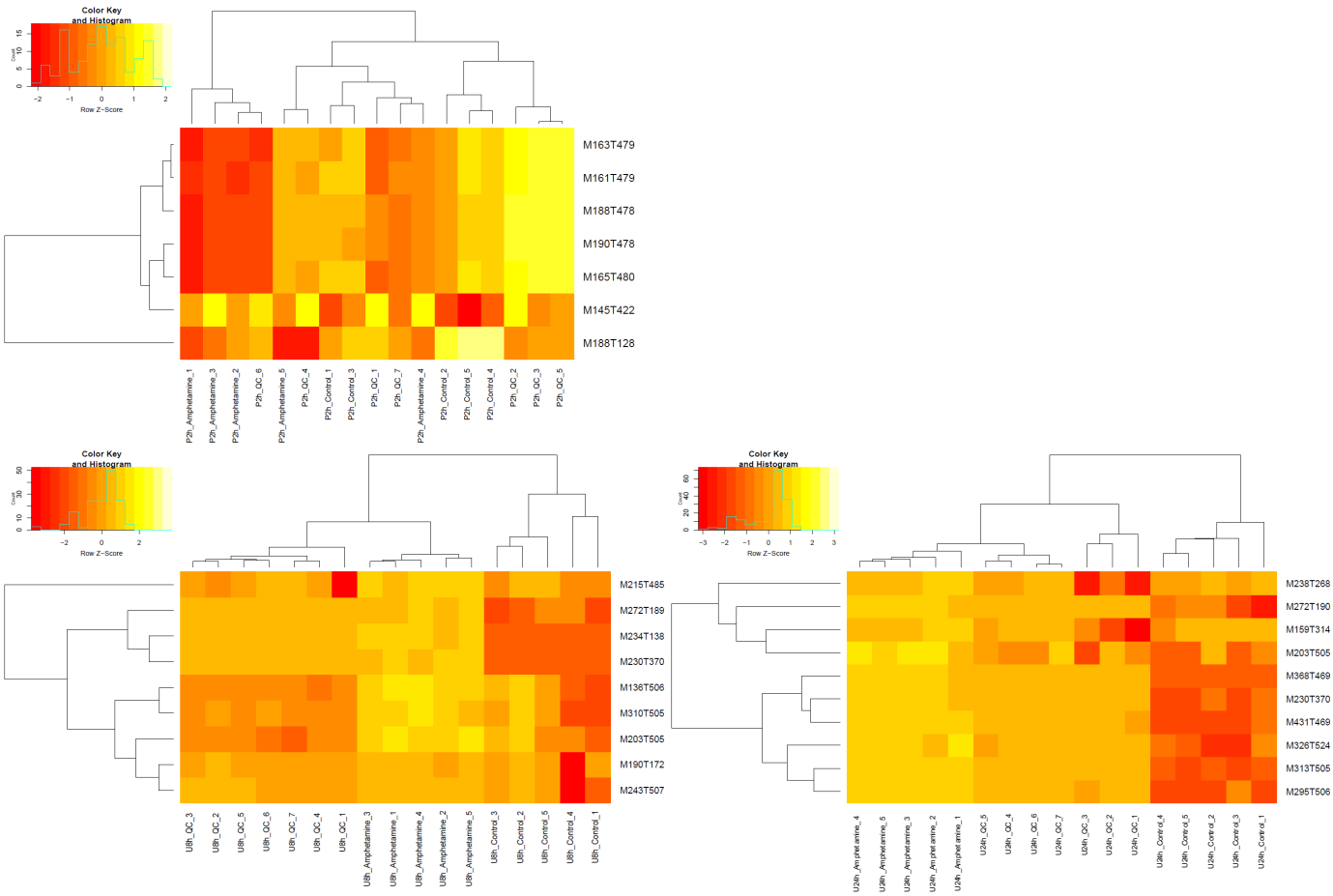

Fig. S6. Results of heat map of hierarchical clustering for plasma and urine samples after analysis using normal phase chromatography and negative ionization mode. **a** = plasma 2 h; **b** = urine 8 h; **c** = urine 24 h.

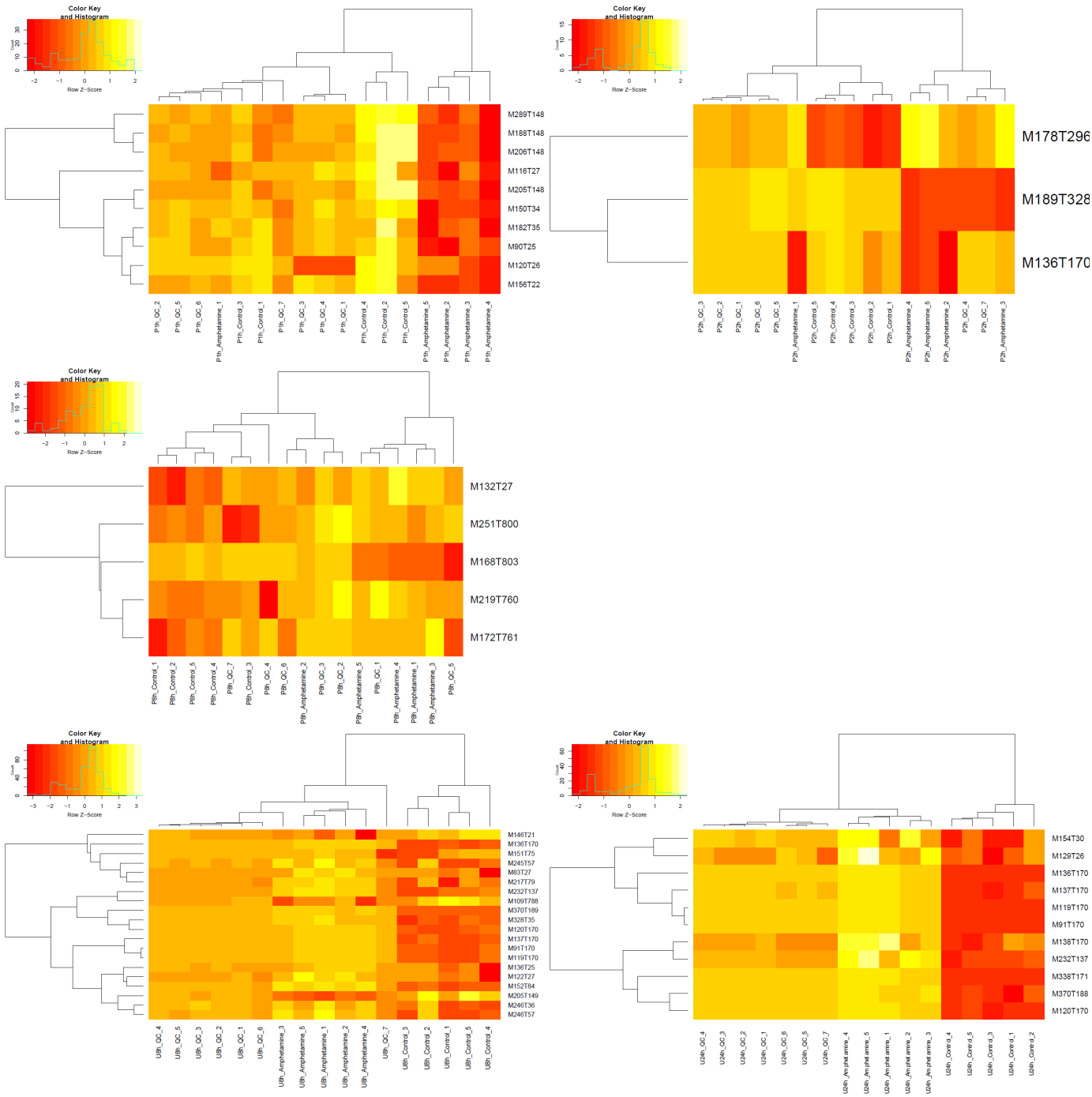

Fig. S7. Results of heat map of hierarchical clustering for plasma and urine samples after analysis using reversed phase chromatography and positive ionization mode. **a** = plasma 1 h; **b** = plasma 2 h; c = plasma 8 h; **d** = urine 8 h; **e** = urine 24 h.

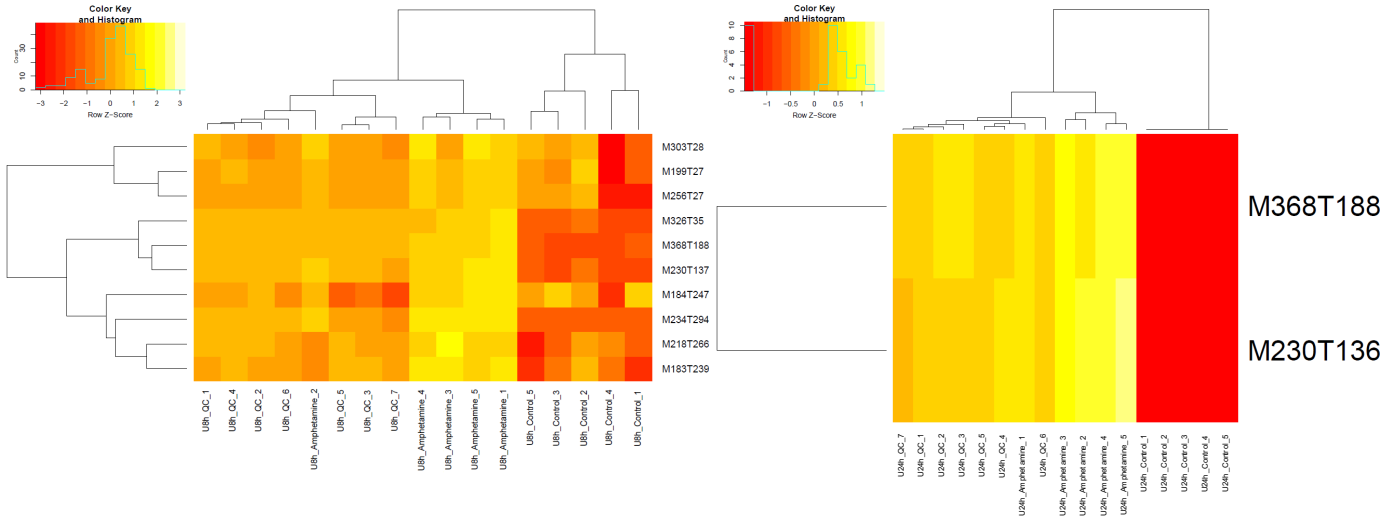

Fig. S8. Results of heat map of hierarchical clustering for urine samples after analysis using reversed phase chromatography and negative ionization mode. **a** = urine 8 h; **b** = urine 24 h.

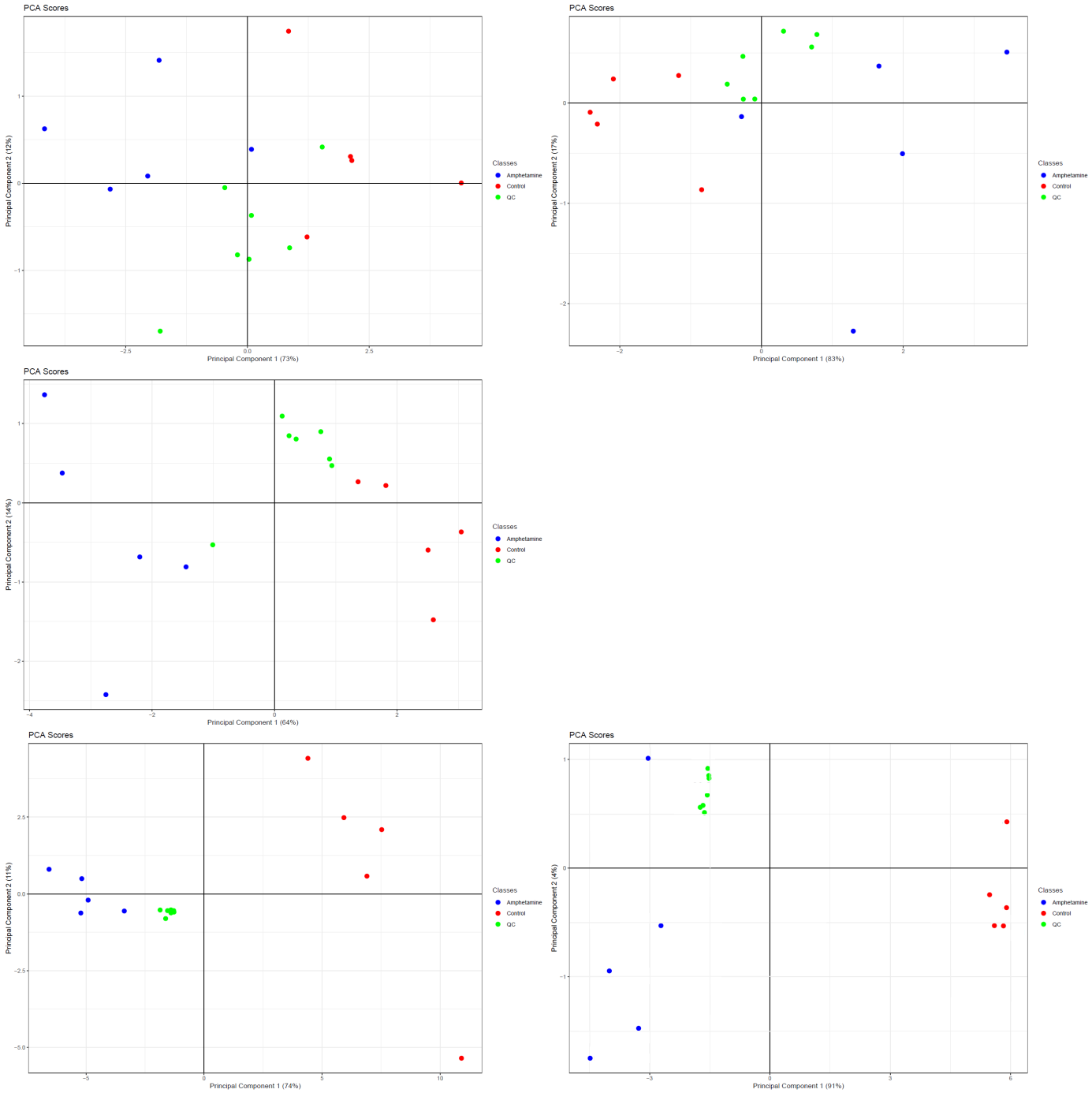

Fig. S9. Results of scores of principal component analysis for plasma and urine samples after analysis using normal phase chromatography and positive ionization mode. **a** = plasma 1 h; **b** = plasma 2 h; **c** = plasma 8 h; **d** = urine 8 h; **e** = urine 24 h.

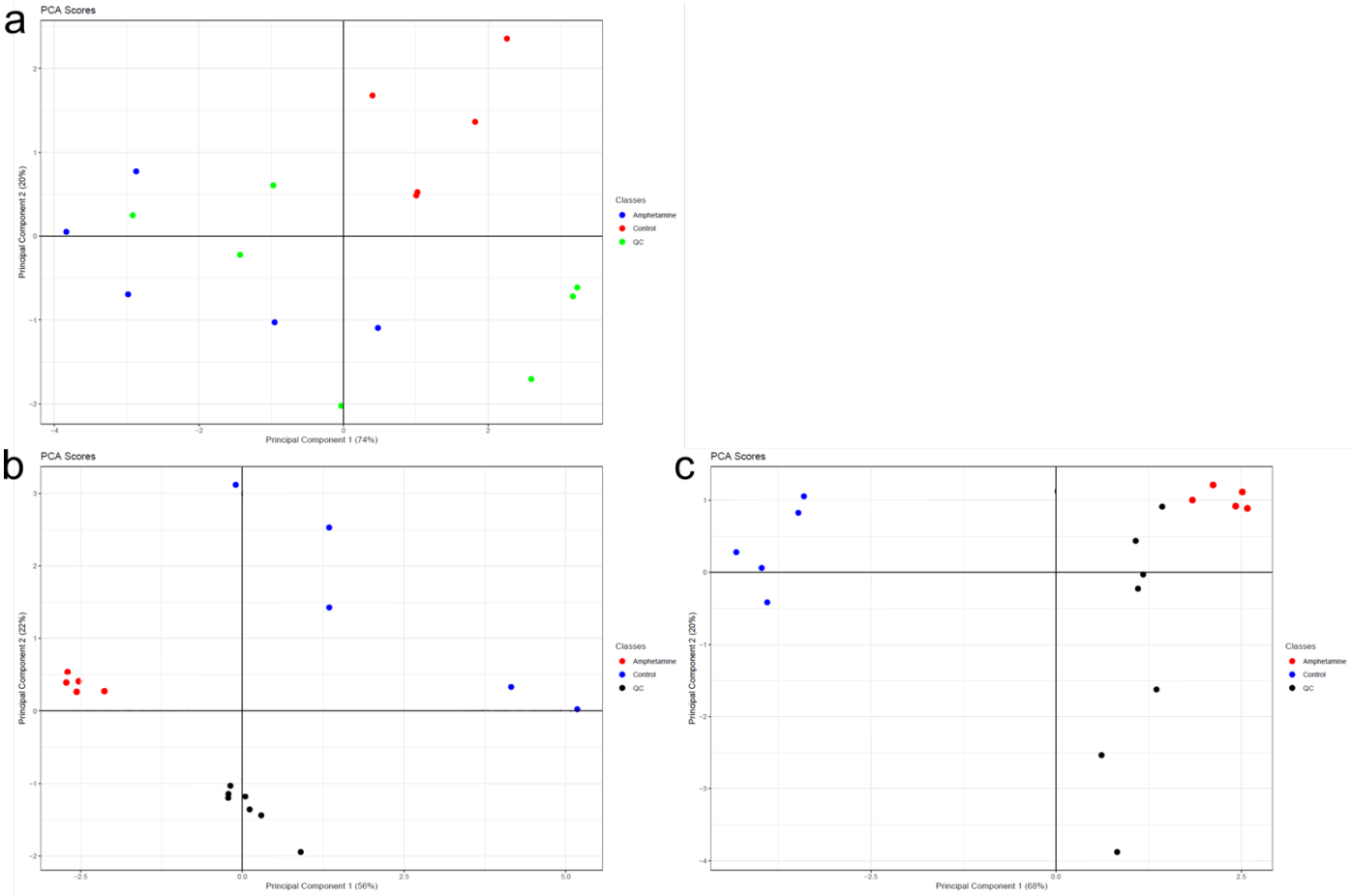

Fig. S10. Results of scores of principal component analysis for plasma and urine samples after analysis using normal phase chromatography and negative ionization mode. **a** = plasma 2 h; **b** = urine 8 h; **c** = urine 24 h.

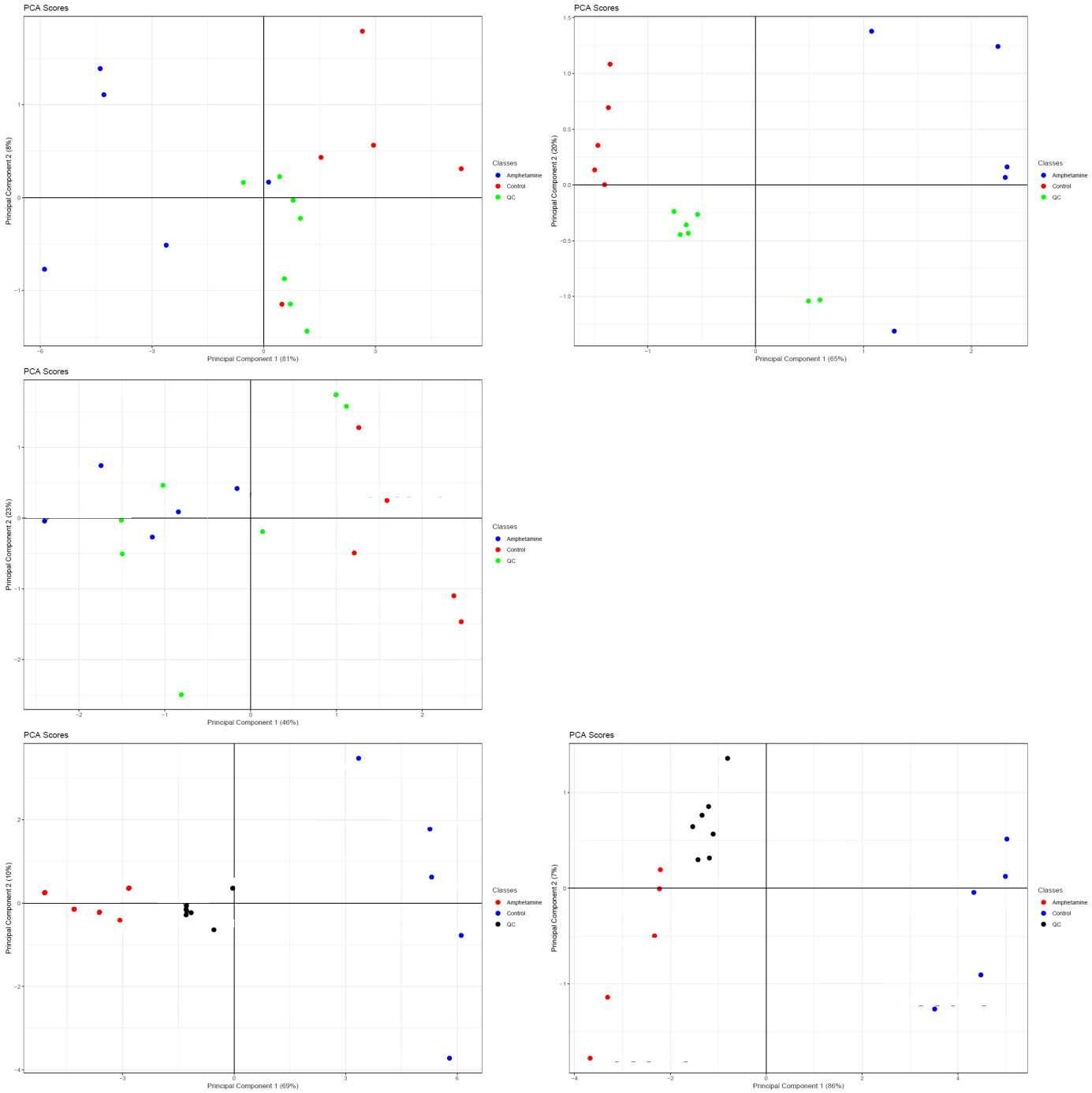

Fig. S11. Results of scores of principal component analysis for plasma and urine samples after analysis using reversed phase chromatography and positive ionization mode. **a** = plasma 1 h; **b** = plasma 2 h; **c** = plasma 8 h; **d** = urine 8 h; **e** = urine 24 h.

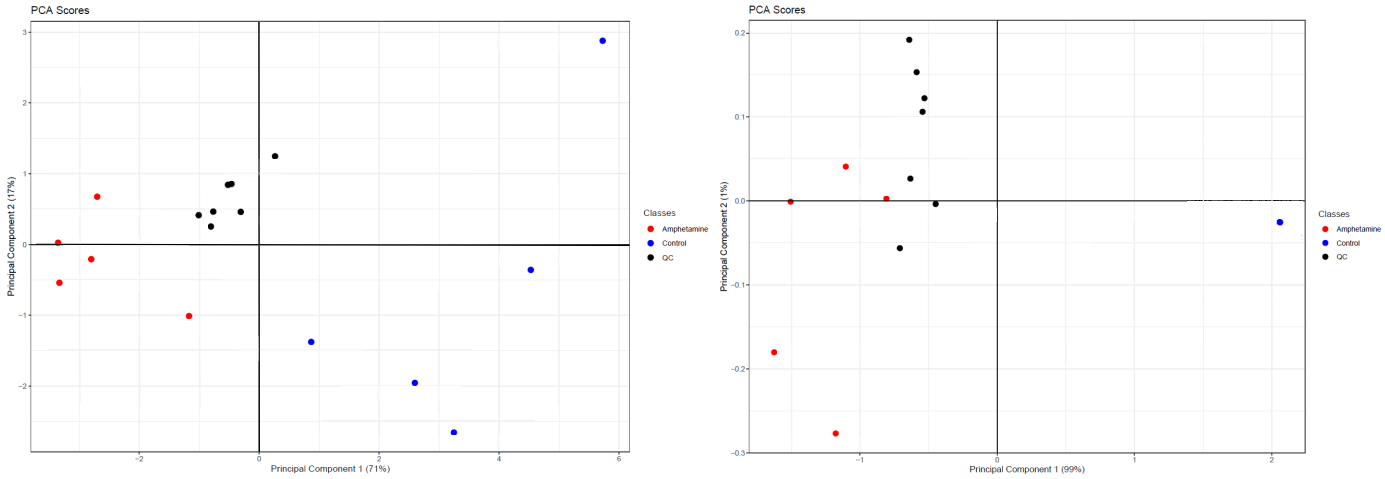

Fig. S12. Results of scores of principal component analysis for urine samples after analysis using reversed phase chromatography and negative ionization mode. **a** = urine 8 h; **b** = urine 24 h.

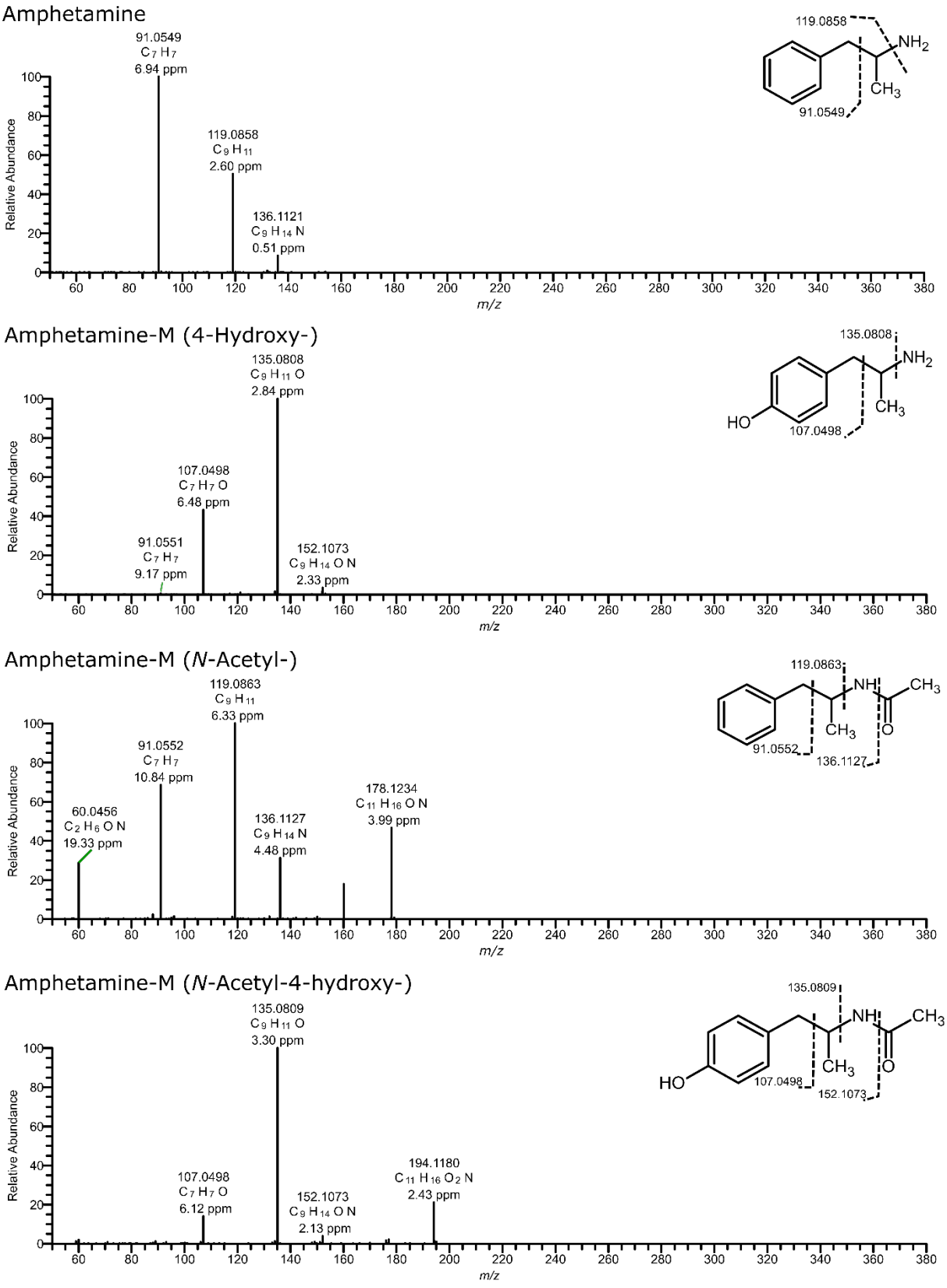

Fig. S13. LC-HRMS/MS spectra of amphetamine metabolites. Fragments with accurate mass, calculated elemental formula, and mass error value in parts per million (ppm).

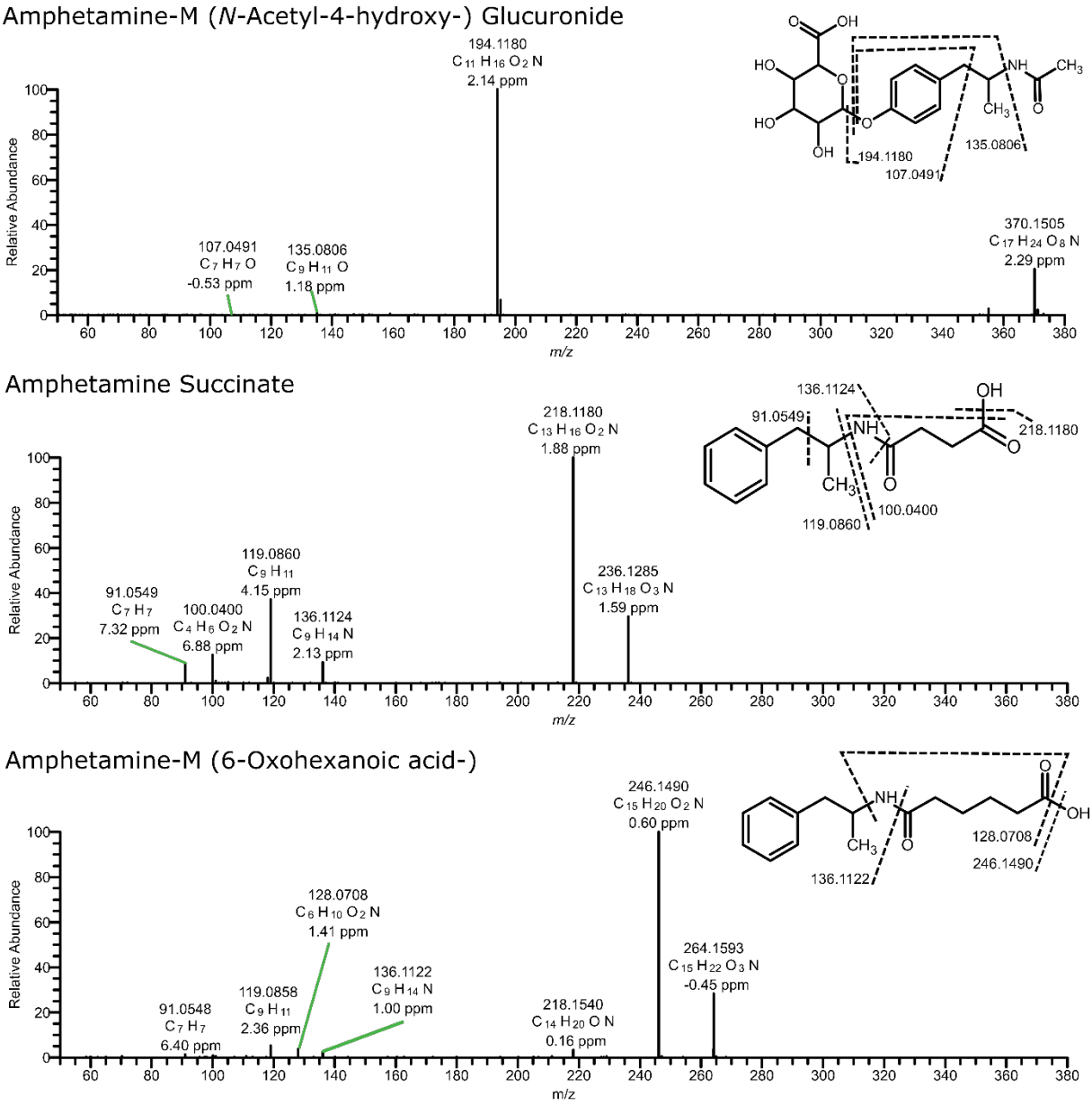

Fig. S13. Continued.

3.5. In Vitro and In Vivo Toxicometabolomics of the Synthetic Cathinone PCYP Studied by Means of LC-HRMS/MS

(DOI: 10.3390/metabo12121209)[94]

Author Contributions:

Selina Hemmer conducted and evaluated the experiments as well as composed the manuscript; Folker Westphal and Benedikt Pulver provided the investigated new psychoactive substance; Lea Wagmann and Markus R. Meyer assisted with the design of the experiments, the interpretation of the analytical experiments, and scientific discussions.

metabolites

MDPI

Article

In Vitro and In Vivo Toxicometabolomics of the Synthetic Cathinone PCYP Studied by Means of LC-HRMS/MS

Selina Hemmer [1], Lea Wagmann [1], Benedikt Pulver [2], Folker Westphal [2] and Markus R. Meyer [1,*]

[1] Department of Experimental and Clinical Toxicology, Institute of Experimental and Clinical Pharmacology and Toxicology, Center for Molecular Signaling (PZMS), Saarland University, 66421 Homburg, Germany
[2] State Bureau of Criminal Investigation Schleswig-Holstein, 24116 Kiel, Germany
* Correspondence: m.r.meyer@mx.uni-saarland.de

Abstract: Synthetic cathinones are one important group amongst new psychoactive substances (NPS) and limited information is available regarding their toxicokinetics and -dynamics. Over the past few years, nontargeted toxicometabolomics has been increasingly used to study compound-related effects of NPS to identify important exogenous and endogenous biomarkers. In this study, the effects of the synthetic cathinone PCYP (2-cyclohexyl-1-phenyl-2-(1-pyrrolidinyl)-ethanone) on in vitro and in vivo metabolomes were investigated. Pooled human-liver microsomes and blood and urine of male Wistar rats were used to generate in vitro and in vivo data, respectively. Samples were analyzed by liquid chromatography and high-resolution mass spectrometry using an untargeted metabolomics workflow. Statistical evaluation was performed using univariate and multivariate statistics. In total, sixteen phase I and one phase II metabolite of PCYP could be identified as exogenous biomarkers. Five endogenous biomarkers (e.g., adenosine and metabolites of tryptophan metabolism) related to PCYP intake could be identified in rat samples. The present data on the exogenous biomarker of PCYP are crucial for setting up analytical screening procedures. The data on the endogenous biomarker are important for further studies to better understand the physiological changes associated with cathinone abuse but may also serve in the future as additional markers for an intake.

Keywords: toxicometabolomics; PCYP; LC-HRMS; untargeted metabolomics

check for updates

Citation: Hemmer, S.; Wagmann, L.; Pulver, B.; Westphal, F.; Meyer, M.R. In Vitro and In Vivo Toxicometabolomics of the Synthetic Cathinone PCYP Studied by Means of LC-HRMS/MS. *Metabolites* **2022**, *12*, 1209. https://doi.org/10.3390/metabo12121209

Academic Editors: Sarah Wille and Andrea E. Steuer

Received: 17 November 2022
Accepted: 29 November 2022
Published: 2 December 2022

Publisher's Note: MDPI stays neutral with regard to jurisdictional claims in published maps and institutional affiliations.

Copyright: © 2022 by the authors. Licensee MDPI, Basel, Switzerland. This article is an open access article distributed under the terms and conditions of the Creative Commons Attribution (CC BY) license (https://creativecommons.org/licenses/by/4.0/).

1. Introduction

In clinical and forensic toxicology, knowledge about the toxicometabolomics of drugs of abuse (DOAs) is important not only for reliable confirmation of a DOA intake by patients but also for their risk assessment in general [1]. Such knowledge is particularly important when the DOA itself can no longer be detected and metabolites or endogenous biomarkers are the only targets for their detection. At the end of 2020, the European Monitoring Centre for Drugs and Drug Addiction (EMCDDA) reported around 830 new psychoactive substances (NPS), including 156 synthetic cathinones [2]. Due to the structural diversity of NPS and the lack of toxicokinetic information (including metabolic fate), the detection of an intake by patients is an analytical challenge in clinical and forensic toxicology [3,4]. Furthermore, the fluctuating compounds of NPS available on the market make it difficult to regulate them and to evaluate sufficient risk assessment for each compound.

Between 2019 and 2022, 29 synthetic cathinones have been identified for the first time [5]. They are classified as stimulants or amphetamine-type stimulants [6,7]. The pharmacological effects of the different derivates depend on the type of substituents and their location. In preclinical studies, two ways on interaction with monoamine transporters were demonstrated: monoamine transporter blockers such as cocaine or monoamine transporter substrates stimulated the release of neurotransmitters such as amphetamine and MDMA [8,9].

The synthetic cathinone PCYP (2-cyclohexyl-1-phenyl-2-pyrrolidin-1-yl-ethan-1-one) was first detected in March 2019 in the U.S., and in Europe the first case report was published 2020 [5]. Due to the presence of the lipophilic and bulky cyclohexyl ring, PCYP exhibited an up to twofold stronger interaction with dopamine transporters in vitro compared to alpha-pyrrolidinovalerophenone (α-PVP). Therefore, it shows stronger dopaminergic stimulation and higher addictive potential [10]. This biochemical reaction led to desired effects such as stimulation and euphoria, but also to adverse effects including restlessness, anxiety, psychosis, tachycardia, and hyperthermia [5]. So far, no data are available about the metabolic fate of PCYP and the impact of PCYP on endogenous metabolic pathways. To date, only one case report of PCYP intake in Europe has been published [5]. It cannot be excluded that there is, was, and will be more extensive distribution. To uncover such abuse, screening procedures need to be up to date, which is often not possible in cases where the urinary screening targets are not known.

In recent years, toxicometabolomics, a subdiscipline of metabolomics, has increasingly gained interest in the study of the toxicokinetic and -dynamic DOAs [3,11–16]. The application of untargeted toxicometabolomics may allow researchers to find exogenous biomarkers, such as new drug metabolites, and endogenous biomarkers. Not only could these be indicators of acute drug ingestion or sample manipulation, but they could also offer information on the mode of action of the drugs and consumption patterns or could be used to assess the severity of intoxication [17–19]. Due to the lack of authentic human samples, toxicometabolomic studies are often conducted using different in vitro and in vivo models, such as pooled human-liver microsomes (pHLMs), HepaRG cell lines, and/or rats [13–15].

Since data about neither the metabolic pathway of PCYP nor the impact on the metabolome are available, this study aimed to provide the metabolic profile in an in vitro model using pHLM incubation. In conducting an in vivo experiment providing rat plasma and rat urine, the endogenous response to an acute PCYP exposure should be revealed. Analysis will be conducted by liquid chromatography coupled with high-resolution tandem mass spectrometry (LC-HRM/MS) using an untargeted metabolomics workflow. The resulting data should enable us to overcome the analytical challenge in clinical and forensic toxicology to confirm patient intakes of PCYP and to understand its acute and chronic effects.

2. Materials and Methods

2.1. Materials and Chemicals

PCYP hydrochloride was provided by the State Bureau of Criminal Investigation Schleswig-Holstein (E.U. project ADEBAR plus, Kiel, Germany) for research purposes. The chemical purity of >93% and the identity of the compound was verified by MS and nuclear magnetic resonance analysis. Ammonium formate, ammonium acetate, creatinine-d_3, dipotassium phosphate, formic acid, D-glucose-1,2,3,4,5,6,6-d_7, isocitrate dehydrogenase, isocitrate, magnesium chloride, palmitic acid-d_{31}, superoxide dismutase, and tripotassium phosphate were obtained from Merck (Darmstadt, Germany). Acetonitrile, ethanol, methanol (all LC-MS grade), and NADP-Na_2 were from VWR (Darmstadt, Germany). L-Tryptophan-d_5 was obtained from Alsachim (Illkirch-Graffenstaden, France). 1-Palmitoyl-d_9-2-palmitoyl-sn-glycero-3-PC and prostaglandin-E_3-d_9 were from Cayman Chemical (Ann Arbor, MI, USA). Water was purified with a millipore filtration unit (18.2 W × cm water resistance). pHLMs (20 mg microsomal protein × mL^{-1}, 360 pmol total CYP/mg, 26 donors) were obtained from Corning (Amsterdam, The Netherlands). After delivery, pHLMs were thawed at 37 °C, aliquoted, snap-frozen in liquid nitrogen, and stored at −80 °C until use.

2.2. Sample Preparation and Analysis of pHLM Incubation

According to published procedures [3,20], incubations using pHLMs were prepared as follows. PCYP was dissolved freshly in methanol and subsequently diluted with 0.1 M

phosphate buffer to obtain the required concentrations. Incubations were performed using a final PCYP concentration of 0 (blank group) or 50 µM (PCYP group) and 1 mg protein mL^{-1} pHLM at 37 °C. The final incubation mixtures also contained 90 mM phosphate buffer, 5 mM isocitrate, 5 mM Mg^{2+}, 1.2 mM $NADP^{+}$, 200 U/mL superoxide dismutase, and 0.5 U mL^{-1} isocitrate dehydrogenase. A final incubation volume of 50 µL was obtained. The reaction was stopped after 60 min by adding 50 µL of ice-cold acetonitrile and then centrifuged for 2 min at 18,407× *g*. For each group, 5 replicates were prepared. Pooled-quality samples (QC group) were prepared by transferring 20 µL of each replicate incubation into one MS vial. QC samples were used for optimization of the peak-picking parameters and identification of significant features, as described below.

2.3. Study Design In Vivo

Ten adolescent male Wistar rats (Charles River, Sulzfeld, Germany) were housed in a controlled environment (temperature 22 °C, humidity 57 ± 2%, and 12 h light/dark cycle). Studies were approved by an ethics committee (33/2019-Landesamt für Verbraucherschutz, Saarbrücken, Germany). A single dose of 2 mg/kg body weight (BW) PCYP was administered to five rats as aqueous suspension by gastric intubation. Five control rats were administrated only with water. During the study, rats were housed in metabolism cages for 24 h, having water ad libitum. Animal general health aspects were assessed at the time points 30, 60, 120, 360 min, and 24 h after intake.

2.4. Sample Collection In Vivo

Blood samples of 0.5 mL were collected from each rat one hour after administration. For blood sampling, animals were anesthetized with diethyl ether and blood was taken from the *Vena caudalis mediana* using a heparin-coated syringe. Blood samples were centrifuged (1503× *g*, 5 min, 24 °C) and plasma was removed and immediately stored at −80 °C until analysis. Urine was collected separately from the feces over a period of 24 h after administration, aliquoted, frozen, and stored at −80 °C until use.

2.5. Sample Preparation and Analysis of Rat Blood Plasma and Rat Urine

According to Manier and Meyer [21], blood plasma samples were prepared as follows: an amount of 50 µL plasma was transferred into a reaction tube and precipitated using 200 µL of a mixture of methanol and ethanol (1:1, *v*/*v*). The mixture contained 48 µM L-tryptophan-d_5, 8.6 µM creatinine-d_3, 34.8 µM palmitic acid-d_{31}, and 53.4 µM D-glucose-d_7 as internal standard. Samples were shaken for 2 min at 2000 rpm and subsequently centrifuged at 21,130× *g* and 2 °C for 30 min. A volume of 150 µL of the supernatant was transferred into a new reaction tube and evaporated to dryness using a vacuum centrifuge at 1400 rpm and 24 °C for 20 min. The obtained residues were reconstituted in 50 µL of a mixture of acetonitrile and methanol (70:30, *v*/*v*).

Based on Hemmer et al. [15], urine samples were centrifuged at 13,523× *g* at 4 °C for 10 min. Volumes of 100 µL of urine were transferred into reaction tubes and 400 µL methanol, including 48 µM L-tryptophan-d_5, 8.6 µM creatinine-d_3, 34.8 µM palmitic acid-d_{31}, and 53.4 µM D-glucose-d_7 as internal standard, was added. Samples were cooled to −20 °C for 20 min and then centrifuged at 13,523× *g* and 4 °C for 10 min. An amount of 350 µL of the supernatant was transferred into a new reaction tube and evaporated to dryness using a vacuum centrifuge at 1400 rpm and 24 °C. The obtained residues were reconstituted in 50 µL of a mixture of acetonitrile and methanol (70:30, *v*/*v*).

Pooled QC samples were prepared by transferring 50 µL of each sample into one MS vial. These QC samples were also used for optimization of the peak-picking parameters and identification of significant features, as described below (QC group). QC samples, and each sample of control rats (water administration) and PCYP rats (PCYP administration) were stored until use at −80 °C.

2.6. LC-HRMS Apparatus

According to published procedures [3,15,20], analyses were performed using a Thermo Fisher Scientific (TF, Dreieich, Germany) Dionex UltiMate 3000 RS pump consisting of a degasser, a quaternary pump, and an UlitMate Autosampler, coupled with a TF Q Exactive Plus equipped with a heated electrospray ionization (HESI)-II source. Performance of the columns and the mass spectrometer was tested using a test mixture described by Maurer et al. [1,22]. Gradient reversed-phase (RP) elution was performed on a TF Accucore Phenyl-Hexyl column (100 mm × 2.1 mm, 2.6 µm) and hydrophilic interaction chromatography (HILIC) elution using a Merck (Darmstadt, Germany) SeQuant ZIC HILIC (150 mm × 2.1 mm, 3.5 µm). The mobile phase for the RP chromatography consisted of 2 mM aqueous ammonium formate containing acetonitrile (1%, v/v) and formic acid (0.1%, v/v, pH 3, eluent A), as well as 2 mM ammonium formate solution with acetonitrile:methanol (1:1, v/v) containing water (1%, v/v) and formic acid (0.1%, v/v, eluent B). The flow rate was set from 0 to 10 min to 500 µL/min and from 10 to 13.5 min to 800 µL/min using the following gradient: 0–1 min hold 99% A, 1–10 min to 1% A, 10–11.5 min hold 1% A, and 11.5–13.5 min hold 99% A. The gradient elution for HILIC was performed using aqueous ammonium acetate (200 mM, eluent C) and acetonitrile containing formic acid (0.1%, v/v, eluent D). The flow rate was set to 500 µL/min using the following gradient: 0–1 min hold 2% C, 1–5 min to 20% C, 5–8.5 min to 60% C, 8.5–10 min hold 60% C, and 10–12 min hold 2% C. Injection volume was set to 1 µL for all samples. For preparation and cleaning of the injection system, isopropanol:water (90:10, v/v) was used. The following settings were used: wash volume, 100 µL; wash speed, 4000 nL/s; loop wash factor, 2. Column temperature for every analysis was set to 40 °C, maintained by a Dionex UltiMate 3000 RS analytical column heater. HESI-II source conditions were as follows: ionization mode, positive or negative; sheath gas, 60 AU; auxiliary gas, 10 AU; sweep gas, 3 AU; spray voltage, 3.5 kV in positive and −4.0 kV in negative mode; heater temperature 320 °C; ion transfer capillary temperature, 320 °C; and S-lens RF level, 50.0. Mass spectrometry for untargeted metabolomics was performed according to a previously optimized workflow [3,23]. The settings for full-scan (FS) data acquisition were as follows: resolution 140,000 at m/z 200; microscan, 1; automatic gain control (AGC) target, 5e5; maximum injection time, 200 ms; scan range, m/z 50–750; spectrum data type; centroid. All study samples were analyzed in randomized order to avoid potential analyte instability or instrument performance potentially confounding data interpretation. Additionally, one QC injection was performed every five samples to monitor batch effects, as described by Wehrens et al. [24]. Significant features were subsequently identified using PRM. Settings for PRM data acquisition were as follows: resolution, 35,000 at m/z 200; microscans, 1; AGC target, 5e5; maximum injection time, 200 ms; isolation window, m/z 1.0; collisions energy (CE), 10, 20, 35, or 40 eV; spectrum data type, centroid. The inclusion list contained the monoisotopic masses of all significant features and a time window of their retention time ± 60 s. TF Xcalibur software version 3.0.63 was used for data handling.

2.7. Data Processing and Statistical Analysis

Data processing for untargeted metabolomics was performed in an R environment according to previously published workflows [15,23]. TF LC-HRMS/MS RAW files were converted into mzXML files using ProteoWizard [25]. XCMS parameters were optimized using a previously developed strategy, as mentioned by Manier et al. [23]. Peak-picking and alignment parameters are summarized in Table S1. Peak picking was performed using XCMS in an R environment [26,27], and the R package CAMERA [28] was used for the annotation of adducts, artifacts, and isotopes. Feature abundances with a value of zero were replaced by the lowest-measured abundance as a surrogate limit of detection and the whole dataset was then log 10 transformed [24]. Normalization was performed for urine samples using the area of endogenous creatinine from those samples analyzed using HILIC column and positive ionization mode. For plasma samples, normalization was performed using the area of L-tryptophane-d_5. Significant changes in features between

control and PCYP respectively blank and PCYP groups were assumed after Welch's two-sample *t*-test and Bonferroni correction for pHLM [29]; *p*-value < 0.01 for urine, and *p*-value < 0.05 for plasma. Principal component analysis (PCA) and hierarchal clustering were used to investigate patterns in the datasets. For pHLM, t-distributed stochastic neighborhood embedding (t-SNE) [30,31] was used instead of PCA. Names for features were adopted from XCMS using "M" followed by rounded mass and "T" followed by the retention time in seconds. After visual inspection of the extracted ion chromatograms (EIC) of significant features, based on the peak shape quality, the significant features were divided into true and false features [20]. The R scripts can be found on GitHub (https://github.com/sehem/PCYP_Metabolomics.git) and the mzXML files used in this study are available via Metabolights (study identifier MTBLS6469).

2.8. Identification of Significant Features

Significant features were identified by recording MS/MS spectra using the PRM method mentioned above. After conversion to mzXML format using ProteoWizard [25], spectra were imported to NIST MS Search version 2.3 Library. The settings for library and MS/MS search were used according to published procedures [14,15,20]. Metabolites of the synthetic cathinone PCYP were tentatively identified by interpreting their spectra in comparison to that of the parent compound. Identified features were classified on the different levels of identification according to the metabolomics standards initiative (MSI) [32].

3. Results and Discussion

3.1. Study Design

Two different models were used to investigate the toxicometabolomics of the synthetic cathinone PCYP via an untargeted approach. The in vitro model used is common in drug metabolism studies due to its ease of use and low variability [33]. Rat, as in vivo model, was used to investigate the impact of the synthetic cathinone on the rat metabolome. In comparison to cell lines, plasma or urine samples are very complex since the metabolome can also be affected by, for example, food, the microbiome, and drugs used to anesthetize animals [34]. Due to the complexity and influence of the metabolome, animal models are well-suited for studying changes in the metabolome compared to human studies. Animal studies can be performed under standardized and comparable conditions. For example, animals are subject to a uniform sleep–wake rhythm, and they can be kept under the same conditions and obtain the same water and food. Due to their very low genetic variability, it is also possible to obtain reliable results with significantly fewer animals compared to human clinical studies. Compared to in vitro studies, which often only represent certain cell components, cells, or organs, in vivo studies offer the possibility to provide an insight into the whole organism. Besides elucidation of the endogenous response, urine also offers the possibility to analyze for drug metabolites. The knowledge about xenobiotic metabolic pathways is essential for clinical and forensic toxicology to develop suitable analytical screening procedures to detect consumption [5,8,9]. Compared to conventional methods for analyzing metabolic pathways, an untargeted urinary toxicometabolomics approach allows for the detection of metabolites which might be overlooked as they are not expected [3,14,35]. Besides toxicokinetics, there is limited information available about the mode of action of synthetic cathinones, especially of PCYP. This is where the blood plasma comes into play. Plasma samples are of interest with respect to changes in endogenous metabolites that may be affected by the intake of drugs of abuse.

3.2. Untargeted Data Processing and Statistical Analysis

Univariate statistics were performed using volcano plot. False-positive results were prevented by using Bonferroni correction [29] for pHLM-derived data, with *p*-value > 0.01 for urine-derived data, and *p*-value > 0.05 for plasma-derived data. Results of the identification of significant features and their level of identification in accordance with the

MSI [32] are summarized in Tables S2–S4. Annotated isotopes by CAMERA were not further analyzed. Features were analyzed as described above using the PRM method, and MS^2 spectra for PCYP metabolites are shown in Figure S8. For several features, no MS^2 spectra could be recorded due to their low abundance.

Using the four different analytical methods (RP positive, RP negative, HILIC positive, HILIC negative), thirty features, containing eleven isotopes and one adduct, were found in total to be significant in pHLM incubation. Analysis using RP and HILIC and negative ionization mode did not reveal any significant changes. Rat plasma samples, which were taken 1 h after administration, revealed 17 metabolites and 3 isotopes using above-mentioned analytical methods. In urine samples, 122 significant features were found in total containing 16 isotopes and 1 adduct.

Besides univariate statistics, the different datasets were also evaluated regarding the results of multivariate statistics to identify the largest changing features and specific signatures in the data. Since multivariate statistics could only be performed if there were at least two significant features, no data were available for datasets containing no or only one significant feature. For all analyses and matrices, it can be shown that the PCYP and blank or control groups were distinct from each other (Figures S1–S3). Complementary to the scores plot, the loadings plot provided information about which metabolites had the greatest contribution to the separations between groups [36]. Thereby, it can be seen that especially PCYP itself and its metabolites lead to the separation of the individual groups. For data derived from the pHLM incubations (Figure S1), the variance in the first principal component was between 99 and 97% using RP and HILIC in positive ionization mode. These results indicated that the pHLM datasets were highly linear, revealing that the PCA is not suitable for those experiments where only the parent compound and its metabolites are detectable. Therefore, the patterns in the pHLM dataset were evaluated using t-SNE, which is a dimension reduction algorithm that visualizes similarities in datasets [31]. Results of the t-SNEs (Figure S4) showed similar cluster patterns for all analyses. This can be explained by the fact that data derived from pHLM incubations show low variability and only PCYP itself and its metabolites led to the separation of the two groups.

In addition to PCA, hierarchical clustering was also performed. In untargeted metabolomics studies, heat maps of hierarchical clustering can be used to discover clustering patterns in the datasets. For all analyses and matrices, the hierarchical clustering mostly revealed a high distance of samples from blank or control group to those from PCYP and QC groups (Figures S5–S7). However, there was an exception for urine samples separated by HILIC in positive ionization mode (Figure S7C). In this case, two QC samples were clearly separated from other data. Taking a closer look at these two runs, it was observed that the total ion chromatogram of these two samples showed a higher intensity than the other QCs, even though it was the same sample. Reasons for this remain unclear.

3.3. Metabolic Pathways of PCYP

The proposed metabolic pathways of PCYP in the in vitro and in vivo models are summarized in Figure 1. The MS^2 spectra of all PCYP metabolites are shown in Figure S8. Table S5 provides a list of all metabolites in terms of their abundance in each column and matrix. Additionally, Table S5 includes the metabolite identification number (M), the calculated exact mass of the protonated molecule, and the elemental composition of all detected metabolites, respectively. The corresponding retention times of each metabolite for each column are given in Tables S2–S4 in the Supporting Information. Figures S9 and S10 show the reconstructed chromatograms of the most abundant metabolites in pHLM and rat urine.

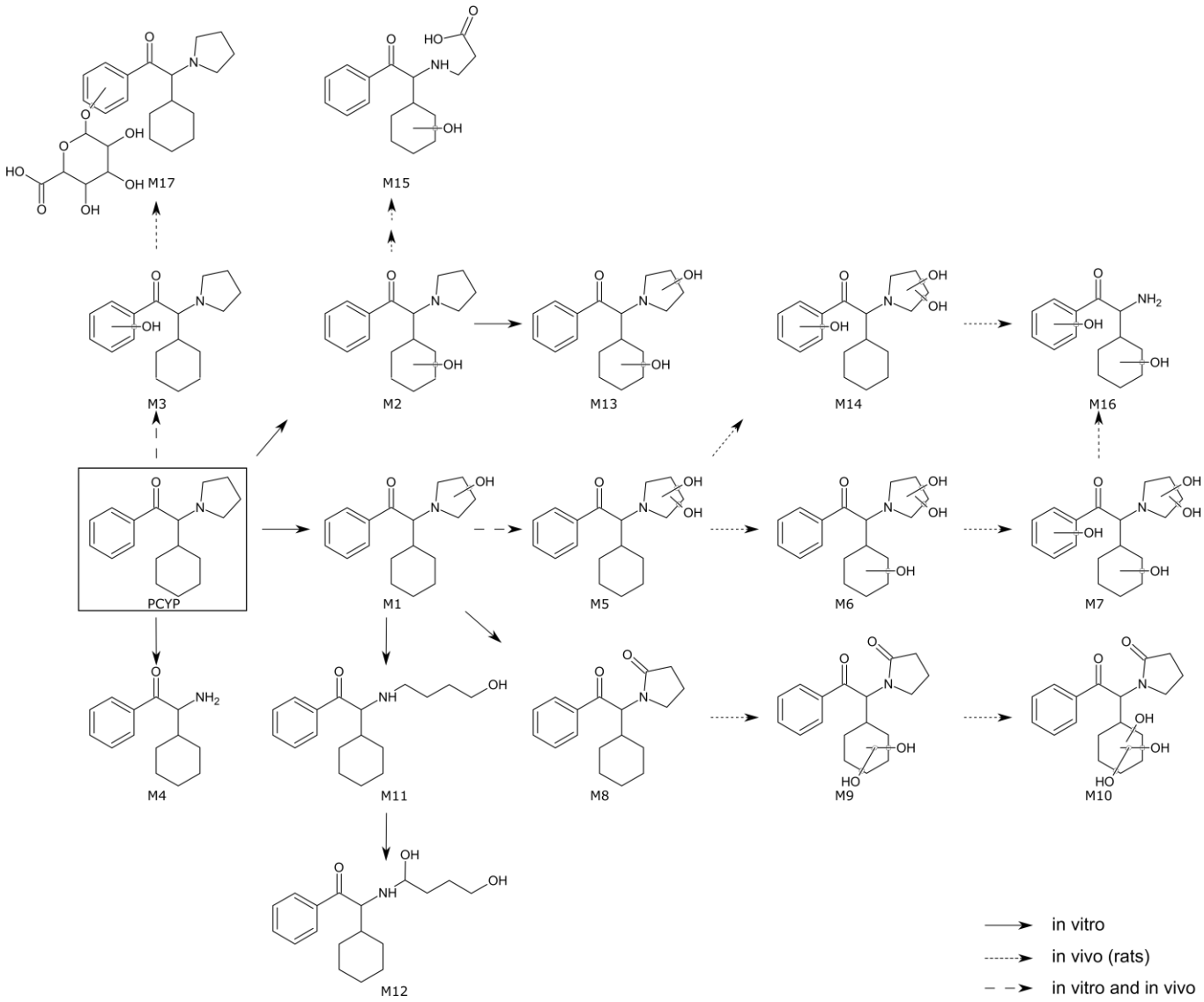

Figure 1. In vitro and in vivo metabolic pathways of PCYP. The parent compound is indicated by a black square, undefined hydroxylation positions are indicated by unspecific bonds. Metabolite identification numbers (M) match with the metabolites listed in Table S5.

In total, sixteen phase I and one phase II metabolite were found in all three matrices using the four different above-mentioned analytical methods. Not metabolized PCYP could only be detected in vitro but not in the in vivo samples. However, this was not surprising since the average elimination half-time of the structure analog α-PVP was reported to be <2.1 h in Sprague–Dawley rats after injection [37]. Regarding the in vitro phase I metabolism, PCYP was reduced by a *N*,*N*-bis-dealkylation (M4), which was also reported for α-PVP [38–41]. In accordance with previous publications, the pyrrolidine ring underwent biotransformation resulting in a mono- (M1) and dihydroxylation (M5), an oxo- (M8) as well as a ring-opened mono- (M11) and dihydroxy metabolite (M12) [3,42]. The opening of the pyrrolidine ring has also previously been observed for the two synthetic cathinones α-PBP and α-PEP and is most likely the result of hydroxylation at the ortho-position of the pyrrolidine ring, followed by a retrohemiaminal reaction [3]. The combination of hydroxylation on hexyl and pyrrolidine ring leading to a dihydroxylation (M13) was also detected in pHLM incubations.

Nine phase I metabolites could be identified in vivo, amongst them the monohydroxylation at the benzyl-ring (M3) and the dihydroxylation at the pyrrolidine ring (M5).

Additionally, a combination of di- (M9) and trihydroxylation (M10) on the hexyl ring and oxidation at the pyrrolidine ring was found in urine samples. The combination of hydroxylation on hexyl and pyrrolidine ring leading in a dihydroxylation (M13) was also detected. Tri- and tetrahydroxylation metabolites were found, resulting in a dihydroxylation on the pyrrolidine ring followed by a monohydroxylation on the hexyl (M6) and/or benzyl ring (M7, M14). Tetrahydroxylation led to a bis-*N*-dealkylation (M16). Another metabolite, which was only detected in urine samples, consisted of hydroxylation on the hexyl ring and pyrrolidine cleavage followed by oxidation to carboxylic acid (M15). The metabolites M5, M6, and M9 could also be observed in rat plasma. Regarding phase II metabolism, only the conjugation with glucuronic acid after hydroxylation of the benzyl ring (M17) could be observed. No other conjugates, such as glucuronic acid or sulfate, could be found. The lower abundance of phase II metabolites can be explained by the fact that drug-metabolizing enzymes such as cytochrome P450 or glucuronosyltransferases have different expressions and functions in different species. Therefore, significantly more phase I metabolites are formed in rat liver compared to humans, whereas more phase II metabolites are formed in humans [43–46].

Since the parent compound could no longer be detected in 24 h urine, analytical procedure should include these metabolites in addition to the parent compound, considering its probability of being not detectable in urine after lower doses or after sampling times later than 24 h after intake. Therefore, reference spectra need to be added to common MS databases to allow detection [22,47]. Nevertheless, authentic human samples are required to fill the gap between in vitro and in vivo assays and to reliably determine which metabolites are useful for screening procedures in humans.

3.4. Effect of PCYP on the Rat Metabolome

Since there is limited information available on the effects of NPS on the metabolome [11,48], untargeted toxicometabolomics have been increasingly used to study their toxicity-related pathways. Toxicometabolomics combines the detection and identification of endogenous and exogenous biomarker. This allows the determination of metabolites of the investigated substance in order to detect an intake by patients, as well as the identification of biomarkers that provide information on the effect of substances on the metabolome in only one experiment [49,50].

The complexity of the metabolome becomes visible by comparing the PCAs of the three investigated matrices (pHLM incubations, plasma samples, and urine samples) in this study (Figures S1–S3). Since the PCAs in pHLM are highly linear and only PCYP and its metabolites were identified as significant features, rat urine and rat plasma samples showed higher variability. In rat plasma samples collected 1 h after administration, three significantly altered metabolites could be identified by MSI level 2 or 3 [32]. In PCYP-treated rats, adenosine was significantly increased. Adenosine is a ubiquitous nucleoside and is consequently involved in many biological processes as a component of DNA or RNA. For example, it plays an important role in energy transfer as adenosine diphosphate (ADP) or -triphosphate (ATP). As cyclic adenosine monophosphate (cAMP), it also plays a role in signal transduction. Furthermore, adenosine itself is both a neurotransmitter and a potent vasodilator [51]. Altered adenosine levels after acute or chronic consumption of drugs of abuse and psychostimulants have already been reported in several studies [52–56]. Other studies have shown that high levels of adenosine induce sleep in rats [57–59]. During the monitoring of the animal general health aspects at the time point 30 min, 60 min, 120 min, 360 min, and 24 h, no significant change in the sleep behavior could be observed between the two groups. Another endogenous metabolite that was significantly increased in the plasma of PCYP-treated rats was 3-methyladipic acid. 3-methyladipic acid itself is a metabolite of the catabolism of the naturally occurring phytanic acid and is involved in biological processes such as lipid peroxidation, fatty acid metabolism, cell signaling, and the lipid metabolism pathway [51]. Quinoline-2-ol was also significantly increased in rat plasma as well as in rat urine of PCYP-treated rats. However, the biological significance of this metabolite is currently unclear.

Urine is distinguished from plasma by being easily collected, rich in metabolites, and capable of reflecting imbalances in all biochemical pathways within an organism [60]. It is well-suited for the identification of novel exogenous drug metabolites or endogenous biomarkers indicative for drug ingestion unless they are not exclusively excreted in feces. In this study, ten PCYP metabolites could be identified in rat urine collected 24 h after administration, which are described in detail above. In addition to quinoline-2-ol, which was also significantly present in rat urine, three other metabolites were identified in rat urine that did not belong to PCYP. Daidzein, is an isoflavone and is known as a biomarker for the consumption of soybeans and other soy products [51]. It was significantly increased in urine of PCYP-treated rats. Since the rats had only water and no food available in their metabolic cage after substance administration, this finding cannot be associated with the consumption of PCYP. The last two metabolites which were significantly changed in rat urine belong to the tryptophan metabolism. Kynurenic acid was significantly decreased in PCYP-treated rats. In the tryptophan metabolism, kynurenic acid is a metabolite of L-kynurenine and also known as neuroprotective agent. Several studies reported a reduced kynurenic acid in mood disorders such as depressive or bipolar disorders [61–63]. Dihydroxyquinoline was increased in PCYP-treated rats. In tryptophan metabolism, 4,6-dihydroxyquinoline and 4,8-dihydroxyquinoline are degradation products of hydroxykynurenamine (HMDB). This observation suggests that PCYP induces the tryptophan metabolism. Kolanos et al. demonstrated in an in vitro experiment, that PCYP, due to its structure, shows strong dopaminergic stimulation [10]. Based on these two observations, it can be hypothesized that synthetic cathinones such as PCYP may directly affect neurotransmission, and thereby affect important metabolic pathways such as tryptophan metabolism. Since the present study provides only a snapshot of the metabolome in rats and only two metabolites of the tryptophan metabolism could be identified, further studies are required to obtain a reliable conclusion.

Furthermore, it is important to keep in mind that a direct correlation to humans is not possible. The few altered endogenous metabolites in this study could only be partly explained regarding their general function in mammals. Since it is very difficult to make a reliable conclusion about a specific pathway based on one or two metabolites, further studies are needed. These studies should be based on a targeted metabolomics approach on the alteration of the tryptophan metabolism after PCYP intake.

4. Conclusions

The present study provides a snapshot on the altered metabolic pathway after acute intake of the synthetic cathinone PCYP. Using untargeted toxicometabolomics, sixteen phase I and one phase II metabolites of PCYP could be identified in vitro and in vivo. The main metabolic reaction in rat urine was the dihydroxylation on the pyrrolidine ring followed by mono- and/or dihydroxylation on the benzyl and/or hexyl ring. Regarding phase II metabolism, only the glucuronidation after hydroxylation on the benzyl ring could be observed. Since there are no data available regarding the metabolic pathways of PCYP, the identified metabolites in this study could be used for detection of PCYP intake.

Additionally, five endogenous metabolites could be identified as being significantly altered after PCYP intake. Particular attention should be paid to the two metabolites which are involved in tryptophan metabolism. Since there are many more metabolites involved in this metabolism, further studies are required to confirm this observation. The results of this study demonstrate how the use of toxicometabolomic workflows can overcome conventional screening methods to identify metabolites and endogenous biomarkers that would not be expected. Thus, the knowledge obtained from this study of the rat metabolome can be applied to similar compounds and provide insights into the effects of the compound (class) on an organism. Overall, this study contributes to the understanding of the influence of synthetic cathinones, especially PCYP, on the mammalian metabolome. However, further studies are essential to support the results of this study and to investigate the applicability to humans.

Supplementary Materials: The following supporting information can be downloaded at: https://www.mdpi.com/article/10.3390/metabo12121209/s1, Table S1: Overview of the peak-picking and alignment parameters used for preprocessing for the reversed-phase (RP) and hydrophilic interaction chromatography (HILIC) column and the respective matrices. Pos = positive, neg = negative, ppm = allowed ppm deviation of mass traces for peak picking, snthresh = signal to noise threshold, mzdiff = minimum difference in m/z for two peaks to be considered as separate, prefilter 1 = minimum of scan points, prefilter 2 = minimum abundance, bw = bandwidth for grouping of peaks across separate chromatograms; Table S2: Overview of the significant features using reversed-phase (RP) and hydrophilic interaction chromatography (HILIC) column in pooled human-liver microsome (pHLM) incubation. Features are sorted according to m/z values, followed by the polarity, the retention time (RT) for the corresponding column in seconds (sec), identity, and the identification level according to MSI. Hyphen (-) means that the feature was not significant using the corresponding column; Table S3: Overview of the significant features using reversed-phase (RP) and hydrophilic interaction chromatography (HILIC) column in rat. Features are sorted according to m/z values, followed by the polarity, the retention time (RT) for the corresponding column in seconds (sec), identity, and the identification level according to MSI. Hyphen (-) means that the feature was not significant using the corresponding column; Table S4: Overview of the significant features using reversed-phase (RP) and hydrophilic interaction chromatography (HILIC) column in rat urine. Features are sorted according to m/z values, followed by the polarity, the retention time (RT) for the corresponding column in seconds (sec), identity, and the identification level according to MSI. Hyphen (-) means that the feature was not significant using the corresponding column; Table S5: Detected PCYP metabolites using reversed-phase (RP) and hydrophilic interaction chromatography (HILIC) column in their corresponding matrices namely pooled human-liver microsomes (H), rat urine (U), and rat plasma (P) in which the metabolites could be detected. Metabolite identification numbers (ID) match with the labeling of the structure in Figure 1. For each metabolite, the calculated exact mass of the protonated molecule and elemental composition are given. Hyphen (-) means that the metabolite was not significant in any matrix of the respective column; Figure S1: Results of scores of principal component analysis of pooled human-liver microsome samples after analysis using reversed-phase (RP) and hydrophilic interaction chromatography (HILIC) in positive ionization mode. A = RP pos, B = HILIC pos; Figure S2: Results of scores of principal component analysis of rat urine samples after analysis using reversed-phase (RP) and hydrophilic interaction chromatography (HILIC) in positive and negative ionization mode. A = RP pos, B = RP neg, C = HILIC pos, D = HILIC neg; Figure S3: Results of scores of principal component analysis of rat plasma samples after analysis using reversed-phase (RP) and hydrophilic interaction chromatography (HILIC) in positive and negative ionization mode. A = PH pos, B = HILIC pos, C = HILIC neg; Figure S4: Results of t-distributed stochastic neighborhood embedding (t-SNE) of pooled human-liver microsome samples after analysis using reversed-phase (RP) and hydrophilic interaction chromatography (HILIC) in positive ionization mode. A = RP pos, B = HILIC pos; Figure S5: Results of heat map of hierarchical clustering of pooled human-liver microsome samples after analysis using reversed-phase (RP) and hydrophilic interaction chromatography (HILIC) in positive ionization mode. A = RP pos, B = HILIC pos; Figure S6: Results of heat map of hierarchical clustering of rat urine samples after analysis using reversed-phase (RP) and hydrophilic interaction chromatography (HILIC) in positive and negative ionization mode. A = RP pos, B = RP neg, C = HILIC pos, D = HILIC neg; Figure S7: Results of heat map of hierarchical clustering of rat plasma samples after analysis using reversed-phase (RP) and hydrophilic interaction chromatography (HILIC) in positive and negative ionization mode. A = RP pos, B = HILIC pos, C = HILIC neg; Figure S8: LC-HRMS/MS spectra of the PCYP metabolites detected in positive ionization mode. Fragments with accurate mass, calculated elemental formula, and mass error value in parts per million (ppm); Figure S9: Reconstructed ion chromatogram of m/z 288.1958 after analysis of one QC sample of pooled human-liver microsome in full scan in positive ionization mode using hydrophilic interaction chromatography (HILIC). Metabolite identification number (M) match with the metabolites listed in Table S5; Figure S10: Reconstructed ion chromatograms of m/z 304.1856, m/z 320.1856, and m/z 336.1805 after analysis of one QC sample of rat urine in full scan in positive ionization mode using hydrophilic interaction chromatography (HILIC). Metabolite identification numbers (M) match with the metabolites listed in Table S5.

Author Contributions: S.H., L.W. and M.R.M. designed the experiments; S.H. performed the experiments; S.H. and M.R.M. analyzed and interpreted the data; B.P. and F.W. provided the reference standard of PCYP; S.H. and M.R.M. wrote and edited the manuscript; S.H. prepared the figures; S.H., L.W., B.P., F.W. and M.R.M. reviewed the manuscript. All authors have read and agreed to the published version of the manuscript.

Funding: This research received no external funding.

Institutional Review Board Statement: The animal study protocol was approved by the ethics committee of Landesamt für Verbraucherschutz, Saarbrücken, Germany (protocol code 33/2019).

Informed Consent Statement: Not applicable.

Data Availability Statement: The R scripts can be found on GitHub (https://github.com/sehem/PCYP_Metabolomics.git) and the mzXML files used in this study are available via Metabolights (www.ebi.ac.uk/metabolights/MTBLS6469 (accessed on 17 November 2022)).

Acknowledgments: The authors would like to thank the E.U.-funded project ADEBAR *plus* (grant No. IZ25-5793-2019-33) for the supply of the chemical standard, as well as Juel Maalouli Schaar, Svenja Fischmann, Sascha K. Manier, Armin A. Weber, Gabriele Ulrich, and Carsten Schröder for their support and/or helpful discussions.

Conflicts of Interest: The authors declare no conflict of interest.

References

1. Maurer, H.H.; Pfleger, K.; Weber, A.A. *Mass Spectral Data of Drugs, Poisons, Pesticides, Pollutants and Their Metabolites*; Wiley-VCH: Weinheim, Germany, 2016.
2. EMCDDA. *European Drug Report 2021*; Publications of of the European Union: Lisabon, Portugal, 2021. [CrossRef]
3. Manier, S.K.; Keller, A.; Schaper, J.; Meyer, M.R. Untargeted metabolomics by high resolution mass spectrometry coupled to normal and reversed phase liquid chromatography as a tool to study the in vitro biotransformation of new psychoactive substances. *Sci. Rep.* **2019**, *9*, 2741. [CrossRef] [PubMed]
4. Wagmann, L.; Jacobs, C.M.; Meyer, M.R. New Psychoactive Substances: Which Biological Matrix is the Best for Clinical Toxicology Screening? *Ther. Drug Monit.* **2022**, *44*, 599–605. [CrossRef] [PubMed]
5. Kuropka, P.; Zawadzki, M.; Szpot, P. A review of synthetic cathinones emerging in recent years (2019–2022). *Forensic Toxicol.* **2022**, 1–22. [CrossRef] [PubMed]
6. Simmler, L.D.; Buser, T.A.; Donzelli, M.; Schramm, Y.; Dieu, L.H.; Huwyler, J.; Chaboz, S.; Hoener, M.C.; Liechti, M.E. Pharmacological characterization of designer cathinones in vitro. *Br. J. Pharmacol.* **2013**, *168*, 458–470. [CrossRef]
7. Simmler, L.D.; Rickli, A.; Hoener, M.C.; Liechti, M.E. Monoamine transporter and receptor interaction profiles of a new series of designer cathinones. *Neuropharmacology* **2014**, *79*, 152–160. [CrossRef]
8. Ellefsen, K.N.; Concheiro, M.; Huestis, M.A. Synthetic cathinone pharmacokinetics, analytical methods, and toxicological findings from human performance and postmortem cases. *Drug Metab. Rev.* **2016**, *48*, 237–265. [CrossRef]
9. Soares, J.; Costa, V.M.; Bastos, M.L.; Carvalho, F.; Capela, J.P. An updated review on synthetic cathinones. *Arch. Toxicol.* **2021**, *95*, 2895–2940. [CrossRef]
10. Kolanos, R.; Sakloth, F.; Jain, A.D.; Partilla, J.S.; Baumann, M.H.; Glennon, R.A. Structural Modification of the Designer Stimulant alpha-Pyrrolidinovalerophenone (alpha-PVP) Influences Potency at Dopamine Transporters. *ACS Chem. Neurosci.* **2015**, *6*, 1726–1731. [CrossRef]
11. Araujo, A.M.; Carvalho, M.; Costa, V.M.; Duarte, J.A.; Dinis-Oliveira, R.J.; Bastos, M.L.; Guedes de Pinho, P.; Carvalho, F. In vivo toxicometabolomics reveals multi-organ and urine metabolic changes in mice upon acute exposure to human-relevant doses of 3,4-methylenedioxypyrovalerone (MDPV). *Arch. Toxicol.* **2021**, *95*, 509–527. [CrossRef]
12. Steuer, A.E.; Kaelin, D.; Boxler, M.I.; Eisenbeiss, L.; Holze, F.; Vizeli, P.; Czerwinska, J.; Dargan, P.I.; Abbate, V.; Liechti, M.E.; et al. Comparative Untargeted Metabolomics Analysis of the Psychostimulants 3,4-Methylenedioxy-Methamphetamine (MDMA), Amphetamine, and the Novel Psychoactive Substance Mephedrone after Controlled Drug Administration to Humans. *Metabolites* **2020**, *10*, 306. [CrossRef]
13. Manier, S.K.; Schwermer, F.; Wagmann, L.; Eckstein, N.; Meyer, M.R. Liquid Chromatography-High-Resolution Mass Spectrometry-Based In Vitro Toxicometabolomics of the Synthetic Cathinones 4-MPD and 4-MEAP in Pooled Human Liver Microsomes. *Metabolites* **2020**, *11*, 3. [CrossRef] [PubMed]
14. Manier, S.K.; Wagmann, L.; Flockerzi, V.; Meyer, M.R. Toxicometabolomics of the new psychoactive substances alpha-PBP and alpha-PEP studied in HepaRG cell incubates by means of untargeted metabolomics revealed unexpected amino acid adducts. *Arch. Toxicol.* **2020**, *94*, 2047–2059. [CrossRef] [PubMed]

15. Hemmer, S.; Wagmann, L.; Meyer, M.R. Altered metabolic pathways elucidated via untargeted in vivo toxicometabolomics in rat urine and plasma samples collected after controlled application of a human equivalent amphetamine dose. *Arch. Toxicol.* **2021**, *95*, 3223–3234. [CrossRef] [PubMed]
16. Zaitsu, K.; Hayashi, Y.; Kusano, M.; Tsuchihashi, H.; Ishii, A. Application of metabolomics to toxicology of drugs of abuse: A mini review of metabolomics approach to acute and chronic toxicity studies. *Drug Metab. Pharmacokinet.* **2016**, *31*, 21–26. [CrossRef] [PubMed]
17. Abraham, A.; Wang, Y.; El Said, K.R.; Plakas, S.M. Characterization of brevetoxin metabolism in Karenia brevis bloom-exposed clams (Mercenaria sp.) by LC-MS/MS. *Toxicon* **2012**, *60*, 1030–1040. [CrossRef]
18. Wang, L.; Wu, N.; Zhao, T.Y.; Li, J. The potential biomarkers of drug addiction: Proteomic and metabolomics challenges. *Biomarkers* **2016**, *21*, 678–685. [CrossRef]
19. Steuer, A.E.; Brockbals, L.; Kraemer, T. Metabolomic Strategies in Biomarker Research-New Approach for Indirect Identification of Drug Consumption and Sample Manipulation in Clinical and Forensic Toxicology? *Front. Chem.* **2019**, *7*, 319. [CrossRef]
20. Hemmer, S.; Manier, S.K.; Fischmann, S.; Westphal, F.; Wagmann, L.; Meyer, M.R. Comparison of Three Untargeted Data Processing Workflows for Evaluating LC-HRMS Metabolomics Data. *Metabolites* **2020**, *10*, 378. [CrossRef]
21. Manier, S.K.; Meyer, M.R. Impact of the used solvent on the reconstitution efficiency of evaporated biosamples for untargeted metabolomics studies. *Metabolomics* **2020**, *16*, 34. [CrossRef]
22. Maurer, H.H.; Meyer, M.R.; Helfer, A.G.; Weber, A.A. *Maurer/Meyer/Helfer/Weber MMHW LC-HR-MS/MS Library of Drugs, Poisons, and Their Metabolites*; Wiley-VCH: Weinheim, Germany, 2018.
23. Manier, S.K.; Keller, A.; Meyer, M.R. Automated optimization of XCMS parameters for improved peak picking of liquid chromatography-mass spectrometry data using the coefficient of variation and parameter sweeping for untargeted metabolomics. *Drug Test. Anal.* **2019**, *11*, 752–761. [CrossRef]
24. Wehrens, R.; Hageman, J.A.; van Eeuwijk, F.; Kooke, R.; Flood, P.J.; Wijnker, E.; Keurentjes, J.J.; Lommen, A.; van Eekelen, H.D.; Hall, R.D.; et al. Improved batch correction in untargeted MS-based metabolomics. *Metabolomics* **2016**, *12*, 88. [CrossRef] [PubMed]
25. Adusumilli, R.; Mallick, P. Data Conversion with ProteoWizard msConvert. *Methods Mol. Biol.* **2017**, *1550*, 339–368. [CrossRef] [PubMed]
26. Smith, C.A.; Want, E.J.; O'Maille, G.; Abagyan, R.; Siuzdak, G. XCMS: Processing mass spectrometry data for metabolite profiling using nonlinear peak alignment, matching, and identification. *Anal. Chem.* **2006**, *78*, 779–787. [CrossRef] [PubMed]
27. Team, R.C. *R: A Language and Environment for Statistical Computing, 3.4.1*; R Foundation for Statistical Computing: Vienna, Austria, 2013.
28. Kuhl, C.; Tautenhahn, R.; Bottcher, C.; Larson, T.R.; Neumann, S. CAMERA: An integrated strategy for compound spectra extraction and annotation of liquid chromatography/mass spectrometry data sets. *Anal. Chem.* **2012**, *84*, 283–289. [CrossRef] [PubMed]
29. Broadhurst, D.I.; Kell, D.B. Statistical strategies for avoiding false discoveries in metabolomics and related experiments. *Metabolomics* **2006**, *2*, 171–196. [CrossRef]
30. van der Maaten, L. Accelerating t-SNE using Tree-Based Algorithms. *J. Mach. Learn. Res.* **2014**, *15*, 3221–3245.
31. van der Maaten, L.; Hinton, G. Visualizing Data using t-SNE. *J. Mach. Learn. Res.* **2008**, *9*, 2579–2605.
32. Sumner, L.W.; Amberg, A.; Barrett, D.; Beale, M.H.; Beger, R.; Daykin, C.A.; Fan, T.W.; Fiehn, O.; Goodacre, R.; Griffin, J.L.; et al. Proposed minimum reporting standards for chemical analysis Chemical Analysis Working Group (CAWG) Metabolomics Standards Initiative (MSI). *Metabolomics* **2007**, *3*, 211–221. [CrossRef]
33. Asha, S.; Vidyavathi, M. Role of human liver microsomes in in vitro metabolism of drugs-a review. *Appl. Biochem. Biotechnol.* **2010**, *160*, 1699–1722. [CrossRef]
34. Barnes, S.; Benton, H.P.; Casazza, K.; Cooper, S.J.; Cui, X.; Du, X.; Engler, J.; Kabarowski, J.H.; Li, S.; Pathmasiri, W.; et al. Training in metabolomics research. I. Designing the experiment, collecting and extracting samples and generating metabolomics data. *J. Mass Spectrom.* **2016**, *51*, 461–475. [CrossRef]
35. Vervliet, P.; Mortele, O.; Gys, C.; Degreef, M.; Lanckmans, K.; Maudens, K.; Covaci, A.; van Nuijs, A.L.N.; Lai, F.Y. Suspect and non-target screening workflows to investigate the in vitro and in vivo metabolism of the synthetic cannabinoid 5Cl-THJ-018. *Drug Test. Anal.* **2019**, *11*, 479–491. [CrossRef] [PubMed]
36. Barnes, S.; Benton, H.P.; Casazza, K.; Cooper, S.J.; Cui, X.; Du, X.; Engler, J.; Kabarowski, J.H.; Li, S.; Pathmasiri, W.; et al. Training in metabolomics research. II. Processing and statistical analysis of metabolomics data, metabolite identification, pathway analysis, applications of metabolomics and its future. *J. Mass Spectrom.* **2016**, *51*, 535–548. [CrossRef]
37. McClenahan, S.; Gunnell, M.; Owens, M. Pharmacokinetics of alpha-Pyrrolidinovalerophenone in Male Rats with and without Vaccination with an alpha-Pyrrolidinovalerophenone Vaccine. *J. Pharm. Pharm. Sci.* **2021**, *24*, 267–276. [CrossRef] [PubMed]
38. Negreira, N.; Erratico, C.; Kosjek, T.; van Nuijs, A.L.; Heath, E.; Neels, H.; Covaci, A. In vitro Phase I and Phase II metabolism of alpha-pyrrolidinovalerophenone (alpha-PVP), methylenedioxypyrovalerone (MDPV) and methedrone by human liver microsomes and human liver cytosol. *Anal. Bioanal. Chem.* **2015**, *407*, 5803–5816. [CrossRef] [PubMed]
39. Tyrkko, E.; Pelander, A.; Ketola, R.A.; Ojanpera, I. In silico and in vitro metabolism studies support identification of designer drugs in human urine by liquid chromatography/quadrupole-time-of-flight mass spectrometry. *Anal. Bioanal. Chem.* **2013**, *405*, 6697–6709. [CrossRef] [PubMed]

40. Franski, R.; Gierczyk, B.; Kasperkowiak, M.; Jankowski, W.; Hoffmann, M. The mechanism of water loss from protonated cathinones. *Rapid Commun. Mass Spectrom.* **2020**, *34*, e8617. [CrossRef]
41. Sauer, C.; Peters, F.T.; Haas, C.; Meyer, M.R.; Fritschi, G.; Maurer, H.H. New designer drug alpha-pyrrolidinovalerophenone (PVP): Studies on its metabolism and toxicological detection in rat urine using gas chromatographic/mass spectrometric techniques. *J. Mass Spectrom.* **2009**, *44*, 952–964. [CrossRef]
42. Ellefsen, K.N.; Wohlfarth, A.; Swortwood, M.J.; Diao, X.; Concheiro, M.; Huestis, M.A. 4-Methoxy-alpha-PVP: In silico prediction, metabolic stability, and metabolite identification by human hepatocyte incubation and high-resolution mass spectrometry. *Forensic Toxicol.* **2016**, *34*, 61–75. [CrossRef]
43. Martignoni, M.; Groothuis, G.M.; de Kanter, R. Species differences between mouse, rat, dog, monkey and human CYP-mediated drug metabolism, inhibition and induction. *Expert Opin. Drug Metab. Toxicol.* **2006**, *2*, 875–894. [CrossRef]
44. Miles, K.K.; Stern, S.T.; Smith, P.C.; Kessler, F.K.; Ali, S.; Ritter, J.K. An investigation of human and rat liver microsomal mycophenolic acid glucuronidation: Evidence for a principal role of UGT1A enzymes and species differences in UGT1A specificity. *Drug Metab. Dispos.* **2005**, *33*, 1513–1520. [CrossRef]
45. Shiratani, H.; Katoh, M.; Nakajima, M.; Yokoi, T. Species differences in UDP-glucuronosyltransferase activities in mice and rats. *Drug Metab. Dispos.* **2008**, *36*, 1745–1752. [CrossRef] [PubMed]
46. Fisher, M.B.; Paine, M.F.; Strelevitz, T.J.; Wrighton, S.A. The role of hepatic and extrahepatic UDP-glucuronosyltransferases in human drug metabolism. *Drug Metab. Rev.* **2001**, *33*, 273–297. [CrossRef]
47. Maurer, H.H.; Wissenbach, D.K.; Weber, A.A. *Maurer/Wissenbach/Weber MWW LC-MSn Library of Drugs, Poisons, and Their Metabolites*, 2nd ed.; Wiley-VCH: Weinheim, Germany, 2018.
48. Olesti, E.; De Toma, I.; Ramaekers, J.G.; Brunt, T.M.; Carbo, M.L.; Fernandez-Aviles, C.; Robledo, P.; Farre, M.; Dierssen, M.; Pozo, O.J.; et al. Metabolomics predicts the pharmacological profile of new psychoactive substances. *J. Psychopharmacol.* **2019**, *33*, 347–354. [CrossRef] [PubMed]
49. Bouhifd, M.; Hartung, T.; Hogberg, H.T.; Kleensang, A.; Zhao, L. Review: Toxicometabolomics. *J. Appl. Toxicol.* **2013**, *33*, 1365–1383. [CrossRef] [PubMed]
50. Milburn, M.V.; Ryals, J.A.; Guo, L. Toxicometabolomics. In *A Comprehensive Guide to Toxicology in Nonclinical Drug Development*; Academic Press: Cambridge, MA, USA, 2013; pp. 875–891. [CrossRef]
51. Wishart, D.S.; Tzur, D.; Knox, C.; Eisner, R.; Guo, A.C.; Young, N.; Cheng, D.; Jewell, K.; Arndt, D.; Sawhney, S.; et al. HMDB: The Human Metabolome Database. *Nucleic Acids Res.* **2007**, *35*, D521–D526. [CrossRef]
52. Nielsen, K.L.; Telving, R.; Andreasen, M.F.; Hasselstrom, J.B.; Johannsen, M. A Metabolomics Study of Retrospective Forensic Data from Whole Blood Samples of Humans Exposed to 3,4-Methylenedioxymethamphetamine: A New Approach for Identifying Drug Metabolites and Changes in Metabolism Related to Drug Consumption. *J. Proteome Res.* **2016**, *15*, 619–627. [CrossRef]
53. Hack, S.P.; Christie, M.J. Adaptations in adenosine signaling in drug dependence: Therapeutic implications. *Crit. Rev. Neurobiol.* **2003**, *15*, 235–274. [CrossRef]
54. Brown, R.M.; Short, J.L. Adenosine A(2A) receptors and their role in drug addiction. *J. Pharm. Pharmacol.* **2008**, *60*, 1409–1430. [CrossRef]
55. Filip, M.; Zaniewska, M.; Frankowska, M.; Wydra, K.; Fuxe, K. The importance of the adenosine A(2A) receptor-dopamine D(2) receptor interaction in drug addiction. *Curr. Med. Chem.* **2012**, *19*, 317–355. [CrossRef]
56. Ballesteros-Yanez, I.; Castillo, C.A.; Merighi, S.; Gessi, S. The Role of Adenosine Receptors in Psychostimulant Addiction. *Front. Pharmacol.* **2017**, *8*, 985. [CrossRef]
57. Borbely, A.A.; Daan, S.; Wirz-Justice, A.; Deboer, T. The two-process model of sleep regulation: A reappraisal. *J. Sleep Res.* **2016**, *25*, 131–143. [CrossRef] [PubMed]
58. Borea, P.A.; Gessi, S.; Merighi, S.; Vincenzi, F.; Varani, K. Pharmacology of Adenosine Receptors: The State of the Art. *Physiol. Rev.* **2018**, *98*, 1591–1625. [CrossRef] [PubMed]
59. Radulovacki, M. Role of adenosine in sleep in rats. *Rev. Clin. Basic Pharm.* **1985**, *5*, 327–339. [PubMed]
60. Khamis, M.M.; Adamko, D.J.; El-Aneed, A. Mass spectrometric based approaches in urine metabolomics and biomarker discovery. *Mass Spectrom. Rev.* **2017**, *36*, 115–134. [CrossRef]
61. Bartoli, F.; Misiak, B.; Callovini, T.; Cavaleri, D.; Cioni, R.M.; Crocamo, C.; Savitz, J.B.; Carra, G. The kynurenine pathway in bipolar disorder: A meta-analysis on the peripheral blood levels of tryptophan and related metabolites. *Mol. Psychiatry* **2021**, *26*, 3419–3429. [CrossRef]
62. Wonodi, I.; Stine, O.C.; Sathyasaikumar, K.V.; Roberts, R.C.; Mitchell, B.D.; Hong, L.E.; Kajii, Y.; Thaker, G.K.; Schwarcz, R. Downregulated kynurenine 3-monooxygenase gene expression and enzyme activity in schizophrenia and genetic association with schizophrenia endophenotypes. *Arch. Gen. Psychiatry* **2011**, *68*, 665–674. [CrossRef]
63. Eskelund, A.; Li, Y.; Budac, D.P.; Muller, H.K.; Gulinello, M.; Sanchez, C.; Wegener, G. Drugs with antidepressant properties affect tryptophan metabolites differently in rodent models with depression-like behavior. *J. Neurochem.* **2017**, *142*, 118–131. [CrossRef]

Supporting Information

In Vitro and In Vivo Toxicometabolomics of the Synthetic Cathinone PCYP Studied by Means of LC-HRMS/MS

Selina Hemmer[1], Lea Wagmann[1], Benedikt Pulver[2], Folker Westphal[2], Markus R. Meyer[1,*]

[1]Department of Experimental and Clinical Toxicology, Institute of Experimental and Clinical Pharmacology and Toxicology, Center for Molecular Signaling (PZMS), Saarland University, Homburg, Germany
[2]State Bureau of Criminal Investigation Schleswig-Holstein, Kiel, Germany

Corresponding author
*Markus R. Meyer, email: markus.meyer@uks.eu

Table S1. Overview of the peak picking and alignment parameters used for preprocessing for the reversed-phase (RP) and hydrophilic interaction chromatography (HILIC) column and the respective matrices. Pos = positive, neg = negative, ppm = allowed ppm deviation of mass traces for peak picking, snthresh = signal to noise threshold, mzdiff = minimum difference in *m/z* for two peaks to be considered as separate, prefilter 1 = minimum of scan points, prefilter 2 = minimum abundance, bw = bandwidth for grouping of peaks across separate chromatograms.

Column	Matrix	Polarity	Peak width, min	Peak width, max	ppm	sntresh	mzdiff	Prefilter 1	Prefilter 2	bw
RP	pHLM	pos	8.9	100	1.8	10	0.018	7	100	5.0
		neg	8.9	15	1.7	27	0.094	5	100	1.0
	Urine	pos	8.9	19	1.0	12	0.012	7	100	2.5
		neg	7.8	15	2.5	18	-0.098	6	100	4.5
	Plasma	pos	8.9	33	1.3	12	0.1	7	100	1.0
		neg	6.8	100	1.8	16	0.01	5	100	1.0
HILIC	pHLM	pos	7.8	29	1.6	17	0.006	6	100	0.5
		neg	7.8	17	2.5	51	0.01	6	1300	1.0
	Urine	pos	8.9	21	1.9	16	0.02	8	100	1.5
		neg	8.9	35	1.3	15	0.022	8	100	1.5
	Plasma	pos	8.9	46	1.4	6	0.034	6	100	0.2
		neg	8.9	25	2.5	15	0.034	6	100	0.9

Table S2. Overview of the significant features using reversed-phase (RP) and hydrophilic interaction chromatography (HILIC) column in pooled human liver microsome incubation. Features are sorted according to *m/z* values, followed by the polarity, the retention time (RT) for the corresponding column in seconds (sec), identity, and the identification level according to MSI. Hyphen (-) means that the feature was not significant using the corresponding column.

m/z	Polarity	RP RT, sec	HILIC RT, sec	Identity	Identification level according to MSI
105.0331	Positive	-	192	PCYP artifact	3
146.0812	Positive	-	61	Unknown	4
158.0812	Positive	-	83, 126	Unknown	4
176.0918	Positive	31	126	Unknown	4
218.1539	Positive	-	224	PCYP-M (*N*-dealkyl-)	3
220.1696	Positive	-	247	Unknown	4
271.1884	Positive	314	-	PCYP-M (dehydro-) isotope	3
272.2008	Positive	314	192	PCYP	1
273.2041	Positive	314	192	PCYP isotope	3
274.2164	Positive	314	195	PCYP isotope	3
275.2197	Positive	314	194	PCYP isotope	3
276.223	Positive	314	-	PCYP isotope	3
286.1801	Positive	214, 235	-	PCYP-M (oxo-)	3
288.1957	Positive	280, 302, 255	222, 259, 244	PCYP-M (hydroxy-)	3
289.199	Positive	-	189, 222, 259, 244	PCYP-M (hydroxy-) isotope	3
290.2113	Positive	306	266	PCYP-M (ring opened hydroxy-)	3
291.2146	Positive	-	205	PCYP-M (ring opened hydroxy-) isotope	3
304.1907	Positive	202, 309	234	PCYP-M (dihydroxy-)	3
305.1939	Positive	309	234, 252	PCYP-M (dihydroxy-) isotope	3
306.2063	Positive	216	-	PCYP-M (ring opened dihydroxy)	3
566.5508	Positive	-	42	Unknown	4

Table S3. Overview of the significant features using reversed-phase (RP) and hydrophilic interaction chromatography (HILIC) column in rat plasma. Features are sorted according to *m/z* values, followed by the polarity, the retention time (RT) for the corresponding column in seconds (sec), identity, and the identification level according to MSI. Hyphen (-) means that the feature was not significant using the corresponding column.

m/z	Polarity	RP RT, sec	HILIC RT, sec	Identity	Identification level according to MSI
146.0599	Positive	-	71	Quinolin-2-ol	2 (NIST msms)
189.0579	Positive	-	66	3-Methyladipic acid $[M+H+H_2O]^+$	2 (NIST msms)
190.0613	Positive	-	67	3-Methyladipic acid $[M+H+H_2O]^+$ isotope	2 (NIST msms)
268.1038	Positive	35,61	248	Adenosine	2 (NIST msms)
269.0878	Positive	-	330	Unknown	4
276.2685	Positive	-	178	Unknown	4
291.2721	Positive	390	-	Unknown	4
304.1904	Positive	306	235	PCYP-M (dihydroxy -)	3
305.1939	Positive	306	235	PCYP-M (dihydroxy-) isotope	3
309.1010	Negative	-	215	Unknown	4
310.1493	Positive	167	-	Unknown	4
312.0945	Negative	-	248	Unknown	4
318.1699	Positive	-	237	PCYP-M (dihydroxy-, oxo)	3
320.1856	Positive	215	290	PCYP-M (trihydroxy-)	3
321.0432	Negative	-	206	Unknown	4
321.1886	Positive	215	-	PCYP-M (trihydroxy-) isotope	3
328.3845	Positive	-	160	Unknown	4
416.3740	Negative	-	159	Unknown	4
562.5880	Negative	24	-	Unknown	4

Table S4. Overview of the significant features using reversed-phase (RP) and hydrophilic interaction chromatography (HILIC) column in rat urine. Features are sorted according to *m/z* values, followed by the polarity, the retention time (RT) for the corresponding column in seconds (sec), identity, and the identification level according to MSI. Hyphen (-) means that the feature was not significant using the corresponding column.

m/z	Polarity	RP RT, sec	HILIC RT, sec	Identity	Identification level according to MSI
146.0602	Positive	244	70	Quinolin-2-ol	2 (NIST msms)
147.0635	Positive	244	-	Quinolin-2-ol isotope	2 (NIST msms)
148.0965	Positive	-	456	Unknown	4
162.0551	Positive	-	230	Dihydroxyquinoline	3 (NIST msms)
163.0584	Positive	-	230	Dihydroxyquinoline isotope	3 (NIST msms)
185.0437	Positive	-	303	Kynurenic acid $[M\text{-}CH_2O_2+Na]^+$	2 (massbank)
186.0470	Positive	-	303	Kynurenic acid $[M\text{-}CH_2O_2+Na]^+$ isotope	2 (massbank)
189.0582	Positive	156	67	Unknown	4
190.0503	Negative	-	176	Unknown	4
190.0614	Positive	-	67	Unknown isotope	4
208.1183	Negative	-	398	Unknown	4
208.4951	Negative	-	320	Unknown	4
208.9913	Negative	-	320	Unknown	4
211.0401	Positive	156	-	Unknown	4
215.0013	Negative	-	301	Unknown	4
219.9996	Negative	-	248	Unknown	4
220.9920	Negative	-	248	Unknown	4
221.0448	Negative	226	-	Unknown	4
239.9966	Negative	203, 151	232, 271	Unknown	4
240.0539	Positive	-	263	Unknown	4
242.0118	Positive	152	271	Unknown	4
242.0122	Negative	-	245	Unknown	4
242.0123	Negative	157	-	Unknown	4

Table S4. Continued.

m/z	Polarity	RP RT, sec	HILIC RT, sec	Identity	Identification level according to MSI
243.0977	Positive	-	472	Unknown	4
243.1817	Positive	-	425	Unknown	4
245.0924	Negative	-	242	Unknown	4
247.9776	Negative	238	-	Unknown	4
250.1439	Positive	-	339	PCYP artifact	3
255.0653	Positive	-	225	Daidzein	2 (massbank)
260.0588	Positive	186	-	Unknown	4
270.0483	Negative	336	-	Unknown	4
271.0390	Negative	-	226	Unknown	4
271.0819	Negative	-	107	Unknown	4
281.1136	Negative	266	329	Unknown	4
283.1290	Positive	266	-	Unknown	4
283.9306	Negative	207, 238	-	Unknown	4
284.1242	Positive	-	468	Unknown	4
285.2286	Positive	-	456	Unknown	4
285.8645	Negative	266	-	Unknown	4
286.0793	Positive	-	455	Unknown	4
287.1139	Positive	208	-	Unknown	4
288.0901	Positive	218	247	Unknown	4
288.1957	Positive	-	222	PCYP-M (hydroxy-)	3
289.0324	Negative	-	354	Unknown	4
290.9998	Negative	-	246	Unknown	4
297.0973	Negative	-	148	Unknown	4
299.8808	Negative	122	-	Unknown	4
302.1422	Positive	-	68	Unknown	4

Table S4. Continued.

m/z	Polarity	RP RT, sec	HILIC RT, sec	Identity	Identification level according to MSI
302.2108	Positive	-	366	Unknown	4
303.1704	Positive	-	271	Unknown	4
303.2109	Positive	-	366	Unknown isotope	4
304.0070	Negative	-	320	Unknown	4
304.1910	Positive	305	232	PCYP-M (dihydroxy-)	3
305.1942	Positive	305	-	PCYP-M (dihydroxy-) isotope	3
306.1701	Positive	204	296	PCYP-M (hydroxy + pyrrolidin cleavage with oxidation to COOH)	3
307.0578	Positive	312	-	Unknown	4
307.0749	Positive	249	-	Unknown	4
309.0067	Negative	-	247	Unknown	4
310.0720	Positive	218	247	Unknown	4
311.2119	Positive	320	218	Unknown	4
312.2151	Positive	-	218	Unknown isotope	4
316.1546	Negative	-	236	Unknown	4
317.0329	Negative	-	241	Unknown	4
318.1702	Positive	222	195, 233, 318	PCYP-M (dihydroxy-, oxo)	3
319.1266	Positive	245	-	Unknown	4
319.1734	Positive	222	233, 318	PCYP-M (dihydroxy-, oxo) isotope	3
320.1859	Positive	214, 232	264, 302	PCYP-M (trihydroxy-)	3
321.1892	Positive	214, 232	302	PCYP-M (trihydroxy-) isotope	3
322.2015	Positive	193	-	Unknown	4
323.2048	Positive	192	296	Unknown isotope	4

Table S4. Continued

m/z	Polarity	RP RT, sec	HILIC RT, sec	Identity	Identification level according to MSI
324.9200	Negative	-	234	Unknown	4
325.0855	Positive	206	305	Unknown	4
326.0460	Positive	-	246	Unknown	4
327.1079	Negative	-	176	Unknown	4
327.2069	Positive	243	273	Unknown	4
331.0851	Negative	-	235	Unknown	4
332.1491	Positive	-	86	Unknown	4
334.0101	Negative	-	226	Unknown	4
334.1108	Positive	-	69	Unknown	4
334.1651	Positive	188, 248	115, 324	PCYP-M (trihydroxy-, oxo)	3
335.0223	Positive	-	324	PCYP-M (trihydroxy-, oxo) isotope	3
335.9012	Negative	235	-	Unknown	4
336.1807	Positive	176, 197	323, 341	PCYP-M (tetrahydroxy-)	3
337.1807	Positive	176	323, 341	PCYP-M (tetrahydroxy-) isotope	3
338.0414	Negative	-	241	Unknown	4
341.1861	Positive	210	375	Unknown	4
343.2019	Positive	-	321	Unknown	4
343.8885	Negative	182	-	Unknown	4
346.1433	Positive	-	245	Unknown	4
347.1466	Positive	-	245	Unknown	4
347.2541	Positive	-	374	Unknown	4
349.0703	Negative	-	248	Unknown	4
351.0858	Positive	-	114	Unknown	4
352.0487	Positive	-	225	Unknown	4

Table S4. Continued.

m/z	Polarity	RP RT, sec	HILIC RT, sec	Identity	Identification level according to MSI
353.0329	Negative	-	245	Unknown	4
356.1471	Positive	247	-	Unknown	4
360.1920	Positive	-	202, 344	Unknown	4
361.1952	Positive	-	344	Unknown isotope	4
365.2357	Negative	-	146	Unknown	4
367.0484	Negative	-	240	Unknown	4
371.1338	Negative	225	-	Unknown	4
372.1212	Positive	-	114	Unknown	4
376.1426	Positive	271	-	Unknown	4
380.0548	Negative	-	246	Unknown	4
390.1762	Positive	225	-	Unknown	4
391.0682	Negative	-	223	Unknown	4
426.1333	Positive	-	247	Unknown	4
462.0523	Negative	-	320	Unknown	4
464.2285	Positive	-	393	PCYP-M (hydroxy-glucuronide-)	3
465.2155	Positive	317	360	Unknown	4
466.2189	Positive	-	360	Unknown isotope	4
573.3299	Negative	-	139	Unknown	4

Table S5. Detected PCYP metabolites using reversed-phase (RP) and hydrophilic interaction chromatography (HILIC) column in their corresponding matrices namely pooled human liver microsomes (H), rat urine (U), and rat plasma (P) in which the metabolites could be detected. Metabolite identification numbers (ID) match with the labeling of the structure in Figure 1. For each metabolite the calculated exact mass of the protonated molecule and elemental composition are given. Hyphen (-) means that the metabolite was not significant in any matrix of the respective column.

Metabolite-ID	Calculated exact mass, *m/z*	Elemental composition	RP	HILIC
PCYP	272.2009	$C_{18}H_{25}NO$	H	H
M1	288.1958	$C_{18}H_{25}NO_2$	H	H
M2	288.1958	$C_{18}H_{25}NO_2$	H	H
M3	288.1958	$C_{18}H_{25}NO_2$	H	H, U
M4	218.1539	$C_{14}H_{19}NO$	-	H
M5	304.1907	$C_{18}H_{25}NO_3$	H, U, P	H, U, P
M6	320.1856	$C_{18}H_{25}NO_4$	U, P	U, P
M7	336.1805	$C_{18}H_{25}NO_5$	U	U
M8	286.1802	$C_{18}H_{23}NO_2$	H	-
M9	318.1700	$C_{18}H_{23}NO_3$	U, P	U, P
M10	334.1649	$C_{18}H_{25}NO_5$	U	U
M11	290.2115	$C_{18}H_{27}NO_2$	H	H
M12	306.2064	$C_{18}H_{27}NO_3$	H	-
M13	304.1907	$C_{18}H_{25}NO_3$	H	-
M14	320.1856	$C_{18}H_{25}NO_4$	U	U
M15	306.1700	$C_{17}H_{23}NO_4$	U	U
M16	250.1438	$C_{14}H_{19}NO_3$	-	U
M17	464.2279	$C_{24}H_{33}NO_8$	-	U

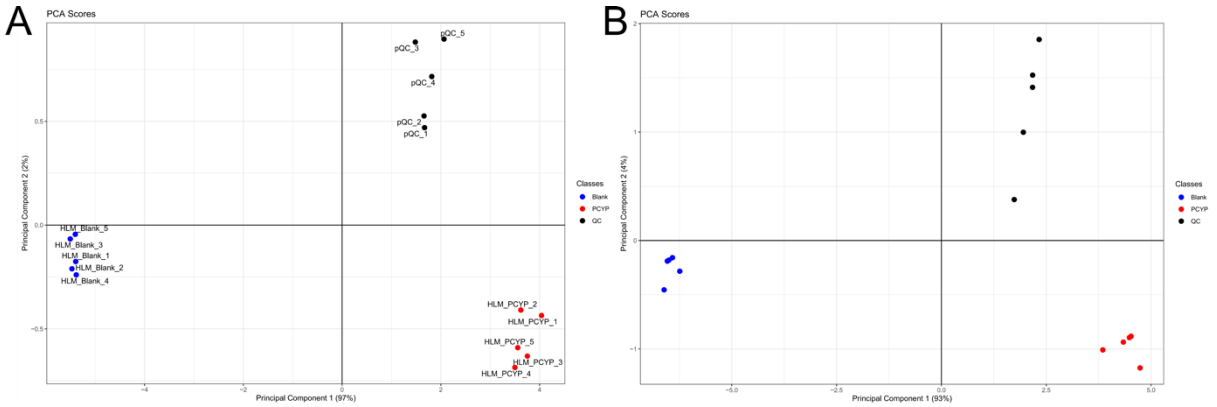

Figure S1. Results of scores of principal component analysis of pooled human liver microsome samples after analysis using reversed-phase (RP) and hydrophilic interaction chromatography (HILIC) in positive ionization mode. A = RP pos, B = HILIC pos.

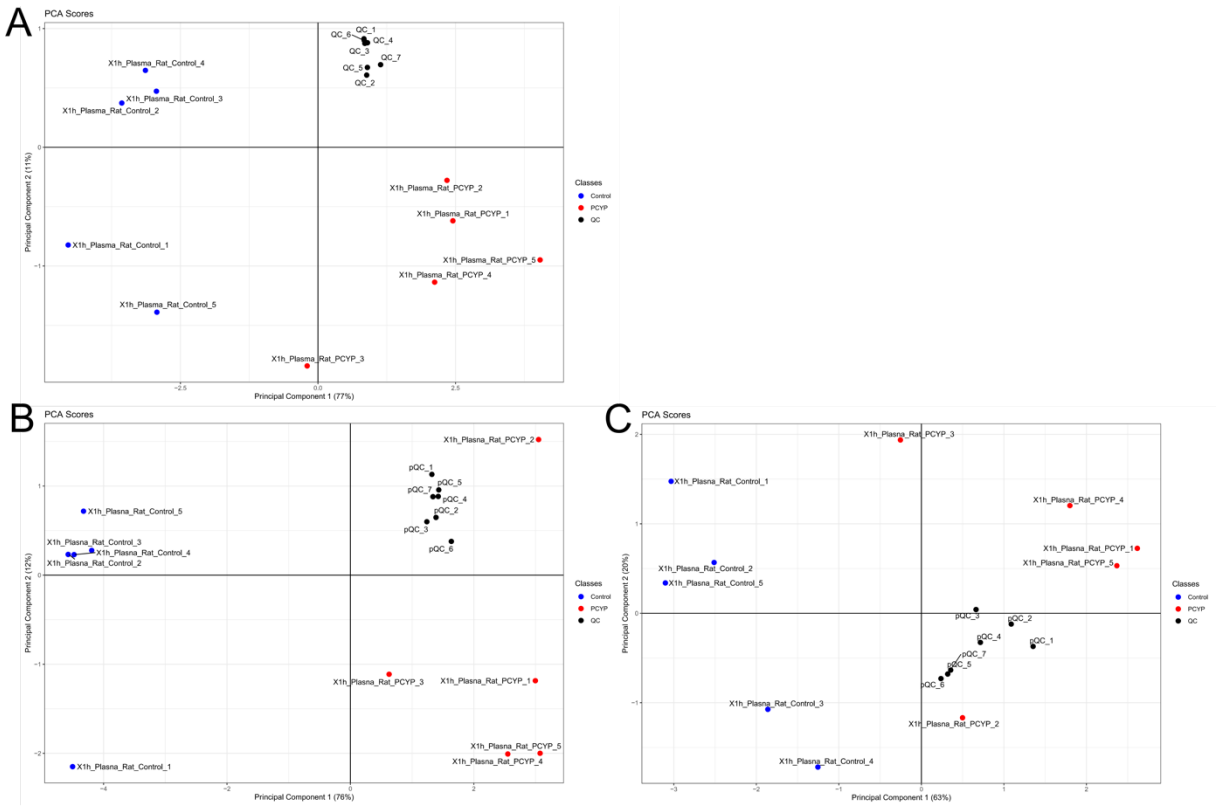

Figure S2. Results of scores of principal component analysis of rat plasma samples after analysis using reversed-phase (RP) and hydrophilic interaction chromatography (HILIC) in positive and negative ionization mode. A = PH pos, B = HILIC pos, C = HILIC neg.

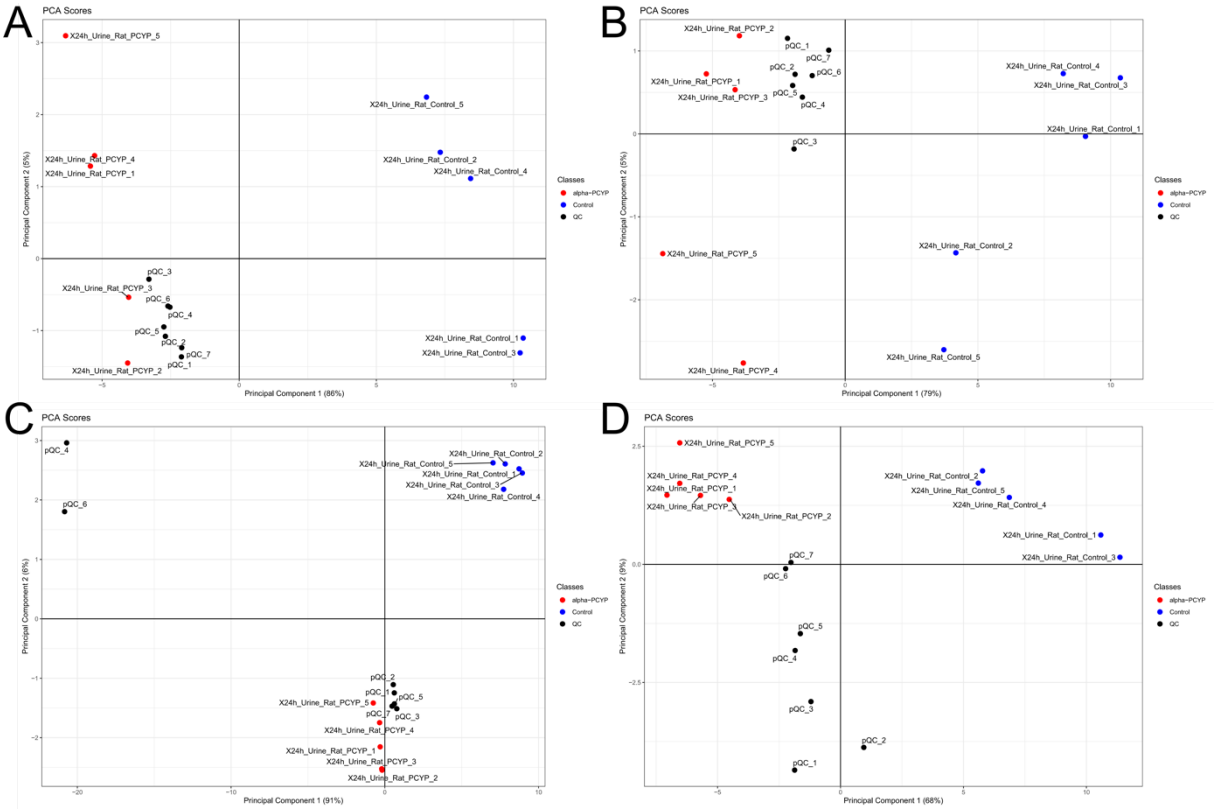

Figure S3. Results of scores of principal component analysis of rat urine samples after analysis using reversed-phase (RP) and hydrophilic interaction chromatography (HILIC) in positive and negative ionization mode. A = RP pos, B = RP neg, C = HILIC pos, D = HILIC neg.

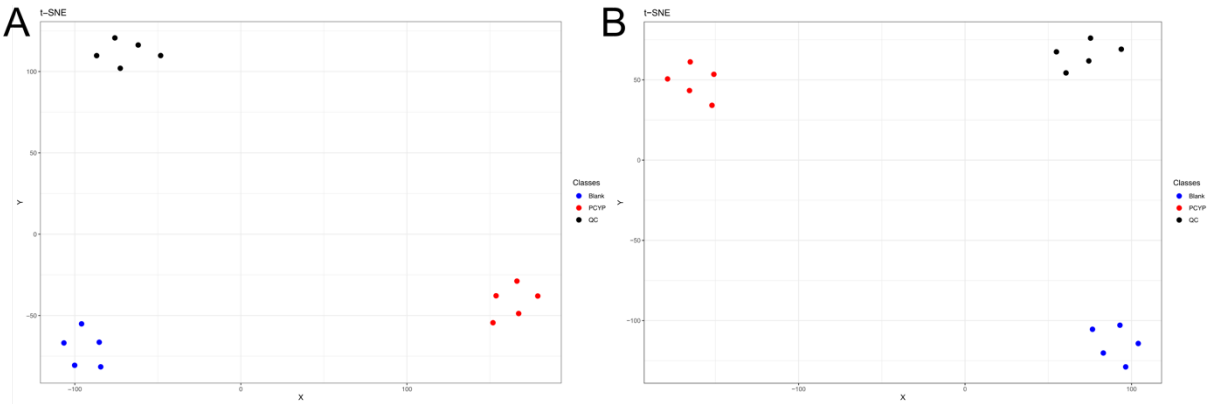

Figure S4. Results of t-distributed stochastic neighborhood embedding (t-SNE) of pooled human liver microsome samples after analysis using reversed-phase (RP) and hydrophilic interaction chromatography (HILIC) in positive ionization mode. A = RP pos, B = HILIC pos.

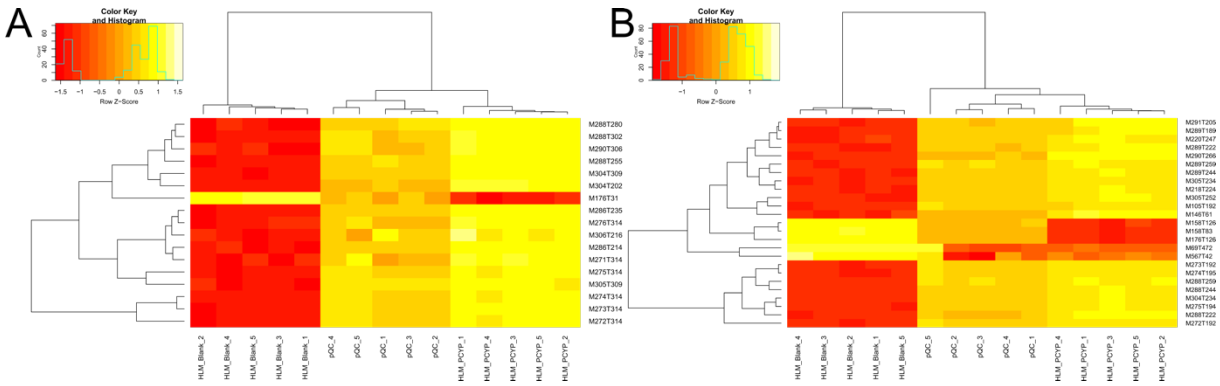

Figure S5. Results of heat map of hierarchical clustering of pooled human liver microsome samples after analysis using reversed-phase (RP) and hydrophilic interaction chromatography (HILIC) in positive ionization mode. A = RP pos, B = HILIC pos.

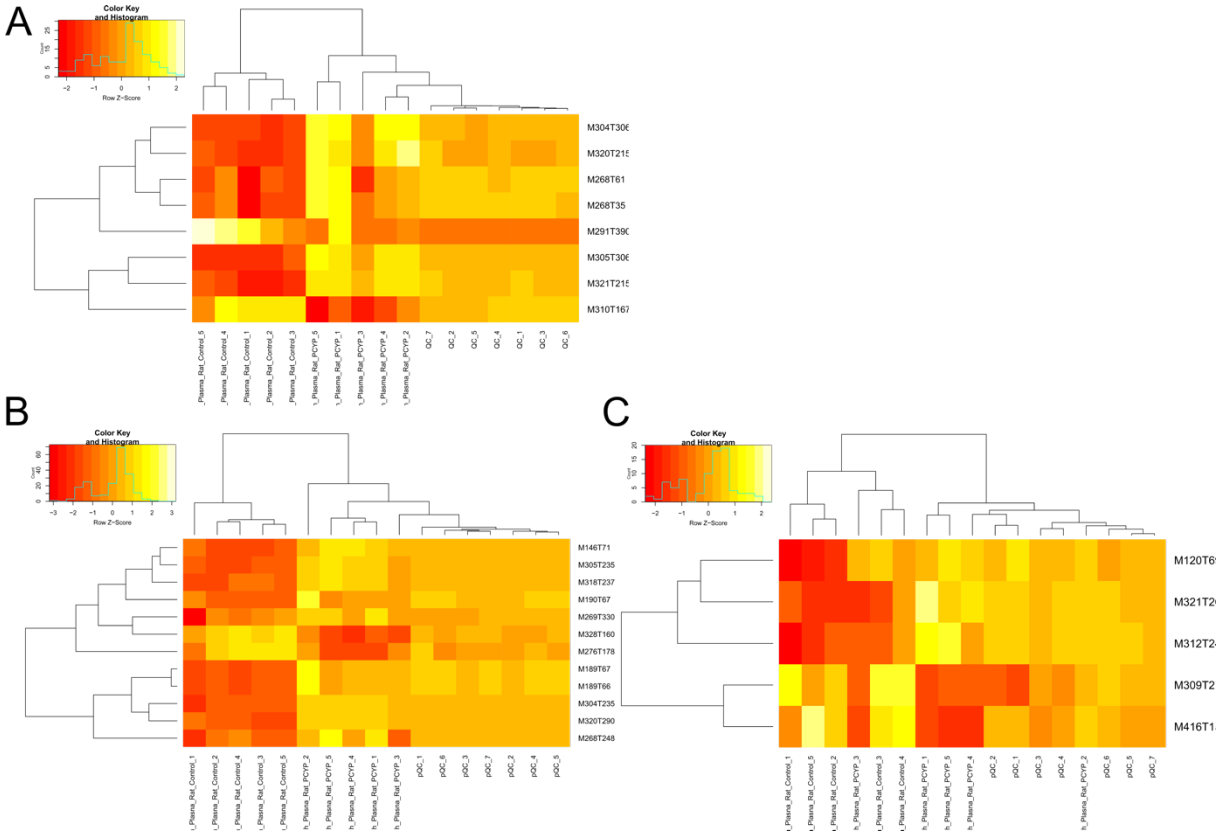

Figure S6. Results of heat map of hierarchical clustering of rat plasma samples after analysis using reversed-phase (RP) and hydrophilic interaction chromatography (HILIC) in positive and negative ionization mode. A = RP pos, B = HILIC pos, C = HILIC neg.

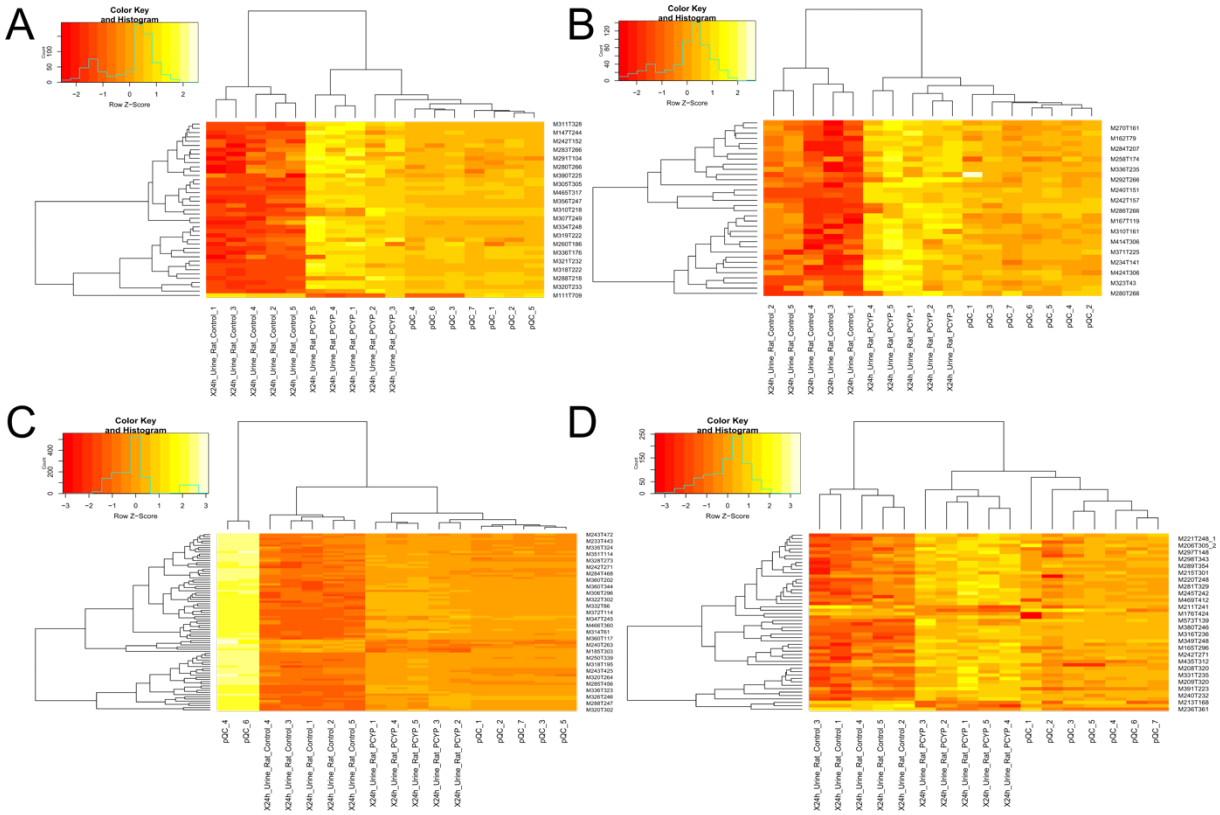

Figure S7. Results of heat map of hierarchical clustering of rat urine samples after analysis using reversed-phase (RP) and hydrophilic interaction chromatography (HILIC) in positive and negative ionization mode. A = RP pos, B = RP neg, C = HILIC pos, D = HILIC neg.

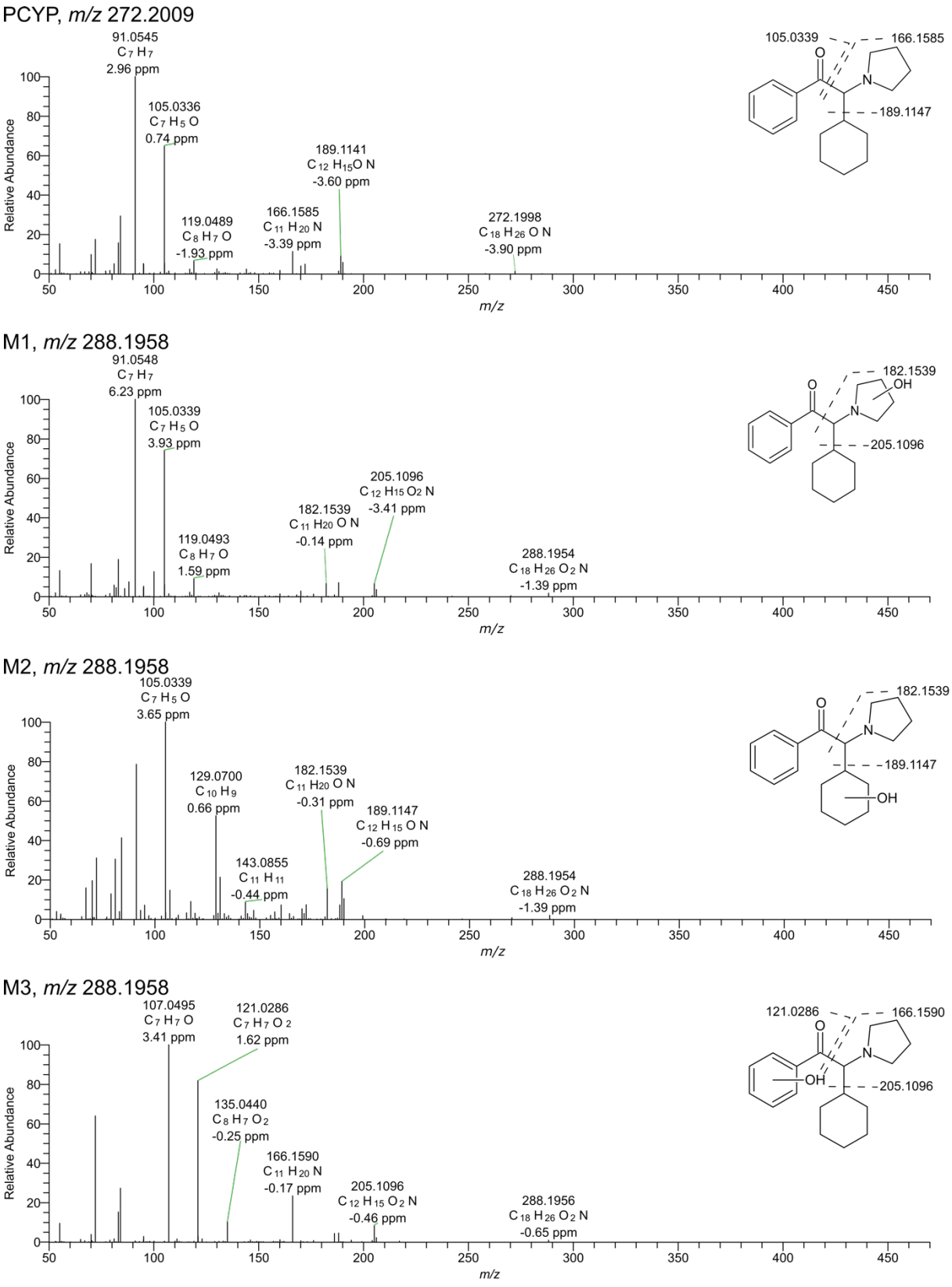

Figure S8. LC-HRMS/MS spectra of the PCYP metabolites detected in positive ionization mode. Fragments with accurate mass, calculated elemental formula, and mass error value in parts per million (ppm).

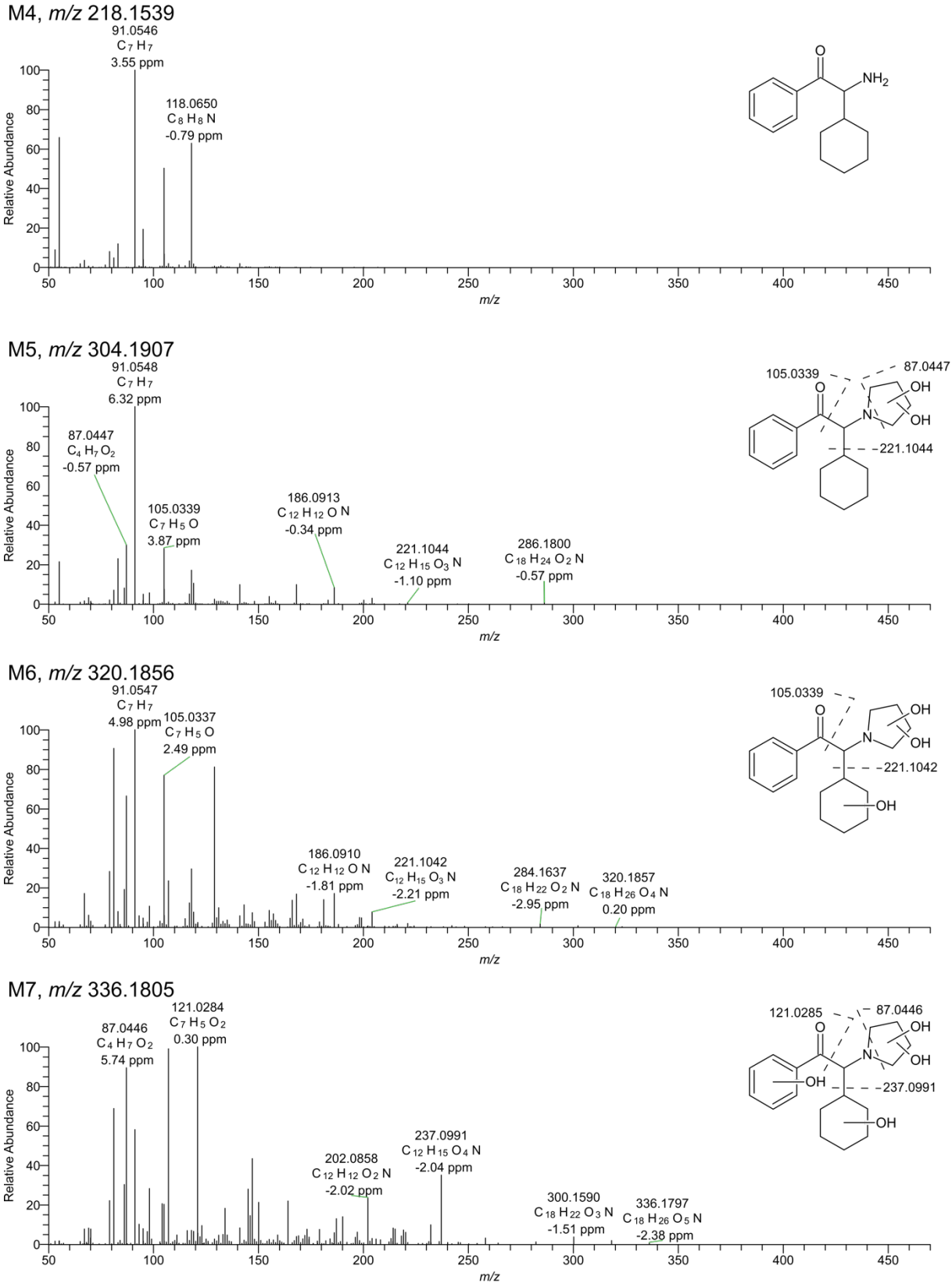

Figure S8. Continued.

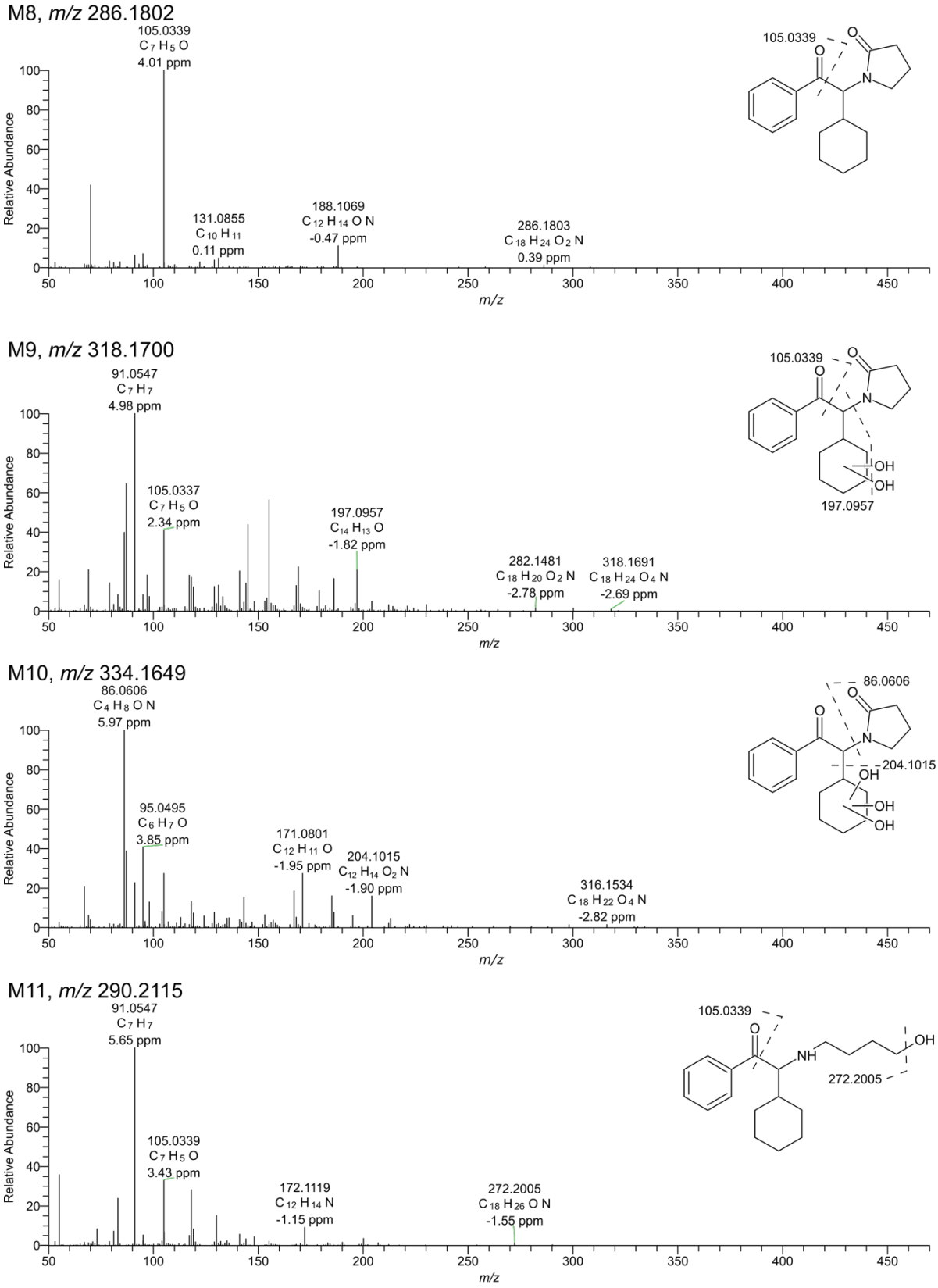

Figure S8. Continued.

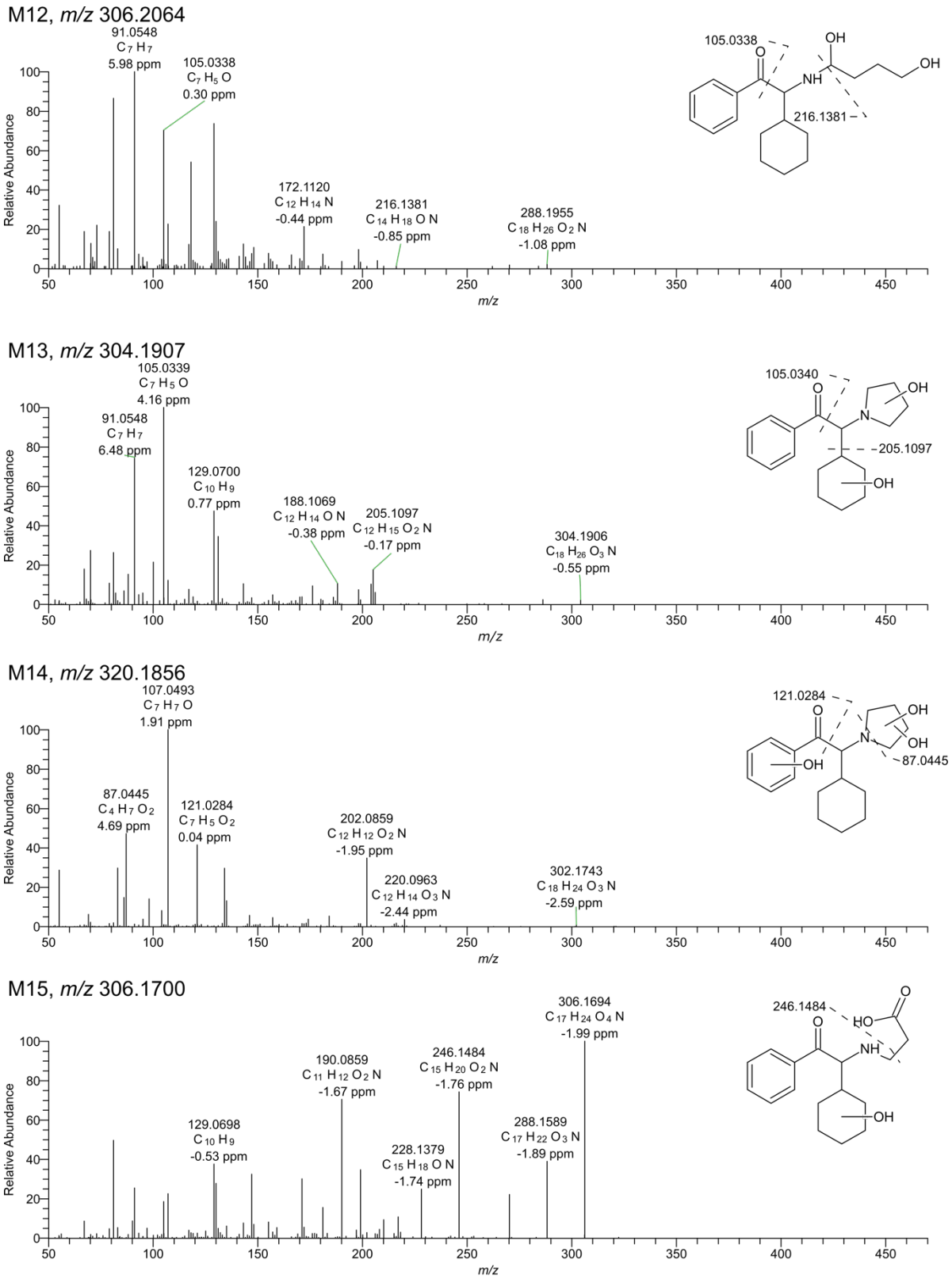

Figure S8. Continued.

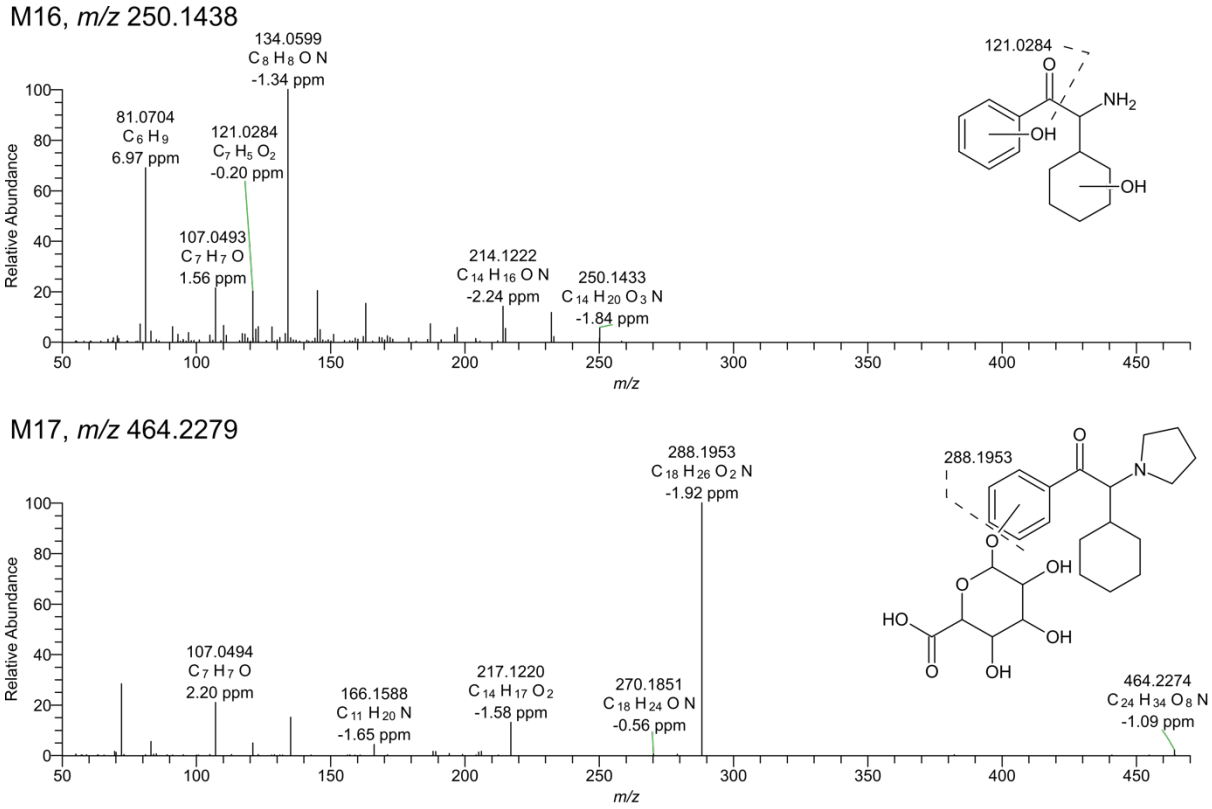

Figure S8. Continued.

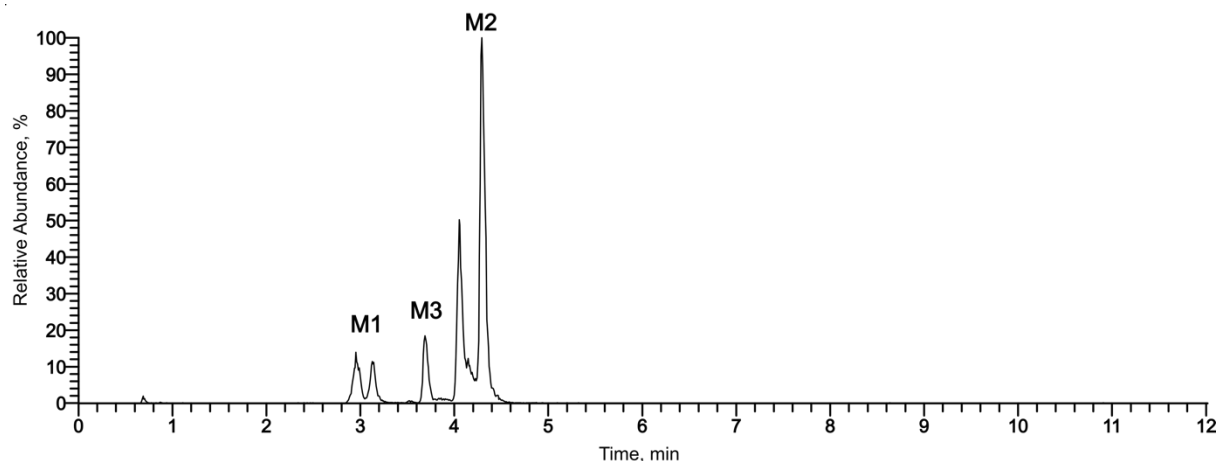

Figure S9. Reconstructed ion chromatogram of *m/z* 288.1958 after analysis of one QC sample of pooled human liver microsome in full scan in positive ionization mode using hydrophilic interaction chromatography (HILIC). Metabolite identification number (M) match with the metabolites listed in Table S5.

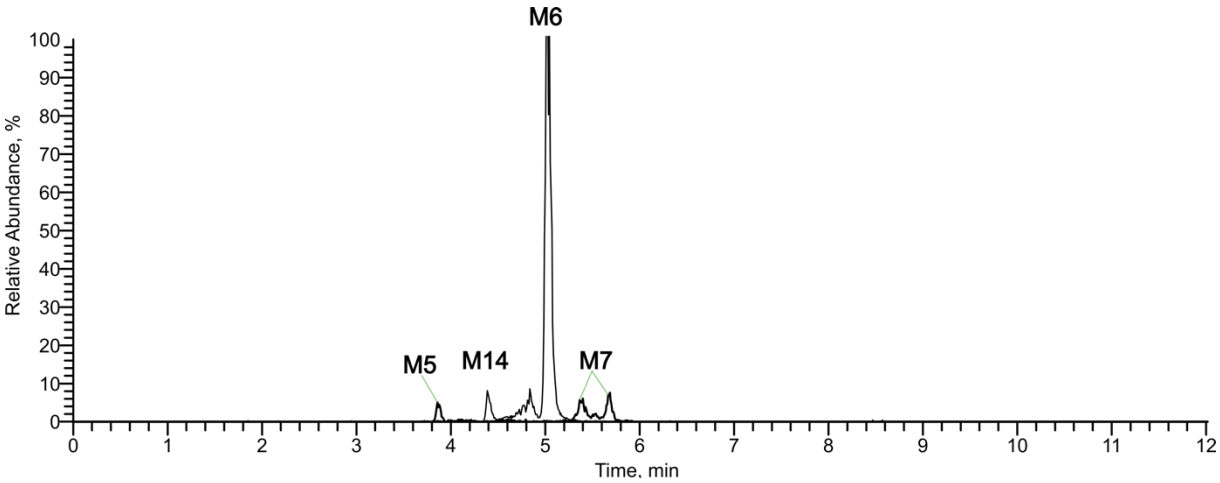

Figure S10. Reconstructed ion chromatograms of *m/z* 304.1856, *m/z* 320.1856, and *m/z* 336.1805 after analysis of one QC sample of rat urine in full scan in positive ionization mode using hydrophilic interaction chromatography (HILIC). Metabolite identification numbers (M) match with the metabolites listed in Table S5.

4. Discussion

In an untargeted toxicometabolomics workflow, each step poses various key challenges that require individual optimization for both analytical setup and biological question. Therefore, the initial three studies focused on optimizing the workflow for untargeted toxicometabolomics studies by means of LC-HRMS. Optimization was performed for critical steps such as sample preparation, data acquisition, and data analysis.

With effects for metabolite extraction and subsequent detection, sample preparation is a critical step in achieving comprehensive analyte coverage in metabolomics.[12,95] As key biological matrix in metabolomics studies, urine has several advantages such as non-invasive sample collection, comparatively low sample complexity, and reflection of both endogenous and exogenous metabolic profile among others.[96,97] However, urine exhibits a variety of metabolite concentrations and is susceptible to variable and unpredictable dilution.[97] As such, and due to the high chemical diversity of metabolites, appropriate sample preparation is required. Thus, the first study systematically examined the impact of various extraction solvents in combination with different reconstitution solvents on the analytical data of untargeted LC-HRMS toxicometabolomics analysis of urine samples from rat and human. Results were evaluated based on the total feature count, feature detectability, and reproducibility of selected compounds. The findings revealed that reconstitution solvents had a more significant effect on the recovery of the compounds compared to extraction solvents. This is in line with the results of the study by Manier and Meyer, who investigated the effect of reconstitution solvents on evaporated human plasma samples and found also a major impact of solvent composition on analyte recovery.[98] Furthermore, the choice of chromatographic system plays a crucial role for the different extraction and reconstitution solvents. Additionally, increasing the amount of extraction solvent enhanced the extraction of rat urine. In contrast, a lower amount of extraction solvent was required for human urine. This may be due to the higher protein concentration in rat urine, which requires a large amount of solvent for protein precipitation.[99] The results of the study demonstrate the importance of adapting sample preparation protocols to the specific biomatrix, and species investigated, as well as the chromatographic system employed.

One of the major challenges in the development of analytical methods for untargeted toxicometabolomics is the analysis of the diverse physicochemical properties of the analytes, which are often unknown. This includes detecting both endogenous and exogenous biomarkers, such as new drug metabolites. To cover a wide range, a universal separating and detecting system is required. Both reversed-phase (RP) and normal-phase or hydrophilic interaction

chromatography (HILIC) are used in untargeted approaches.[1] In addition to the baseline separation of all molecules, the resolution of even small differences in structure and molecular mass plays a crucial role in the precise annotation, identification, and interpretation of data.[18] Several studies have examined the impact of various columns on targeted metabolomics studies or selected metabolite libraries.[100-102] However, few studies have compared columns in untargeted metabolomics studies. Most of these studies have only compared columns using a single type of separation method or a single matrix.[103,104] Therefore, in the second study the influence of three different RP, two HILIC, and one porous graphitic carbon column were investigated by comparing the chromatographic resolution of selected compounds and the outcome of an untargeted toxicometabolomics study using pHLM, rat plasma, and rat urine as matrices. The results of this study emphasized that the outcome of an untargeted toxicometabolomics study might be highly influenced by the analytical column, which is in line with findings from current literature.[17,19,105,106] Despite nearly identical stationary phases chemistries, there were identifiable distinctions among columns. Criscuolo et al. demonstrated that it is necessary to consider not only the chemistry of the stationary phase, but also the different types of particles or their size, among other factors.[107] Variations were observed not only between different matrices but also in terms of substance detectability. For instance, using a Phenyl-Hexyl column may retain mainly non-polar metabolites with an aromatic hydrocarbon structure, and may less retain e.g. fatty acids. However, the study has some limitations, such as a limited selection of columns or the selection of endogenous compounds. It is important to keep these limitations in mind. Nonetheless, the study demonstrates that the selection of the column, and thus the analytical method, must be tested in advance for an untargeted toxicometabolomics study and adapted to each matrix and set of investigated substances to achieve the best possible results.

After data generation, extensive data processing is required to interpret metabolomics results accurately, evaluate sample classification and/or discrimination, and discover biomarkers from the intricate and information-rich raw data files. Several software options are available for this purpose, but they can differ regarding their algorithm and thus influence the outcome of a study.[27] In the third study, a dataset of pHLM incubation of the synthetic cannabinoid A-CHMINACA was used to evaluate the data processing of three different software workflows.[91] These three workflows included the commercial software Compound Discoverer 3.1, as well as two open-source solution: XCMS Online combined with MetaboAnalyst 4.0 and a manually programmed tool using R. Additionally, the metabolic fate of A-CHMINACA in pHLM was investigated. Results indicate that commercial software, like Compound Discoverer, are user-

friendly black boxes with limitations in preprocessing parameters, normalization techniques, and statistical analysis. Open-source software, on the other hand, offer more transparency in methodology but require the customization of parameters and advanced programming skills. Online tools, like XCMS Online, require less programming knowledge, but often have limited parameter specifications. Fernández-Ochoa et al. compared the commercially Agilent Profinder software with an open-source R pipeline and drew a similar conclusion.[108] The study also found out that the vendor-based software is easy to use and produces better quality graphics. However, the open-source methods are more effective in correcting drift between and within batches. Additionally, the statistical methods used in the open-source pipeline achieved better classification results, indicating higher data quality. Therefore, their conclusion was that the open-source method is often more suitable for a large number of samples due to its higher capacity and versatility.[108] Nevertheless, for complex biological questions, manually programmed tools are typically superior, as they provide numerous packages and adaptability, including normalization to an endogenous marker. Nonetheless, comparing various software tools is challenging as it is highly depending on the selected parameters.[85] Concerning the in vitro metabolism of A-CHMINACA, the primary metabolic reactions involved hydroxylation of the adamantyl-ring and *N*-dealkylation of the indazole-3-carbaldehyde moiety. Although all three workflows identified the most important metabolites, the simplicity and low complexity of the dataset did not require any normalization compared to complex plasma or urine samples. The last two studies investigated the influence of DOAs in vitro and in vivo using untargeted toxicometabolomics. The purpose of the studies was to gain insights into the endogenous response in the rat metabolome after acute exposure, as well as information on the metabolic profile in vitro and in vivo, thus allowing the establishment of suitable biomarkers to verify the intake of the respective DOA.

The fourth study offered new insights into the metabolic profiling of rat plasma and urine in response to acute amphetamine exposure and additional urinary metabolites/biomarkers to detect amphetamine uptake, complemented previous studies.[93] Compared to a prior study conducted with humans, which mainly observed various metabolites related to energy metabolism, the findings from rats indicated a decrease in amino acids following exposure to amphetamine.[109] Furthermore, four new potential biomarkers were identified in rat urine: *N*-acetylamphetamine, *N*-acetyl-4-hydroxyamphetamine, *N*-acetyl-4-hydroxyamphetamine glucuronide, and amphetamine succinate. While this study is only a snapshot of the rat metabolome and cannot be directly extrapolated to humans, it is another piece of the puzzle to better understand acute and chronic effects and to support future targeted studies in humans that

require fewer subjects. The varied results of the two studies highlight the importance of comprehensive investigations and different analytical approaches when researching differences in metabolomics. A good example of the benefits of untargeted toxicometabolomics studies is amphetamine succinate. Studies like this one can detect metabolites that would not be expected or sought in a targeted approach.

The fifth study provides the metabolic profile in an in vitro model using pHLM incubation while the in vivo experiments provide insights into the endogenous response of rat plasma and urine to acute exposure of the synthetic cathinone PCYP.[94] A total of sixteen phase I metabolites, of which nine were found in vivo, and one phase II metabolite of PCYP were identified as exogenous biomarkers. The main metabolic reaction in rat urine was the dihydroxylation at the pyrrolidine ring, followed by mono- and/or dihydroxylation at the benzyl and/or hexyl rings. These metabolites offer the possibility of establishing analytical screening procedures to overcome the analytical challenge in clinical and forensic toxicology and to confirm patient intake. Furthermore, metabolites of tryptophan metabolism and adenosine were also found related to PCYP intake. Suggesting that synthetic cathinones such as PCYP may directly affect neurotransmission and thereby influence important metabolic pathways such as tryptophan metabolism. These findings provide additional markers of cathinone abuse, improve our understanding of the associated physiological changes, and thus demonstrate the advantages of an untargeted toxicometabolomics study. Specifically, it permits exploration of both biomarkers and mode of action in a single study, which proves particularly advantageous for highly fluctuating substances such as NPS, for which both toxicokinetic and toxicodynamic data are lacking. Nevertheless, it is important to note that this study provides only a snapshot of the rat metabolome. Further studies using targeted toxicometabolomics approaches are needed to investigate the changes in tryptophan metabolism after PCYP ingestion and its applicability to humans.

5. Conclusion

Based on the results of the different studies, it can be concluded that there are different influences in an untargeted toxicometabolomics approach, which affect the outcome of a study in varying degrees. Starting with the sample preparation, which is an essential and important step for the extraction and detection of various metabolite. The analytical method used, where in an LC-MS approach especially the analytical column used has a strong influence and therefore needs to be adapted for each matrix and regarding toxicometabolomics, also for the substance to be investigated. Finally, data processing also plays an important role in the correct extraction of information. Although raw files may be identical, not all data processing software is appropriate for every biological question. Studies have shown there is no standardized procedure for untargeted toxicometabolomics. Therefore, instead of simply applying a standard procedure, researchers should optimize corresponding procedures and parameters beforehand to the study question to achieve the best results possible. Even with ideal parameter optimization, a single metabolomics study remains only a snapshot that captures only a single moment in time.

In addition to the optimization strategies of an untargeted toxicometabolomics approach, the two untargeted toxicometabolomics studies have shown how the use of toxicometabolomics workflows overcome conventional screening methods to identify metabolites and endogenous biomarkers that would not be expected. It allows for acquisition of both toxicokinetic data and information on the mode of action of DOA within one study. Even for classical DOAs such as amphetamine, which seem to be well studied toxicologically, metabolomics is expected to reveal new insights or hidden modes of actions. Nevertheless, untargeted toxicometabolomics can be a time-consuming process yielding only individual metabolites that can be assessed only in terms of their physiological function rather than within a biological context. Furthermore, a single toxicometabolomics study is merely a snapshot, capturing only a moment in time, and therefore further studies are usually required to support or refute the biological interpretation. Nonetheless, these metabolites are useful for initiating further targeted studies and even conducting human studies.

Another advantage of untargeted toxicometabolomics is the reduced number of animals required for in vivo experiments. For an in vivo study, a small number of animals per group is necessary to achieve significant results owing to their genetic identity, uniform sleep/wake rhythm, and consistent diet. The utilization of even a small dose to observe an effect on the metabolome helps to minimize pain and suffering experienced by the test animals.

Nevertheless, it is essential to emphasize that the complete organism is mandatory to verify useful endogenous biomarkers in the context of toxicometabolomics. Furthermore, a preliminary study is conducted, which is followed by a specific study to interpret the biomarkers biologically. Despite using fewer animals, the targeted study still necessitates additional laboratory animals. Subsequently, extrapolation to humans must be examined to apply the findings to the human population.

6. References

1 Barnes, S. *et al.* Training in metabolomics research. I. Designing the experiment, collecting and extracting samples and generating metabolomics data. *J Mass Spectrom* **51**, 461-475, doi:10.1002/jms.3782 (2016).

2 Liu, X. & Locasale, J. W. Metabolomics: A Primer. *Trends Biochem Sci* **42**, 274-284, doi:10.1016/j.tibs.2017.01.004 (2017).

3 Bouhifd, M., Hartung, T., Hogberg, H. T., Kleensang, A. & Zhao, L. Review: toxicometabolomics. *J Appl Toxicol* **33**, 1365-1383, doi:10.1002/jat.2874 (2013).

4 Oliver, S. G., Winson, M. K., Kell, D. B. & Baganz, F. Systematic functional analysis of the yeast genome. *Trends Biotechnol* **16**, 373-378, doi:10.1016/s0167-7799(98)01214-1 (1998).

5 Araujo, A. M., Carvalho, F., Guedes de Pinho, P. & Carvalho, M. Toxicometabolomics: Small Molecules to Answer Big Toxicological Questions. *Metabolites* **11**, doi:10.3390/metabo11100692 (2021).

6 German, J. B., Hammock, B. D. & Watkins, S. M. Metabolomics: building on a century of biochemistry to guide human health. *Metabolomics* **1**, 3-9, doi:10.1007/s11306-005-1102-8 (2005).

7 Castillo-Peinado, L. S. & Luque de Castro, M. D. Present and foreseeable future of metabolomics in forensic analysis. *Anal Chim Acta* **925**, 1-15, doi:10.1016/j.aca.2016.04.040 (2016).

8 Agin, A. *et al.* Metabolomics – an overview. From basic principles to potential biomarkers (part 1). *Médecine Nucléaire* **40**, 4-10, doi:10.1016/j.mednuc.2015.12.006 (2016).

9 Gertsman, I. & Barshop, B. A. Promises and pitfalls of untargeted metabolomics. *J Inherit Metab Dis* **41**, 355-366, doi:10.1007/s10545-017-0130-7 (2018).

10 Schrimpe-Rutledge, A. C., Codreanu, S. G., Sherrod, S. D. & McLean, J. A. Untargeted Metabolomics Strategies-Challenges and Emerging Directions. *J Am Soc Mass Spectrom* **27**, 1897-1905, doi:10.1007/s13361-016-1469-y (2016).

11 Álvarez-Sánchez, B., Priego-Capote, F. & Luque de Castro, M. D. Metabolomics analysis I. Selection of biological samples and practical aspects preceding sample preparation. *TrAC Trends in Analytical Chemistry* **29**, 111-119, doi:10.1016/j.trac.2009.12.003 (2010).

12 Ivanisevic, J. & Want, E. J. From Samples to Insights into Metabolism: Uncovering Biologically Relevant Information in LC-HRMS Metabolomics Data. *Metabolites* **9** (2019).

13 Bi, H. *et al.* The key points in the pre-analytical procedures of blood and urine samples in metabolomics studies. *Metabolomics* **16**, 68, doi:10.1007/s11306-020-01666-2 (2020).

14 Garwolińska, D., Kot-Wasik, A. & Hewelt-Belka, W. Pre-analytical aspects in metabolomics of human biofluids – sample collection, handling, transport, and storage. *Molecular Omics* **19**, 95-104, doi:10.1039/D2MO00212D (2023).

15 González-Domínguez, R., González-Domínguez, Á., Sayago, A. & Fernández-Recamales, Á. Recommendations and Best Practices for Standardizing the Pre-Analytical Processing of Blood and Urine Samples in Metabolomics. *Metabolites* **10** (2020).

16 Stevens, V. L., Hoover, E., Wang, Y. & Zanetti, K. A. Pre-Analytical Factors that Affect Metabolite Stability in Human Urine, Plasma, and Serum: A Review. *Metabolites* **9** (2019).

17 Zeki, Ö. C., Eylem, C. C., Reçber, T., Kır, S. & Nemutlu, E. Integration of GC–MS and LC–MS for untargeted metabolomics profiling. *Journal of Pharmaceutical and Biomedical Analysis* **190**, 113509, doi:10.1016/j.jpba.2020.113509 (2020).

18 Harrieder, E. M., Kretschmer, F., Bocker, S. & Witting, M. Current state-of-the-art of separation methods used in LC-MS based metabolomics and lipidomics. *J Chromatogr B Analyt Technol Biomed Life Sci* **1188**, 123069, doi:10.1016/j.jchromb.2021.123069 (2022).

19 Patti, G. J. Separation strategies for untargeted metabolomics. *J Sep Sci* **34**, 3460-3469, doi:10.1002/jssc.201100532 (2011).

20 Gika, H., Virgiliou, C., Theodoridis, G., Plumb, R. S. & Wilson, I. D. Untargeted LC/MS-based metabolic phenotyping (metabonomics/metabolomics): The state of the art. *J Chromatogr B Analyt Technol Biomed Life Sci* **1117**, 136-147, doi:10.1016/j.jchromb.2019.04.009 (2019).

21 Barnes, S. *et al.* Training in metabolomics research. II. Processing and statistical analysis of metabolomics data, metabolite identification, pathway analysis, applications of metabolomics and its future. *J Mass Spectrom* **51**, 535-548, doi:10.1002/jms.3780 (2016).

22 Tautenhahn, R., Patti, G. J., Rinehart, D. & Siuzdak, G. XCMS Online: A Web-Based Platform to Process Untargeted Metabolomic Data. *Analytical Chemistry* **84**, 5035-5039, doi:10.1021/ac300698c (2012).

23 Gowda, H. *et al.* Interactive XCMS Online: Simplifying Advanced Metabolomic Data Processing and Subsequent Statistical Analyses. *Analytical Chemistry* **86**, 6931-6939, doi:10.1021/ac500734c (2014).

24 Chong, J., Wishart, D. S. & Xia, J. Using MetaboAnalyst 4.0 for Comprehensive and Integrative Metabolomics Data Analysis. *Current Protocols in Bioinformatics* **68**, e86, doi:doi.org/10.1002/cpbi.86 (2019).

25 Pluskal, T., Castillo, S., Villar-Briones, A. & Orešič, M. MZmine 2: Modular framework for processing, visualizing, and analyzing mass spectrometry-based molecular profile data. *BMC Bioinformatics* **11**, 395, doi:10.1186/1471-2105-11-395 (2010).

26 Röst, H. L. *et al.* OpenMS: a flexible open-source software platform for mass spectrometry data analysis. *Nature Methods* **13**, 741-748, doi:10.1038/nmeth.3959 (2016).

27 Rafiei, A. & Sleno, L. Comparison of peak-picking workflows for untargeted liquid chromatography/high-resolution mass spectrometry metabolomics data analysis. *Rapid Communications in Mass Spectrometry* **29**, 119-127, doi:10.1002/rcm.7094 (2015).

28 Anwardeen, N. R., Diboun, I., Mokrab, Y., Althani, A. A. & Elrayess, M. A. Statistical methods and resources for biomarker discovery using metabolomics. *BMC Bioinformatics* **24**, 250, doi:10.1186/s12859-023-05383-0 (2023).

29 Johnson, C. H., Ivanisevic, J. & Siuzdak, G. Metabolomics: beyond biomarkers and towards mechanisms. *Nat Rev Mol Cell Biol* **17**, 451-459, doi:10.1038/nrm.2016.25 (2016).

30 Crocq, M. A. Historical and cultural aspects of man's relationship with addictive drugs. *Dialogues Clin Neurosci* **9**, 355-361, doi:10.31887/DCNS.2007.9.4/macrocq (2007).

31 Vetulani, J. Drug addiction. Part I. Psychoactive substances in the past and presence. *Pol J Pharmacol* **53**, 201-214 (2001).

32 Jones, A. W. Early drug discovery and the rise of pharmaceutical chemistry. *Drug Test Anal* **3**, 337-344, doi:10.1002/dta.301 (2011).

33 Brook, K., Bennett, J. & Desai, S. P. The Chemical History of Morphine: An 8000-year Journey, from Resin to de-novo Synthesis. *J Anesth Hist* **3**, 50-55, doi:10.1016/j.janh.2017.02.001 (2017).

34 Calatayud, J. & González, Á. History of the Development and Evolution of Local Anesthesia Since the Coca Leaf. *Anesthesiology* **98**, 1503-1508, doi:10.1097/00000542-200306000-00031 (2003).

35 Rishton, G. M. Natural products as a robust source of new drugs and drug leads: past successes and present day issues. *Am J Cardiol* **101**, 43D-49D, doi:10.1016/j.amjcard.2008.02.007 (2008).

36 Cunha-Oliveira, T., Rego, A. C., Carvalho, F. & Oliveira, C. R. in *Principles of Addiction* (ed Peter M. Miller) 159-175 (Academic Press, 2013).

37 Sneader, W. The discovery of heroin. *The Lancet* **352**, 1697-1699, doi:10.1016/S0140-6736(98)07115-3 (1998).

38 Böllinger, L. Drug Law and Policy in Germany and the European Community: Recent Developments. *Journal of Drug Issues* **34**, 491-510, doi:10.1177/002204260403400302 (2004).

39 Borden, S. A. *et al.* Mass Spectrometry Analysis of Drugs of Abuse: Challenges and Emerging Strategies. *Mass Spectrom Rev* **39**, 703-744, doi:10.1002/mas.21624 (2020).

40 Peters, F. T. & Martinez-Ramirez, J. A. Analytical toxicology of emerging drugs of abuse. *Ther Drug Monit* **32**, 532-539, doi:10.1097/FTD.0b013e3181f33411 (2010).

41 UNODC. The Challenge of New Psychoactive Substances: A Report from the Global SMART Programme, 2013. (2013). <https://www.unodc.org/documents/scientific/NPS_Report.pdf>.

42 UNODC. World Drug Report 2023 - Booklet 1. (2023). <https://www.unodc.org/res/WDR-2023/WDR23_Exsum_fin_SP.pdf>.

43 Shafi, A., Berry, A. J., Sumnall, H., Wood, D. M. & Tracy, D. K. New psychoactive substances: a review and updates. *Ther Adv Psychopharmacol* **10**, 2045125320967197, doi:10.1177/2045125320967197 (2020).

44 Smith, J. P., Sutcliffe, O. B. & Banks, C. E. An overview of recent developments in the analytical detection of new psychoactive substances (NPSs). *Analyst* **140**, 4932-4948, doi:10.1039/c5an00797f (2015).

45 UNODC. World Drug Report 2022 - Booklet 4. (2022). <https://www.unodc.org/res/wdr2022/MS/WDR22_Booklet_4.pdf>.

46 EMCDDA. European Drug Report 2023: Trends and Developments *Publications of the European Union* (2023). <https://www.emcdda.europa.eu/publications/european-drug-report/2023_en>.

47 Nelson, M. E., Bryant, S. M. & Aks, S. E. Emerging drugs of abuse. *Dis Mon* **60**, 110-132, doi:10.1016/j.disamonth.2014.01.001 (2014).

48 Cannaert, A. *et al.* Synthesis and in Vitro Cannabinoid Receptor 1 Activity of Recently Detected Synthetic Cannabinoids 4F-MDMB-BICA, 5F-MPP-PICA, MMB-4en-PICA, CUMYL-CBMICA, ADB-BINACA, APP-BINACA, 4F-MDMB-BINACA, MDMB-4en-PINACA, A-CHMINACA, 5F-AB-P7AICA, 5F-MDMB-P7AICA, and 5F-AP7AICA. *ACS Chemical Neuroscience* **11**, 4434-4446, doi:10.1021/acschemneuro.0c00644 (2020).

49 Banister, S. D. *et al.* The chemistry and pharmacology of putative synthetic cannabinoid receptor agonist (SCRA) new psychoactive substances (NPS) 5F-PY-PICA, 5F-PY-PINACA, and their analogs. *Drug Testing and Analysis* **11**, 976-989, doi:10.1002/dta.2583 (2019).

50 Castaneto, M. S. *et al.* Synthetic cannabinoids: Epidemiology, pharmacodynamics, and clinical implications. *Drug and Alcohol Dependence* **144**, 12-41, doi:10.1016/j.drugalcdep.2014.08.005 (2014).

51 Pertwee, G. R. Receptors and Channels Targeted by Synthetic Cannabinoid Receptor Agonists and Antagonists. *Current Medicinal Chemistry* **17**, 1360-1381, doi:10.2174/092986710790980050 (2010).

52 Ciucă Anghel, D.-M., Nițescu, G. V., Tiron, A.-T., Guțu, C. M. & Baconi, D. L. Understanding the Mechanisms of Action and Effects of Drugs of Abuse. *Molecules* **28** (2023).

53 EMCDDA. European Drug Report 2018. *Publications of the European Union* (2018). <http://www.emcdda.europa.eu/system/files/publications/8585/20181816_TDAT18001ENN_PDF.pdf>.

54 Soares, J., Costa, V. M., Bastos, M. d. L., Carvalho, F. & Capela, J. P. An updated review on synthetic cathinones. *Archives of Toxicology* **95**, 2895-2940, doi:10.1007/s00204-021-03083-3 (2021).

55 Kuropka, P., Zawadzki, M. & Szpot, P. A review of synthetic cathinones emerging in recent years (2019–2022). *Forensic Toxicology* **41**, 25-46, doi:10.1007/s11419-022-00639-5 (2023).

56 Ellefsen, K. N., Concheiro, M. & Huestis, M. A. Synthetic cathinone pharmacokinetics, analytical methods, and toxicological findings from human performance and postmortem cases. *Drug Metabolism Reviews* **48**, 237-265, doi:10.1080/03602532.2016.1188937 (2016).

57 Baumann, M. H. *et al.* Powerful cocaine-like actions of 3,4-methylenedioxypyrovalerone (MDPV), a principal constituent of psychoactive 'bath salts' products. *Neuropsychopharmacology* **38**, 552-562, doi:10.1038/npp.2012.204 (2013).

58 Eshleman, A. J. *et al.* Substituted methcathinones differ in transporter and receptor interactions. *Biochem Pharmacol* **85**, 1803-1815, doi:10.1016/j.bcp.2013.04.004 (2013).

59 Iversen, L. *et al.* Neurochemical profiles of some novel psychoactive substances. *European Journal of Pharmacology* **700**, 147-151, doi:10.1016/j.ejphar.2012.12.006 (2013).

60 Lopez-Arnau, R., Martinez-Clemente, J., Pubill, D., Escubedo, E. & Camarasa, J. Comparative neuropharmacology of three psychostimulant cathinone derivatives: butylone, mephedrone and methylone. *Br J Pharmacol* **167**, 407-420, doi:10.1111/j.1476-5381.2012.01998.x (2012).

61 Saha, K. *et al.* 'Second-generation' mephedrone analogs, 4-MEC and 4-MePPP, differentially affect monoamine transporter function. *Neuropsychopharmacology* **40**, 1321-1331, doi:10.1038/npp.2014.325 (2015).

62 Simmler, L. D. *et al.* Pharmacological characterization of designer cathinones in vitro. *British Journal of Pharmacology* **168**, 458-470, doi:10.1111/j.1476-5381.2012.02145.x (2013).

63 Simmler, L. D., Rickli, A., Hoener, M. C. & Liechti, M. E. Monoamine transporter and receptor interaction profiles of a new series of designer cathinones. *Neuropharmacology* **79**, 152-160, doi:10.1016/j.neuropharm.2013.11.008 (2014).

64 Eshleman, A. J. *et al.* Structure-activity relationships of bath salt components: substituted cathinones and benzofurans at biogenic amine transporters. *Psychopharmacology* **236**, 939-952, doi:10.1007/s00213-018-5059-5 (2019).

65 Liechti, M. Novel psychoactive substances (designer drugs): overview and pharmacology of modulators of monoamine signalling. *Swiss Medical Weekly* **144**, w14043, doi:10.4414/smw.2015.14043 (2015).

66 Zawilska, J. B. & Wojcieszak, J. Designer cathinones—An emerging class of novel recreational drugs. *Forensic Science International* **231**, 42-53, doi:10.1016/j.forsciint.2013.04.015 (2013).

67 Meyer, M. R. New psychoactive substances: an overview on recent publications on their toxicodynamics and toxicokinetics. *Arch Toxicol* **90**, 2421-2444, doi:10.1007/s00204-016-1812-x (2016).

68 Wagmann, L., Jacobs, C. M. & Meyer, M. R. New Psychoactive Substances: Which Biological Matrix Is the Best for Clinical Toxicology Screening? *Ther Drug Monit* **44**, 599-605, doi:10.1097/FTD.0000000000000974 (2022).

69 Langman, L. J. & Kapur, B. M. Toxicology: Then and now. *Clinical Biochemistry* **39**, 498-510, doi:10.1016/j.clinbiochem.2006.03.004 (2006).

70 Pappas, A. A., Massoll, N. A. & Cannon, D. J. Toxicology: past, present, and future. *Ann Clin Lab Sci* **29**, 253-262 (1999).

71 Duffus, J. H., Nordberg, M. & Templeton, D. M. Glossary of terms used in toxicology, 2nd edition (IUPAC Recommendations 2007). **79**, 1153-1344, doi:10.1351/pac200779071153 (2007).

72 Maurer, H. H. Demands on scientific studies in clinical toxicology. *Forensic Sci Int* **165**, 194-198, doi:10.1016/j.forsciint.2006.05.019 (2007).

73 Brandt, S. D., King, L. A. & Evans-Brown, M. The new drug phenomenon. *Drug Test Anal* **6**, 587-597, doi:10.1002/dta.1686 (2014).

74 Peters, F. T. Recent developments in urinalysis of metabolites of new psychoactive substances using LC-MS. *Bioanalysis* **6**, 2083-2107, doi:10.4155/bio.14.168 (2014).

75 Meyer, M. R. & Peters, F. T. Analytical toxicology of emerging drugs of abuse--an update. *Ther Drug Monit* **34**, 615-621, doi:10.1097/FTD.0b013e31826d0915 (2012).

76 Wagmann, L. *et al.* How to Study the Metabolism of New Psychoactive Substances for the Purpose of Toxicological Screenings—A Follow-Up Study Comparing Pooled Human Liver S9, HepaRG Cells, and Zebrafish Larvae. *Frontiers in Chemistry* **8** (2020).

77 Richter, L. H. J., Flockerzi, V., Maurer, H. H. & Meyer, M. R. Pooled human liver preparations, HepaRG, or HepG2 cell lines for metabolism studies of new psychoactive substances? A study using MDMA, MDBD, butylone, MDPPP, MDPV, MDPB, 5-MAPB, and 5-API as examples. *Journal of Pharmaceutical and Biomedical Analysis* **143**, 32-42, doi:10.1016/j.jpba.2017.05.028 (2017).

78 Manier, S. K., Richter, L. H. J., Schäper, J., Maurer, H. H. & Meyer, M. R. Different in vitro and in vivo tools for elucidating the human metabolism of alpha-cathinone-derived drugs of abuse. *Drug Testing and Analysis* **10**, 1119-1130, doi:10.1002/dta.2355 (2018).

79 Gampfer, T. M., Wagmann, L., Belkacemi, A., Flockerzi, V. & Meyer, M. R. Cytotoxicity, metabolism, and isozyme mapping of the synthetic cannabinoids JWH-200, A-796260, and 5F-EMB-PINACA studied by means of in vitro systems. *Archives of Toxicology* **95**, 3539-3557, doi:10.1007/s00204-021-03148-3 (2021).

80 Gampfer, T. M. *et al.* A simplified strategy to assess the cytotoxicity of new psychoactive substances in HepG2 cells using a high content screening assay – Exemplified for nine compounds. *Toxicology* **476**, 153258, doi:10.1016/j.tox.2022.153258 (2022).

81 Wagmann, L., Maurer, H. H. & Meyer, M. R. Inhibition and stimulation of the human breast cancer resistance protein as in vitro predictor of drug–drug interactions of drugs

of abuse. *Archives of Toxicology* **92**, 2875-2884, doi:10.1007/s00204-018-2276-y (2018).

82 Fan, E. *et al.* Acute exposure to N-Ethylpentylone induces developmental toxicity and dopaminergic receptor-regulated aberrances in zebrafish larvae. *Toxicology and Applied Pharmacology* **417**, 115477, doi:10.1016/j.taap.2021.115477 (2021).

83 Matsunaga, T. *et al.* Structure-activity relationship for toxicity of α-pyrrolidinophenones in human aortic endothelial cells. *Forensic Toxicology* **35**, 309-316, doi:10.1007/s11419-017-0359-8 (2017).

84 Szeremeta, M., Pietrowska, K., Niemcunowicz-Janica, A., Kretowski, A. & Ciborowski, M. Applications of Metabolomics in Forensic Toxicology and Forensic Medicine. *Int J Mol Sci* **22**, doi:10.3390/ijms22063010 (2021).

85 Steuer, A., Brockbals, L. & Kraemer, T. Untargeted metabolomics approaches to improve casework in clinical and forensic toxicology—"Where are we standing and where are we heading?". *Wiley Interdisciplinary Reviews: Forensic Science* **4**, doi:10.1002/wfs2.1449 (2021).

86 Steuer, A. E., Brockbals, L. & Kraemer, T. Metabolomic Strategies in Biomarker Research-New Approach for Indirect Identification of Drug Consumption and Sample Manipulation in Clinical and Forensic Toxicology? *Front Chem* **7**, 319, doi:10.3389/fchem.2019.00319 (2019).

87 Zaitsu, K., Hayashi, Y., Kusano, M., Tsuchihashi, H. & Ishii, A. Application of metabolomics to toxicology of drugs of abuse: A mini review of metabolomics approach to acute and chronic toxicity studies. *Drug Metabolism and Pharmacokinetics* **31**, 21-26, doi:10.1016/j.dmpk.2015.10.002 (2016).

88 Manier, S. K. & Meyer, M. R. Current Situation of the Metabolomics Techniques Used for the Metabolism Studies of New Psychoactive Substances. *Therapeutic Drug Monitoring* **42** (2020).

89 Dinis-Oliveira, R. J. Metabolomics of drugs of abuse: a more realistic view of the toxicological complexity. *Bioanalysis* **6**, 3155-3159, doi:10.4155/bio.14.260 (2014).

90 Van Norman, G. A. Limitations of Animal Studies for Predicting Toxicity in Clinical Trials: Is it Time to Rethink Our Current Approach? *JACC: Basic to Translational Science* **4**, 845-854, doi:10.1016/j.jacbts.2019.10.008 (2019).

91 Hemmer, S. *et al.* Comparison of Three Untargeted Data Processing Workflows for Evaluating LC-HRMS Metabolomics Data. *Metabolites* **10**, doi:10.3390/metabo10090378 (2020).

92 Hemmer, S. *et al.* Addendum: Hemmer, S., et al. Comparison of Three Untargeted Data Processing Workflows for Evaluating LC-HRMS Metabolomics Data. Metabolites 2020, 10, 378. *Metabolites* **10** (2020).

93 Hemmer, S., Wagmann, L. & Meyer, M. R. Altered metabolic pathways elucidated via untargeted in vivo toxicometabolomics in rat urine and plasma samples collected after controlled application of a human equivalent amphetamine dose. *Arch Toxicol* **95**, 3223-3234, doi:10.1007/s00204-021-03135-8 (2021).

94 Hemmer, S., Wagmann, L., Pulver, B., Westphal, F. & Meyer, M. R. In Vitro and In Vivo Toxicometabolomics of the Synthetic Cathinone PCYP Studied by Means of LC-HRMS/MS. *Metabolites* **12**, doi:10.3390/metabo12121209 (2022).

95 Gong, Z.-G., Hu, J., Wu, X. & Xu, Y.-J. The Recent Developments in Sample Preparation for Mass Spectrometry-Based Metabolomics. *Critical Reviews in Analytical Chemistry* **47**, 325-331, doi:10.1080/10408347.2017.1289836 (2017).

96 Ryan, D., Robards, K., Prenzler, P. D. & Kendall, M. Recent and potential developments in the analysis of urine: A review. *Analytica Chimica Acta* **684**, 17-29, doi:10.1016/j.aca.2010.10.035 (2011).

97 Want, E. J. *et al.* Global metabolic profiling procedures for urine using UPLC–MS. *Nature Protocols* **5**, 1005-1018, doi:10.1038/nprot.2010.50 (2010).

98 Manier, S. K. & Meyer, M. R. Impact of the used solvent on the reconstitution efficiency of evaporated biosamples for untargeted metabolomics studies. *Metabolomics* **16**, 34, doi:10.1007/s11306-019-1631-1 (2020).

99 Olson, M. J., Johnson, J. T. & Reidy, C. A. A comparison of male rat and human urinary proteins: implications for human resistance to hyaline droplet nephropathy. *Toxicol Appl Pharmacol* **102**, 524-536, doi:10.1016/0041-008x(90)90047-x (1990).

100 Diamantidou, D., Sampsonidis, I., Liapikos, T., Gika, H. & Theodoridis, G. Liquid chromatography-mass spectrometry metabolite library for metabolomics: Evaluating column suitability using a scoring approach. *J Chromatogr A* **1690**, 463779, doi:10.1016/j.chroma.2023.463779 (2023).

101 Elmsjo, A. *et al.* Method selectivity evaluation using the co-feature ratio in LC/MS metabolomics: Comparison of HILIC stationary phase performance for the analysis of plasma, urine and cell extracts. *J Chromatogr A* **1568**, 49-56, doi:10.1016/j.chroma.2018.05.007 (2018).

102 Wernisch, S. & Pennathur, S. Evaluation of coverage, retention patterns, and selectivity of seven liquid chromatographic methods for metabolomics. *Anal Bioanal Chem* **408**, 6079-6091, doi:10.1007/s00216-016-9716-4 (2016).

103 Sonnenberg, R. A., Naz, S., Cougnaud, L. & Vuckovic, D. Comparison of underivatized silica and zwitterionic sulfobetaine hydrophilic interaction liquid chromatography stationary phases for global metabolomics of human plasma. *J Chromatogr A* **1608**, 460419, doi:10.1016/j.chroma.2019.460419 (2019).

104 Si-Hung, L., Causon, T. J. & Hann, S. Comparison of fully wettable RPLC stationary phases for LC-MS-based cellular metabolomics. *Electrophoresis* **38**, 2287-2295, doi:10.1002/elps.201700157 (2017).

105 Moreno-Torres, M. *et al.* Factors that influence the quality of metabolomics data in in vitro cell toxicity studies: a systematic survey. *Scientific Reports* **11**, 22119, doi:10.1038/s41598-021-01652-1 (2021).

106 Alseekh, S. *et al.* Mass spectrometry-based metabolomics: a guide for annotation, quantification and best reporting practices. *Nature Methods* **18**, 747-756, doi:10.1038/s41592-021-01197-1 (2021).

107 Criscuolo, A., Zeller, M., Cook, K., Angelidou, G. & Fedorova, M. Rational selection of reverse phase columns for high throughput LC-MS lipidomics. *Chem Phys Lipids* **221**, 120-127, doi:10.1016/j.chemphyslip.2019.03.006 (2019).

108 Fernandez-Ochoa, A. *et al.* A Case Report of Switching from Specific Vendor-Based to R-Based Pipelines for Untargeted LC-MS Metabolomics. *Metabolites* **10**, doi:10.3390/metabo10010028 (2020).

109 Steuer, A. E. *et al.* Comparative Untargeted Metabolomics Analysis of the Psychostimulants 3,4-Methylenedioxy-Methamphetamine (MDMA), Amphetamine, and the Novel Psychoactive Substance Mephedrone after Controlled Drug Administration to Humans. *Metabolites* **10** (2020).

7. Abbreviations

ANOVA	analysis of variance
DOA	drugs of abuse
EMCDDA	European Monitoring Center for Drugs and Drug Addiction
GC	gas chromatography
GC-MS	gas chromatography coupled to mass spectrometry
HILIC	hydrophilic interaction chromatography
LC	liquid chromatography
LC-HRMS	liquid chromatography coupled to high resolution mass spectrometry
MS	mass spectrometry
NMR	nuclear magnetic resonance
NPS	new psychoactive substances
PCA	principal component analysis
PCYP	alpha-pyrrolidinocyclohexanophenone
pHLM	pooled human liver microsomes
PLSDA	partial least-squares discriminant analysis
RP	reversed-phase